SOUVENIR & ABSTRACTS

International Conference on Quantum Effects in Solids of Today (I-ConQuEST)

&

K.S. Krishnan Discussion Meeting on Frontiers in Quantum Science (FQS2010)

&

Indo-US Workshop on Physics & Applications of Quantum Phases in Condensed Matter

December 20 to 23, 2010

National Physical Laboratory

New Delhi (India)

Area-wise CSIR Institute/laboratories

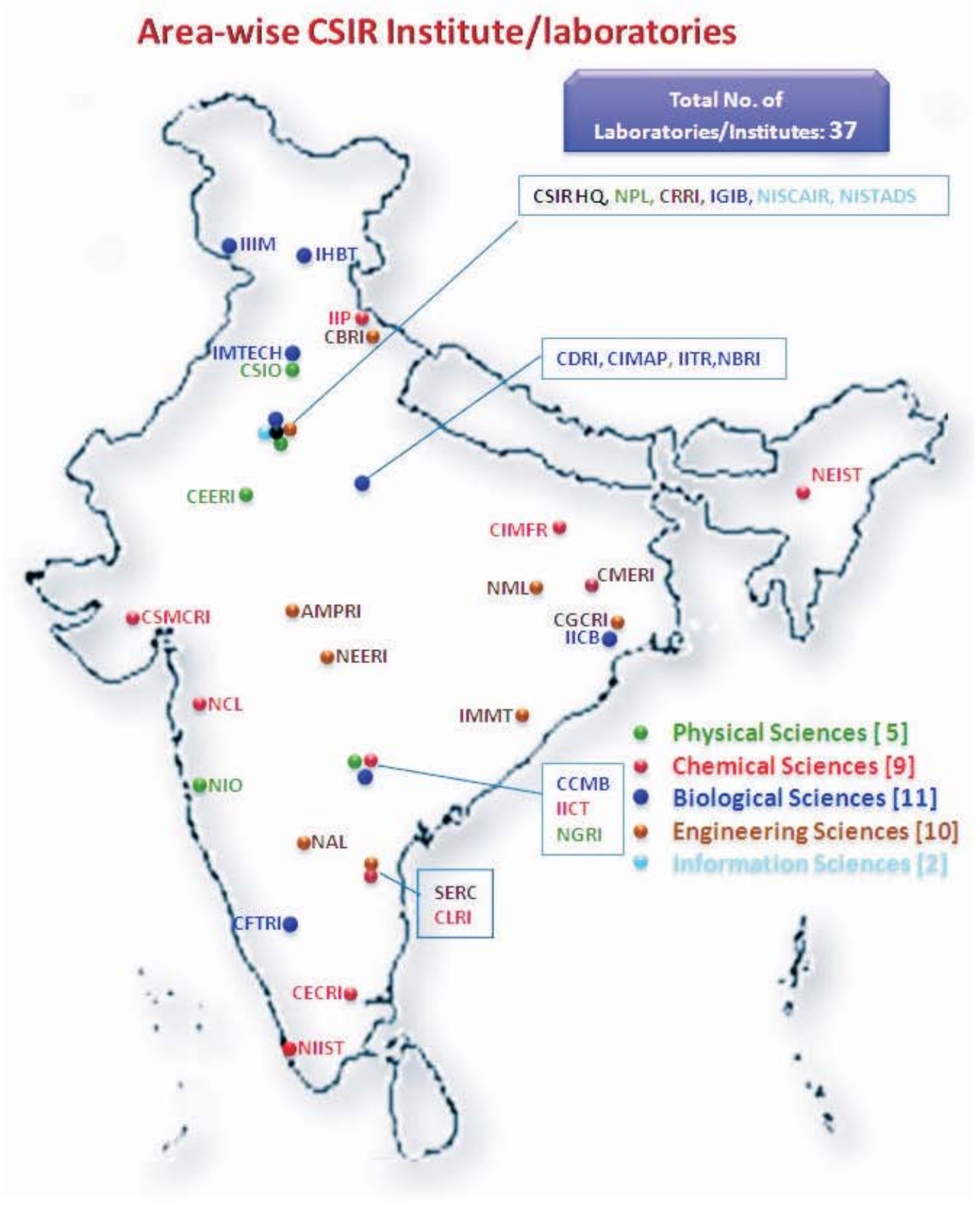

SOUVENIR & ABSTRACTS

International Conference on Quantum Effects in Solids of Today (I-ConQuEST)

&

K.S. Krishnan Discussion Meeting on Frontiers in Quantum Science (FQS2010)

&

Indo-US Workshop on Physics & Applications of Quantum Phases in Condensed Matter

December 20 to 23, 2010

National Physical Laboratory

New Delhi (India)

कपिल सिब्बल
Kapil Sibal

सत्यमेव जयते

मंत्री
मानव संसाधन विकास;
विज्ञान और प्रौद्योगिकी एवं पृथ्वी विज्ञान;
संचार एवं सूचना प्रौद्योगिकी
भारत सरकार, नई दिल्ली

MINISTER OF
HUMAN RESOURCE DEVELOPMENT
SCIENCE & TECHNOLOGY AND EARTH SCIENCES;
COMMUNICATIONS AND INFORMATION TECHNOLOGY
GOVERNMENT OF INDIA
NEW DELHI - 110001

Message

I am pleased to know that the National Physical Laboratory (CSIR), New Delhi is organizing an "International Conference on Quantum Effects in Solids of Today (I-ConQuEST)" during 20th to 23rd December, 2010. Quantum phenomena based applications are gaining momentum primarily because quantum mechanics has been enormously successful in explaining the microscopic phenomena in practically all the branches of Physics and even the discovery of nanotechnology owes its roots to quantum theory. Our increasing ability to manipulate matter at very low temperatures and in very small dimensions continues to open up new areas where we can tailor materials whose behavior depends crucially on the quirks of quantum mechanics.

I am happy to note that this Conference will assemble researchers from variety of disciplines related to "quantum phenomena in solids", thereby providing a strong synergy to the future research endeavours in this exciting area, through such a useful event. I hope that all the participants will have an academically stimulating meeting and I wish the conference all the success.

Dated : 6th December, 2010

(Kapil Sibal)

Anusandhan Bhawan, 2, Rafi Marg, New Delhi-110001 Ph: 011-23316766, 23714230 Fax : 011-23316745

प्रो. समीर के. ब्रह्मचारी
महानिदेशक, वै.औ.अ.प.
एवं सचिव, भारत सरकार
वैज्ञानिक और औद्योगिक अनुसंधान विभाग

Prof. Samir K. Brahmachari
Director General, CSIR
& Secretary, Government of India
Department of Scientific & Industrial Research

वैज्ञानिक तथा औद्योगिक अनुसंधान परिषद्
अनुसंधान भवन, 2, रफी मार्ग, नई दिल्ली-110001
COUNCIL OF SCIENTIFIC & INDUSTRIAL RESEARCH
Anusandhan Bhawan, 2, Rafi Marg, New Delhi-110001

Message

I am immensely pleased to know that the National Physical Laboratory, a constituent laboratory of the Council of Scientific and Industrial Research (CSIR), is holding an International Conference on *"Quantum Effects in Solids of Today"*, which is scheduled to be held during December 20-23, 2010.

Devices based on quantum effects are now very familiar to all. From well-known lasers, transistors, electron microscope and magnetic imaging devices to spintronics-based devices, quantum computing, these devices have revolutionized the framework of modern science and technology. It may not be an exaggeration to suggest that quantum effects will dominate the course of technology development in the 21st century. This conference assumes special significance for National Physical Laboratory in view of the rapidly changing scenario of standards, which is gradually shifting from conventional metrology towards quantum metrology, based on several quantum-related phenomena.

It is heartening to observe that special emphasis in this conference has been laid on the participation of young researchers. I am sure that this conference would provide a suitable platform for researchers from India and abroad to discuss the latest trends in modern quantum related materials and how these are being harnessed for technological applications.

I warmly welcome all delegates, congratulate the organizers and send my best wishes for the success of the event.

[Samir K Brahmachari]

New Delhi

December 6, 2010

Telephone Office : 91-11-23710472, 23717053; Fax: 91-11-23710618; Residence : 91-11-26842276
E-mail : dgcsir@csir.res.in & dg@csir.res.in

This is book of abstracts of the International Conference on ***"Quantum Effects in Solids of Today"*** *from December 20 to 23 at the National Physical Laboratory, New Delhi. Quantum effects in solids become visible at low temperatures. In nanomaterials the electronic confinement and consequent discrete nature of energy states lead to interesting behaviour. Graphene shows a quantum behaviour which is unique. Cuprates, pnictides, manganites and topological insulators are exotic states of matter, and as of now we lack basic understanding of their behaviour. Interfaces between insulating and non-magnetic perovskites, exhibit two dimensional electron gas with superconductivity. There is rich and exciting physics in new forms of quantum order in intercalcated compounds, ferroelectrics and multiferroic materials in the neighbourhood of quantum phase transitions. All these and many more quantum phenomena in a variety of systems are presented here in the abstracts of papers for the above International Conference at NPL. In this conference there are about 50 invited talks and about 100 poster presentations. These deal broadly with areas like electron-electron correlations, heavy fermion systems, transport in mesoscopic systems, fractional quantum Hall effect and topological insulators. It is also appropriate that when NPL India is organizing the conference, applications of some of these new developments to quantum metrology are emphasized.*

We thank all the contributors for their cooperation and for responding to our request to submit abstract in time. We look forward to a stimulating conference.

Organizing Committee I-ConQuEST-2010

CONTENTS

LIST OF SPONSORS

Council of Scientific & Industrial Research, New Delhi

Institute of Mathematical Sciences, Chennai

Indo-US S&T Forum, New Delhi

Department of Science & Technology, New Delhi

Department of Information Technology, New Delhi

Defence Research & Development Organization, New Delhi

Indian National Science Academy, New Delhi

Tata Institute of Fundamental Research, Mumbai

Jawaharlal Nehru Centre for Advanced Scientific Research, Bangalore

Central Electronics Engineering Research Institute, Pilani

National Engineering Institute for Science & Technology, Jorhat

National Geophysical Research Institute, Hyderabad

National Institute for Interdisciplinary Science & Technology, Thiruvananthapuram

National Environmental Engineering Research Institute, Nagpur

National Metallurgical Laboratory, Jamshedpur

Advanced Materials and Processes Research Institute, Bhopal

National Institute of Science Communication and Information Resources, New Delhi

Central Drug Research Institute, Lucknow

Indian Institute of Toxicology Research, Lucknow

Central Road Research Institute, New Delhi

National Accreditation Board for Testing and Calibration Laboratories, New Delhi

Central Leather Research Institute, Chennai

Unit for R&D of Information Products, Pune

Institute of Himalayan Bioresource Technology, Palampur

Institute of Genomics & Integrative Biology, Delhi

Laser Science Services (I) Pvt. Limited, Mumbai

Carl Zeiss India, New Delhi

Mack International, Mumbai

Excel Instruments, Mumbai

Specialise Instruments Marketing Company, Mumbai

The Tinsley Group Limited (India), Delhi

Con-Serv Enterprises, Mumbai

IR Technology Services Pvt. Limited, Noida

Pfeiffer Vacuum India Limited, Secundrabad

Syndicate Bank, NPL-Pusa, New Delhi

Amit Air Products, New Delhi

Bruker India Scientific Pvt. Ltd., New Delhi

Riber SA, France

Goodwill Cryogenics Enterprises, Mumbai

Emmtech Calibration, Faridabad (Haryana)

Belz Instruments Pvt. Limited, Faridabad

Ekta Marketing Corporation, Delhi

Katsun Automation Pvt. Limited, New Delhi

Vico Scientific Sales, New Delhi

Stirling Cryogenics India, New Delhi

Inkarp Instruments Pvt. Limited, Hyderabad

Linde Engineering Pvt. Limited, Vadodara

I-ConQuEST 2010

A B S T R A C T S

KEYNOTE LECTURE

NEWS FROM QUANTUM EFFECTS IN TWO-DIMENSIONAL SYSTEMS

Klaus v. Klitzing

Max-Planck-Institut für Festkörperforschung, Heisenbergstr.1, D-70569 Stuttgart, Germany

25 years after the Nobel Prize in Physics for the quantum Hall effect, the Nobel Prize 2010 for graphene throw light again on the fascinating physics of two-dimensional electron systems with interesting quantum phenomena.

The talk will concentrate on modern topics of two-dimensional electron systems in strong magnetic fields including discussions about applications of the quantum Hall effect in metrology and new experiments on mono and double layers of two-dimensional systems.

Plenary Lectures

COMPOSITE FERMION THEORY OF FRACTIONAL QUANTUM HALL EFFECT IN GRAPHENE

J.K. JAIN

Pennsylvania State University, USA
Email: jain@phys.psu.edu

Graphene is a realization of a two dimensional electron system that exhibits the fractional quantum Hall effect (FQHE) under the application of a strong magnetic field. I will present theoretical studies that demonstrate that composite fermions are formed in graphene as well, but the spin and valley degeneracies and the linear dispersion of electrons produce interesting new physics relative to that in the usual two-dimensional GaAs systems. Composite fermion theory allows detailed predictions about FQHE in graphene in regimes when either or both of the spin and valley degeneracies are broken. I will discuss the relevance of our theory to recent experiments. This work has been performed in collaboration with Csabe Toke.

STUDIES OF TIME-REVERSAL-SYMMETRY-BREAKING IN UNCONVENTIONAL SUPERCONDUCTORS

AHARON KAPITULNIK

Stanford University, USA
Email: aharonk@stanford.edu

BCS theory of conventional superconductivity is based on pairing of each electron state with its exact time reverse, resulting in a coherent condensate of spin singlet pairs, which is insensitive to non-magnetic scattering (Andserson theorem). Such superconductors are characterized by an order parameter which breaks U(1)-gauge symmetry leading to the basic properties, such as the Meissner effect, persistent current and flux quantization. By contrast, unconventional superconductors exhibit additional broken symmetries, which lead often to distinctive superconducting phases with unique properties including sensitivity to non-magnetic scattering. Of particular interest to us is the case of time reversal symmetry breaking (TRSB) which involves magnetism and is predicted to exhibit some anomalous properties. In this talk we will review our recent studies of TRSB in several systems including the triplet superconductor Sr_2RuO_4, the pseudogap state of high temperature superconductors, and the inverse proximity effect in superconductor/ferromagnet bilayer structures.

QUANTUM OSCILLATIONS OF SURFACE ELECTRONS IN TOPOLOGICAL INSULATORS

N.P. Ong

Department of Physics, Princeton University, USA
Email: npo@princeton.edu

Topological insulators (Tls) are predictged to display unusal surface states which traverse the bulk energy gap. These surface states in Tls are massless Dirac states. Unlike the Dirac states in graphene, the electrons have only one spin degree of freedom on each surface. Strong spin-orbit coupling locks the spin perpendicular to the wavevector k (Rashba term), so that states on opposite surfaces in a crystal have different helicities, Surface probes (ARPES and STM) have been very successful in investigating these novel states in bismuth based semimetals. By as-grown crystals can exceed the surface term by factors of 100,00 to a million. Recently, we have obtained crystals of Bi_2Te_3 that display non-metallic resistivity profiles. The surface states are detected as distinct, if weak, Shubnikov de Haas (SdH) oscillations in the Hall channel. From the SdH amplitudes, we deduce sizeable surface mobilites of 10,000 cm^2/Vs, with large metallicity factors $k_{f/\sim 100.}$ The Fermi velocity inferred is in good agreement with ARPES results. A striking weak-field Hall anomaly provides confirmation of these numbers. I will provide a brief introduction to the topic and describe the transport evidence as well as recent results on the high field quantization of the Dirac states.

CORRELATION BETWEEN SPIN FLUCTUATIONS AND PAIRING IN ELECTRON-DOPED CUPRATES

R. L. Greene

Department of Physics, CNAM, University of Maryland, USA
Email: rgreene@squid.umd.edu

The origin of the electron pairing in high-T_c cuprate superconductors is still unresolved in spite of over 20 years of research on these materials. Most research has focused on hole-doped cuprates, which have a "pseudogap" phase of unknown origin in the under doped region of the phase diagram. In contrast, electron-doped cuprates have a "pseudogap" whose origin is known to come from antiferromagnetic spin density wave (SDW) fluctuations [1]. Here we report a detailed analysis of very low temperature transport measurements (30mK < T< 2K) on electron-doped $La_{2-x}Ce_xCuO_4$ ($0.10 < x < 0.21$) films in the normal state (H >Hc2). Most significantly, we find a direct correlation between the strength of the linear-in-temperature resistivity and the superconducting transition temperature (T_c). This strongly suggests that pairing and normal state scattering are both caused by the same coupling, most likely to SDW fluctuations since no other excitations are known to exist at low temperatures in the n-doped cuprates. A correlation between T-linear resistivity and T_c has also been found in hole-doped cuprates [2], however, in this case the scattering responsible for the T linear term is unknown and the measurements have not been done at low enough temperatures to access the ground state. Since the superconductivity originates in the CuO_2 planes for both electron- and hole-doped cuprates, our work suggests that the spin fluctuations must play the dominant role in the pairing for all (both hole- and electron-doped) cuprate high-T_c superconductors!

REFERENCES

1. P. Armitage, P. Fournier, and R. L. Greene, Rev. Mod. Phys. 82, 2421 (2010)
2. For a summary and other references see; L. Taillefer, arXiv: 1003.2972

Collaborators on this work are: K. Jin, N. P. Butch, G. Droulers, K. Kirshenbaum, X. H. Zhang, P. Bach, and J. Paglione.

PHENOMENOLOGICAL GINZBURG LANDAU LIKE THEORY FOR HIGH TEMPERATURE SUPERCONDUCTIVITY IN THE CUPRATES

S. Banerjee,[1] T.V. Ramakrishnan,[2] C. Dasgupta[1]

[1]*Department of Physics, Indian Institute of Science, Bangalore - 560012*
[2]*Department of Physics, Banadras Hindu University, Varanasi-221005*
Email: vrama@bhu.ac.in

An experimentally inspired theory for cuprate superconductivity, with nearest neighbour spin singlet (bond) cooper pairs are the basic low energy degrees of freedom, is described here. The electrons responsible for superconductivity reside primarily on the sites of the square planar Copper lattice with weak interplanar coupling. We hypothesize a simple functional of Yij = Ym=Dmexp (ifm) which mimics the well known GL functional for superconductivity. An 'antiferromagnetic' nearest neighbour coupling of the form Re (Ym*Yn) where m and n are nearest neighbours in the bon centre lattice, leads to superconductive long range order below Tc>. The bond pair magnitude (without long range phase coherence) is sizeable below a crossover temperature obtained by us from the functional, and identified with pseudogap temperature T*. In a magnetic analogy, the d-wave symmetry superconducting order translates into the Neel antiferromagnetic LRO found by us.

The coefficients of the functional are inspired by experiment. We make predictions for Tc (x) as a function of hole doping x, for the superfluid density rs (x,T), the specific heat (without and with a magnetic field) and the vortex structure, and compare our results successfully with experiments. We also generalize the theory to include coupling to electrons (hopping on the same square lattice and forming Cooper pairs), calculate the single particle spectral function as affected by inevitable low energy Cooper pair (phase) fluctuations, and compare our results with recent high resolution ARPES results on Fermi arcs, filling of the antinodal pseudogap, 'bending' of Dk below Tc etc.

ELECTRIC FIELD TUNING OF THE $LaAlO_3/SrTiO_3$ INTERFACE GROUNDSTATE

Caviglia[1], N. Reyren[1], S. Gariglio[1], C. Cancellieri[1], S. Thiel[2], G. Hammerl[2], D. Jaccard[1], M. Gabay[3], T. Schneider[4], J. Mannhart[2], J.-M. Triscone[1*]

[1]*DPMC, University of Geneva, 24 quai E.-Ansermet, 1211 Geneva 4, Switzerland.*

[2] *Experimental Physics VI, Center for Electronic Correlations and Magnetism, Institute of Physics, University of Augsburg, D-86135 Augsburg, Germany.*

[3] *Laboratoire de Physique des Solides, Bat 510, Université d'Orsay, 91405 Orsay, Cedex, France.*

[4]*Physik Institut, University of Zurich, Winterthurerstrasse 190, 8057 Zurich, Switzerland.*
Email: Jean-Marc.Triscone@unige.ch

At interfaces between complex oxides, electronic systems with unusual properties can be generated [1,2]. A striking example is the interface between LaAlO3 and SrTiO3, two good insulating perovskites, which was found in 2004 to be conducting with a high mobility [3]. The ground state of this system is a superconducting condensate, with a critical temperature of about 200 mK [4]. The characteristics observed in the normal and superconducting states are consistent with a two-dimensional electronic system. Field effect experiments revealed the sensitivity of the normal and superconducting states to the carrier density. In particular, the electric field allows the tuning of the critical temperature between 200 mK and 0 K and thus the on-off switching of superconductivity. The system phase diagram reveals a superconducting pocket with an underdoped and an overdoped regime [5]. Magnetoconductance measurements allow a superconductor-insulator and a superconductor-metal phase transition in the underdoped and overdoped regimes respectively to be identified. A large, interfacially generated, tunable spin-orbit coupling and a remarkable correlation between the spin-orbit coupling strength and the system phase diagram are other hallmarks of this fascinating system [6].

REFERENCES

1. See for instance, "Enter the oxides", J. Heber, Nature 459, 28 (2009).
2. J. Mannhart and D. Schlom, Science 327, 1607 (2010).
3. Ohtomo, H. Y. Hwang, Nature 427, 423 (2004).
4. N. Reyren, S. Thiel, A. D. Caviglia, L. Fitting Kourkoutis, G. Hammerl, C. Richter, C. W. Schneider, T. Kopp, A.-S. Ruetschi, D. Jaccard, M. Gabay, D. A. Muller, J.-M. Triscone and J. Mannhart, Science 317, 1196 (2007).
5. Caviglia, S. Gariglio, N. Reyren, D. Jaccard, T. Schneider, M. Gabay, S. Thiel, G. Hammerl, J. Mannhart, and J.-M. Triscone, Nature 456, 624 (2008).
6. A.D. Caviglia, M. Gabay, S. Gariglio, N. Reyren, C. Cancellieri, and J.-M. , Physical Review 104, 126803 (2010).

RAMAN SCATTERING AND ULTRAFAST PUMP-PROBE STUDY OF IRON PNICTIDE SUPERCONDUCTORS

A.K. Sood

Department of Physics, Indian Institute of Science, Bangalore
Email: asood@physics.iisc.ernet.in

The talk will cover our recent Raman studies of iron pnictide superconductors as a function of temperature. We will also present differential reflectivity pump-probe experiments carried out using 40fs laser pulses on parent and doped 122 iron pnictide single crystals. In $FeSe_{0.82}$, a phonon mode near 100 cm^{-1} exhibits a sharp increase by ~5% in the frequency below a temperature T_s (~100 K) attributed to strong spin-phonon coupling and onset of short-range antiferromagnetic order. In addition, two high frequency modes are observed at 1350 cm^{-1} and 1600 cm^{-1}, attributed to electronic Raman scattering from (x^2-y^2) to *xz/yz* d-orbitals of Fe [1]. In $CeFeAsO_{0.9}F_{0.1}$, we find evidence for strong coupling between the phonons and crystal field excitations [2]. Below the superconducting transition temperature, the phonon mode near 280 cm^{-1} shows softening, signaling its coupling with the superconducting gap. In $Ca(Fe_{0.95}Co_{0.05})_2As_2$ also, the phonon mode near 260 cm^{-1} shows coupling with the superconducting gap [3]. First-principles density-functional-theory-based calculations have also been done to determine the effects of the strength of on-site electron correlation, magnetic ordering, and spin-phonon coupling [4].

I thank all my coauthors mentioned in the references below for their valuable contributions to the ongoing collaboration.

REFERENCES

1. Pradeep Kumar, Anil Kumar, Surajit Saha, D.V.S. Muthu, J. Prakash, S. Patnaik, U.V. Waghmare, A.K. Ganguli and A.K. Sood, Anomalous Raman Scattering from Phonons and Electrons of Superconducting $FeSe_{0.82}$, Solid State Communication (Fast Track) 150, 557-560 (2010).
2. Pradeep Kumar, Anil Kumar, Surajit Saha, D.V.S. Muthu, J. Prakash, U.V. Waghmare, A.K. Ganguli and A.K. Sood, Temperature-dependent Raman study of $CeFeAsO_{0.9}F_{0.1}$ Superconductor: Crystal field excitations, phonons and their coupling, J. of Phys. Cond. Matt. 22, 255402 (2010)
3. Pradeep Kumar, A. Bera, D.V.S. Muthu, Anil Kumar, U.V. Waghmare, H. Luminita, S. Singh, R. Buchner and A.K. Sood, Raman evidence for superconducting gap and spin-phonon coupling in superconductor $Ca(Fe_{0.95}Co_{0.05})_2As_2$. (To be published)
4. Anil Kumar, Pradeep Kumar, Umesh V. Waghmare and A.K. Sood, First-principles analysis of electron correlation, spin ordering and phonons in the normal state of $FeSe_{1-x}$, J. Phys. Cond. Matt. 22, 385701 (2010)

Invited Lectures

ELECTRICAL QUANTUM METROLOGY: IT'S FUNDAMENTAL

Franz Josef Ahlers

Electrical Quantum Metrology, Physikalisch-Technische Bundesanstyalt, Bundesallee 100, 38116 Braunschweig, Germany.
Email: Franz-Josef.Ahlers@ptb.de

Electrical Metrology means, at its heart, quantum metrology: the traceability of the units of voltage and resistance to Planck's constant *h* and elementary charge *e* realized by the Josephson and quantum Hall effects has (r) evolutionized the field during the last 20 years. Electrical units due to their extremely good reproducibility are even likely candidates to replace the artifact based definition of the kilogram by one based on Planck"s constant. Having reached maturity for the DC quantitites Volt and Ω, modern quantum standards find more and more application also in the AC regime, while at the same time progress in materials technology or new discoveries still is opening perspectives for improvement of their basic building blocks, the quantum devices. In my talk I will review the current state of the art in electrical quantum metrology, and I will take a loot at some of the developments expected for the future.

GRAPHENE: SETTING NEW STANDARDS

Alexander Tzalenchuk[1], T.J.B.M. Janssen[1], Samuel Lara-Avila[2], Alexei Kalaboukhov[2], Sara Paolillo[2,3], Mikael Syväjärvi[4], Rositza Yakimova[4], Olga Kazakova[1], Sergey Kopylov[5], Vladimir Fal'ko[5], Sergey Kubatkin[2]

[1]National Physical Laboratory, TW11 0LW Teddington, UK,
[2]Department of Microtechnology and Nanoscience, Chalmers University of Technology, S-412 96 Göteborg, Sweden,
[3]Department of Physics, Politecnico di Milano, 20133 Milano, Italy,
[4]Department of Physics, Chemistry and Biology (IFM), Linköping University, S-581 83 Linköping, Sweden,
[5]Physics Department, Lancaster University, Lancaster, LA1 4YB, UK
Email: alexander.tzalenchuk@npl.co.uk

We report progress in development of a quantum Hall effect (QHE) resistance standard based on large area monolayer graphene on silicon carbide [1,2]. Epitaxial graphene devices demonstrate extraordinary robustness of the h/2e2 plateau, accurately quantized to at least a part in a billion over a broad range of magnetic field, temperature and measurement current. This robustness, which we attribute to the pinning of ν=2 filling factor provided by charge transfer between the SiC surface and graphene layer, makes epitaxial graphene ideally suited for quantum resistance metrology. We believe that the new results on graphene will help expand the horizon of quantum metrology and advance the understanding of both graphene and QHE.

REFERENCES

1. A Tzalenchuk et al., Nature Nanotechnology 5, 186 (2010).
2. TJBM Janssen et al., arXiv:1009. 3450

ANDREEV REFLECTION SPECTROSCOPY ON EPITAXIAL THIN FILMS OF SUPERCONDUCTING $Ba(Fe_{0.92}Co_{0.08})_2As_2$

Venkat Chandrasekhar

Department of Physics and Astronomy, Northwestern University, USA
Email: v-chandrasekhar@northwestern.edu

The normal state properties of the ferropnictide superconductors might hold the key to understanding high temperature superconductors that are not understood within the context of the BCS formalism. We have performed point-contact Andreev reflection spectroscopy on extremely high quality epitaxial thin films of $Ba(Fe_{0.02}Co_{0.08})_2As_2$, below and above the superconducting transition temperature (T_c). The Andreev reflection signal shows an unusual temperature dependence that remains up to $1.3T_c$. Andreev reflection in the normal state of a superconductor can be understood in the model of phase-incoherent pairs that was proposed in the context of the pseudogap in the cuprates. Within this model, if the stiffness of the phase of the order parameter is low, T_c can be significantly lower than the temperature where pair formation takes place and phase-incoherent superconducting pairs participate in normal state Andreev reflection. However, according to this model, phase fluctuations can be important only for materials with low superfluid density. It is known that the superfluid density in the ferropnicties is high and comparable to the conventional elemental superconductors. Therefore, our observations suggest that the importance of phase fluctuations in the unconventional superconductors with high superfluid density should be reconsidered.

THEORY OF HIGH TC SUPERCONDUCTIVITY

G. Baskaran

The Institute of Mathematical Sciences, Chennial-600 113
Email: baskaran@imsc.res.in

Any theory that attempts to explain high Tc superconducity in cuprates faces a plethora of experimental results that have been accumulated in the last 24 years. Instead of constraining the theories, many new experiments seem to lend support to different mechanisms and theories. It is a confusing situation, somewhat related to 'cherry picking'. I will focuss on some well known phenomena, i) 41meV neutron resonance, ii) stripes seen in STM, iii) small Fermi pockets seen in quantum oscillations and iv) 'kink' in APRWS, and argue that when correctly interpreted they help one to fix the theory some what uniquely and lend a strong support to the resonating valence bond mechanism of high temperature superconductivity as the right theory.

TRANSPORT PROPERTIES OF TWO-DIMENSIONAL ELECTRON GAS AT THE MOTT-INSULATOR/BAND-INSULATOR $LaTiO_3/SrTiO_3$ INTERFACE

J. Lesueur[1], J. Biscaras[1], N. Bergeal[1], A. Kushwaha[2], T. Wolf[1], A. Rastogi[2], R.C. Budhani[2-3]

[1]LPEM- UMR8213/CNRS - ESPCI ParisTech, 10 rue Vauquelin - 75005 Paris
[2]Condensed Matter - Low Dimensional Systems Laboratory,
Department of Physics,Indian Institute of Technology Kanpur, Kanpur 208016, India and
[3]National Physical Laboratory, New Delhi - 110012, India.
Email: jerome.lesueur@espci.fr

Transition metal oxides display a great variety of quantum electronic behaviors where correlations often play an important role. The achievement of high quality epitaxial interfaces involving such materials gives a unique opportunity to engineer artificial materials where new electronic orders take place. It has been shown recently that a two-dimensional electron gas could form at the interface of two insulators such as $LaAlO_3$ and $SrTiO_3$ [1], or $LaTiO_3$ (a Mott insulator) and $SrTiO_3$ [2].

We present low temperature transport and magneto-transport measurements on $LaTiO_3/SrTiO_3$ hetero-structures, whose properties can be modulated by field effect using a metallic gate on the back of the substrate. The corresponding phase diagram has been investigated, and superconductivity evidenced for the first time in this system which involves a Mott insulator [3]. We will discuss the role of the confinement potential and the $SrTiO_3$ band structure on the phase diagram, and show the specific role of the spin-orbit coupling measured by localization corrections to the magnetoconductivity. Finally, the superconducting to insulator transition will be analyzed.

REFERENCES

1. N. Reyren et al, Science 317, 1196 (2007)
2. A. Ohtomo et al, Nature 419, 378 (2002)
3. J. Biscaras et al, arXiv: 1002.3737v2 ; to appear in Nature Communications (2010)

QUANTIFYING SPIN HALL EFFECTS IN METALS

A. Hoffmann,[*,1] O. Mosendz,[2] G. Mihajloviæ,[2] V. Vlaminck,[1] J. E. Pearson,[1] F. Y. Fradin,[1]
S. D. Bader,[1,3] G. E. W. Bauer,[4] and M. A. Garcia[5]

[1]*Materials Science Division, Argonne National Laboratory, Argonne, IL 60439, U.S.A.*
[2] *San Jose Research Center, Hitachi Global Storage Technologies, San Jose, CA 95135, U.S.A.*
[3] *Center for Nanoscale Materials, Argonne National Laboratory, Argonne, IL 60439, U.S.A.*
[4] *Kavli Institute of NanoScience, Delft University of Technology, 2628 CJ Delft, The Netherlands*
[5] *Institute for Ceramics and Glass, Spanish Council for Scientific Research, 28049 Madrid, Spain*
Email: Hoffmann@anl.gov

Spin Hall effects intermix spin and charge currents even in nonmagnetic materials and, therefore, offer the possibility to generate and detect spin currents without the need for using ferromagnetic materials. In order to gain insight into the underlying physical mechanism and to identify technologically relevant materials, it is important to quantify the spin Hall angle γ, which is a direct measure of the charge-to-spin (and vice versa) conversion efficiency. Towards this end we utilized non-local transport measurements with double Hall bars fabricated from gold and copper [1]. In principle, this geometry permits the study of spin currents both generated and detected via spin Hall effects. We observe an unusual non-local resistivity that changes sign as a function of temperature. However, this result is quantitatively similar in gold and copper, indicating that the non-local signals are not due to spin transport. In fact, the whole temperature dependence of the non-local resistivity can be explained by combining diffusive and quasi-ballistic charge transport leading to an upper limit of $\gamma < 0.027$ for gold at room temperature.

Furthermore, we developed an approach based on spin pumping, which enables us to quantify even small spin Hall angles with high accuracy. Spin pumping utilizes microwave excitation of a ferromagnetic layer adjacent to a normal metal to generate a homogeneous *dc* spin current over a macroscopic area. In this geometry voltage from spin Hall effects scale with the device dimension. We integrated ferromagnet/normal metal bilayers into a co-planar waveguide and determined the spin Hall angle for a variety of non-magnetic materials (Pt, Pd, Au, and Mo) at room temperature [2,3]. In addition, using a similar approach we found that a MgO tunnel-barrier suppresses spin pumping at the ferromagnet/normal metal interface [4].

This work was supported by the U.S. Department of Energy, Office of Science, Basic Energy Sciences, under contract No. DE-AC02-06CH11357 and WU-IST through project MACALO (no. 257159).

REFERENCES

1. G. Mihajloviæ, J. E. Pearson, M. A. Garcia, S. D. Bader, and A. Hoffmann, Phys. Rev. Lett. **103**, 166601 (2009).
2. O. Mosendz, J. E. Pearson, F. Y. Fradin, G. E. W. Bauer, S. D. Bader, and A. Hoffmann, Phys. Rev. Lett. **104**, 046601 (2010).
3. O. Mosendz, V. Vlaminck, J. E. Pearson, F. Y. Fradin, G. E. W. Bauer, S. D. Bader, and A. Hoffmann, arXiv:1009.5089.
4. O. Mosendz, J. E. Pearson, F. Y. Fradin, S. D. Bader, and A. Hoffmann, Appl. Phys. Lett. **96**, 022502 (2010).

NEW COLLECTIVE MODES IN FRACTIONAL QUANTUM HALL EFFECT : MODE SPLITTING, HIGH ENERGY ROTONS, AND SPIN ROTONS

Sudhansu S. Mandal

Indian Association for the Cultivation of Science, Jadavpur, Kolkata 700 032, India
Email: tpsm@iacs.res.in

In analogy to Feynman's theory of roton in superfluid 4He, the theory of collective excitations based on the single mode approximation in fractional quantum Hall state 1/3 predicts a roton minimum and a gap at long wavelength. These predictions are verified in inelastic light scattering experiments. In this theory, the excited state is the density wave modulation over the Laughlin ground state. The collective behaviour of electrons in fractional quantum Hall effect results in the creation of so-called composite fermions, quasi-particles formed by electrons attached to an even number of quantized vortices, each having one unit of flux quantum hc/e. This leads to formation of Ë levels–effective kinetic energy levels resembling Landau levels for such quasi-particles. In the ground state of filling factor 1/3, $\Lambda = 0$ level is fully filled by the composite fermions. The composite fermion (CF) theory predicts collective mode which has good resemblance with that of SMA. The collective mode corresponds to an excitation of CF from $\Lambda = 0$ level to $\Lambda = 1$ level at filling factor $\nu = 1/3$. Moreover, the CF theory allows excitations into higher Λ levels. It is not,however, a priori clear whether these excitations will provide any new mode at all. In this talk, I will present our extensive numerical calculation upto 200 particles to show the splitting of collective mode as we decrease wavelength and appearance of roton minima at high energy collective modes. These predictions are successfully verified in inelastic light scattering experiments. The evidence of formation of quasi-particle levels up to high energies demonstrates the robustness of topological order in the fractional quantum Hall effect. Apart from these neutral spinless modes, the spin modes are also possible when a CF is excited into another empty Λ level with reversed spin. In this talk, I will present how the CF theory predicts roton minima in collective spin modes in several fractional quantum Hall states. These spin rotons are also observed in inelastic light scattering experiments.

A NEW GENERATION OF MODELING HIGHLY RESOLVED SPECTROSCOPIES: CUPRATES, PNICTIDES AND TOPOLOGICAL INSULATORS

Arun Bansil

Physics Department, Northeastern University, Boston, Massachusetts
Email: bansil@lepton.neu.edu

We stand at the threshold of a new 'golden age' of spectroscopic studies of materials for unraveling how charge, spin, orbital and lattice degrees of freedom interact to produce emergent phenomena and exotic states of matter. In this connection, the need for realistic modeling of various highly resolved spectroscopies is becoming of critical importance in providing discriminating tests of competing theoretical models and as a rational basis for future experimentation. In this talk, I will discuss how as we move to model spectroscopic data from a qualitative to a quantitative level, surprising new insights into the nature of electronic states and correlation effects are obtained in high-temperature cuprate superconductors and other complex materials.[1-7] Illustrative examples in cuprates include: (i) Asymmetry of the scanning tunneling (STM) spectrum between positive and negative bias voltages and the extent to which it comes about within the conventional picture; (ii) Origin of the 'high-energy kink' or the 'waterfall effect' in the photoemission spectrum (ARPES) and the interplay therein between effects of the matrix element and the presence of strong coupling of the quasiparticles to electronic excitations; and (iii) The nature of the dichroic signal in photoemission and its relationship to the time-reversal symmetry breaking in the cuprates. I will also comment on our recent work on the manganites and topological insulators.

REFERENCES

1. V. Arpiainen, A. Bansil, and M. Lindroos, Phys. Rev. Letters 103, 067005 (2009).
2. B. Barbiellini, A. Koizumi, P. E. Mijnarends: W. Al-Sawai, H. Lin, T. Nagao, K. Hirota, M. Itou,Y. Sakurai, and A. Bansil, Phys. Rev. Letters 102, 206402 (2009).
3. D. Hsieh, Y. Xia, D. Qian, L. Wray, J. H. Dil, F. Meier, J. Osterwalder, L. Patthey, J. G. Checkelsky, N. P. Ong, A. V. Fedorov, H. Lin, A. Bansil, D. Grauer, Y. S. Hor, R. J. Cava, and M. Z. Hasan, Nature 460, 1101 (2009).
4. Y. Xia, D. Qian, D. Hsieh, L. Wray, A. Pal, H. Lin, A. Bansil, D. Grauer, Y. S. Hor, R. J. Cava, M. Z. Hasan, Nature Physics 5, 398 (2009).
5. J. Nieminen, H. Lin, R. S. Markiewicz, A. Bansil, Phys. Rev. Letters 102, 037001 (2009).
6. H. Lin, L.A. Wray, Y. Xia, S. Xu, S. Jia, R.J. Cava, A. Bansil, M.Z. Hasan, Nature Materials 9, 546 (2010).
7. Hsin Lin, R.S. Markiewicz, L.A. Wray, L. Fu, M.Z. Hasan, A. Bansil, Phys. Rev. Letters 105, 036404 (2010).

COMPOSITE FERMIONS WITH A VALLEY DEGREE OF FREEDOM

Medini Padmanabhan, Tayfun Gokmen and Mansour Shayegan

Department of Electrical Engineering, Princeton University, USA
Email: pmedini@gmail.com

This talk explores the Physics of the fractional quantum Hall (FQH) effect in two dimensional electron systems confined to AIAs quantum wells. In addition to spin, these electrons also possess a valley degree of freedom which raises the exciting possibility of transfer of this characteristic to the composite fermions (CFs). We experimentally tune the valley occupation in our system via the application of strain.

We find that the CFs formed around the Landau leel filling factors of v=3/1 and ½ are fully spin polarized but possess a valley degree of freedom of their own. The response of the various FQH states to stain is captured by a CL Landau level fan diagram drawn for a single spin, two valley system [1]. A comparison of the valley polarization enegies of CGs around v=3/1 and ½ reveal a particle hole symmetry breaking in our system [2]. We also present evidence for anisotropy of the CF Fermi contour.

We also report the observation of persistent FQH states at v=1/3 and 5/3 at zero strain when the two valleys are degenerate [3]. In the CF picture these FQH states are analogous to the integer quantum Hall sate at v=1, which is known to form a quantum Hall ferromagnet in the limit of zero valley splitting. We compare the energy gaps measured at v =1/3 and 5/3 to the theory developed for single valley, two spin systems and find that the gaps and their rates of rise with strain are much smaller than predicted.

OXIDE NANOELECTRONICS ON DEMAND

Jeremy Levy

Department of Physics and Astronomy
University of Pittsburgh, Pittsburgh, PA 15260 3401 USA
Email: jlevy@pitt.edu

Electronic confinement at nanoscale dimensions remains a central means of science and technology. I will describe a method for producing extreme nanoscale electronic confinement at the interface between two normally insulating oxides, $LaAlO_3$ and $SrTiO_3$. Using a conductive atomic-force-microscope probe, we can create nanoscale conducting islands, wires, tunnel junctions, diodes, transistors and photoreceivers with spatial dimensions comparable to the diameter of a single-wall carbon nanotube (~2nm). These structures are created in ambient conditions at room temperature, and can be erased and rewritten repeatedly. This new, on-demand nanoelectronics platform has the potential for widespread scientific and technological exploitation. This work is supported by ARO AFOSR, DARPA, NSF and the Fine Foundation.

EVALUATION OF TWO LEVEL SYSTEMS IN SUPERCONDUCTING RESONATORS USING POWER AND TEMPERATURE DEPENDENCE OF LOSS AND FREQUENCY

David P. Pappas

National Institute of Standards and Technology, Boulder, Co USA
Email: David.Pappas@NIST.gov

High quality factor, i.e low, resonators are important for quantum information storage and addressing [1,2]. In this work we study the resonance frequency and loss in superconducting coplanar waveguide resonators as a function of power and temperature [3-4]. We find that there is increased loss at low power and low temperature [5]. The increased loss is attributed to the existence of two level system (TLS) at the surfaces, interfaces, and in the bulk of insulators deposited on the structures [6]. We show that both the power dependence of the loss and the temperature dependence of the resonant frequency can be used to find the zero temperature TLS contribution to the loss[7]. The frequency data at high power is shown to agree well with the low power TLS loss results. This allows for a relatively fast measurement of the TLS loss. As an example, we measured the properties of amorphous AlO_x deposited on the resonators and find a TLS loss tangent of $1x10^{-3}$. For a more dramatic example, we have been able to prepare extremely low loss resonators using TiN. Thin films of TiN were sputter-deposited onto Si substrates. At high power, internal quality factors (Q_i) higher than 10^7 were measured for TiN with predominantly a (200)-TiN orientation. Elliposometry and Auger measurements indicate that the (200)-TiN growth on the bare Si substrates is stabilized with the formation of the thin, ~2nm, layer of SiN during the pre-deposition procedure. In the single photon regime, Q_i's of exceeded $8x10^5$. These results are very promising for applications in quantum computing, where it is critical to have long lifetimes, i.e high $Q_{i,}$ at low power.

NANOPLATFORMS FOR PHOTONICS AND MEDICINE

Srinivas Sridhar

Arts and Sciences Distinguished Professor of Physics,
Director, IGERT Nanomedicine Science and Technology NCI/NSF Program
Director, Electronic Materials Research Institute, Northeastern University
Email: s.sridhar@neu.edu

Nanotechnology has profound impact in photonics and nanomedicine. I discuss recent developments in nanotechnologies utilized in medicine, imaging and communications. At Northeastern University we have established a multi-disciplinary research and education program that utilizes nanotechnology to address key problems in medicine. Some of the principal research projects are to develop the science and technology of multi-functional nanoparticles (gold, iron-gold, polymeric, micelles, nanoassemblies) for probing cellular processes and for targeted delivery for cancer, infectious and cardiovascular diseases; metallic nanoparticles for embryonic stem cell tracking; magnetic nanoparticles for targeted delivery and MRI contrast enhancement, and nanotemplates for assembly and controlled release of drugs.

Nanoscale optical elements offer the potential of entirely new modalities of imaging with sub-wavelength resolution utilizing the phenomenon of negative refraction. We have developed new types of superlenses and ultra-short focal microlenses using nanolithographic techniques in InP/InGaAsP semiconductor heterostructures at near infrared frequencies. These devices and the accompanying concepts offer the prospect of major developments in imaging and optoelectronics.

Supported by the National Science Foundation and Air Force Research Laboratories.

ELECTRONIC AND TRANSPORT PROPERTIES OF NANO-GRAPHENE SYSTEMS

KATSUNORI WAKABAYASHI[1,2]

[1]International Center for Materials Nanoarchitoctonics(MANA), National Institute for Materials Science(NIMS), Namiki 1-1, Tsukuba 305-0044, Japan
[2]PRESTO, Japan Science and Technology Agency (JST), Kawaguchi, 332-0012, Japan
Email: ka.wakaba@gmail.com

The successive fabrication of graphene devices [1] has initiated intensive and diverse research on carbon related systems. The honeycomb crystal structure of single layer graphene consists of two nonequivalent sublattices and results in a unique band structure for the itinerant p-electrons near the Fermi energy which behave as massless Dirac fermion. In graphene, the presence of edges can have strong implications for the spectrum of the p-electrons. In graphene nanoribbons with zigzag edges, localized states appear at the edge with energies close to the Fermi level.[2] In contrast, edge states are absent for ribbons with armchair edges. Recent experiments have succeeded to synthesize graphene nanoribbons using lithography techniques[3] and chemical techniques.[4]

In my talk, we focus on edge and geometry effects of the electronic properties of graphene nanoribbons.

1) In zigzag nanoribbons, for disorder without inter-valley scattering a single perfectly conducting channel emerges associated with such a chiral mode due to edge states, i.e. the absence of the localization.[5]
2) In armchair nanoribbons, the single-channel transport subjected to long-ranged impurities is nearly perfectly conducting, where the backward scattering matrix elements in the lowest order vanish as a manifestation of internal phase structures of the wavefunction.[6] This phase structure can be related to the existence of Berry phase.[7]
3) Nano-graphene junctions are shown to have the zero-conductance anti-resonances associated with the edge states. The relation between the condition of the resonances and geometry is discussed.[8]
4) Finally, we will discuss the effect of edge chemical modification on magnetic properties of nanographene systems.[9]

REFERENCES

1. K. S. Novoselov, A. K. Geim, S. V. Morozov, et.al., Science, 306 (2004) 666.
2. M. Fujita, K. Wakabayashi, et.al, J. Phys. Soc. Jpn. 65 (1996) 1920.
3. M. Y. Han, B. Oezyilmaz, Y. Zhang, and P. Kim, Phys. Rev. Lett. 98 (2007) 206805.
4. X. Li, X. Wang, L. Zhang, S. Lee, H. Dai, Science 31, (2008) 122.
5. K. Wakabayashi, et.al., Phys. Rev. Lett. 99 (2007) 036601; CARBON 47 (2009) 124; New J. Phys. 11 (2009) 095016.
6. M. Yamamoto, Y. Takane, and K. Wakabayashi, Phys. Rev. B79 (2009) 125421.
7. K. Sasaki, K. Wakabayashi, T. Enoki, New J. Phys. 12 (2010) 083023.
8. M. Yamamoto and K. Wakabayashi, Appl. Phys. Lett. 95 (2009) 082109.
9. K. Wakabayashi, S. Okada et.al., J. Phys. Soc. Jpn. 79 (2010) 034706.

ELECTROMECHANICALLY PERTURBING THE QUANTUM HALL STATE USING SUSPENDED GRAPHENE RESONATORS

Mandar Deshmukh

Tata Institute of Fundamental Research, Mumbai
Email: deshmukh@tifr.res.in

Using suspended graphene resonators we try to answer the following question- how does the quantum Hall state get perturbed when the Hall bar vibrates with an amplitude – 5nm. Resistance changes measured in the quantum Hall state at the electromechanical resonance can result from scattering and also due to modulation of the energy landscape. Experimentally measured, only at the electro mechanical resonance of the suspended grapheme the changes in two probe resistance are measurable and correlate with the quantum Hall features.

QUANTUM EFFECTS ON NOISE IN GRAPHENE

Arindam Ghosh

Indian Institute of Science, Bangalore
Email: arindam@physics.iisc.ernet.in

As an ideal two-dimensional semiconductor graphene has generated great interest in both concepts of fundamental physics and device applications. Graphene is a promising material as the active component in flexible ultra-fast electronics, offering advantages in the form of high carrier mobility, robustness, and miniaturization. The physics of graphene is a bridge between quantum field theory and condensed matter physics due to the special quality of the graphene quasiparticles behaving as massless two dimensional Dirac fermions. Several new phenomena such as the half-integer quantum hall effect, Klein tunneling etc. are manifestations of the uniqueness of graphene's quantum mechanical behaviour. In this talk I shall highlight a phenomenon where the quantum nature of grapheme, as well as its unique band structure play crucial role. Specifically, it will be shown that the low-frequency conductivity fluctuation, or 1/f noise, is sensitive to the ability of graphene to screen external potential fluctuations, which depends on the band structure of graphene in general. From experiments with a wide variety of devices from graphene we have established that the low-frequency 1/f noise can distinguish between the linear and parabolic bands, and hence can be used to separate single layer graphene from the multilayered ones. Apart from being crucial to designing electronic devices from graphene, the results can also be important to characterize graphene nanoribbons, where quantum confinement effects play key role. Results from our experiments on graphene nanoribbons will also be presented.

PHASE-FLUCTUATION DRIVEN PSEUDOGAP STATE IN A DISORDERED S-WAVE SUPERCONDUCTOR: NbN

Pratap Raychaudhuri

Tata Institute of Fundamental Research, Mumbai, India.
Email: prataparya@gmail.com

Understanding the role of interaction and disorder is at the heart of understanding of collective behavior of many-body quantum systems, such as High temperature superconductors, quantum Hall effect and superfluid He. In superconductors, where the order parameter is described by a complex order parameter with an amplitude and phase, the presence of strong disorder poses an intriguing question: Is the destruction of the superconducting state always associated with the vanishing or the amplitude or could strong phase fluctuations destroy the superconducting state even when the amplitude of the superconducting pairing remains finite? The latter, if true, would give rise to novel electronic states with finite superconducting pairing amplitude (and hence finite density of Cooper pairs) but no global superconductivity.

In this talk I will describe our attempts to answer this question, by extracting all the key parameters of the superconducting state, on a set of NbN thin films with controlled amount of disorder. The disorder in these films are tuned from moderately clean limit to the Anderson metal-insulator transition. Using a combination of low temperature scanning tunneling spectroscopy, penetration depth, and magnetotransport measurements I will show that close to the Anderson limit, strong phase fluctuations give rise to pseudogaped state, similar to high temperature cuprates. Finally, I will show signatures that unambiguously identify phase fluctuations as a dominant mechanism for the destruction of superconductivity in strongly disordered s-wave superconductors.

REFERENCES

1. Phys. Rev. B 77, 214503 (2008)
2. Phys. Rev. B 79, 094509 (2009)
3. Appl. Phys. Lett. 94, 262501 (2009)
4. Phys. Rev. B 80, 134514 (2009)
5. Appl. Phys. Lett. 96, 072509 (2010)
6. arXiv:1006.4143.

ATOMIC PHYSICS AND QUANTUM OPTICS USING CIRCUITS: A BRIEF OVERVIEW OF SUPERCONDUCTING QUBITS

Franco Nori

Advanced Science Institute, RIKEN, Saitama, Japan, Physics Department, University of Michigan, Ann Arbor, MI, USA
Email: fnori@riken.jp

Superconducting (SC) circuits can behave like atoms making transitions between a few energy levels. Such circuits can test quantum mechanics at macroscopic scales can be used to conduct atomic-physics experiments on a silicon chip. This presentation overviews a few of our theoretical studies on SC circuits and quantum information processing (QIP) including: SC qubits for photon generation and for lasing; 2-1 photon coexistence; cooling qubits and their environment; using SC qubits to probe nearby defects; hybrid circuits involving both charge and flux qubits; quantum tomography in SC circuits; preparation of macroscopic quantum superposition states of a cavity field via coupling to a SC qubit; generation of nonclassical photon states using a SC qubit in a microcavity; and controllable couplings among qubits. These controllable couplings between qubits can be achieved either directly or indirectly [for instance, with or without coupler circuits; as well as with or without 'data buses' like resonators (e.g. electromagnetic fields in cavities, LC circuits, or transmission line resonators)].

PHASE COEXISTENCE AND MAGNETIC FRUSTRATION IN CORRELATED OXIDES

HARI SRIKKANTH

Physics Department, University of South Florida, Tampa, FL (USA)
Email: sharihar@usf.edu

Magnetism in several classes of complex oxides is strongly influenced by electron correlation effects leading to intrinsic phase separation Geometric frustration, valence fluctuations, internal strain and low dimensionality are all known to lead to rich cooperative phenomena that result in multiple magnetic transitions and glass-like magnetic ground states. In this talk, we will focus on two materials – single crystals of $LuFe_2O_4$ and single crystals and nanostructures of mixed phase manganite (La,Pr,Ca)MnO_3. We will demonstrate that relatively unconventional experimental methods of RF transverse susceptibility (TS) and magnetocaloric effect (MCE) as being powerful probes of magnetic transitions in strongly correlated oxides. The $LuFe_2O_4$ system is an interesting example of a multiferric material in which the ferroelectricity is purely driven by electron correlations rather than the conventional dipole mechanism. Out studies for the first time reveal the presence of a complex magnetic phase diagram with two distinct cluster glass phases at intermediate temperatures followed by kinetic arrest at low temperature. The origin of giant coercivity and other anomalous magnetic properties will be discussed. In LPCMO, we will highlight the subtle balance between coexistence of ferromagnetic metal (FMM), charge ordered insulator (COI) phases that are highly sensitive to strain and dimensionality. New insights into the mechanism of field driven and temperature driven conversion of the COI and FMM phase, and how this process is affected by low dimensionality in nanostructructed oxides, will be discussed.

This research is in collaboration with David Mandrus (Oak Ridge National Lab) and Sang-Wook Cheong (Rutgers University).

*Work at USF supported by the US Department of Energy and Army Research Office.

CO-EXISTENCE OF MOBILE AND LOCALIZED CHARGE CARRIERS IN COLOSSAL MAGNETORESISTIVE MANGANITES

Anjan Gupta

Indian Institute of Technology, Kanpur
Email: anjankg@iitk.ac.in

The coupling of charge, lattice and spin degrees of freedom in CMR manganites gives rise to a number of phases and some very intriguing physics. The electrons in manganites get trapped into local lattice distortions due to the Jan-Teller electron-lattice coupling giving rise to small polarons. The polaronic signatures are seen in the activated nature of the bulk transport and also as a suppression of spectral weight near the Fermi energy in different spectroscopic measurements. With the onset of ferromagnetic ordering with cooling the polaron mobility is enhanced due to the Zener double exchange, which leads to the well known CMR behavior. In the tunneling spectra of a number of epitaxial CMR manganite thin films we find a pseudogap which becomes more pronounced with cooling, in the metallic phase. While the density of states (DOS) at Fermi energy is found to increase with cooling, which is consistent with the bulk insulator-metal transition but inconsistent with the pseudogap enhancement. Similarly in charge-ordered manganite films we find a more robust gap but with some states near the Fermi energy. We discuss these findings in terms of two types of coexisting carriers in manganites.

BORN EFFECTIVE CHARGES, SPONTANEOUS POLARIZATION AND OPTICAL PROPERTIES OF BISMUTH TITANATE FROM FIRST-PRINCIPLES

R. Prasad

Department of Physics, Indian Institute of Technology, Kanpur
Email: rprasad@iitk.ac.in

Bismuth titanate ($Bi_4Ti_3O_{12}$ or, BiT), a ferroelectric perovskite oxide, has received tremendous attention, especially in thin film form, due to its promise in nonvolatile ferroelectric random access memory applications. BiT has a reasonably large spontaneous polarization (P_s), a high Curie temperature (948 K), low processing temperature (< 700°C) in thin film form, lead (Pb) free nature, fatigue resistance with lanthanide doping on Pt electrodes and low permittivity. These attributes make this material suitable for various applications *e.g.* memories, piezoelectric devices and electro optic devices.

Here, we present the results of our first-principles calculations of the band structure, density of states, the Born effective charge tensors and optical properties for the ferroelectric (ground state *B1a1*) and paraelectric (*I4/mmm*) phases of bismuth titanate. The calculations are done using the generalized gradient approximation (GGA) as well as the local density approximation (LDA) of the density functional theory. In contrast to the literature, our calculations on *B1a1* structure using GGA and LDA yield smaller indirect band gaps as compared to the direct band gaps, in agreement with the experimental data. The density of states shows considerable hybridization among Ti 3*d*, Bi 6*p* and O 2*p* states indicating covalent nature of the bonds leading to the ferroelectric instability. The Born effective charge tensors of the constituent ions for the ground state (*B1a1*) and paraelectric (*I4/mmm*) structures were calculated using the Berry phase method. This is followed by the calculation of the spontaneous polarization for the ferroelectric *B1a1* phase using the Born effective charge tensors of the individual ions. The calculated value for the spontaneous polarization of ferroelectric bismuth titanate using different Born effective charges was found to be in the range of 55±13 μC/cm^2 in comparison to the reported experimental value of (50±10 μC/cm^2) for single crystals. The origin of ferroelectricity is attributed to the relatively large displacements of those oxygen ions in the TiO_6 octahedra that lie along the *a*-axis of the bismuth titanate crystal.

INFLUENCE OF ELECTRONIC STRUCTURE ON FERROIC PROPERTIES OF SOLIDS

RATNAMALA CHATTERJEE

Magnetics & Advanced Ceramics Laboratory,
Physics Department, I.I.T Delhi, Hauz-Khas, N.Delhi-110016
Email: rmala@physics.iitd.ac.in

Among the solids of today "multiferroic" materials hold a special place. This broad topic encompasses various categories of materials that show more than one ferroic properties, viz., ferroelsatic / ferroelectric / ferromagnetic. *Magnetoelectric materials, ferromagnetic shape memory alloys* etc. fall under this category. In this context, I would discuss two recent results of interest obtained by our lab that depict the effect of electronic structure of materials on (i) magnetoelectric coupling and (ii) ferroelsaticity of materials.

(i) Magnetoelectric effect caused by interfacial bonding in Fe-implanted $BaTiO_3$ crystal - we experimentally demonstrate (see Fig.1) the magnetoelectric effect in a multilayered structure of Fe-$BaTiO_3$-Fe, with ~ 70 Å $BaTiO_3$ (BT) sandwiched between 2 layers of implanted Fe which was further treated by swift heavy ion (Ag^{+15}) induced ion beam mixing/annealing. Due to this specific experimental procedure, condition of atomic orbital overlap between the Fe and Ti atoms could be favored and the Fe-implanted BT crystal shows an ME effect arising from interfacial bonding at Fe/BT interface, as theoretically proposed by Duan *et al.*[1]

(ii) Control of magnetic field induced strain in Ni-Mn-Ga by twin-boundary motion of martensitic variants -interrelation of magnetic and structural subsystems in these alloys leads to unusual magnetoelastic and thermoelastic properties observed in them. Magnetic field induced

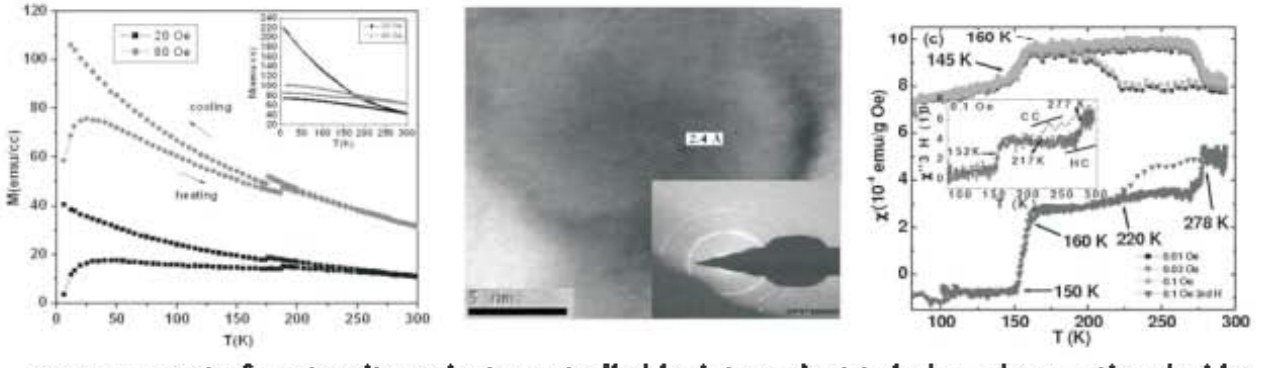

rearrangement of martensite variants controlled by intervariant twin-boundary motion decides the amount of magnetic field induced strain (MFIS) in the Ni-Mn-Ga alloys. Through the results of fundamental & third order *ac* susceptibility measurements in a $Ni_{48}Mn_{29}Ga_{22}$ single crystal we demonstrate[2] that the magnetic subsystem in Ni-Mn-Ga is unstable at low temperatures not only for metastable modulated crystal structure, but also for very stable nonmodulated tetragonal structure, leading to ~6% MFIS in this Heusler alloy single crystal.

REFERENCES

1. C. G. Duan, S. S. Jaswal and E. T. Tsymbol, Phys. Rev. Lett. 97, 047201 (2006).
2. S. K. Srivastava, V. K. Srivastava, A. Joshi, P. Kamasa, L. K. Varga, V. V. Khovaylo and R. Chatterjee, Appl. Phys. Lett. 97, 122505 (2010)

MAGNONS AND SPINONS IN THE TWO-CHAIN SPIN LADDER : THEORY AND EXPERIMENTS IN BPCB

B. Normad

Renmin University, Beijing, China
Email: bruce.normand@gmail.com

While many properties of the two-chain spin ladder were computed theoretically in the 1990s, experimental studies are catching up only now, because of the organometallic compound (C_5H_12N)_2CuBr_4 (BPCB). In this quasi-one –dimensional system of unfrustrated ladder units, whose energy scales match laboratory magnetic fields, it is possible to investigate quantum disordered, quantum critical, spin Luttinger-liquid, 3D magnetically ordered and fully saturated phases. This presentation reviews the range of experiments performed on BPCB, and introduces a complete bond-operator theory which describes with quantitative accuracy both thermodynamic properties and dynamical excitations at all fields and temperatures in the gapped regime. The field-tuned spinon continuum in the gapless regime, seen beautifully in experiment, is described with similar accuracy at zero temperature using a Bethe-Ansatz method.

FRACTIONAL SPIN TEXTURES IN THE FRUSTRATED MAGNET SCGO

KEDAR S. DAMLE

Department of Condensed Matter Physics,
Tata Institute of Fundamental Research, Mumbai, India
Email: kedar@theory.tifr.res.in

We consider the archetypal frustrated antiferromagnet $SrCr_9Ga_{12}O_{19}$ in its well known spin-liquid state, and demonstrate analytically that a Cr^{3+} S=3/2 ion is direct proximity to a pair of vacancies (in disordered p<1 samples) is cloaked by a spatially extended spin texture that encodes the correlations of the parent spin-liquid. In the spin-liquid regime, the combined object has a magnetic response identical to a classical spin of length S/2=3/4, which dominates over the small intrinsic susceptibility of the pure system. This fractional-spin texture leaves an unmistakable imprint on the measured[71] Ga nuclear magnetic resonance (NMR) lineshapes, which we compute using Monte-Carlo simulation and compare with experimental data.

*Collaborators:ArnabSenand RoderichMoessner

REFERENES

1. arXiv:1007.4507, submitted to Phys.Rev.Lett.

MACROSCOPIC ENTANGLEMENT NEAR QUANTUM PHASE TRANSITIONS

V. Subrahmanyam

Department of Physics,Indian Institute of Technology, Kanpur 208016, India.
E-mail:vmani@iitk.ac.in

Quantum entanglement between two parts of a system is measured by the von Neumann entropy of the subsystem. Entanglement between two spatially-distinct blocks of a system does not have a thermodynamic limit, as the block entropy scales logarithmically with the system size. Thus, this entanglement cannot describe quantum phase transitions and the associated thermodynamic singularity.

Here we will discuss a Multi-Species entanglement which is defined for a bipartite system as the entanglement between different species of particles. It is shown to exist in the thermodynamic limit of the system size going to infinity.

This macroscopic entanglement, as it can exhibit singular behavior, is capable of tracking quantum phase transitions. The entanglement between up and down spins has been analytically calculated for the one-dimensional Ising model in a transverse magnetic field, a prototypical model of quantum phase transitions and critical phenomena. As the coupling strength is varied, the first derivative of the entanglement shows a jump discontinuity and the second derivative diverges near the quantum critical points.

SCANNING TUNNELING SPECTROSCOPY OF SUPERCONDUCTING SILICON AND DIAMOND

H. Courtois[1], F. Dahlem[1], O. A. Williams[2], T. Kociniewski[3], P. Achatz[1], J. Boulmer[3], D. Débarre[3], C. Marcenat[2], C. Winkelmann[1], E. Bustarret[1]

[1]*Institut Néel, CNRS & Université Joseph Fourier, 25 avenue des Martyrs, 38042 Grenoble, France*
[2]*Institute for Materials Research, Hasselt University, Wetenschapspark 1, B-3590 Diepenbeek, Belgium*
[3]*Institut d'Electronique Fondamentale, CNRS and Université Paris Sud, 91405 Orsay, France*
[4]*CEA, Institut Nanosciences et Cryogénie, SPSMS-LATEQS, 17 rue des Martyrs, 38054 Grenoble, France*
Email : Herve.Courtois@grenoble.cnrs.fr

Heavily doped group IV covalent semiconductors [1] constitute a new family of superconductors as a low-temperature superconductivity has been recently discovered in boron-doped silicon and in diamond. The evolution of the critical temperature versus boron doping is different in these two materials, raising the general question of nature of their superconductivity. As a unique tool of investigation, our milliKelvin scanning tunneling microscope (STM) [2] can bring important contributions to this question.

In my talk, I will review our recent experiments on superconducting doped semiconductors. We performed the first tunneling spectroscopy of superconducting heavily boron-doped silicon, which shows the conventional (BCS) nature of its local superconductivity (Fig. 1, [3]). In polycrystalline boron-doped diamond thin films, our scanning tunneling spectroscopy study demonstrates the strong correlation between the local superconductivity strength and the granular structure of the films (Fig. 2,[4].

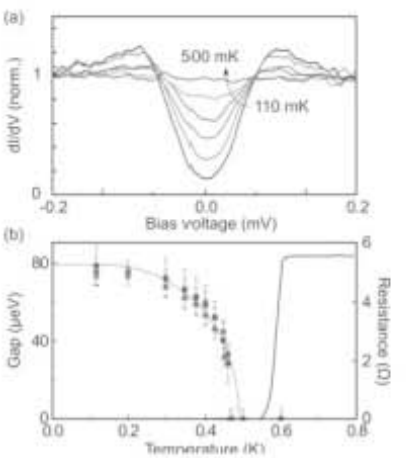

Fig. 1: a) Differential conductance dI/dV spectra in heavily boron-doped silicon at 110; 350; 425; 440; 460 and 500 mK. b) Left axis: local superconducting gap at three different positions (▽, ▽, ▽). The dotted line is a fit to the BCS model. Right axis: macroscopic superconductive resistive transition.

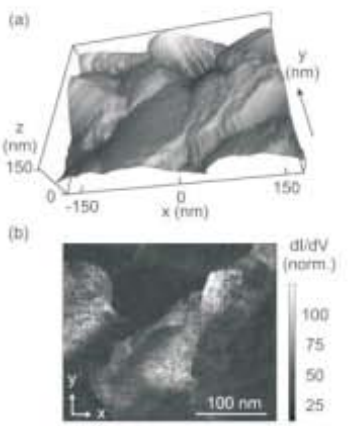

Fig. 2: a) Scanning tunneling topography on boron-doped polycrystalline diamond film showing faceted granular morphology. b) Local differential conductance image acquired simultaneously.

REFERENCES

1. X. Blase, E. Bustarret, C. Chapelier, T. Klein and C. Marcenat, Nature Materials 8, 375 (2009).
2. N. Moussy, H. Courtois and B. Pannetier, Review of Scientific Instruments 72, 128 (2001); A.K. Gupta, L. Crétinon, N. Moussy, B. Pannetier and H. Courtois, Physical Review B 69, 104514 (2004).
3. F. Dahlem, C. Marcenat, L. Pascal, P. Achatz, T. Klein, J. Boulmer, T. Kociniewski, D. Débarre, E. Bustarret and H. Courtois, Physical Review B Rapid Communications, to appear (2010).
4. F. Dahlem, P. Achatz, O. A. Williams, D. Araujo, E. Bustarret and H. Courtois, Physical Review B 82, 0333006 (2010).

SUPERCONDUCTIVITY IN MATERIALS WITHOUT INVERSION SYMMETRY: SIMPLE VS. CORRELATED SYSTEMS

E. Bauer[1], F. Kneidinger[1], R.T. Khan[1], G. Hilscher[1], H. Michor[1], E. Royanian[1], E.-W. Scheidt[2], K. Miliyanchuk[3], C. Blaas-Schenner[3], D. Reith[3], N. Melnychenko-Koblyuk[3], R. Podloucky[3], P. Rogl[3]

[1]*Institute of Solid State Physics, Vienna University of Technology, A-1040 Wien, Austria*
[2]*Chemische Physik und Materialwissenschaften, Universität Augsburg, D-86159 Augsburg,Germany*
[3]*Institute of Physical Chemistry, University of Vienna, A-1090 Wien, Austria*
Email: bauer@ifp.tuwien.ac.at

Superconductors missing a centre of symmetry in the crystal structure are subject to peculiar band splitting, which is detrimental to certain kinds of Cooper pairing channels. In particular, spin triplet pairing was claimed to become unlikely under such circumstances. Ternary $CePt_3Si$ is the first representative of heavy fermion superconductors without inversion symmetry (T_c = 0.75 K, T_N = 2.2 K), however, distinguished by a SC order parameter which is composed of spin-singlet and spin-triplet components, assuring extraordinarily large upper critical field values.

In the present work, experimental and theoretical findings made on strongly correlated electron system $CePt_3Si$ are discussed and compared with novel Ba, Sr and Mo based superconductors which miss both, inversion symmetry and strong electron correlations. These preconditions set the stage for reliable electronic structure calculations, which prove the splitting of electronic bands due to missing inversion symmetry.

This work was supported by the Austrian FWF P22295

$K_2Cr_8O_{16}$: AN UNSUAL EXAMPLE OF A CHARGE ORDERED FERROMAGNET

Priya Mahadevan,[1] Abhinav Kumar,[1] Debraj Choudhury,[2] D.D. Sarma[2]

[1]*Department of Material Science, S. N. Bose National Centre for Basic Sciences, Kolkata-700098*
[2]*Solid State and Structural Chemistry Unit, Indian Institute of Science, Bangalore 560012*
Email: sarma.dd@gmail.com

$K_2Cr_8O_{16}$, a recently1 explored member of the Hollandite series, exhibits many unusual behaviors, which are still not fully understood. It undergoes a paramagnetic to ferromagnetic transition at about 180 K. The system has an unusual half metallic ferromagnetic state at higher temperatures and an intriguing metal-to-insulator transition (MIT) on cooling below ~95 K. This MIT appears to have only a subtle influence on the magnetization, giving rise to a less common example of a ferromagnetic insulating ground state. These unusual properties raise many questions concerning the origin of the magnetism in the insulating and the metallic states of this compound.

Analyzing the electronic and magnetic properties within first principle electronic structure calculations, we find2 that K acts like a donor. The doped electrons associated with the introduction of K in the lattice, induces a charge ordered and insulating ground state and interestingly also introduces a ferromagnetic coupling between the Cr ions. The primary considerations driving the charge ordering are found to be electrostatic ones with the charge being localized on two Cr atoms that minimize the electrostatic energy. The structural distortion that accompanies the ordering, generates a pathway for the electron localized on one site to hop on to the neighboring sites, a process more favorable in the ferromagnetic case, thus, giving rise to a rare example of a charge-order driven ferromagnetic insulator.

We thank Profs. A. Chainani, O. Karis T. Konishi, Y. Ohta, and Y. Ueda for valuable discussions and for sharing unpublished results.

REFERENCES

1. Kunihiro Hasegawa et al., Phys. Rev. Lett. 103, 146403(2009).
2. Priya Mahadevan, Abhinav Kumar, Debraj Choudhury and D.D. Sarma, Phys. Rev. Lett. 104, 256401 (2010).
3. O. Tamada et al., J. Solid State Chem. 126, 1 (1996)
4. M. Sakamaki, T. Konishi, and Y. Ohta, Phys. Rev. B 80, 024416 (2009).

QUANTUM CHARGE/SPIN FLUCTUATIONS OF CORRELATED ELECTRONS IN QUASI-TRIANGULAR LATTICE ORGANICS

Kazushi Kanoda

Department of Applied Physics, University of Tokyo, Bunkyo-ku, Tokyo 113-8656, Japan
Email: kanoda@ap.t.u-tokyo.ac.jp

Mott transition is a metal-insulator transition induced by electron-electron Coulomb interaction and essentially a phenomenon in the charge degrees of freedom. When the lattice is triangular, antiferromagnetically interacting spins suffer from geometrical frustration against ordering. So, the correlated electrons on triangular lattice in the vicinity of Mott transition are in an intriguing situation where both the charge and spin degrees of freedom possibly exhibit quantum fluctuations.

The family of layered organic conductors, κ-$(ET)_2X$, whose bandwidth is comparable with the Coulomb repulsive energy and controllable by pressure, are model systems of interacting electrons on anisotropic triangular lattice [1]. In this conference, I review our experimental study on κ-$(ET)_2X$ in the light of the above mentioned issues. First, I present the spin-liquid behavior [2], Mott transition [3] and superconductivity in κ-$(ET)_2Cu_2(CN)_3$ [4], which is a half-filled band system with nearly isotropic triangular lattice. Second, I show the magnetic characterization of the pressure-driven Mott criticality [5] in κ-$(ET)_2Cu[N(CN)_2]Cl$, which was previously studied by transport measurements [6]. Third, I report the anomalous magnetic and transport properties of the model systems of doped triangular lattices, κ-$(ET)_4Hg_{3-d}X_8$ [X=Br, Cl], and discuss the results in terms of doped-Mott insulator, which is possibly a doped spin liquid [7].

This presentation is based on the work in collaboration with K. Miyagawa, Y. Shimizu, F. Kagawa, Y. Kurosaki, T. Furukawa, H. Hashiba, H. Oike, H. Kasahara, H. Taniguchi, S. Yamashita, Y. Nakazawa, M. Maesato and G. Saito.

REFERENCES

1. K. Kanoda, Hyperfine Interactions **104** (1997) 235; Physica C **282-287** (1997) 299; J. Phys. Soc. Jpn. **75** (2006) 051007.
2. Y. Shimizu *et al.*, Phys. Rev. Lett. **91** (2003) 107001 ; Y. Shimizu et al., Phys. Rev. B **73** (2006) 140407; S. Yamashita *et al.*, Nature Phys. **4** (2008) 459.
3. Y. Kurosaki *et al.*, Phys. Rev. Lett. **95** (2005) 177001.
4. Y. Shimizu *et al.*, Phys. Rev. B **81** (2010) 224508.
5. F. Kagawa *et al.*, Nature Phys. **5** (2009) 880.
6. F. Kagawa *et al.*, Nature **436** (2005) 534
7. H. Oike *et al.*, Physica B 404 (2009) 376 and unpublished.

DISORDER, MAGNETISM AND TRANSPORT IN THE DOUBLE PEROVSKITES

Pinaki Majumdar

Harish-Chandra Research Institute, Allahabad
Email: pinaki@mri.ernet.in

The double perovskits are well known for highTc ferromagnetic phases. The bulk magnetic state and transport depends sensitively on preparative conditions due to the presence of antisite disorder. I will discuss the impact of disorder on the ferromagnetic state and move on to possible antiferromagtnetic phases in these materials. The antiferro phases seem to survive disorder better than the ferromagnetic phase, and also exhibit an unusual large positive magnetoresistance.

MAGNETISM AND SUPERCONDUCTIVITY OF PURE AND DOPED $EuFe_2As_2$

ANUPAM[1], P.L. PAULOSE[2], H. JEEVAN[3], C. GEIBEL[3] Z. HOSSAIN[1]

[1]Department of Physics, IIT Kanpur, Kanpur-208016, India
[2]T.I.F.R, Homi Bhabha Road, Mumbai-400 005, India
[3]Max Planck Institute for Chemical Physics of Solids, 01187 Dresden, Germany
Email: zakir@iitk.ac.in

Superconductivity in iron arsenide compounds is a subject of intense discussion in the scientific community. First iron-arsenide based high temperature superconductor was discovered in F-substituted LaOFeAs with a transition temperature at 26 K [1]. Followed by this four more Fe-based series of compounds were found. Our main interest is in $EuFe_2As_2$ which has a very special place in AFe_2As_2 (A =Ba, Sr, Ca, Eu) series due to the large magnetic moment of Eu2+ (H≈7μB) ions in this compound and hence is an ideal candidate to investigate the interplay between superconductivity and magnetism. This compound exhibits Spin density wave (SDW) transition associated with Fe-moments at 190 K and an antiferromagnetic ordering of Eu2+ ions at 19 K [2]. The SDW transition can be suppressed or weakened either by applying hydrostatic pressure or by chemical pressure which induce superconductivity in this system. We found that 50% potassium doping in $EuFe_2As_2$ leads to the suppression of SDW transition and give rise to superconductivity below 33 K [3, 4]. 151Eu Mössbauer spectroscopy provide clear evidence for the coexistence of short range ordering of the Eu moments with the superconducting state. Superconducting transition temperature decreases for both under K-doped and over K-doped samples with maximum Tc for 50% K-doped sample and hence show a dome type T-x phase diagram similar to high Tc cuprates. Ni doping at iron site destroys the spin density wave and antiferromagnetic transition completely and giving rise to ferromagnetism below 18 K [5]. Our results on 5 % Ni doped $EuFe_2As_2$ exhibit ferromagnetic ordering below 16 K and suppression of SDW transition as confirmed by 57Fe Mössbauer studies. We tried to dope antimony at arsenic site which has larger ionic radii and hence could mimic negative pressure on the lattice. We found that only 5 – 10 % of antimony could go inside the lattice which has no significant influence on the SDW or Eu ordering.

REFERENCES

1. Y. Kamihara, T. Watanabe, M. Hirano, and H. Hosono, J. Am. Chem. Soc. 130, 3296 (2008).
2. H. S. Jeevan, Z. Hossain, Deepa Kasinathan, H. Rosner, C. Geibel, and P. Gegenwart, Phys. Rev. B 78, 052502 (2008).
3. H. S. Jeevan, Z. Hossain, Deepa Kasinathan, H. Rosner, C. Geibel, and P. Gegenwart, Phys. Rev. B 78, 092406 (2008).
4. Anupam, P L Paulose, H S Jeevan, C Geibel and Z Hossain, J. Phys.: Condens. Matter 21, 265701 (2009).
5. Zhi Ren, Xiao Lin, Qian Tao, Shuai Jiang, Zengwei Zhu, Cao Wang, Guanghan Cao, and Zhu'an Xu, PRB 79, 094426 (2009).

SUPERCONDUCTIVITY IN THE $Fe_{1+y}Te_{1"x}Se_x$ SYSTEM: ELUCIDATION OF THE ROLE OF EXCESS Fe

P. L. Paulose+ and C. S. Yadav

Department of Condensed Matter Physics and Materials Science, Tata Institute of Fundamental Research, Mumbai 400005, India.

+E-mail: paulose@tifr.res.in

The recent discovery of iron based superconductors has brought alive the possibility of magnetic spin fluctuation mediated pairing mechanism for superconductivity [1-8]. A common feature observed in the Fe pnictides or chalcogenides is the gradual emergence of the superconductivity when the antiferromagnetic order associated with the Fe-X (X=As/Te) layers is weakened by doping. It has been suggested that in this class of materials the magnetic moments may be soft and depend sensitively on various physical details, which contrasts with the strongly correlated local behavior found in cuprates. $Fe_{1+y}Te$ has a tetragonal anti-PbO type structure and forms in the nonstoichiometric form (0.05 d" y d" 0.22) with the excess iron atoms Fe(2), occupying the octahedral positions randomly. The Fe(2) directly couples to the four nearest neighbour Fe(1) atoms in the Fe planes and could effectively introduce frustration in the underlying antiferromagnetic state as Te is gradually substituted by Se and could lead to a large critical region [9]. It has also been suggested that the excess Fe bearing a local moment in proximity to the Fe layers could offer an interesting opportunity for experimental investigation of the interplay between superconductivity and pair breaking magnetic scattering in the Fe superconductors [10]. A comparative study of the chalcogenide system $Fe_{1.1}Te_{1-x}Se_x$ and the stoichiometric $FeTe_{1-x}Se_x$ is carried out to understand the role of the excess Fe in modifying the superconducting state. The $Fe_{1.1}Te_{1-x}Se_x$ (0 d" x d" 0.55) series is found to be magnetic and its microscopic properties are investigated through Mössbauer spectroscopy. The detailed magnetic phase diagram of $Fe_{1.1}Te_{1-x}Se_x$ reveals the emergence of spin glass state when the antiferromagnetic state is destabilized by the Se substitution. The isomer shift and quadrupolar splitting obtained from the Mössbauer spectroscopy clearly brings out the electronic differences in these two series. There is a clear indication of well developed local moment on Fe network due to the presence of Fe(2), while the stoichiometric series $FeTe_{1-x}Se_x$ display bulk superconductivity with no magnetic ordering. Moreover, the Fe moment and the spin density wave state are drastically affected by the Se substitution and it drives the system to a spin glass state. The magneto transport studies show that there is a strong modification of the electronic state in the stochiometric superconducting state vis-à-vis the nonstoichiometric magnetic system.

REFERENCES

1. Kamihara Y. *et. al.*, *J. Am. Chem. Soc.* **128** (2006) 10012.
2. Kamihara Y. *et. al.*, *J. Am. Chem. Soc.* **130** (2008) 3296.
3. Chen X. H *et. al.*, *Nature* **453** (2008) 761.
4. Chen G. F. *et. al.*, *Phys. Rev. Lett.* **100** (2008) 247002.
5. Ren Zhi-An *et. al.*, *Europhys. Lett.* **83** (2008) 17002.
6. Hsu F. C. *et. al.*, *Proc. Natl. Acad Sci. U.S.A.* **105** (2008) 14262.
7. Fang M. H. *et. al.*, *Phys. Rev. B* **78** (2008) 224503.
8. Sales B. C. *et. al.*, *Phys. Rev. B* **79** (2009) 94521.
9. Fang Chen et al., *Europhys. Lett.* **86** (2009) 67005
10. Zhang L. *et. al.*, *Phys. Rev. B* **79** (2009) 012506.

RECENT ADVANCES IN OXIDES AND OXIDE INTERFACES

T. VENKATESAN

NUSNNI-NanoCore, NUS Singapore
Email: venky@nus.edu.sg

In my talk I will give a progress report on several research fronts in the area of oxide and oxide interfaces being pursued at NanoCore.

The first is the area of diluted magnetic semiconducting oxides where we have seen room temperature ferromagnetism in Ta doped TiO_2. The ferromagnetism is seen in a variety of measurement techniques besides SQUID such as SXMCD, OMCD and also spin polarized photoemission. The origin of the ferromagnetism is shown to arise from cationic defects based on XAS Measurements.

The second area is that of the quasi 2D electron gas seen at the interface of LAO/STO and we show that under special processing conditions, the presence of electronic phase separation with the observation of a variety of magnetic and electronic phases co-existing at the interface.

The third area of interest is the novel concept of 'Nonlinear Insulators' where the defect states in the band gap of oxide insulators provide a way for multiple conductivity states to exist based on the bias currents and voltages. We demonstrate these ideas in resistive switching devices and argue that a large number of oxide insulators (with predominant ionic bonding) fall under the class of "nonlinear insulators" and are not ideal insulators.

MAGNETOTRANSPORT STUDY OF $LaAlO_3/SrTiO_3$ INTERFACES :SPIN ORBIT INTERACTION AND PHASE COHERENT EFFECTS

M. Ben Shalom, D. Rakhmilevitch, A. Palevski, and Y. Dagan*

Raymond and Beverly Sackler School of Physics and Astronomy,
Tel-Aviv University, Tel Aviv 69978, Israel .
Email: yodagan@post.tau.ac.il

The conducting interface formed between $LaAlO_3$ and $SrTiO_3$, which are both non-magnetic and insulating perovskites, unexpectedly exhibits: two dimensional electron gas (2DEG) properties, superconductivity, and possibly magnetic properties. Electric field-induced metal-insulator transition was reported for a layer of $LaAlO_3$ which is thicker than three lattice unit cells. However, the origin of the charge carriers and the thickness of the conducting layer are still under debate.

By applying gate voltage we varied the charge carrier density and the properties of the 2DEG. At low temperatures, the superconducting ground state and T_c can be tuned. The magnetoresistance and Hall Effect are studied for various devices and configurations.

The spin-orbit coupling energy is evaluated as a function of gate voltage. Our results suggest that this interaction plays a dominant role at this interface and may be useful for future oxide based devices, controlling the orbital motion of electrons by acting on their spins.

Using a mesoscopic size device we were able to extract the phase coherence length, L_j. Its temperature dependence suggests that the phase-loss processes are governed by electron-electron interactions.

Finally, Shubniklov-de Haas oscillations at high fields measured along with the Hall resistivity. We fit the data assuming multiple carrier contributions. The comparison between the mobile carrier density inferred from the Hall data and the oscillation frequency suggests multiple valley and spin degeneracy. The small amplitude of the oscillations is discussed within this multiple-band scenario.

INTERLAY OF QUANTUM CRITICALITY AND GEOMETRIC FRUSTRATION IN COLUMBITE

Ribhu Kaul

Department of Physics & Astronomy, 177 Chemistry-Physics Building, 503 Rose Street
University of Kentucky, Lexington, KY 40506-0055
Email: rkk@pa.uky.edu

$CoNb_2O_6$ is a remarkable material. It consists of Ising chains that are coupled in a frustrated anisotropic triangular lattice in the basal plane perpendicular to the chain direction. Applying a strong transverse ûeld tunes the chains through a quantum phase transition into a paramagnetic phase. The interplay between two interesting features of correlated quantum physics, quantum criticality and geometric frustration, produces a rich phase diagram which reflects the fundamental underlying quantum many-body physics.

BOND-OPERATOR FORMALISM FOR SPIN-S DIMERIZED QUANTUM ANTIFERROMAGNETS

Brijesh Kumar

School of Physical Science, Jawaharlal Nehru University, New Delhi
Email: bkumar@mail.jnu.ac.in

The bond operator formalism for spin ½ dimmer problems is generalized to the case of arbitrary spin-S. A low energy mean-field theoretic framework, restricted to triplet excitations (also including quintets in some cases), is developed for studying the dimerized singlet phases. It is applid to some model problems and some real materials. An interesting result from this approach for a system of coupled dimmers interacting via exchange interactions is that under strong frustration the quantum mechanical dimmer phase can survive even in the so called classical limit $S \rightarrow \infty$. That is S being infinite is not necessarily classical. In another application, the tripplon dispersion is calculated for $Bi_2Fe_4O_9$ which is a spin -5/2 Heisenberg problem on dual Shastry-Sutherland lattice. More problems are being investigated using this approach.

STATE-OF-THE-ART SUPERCONDUCTING QUANTUM INTERFERENCE DEVICES FOR INVESTIGATING QUANTUM EFFECTS AT VERY LOW TEMPERATURES

THOMAS SCHURIG

Physikalisch-Technische Bundesanstalt Braunschweig und Berlin
Abbestraße 2-12, D-10587 Berlin, Germany
Email: thomas. schurig@ptb.de

The investigation of quantum effects at low and ultra-low temperatures often requires a very sensitive measurement of weak magnetic fields, small electric currents or voltages. Since its first application more than 30 years ago, Superconducting Quantum Interference Devices (SQUIDs) have been proven as very attractive tools for detecting physical quantities which can be converted to magnetic flux with a very low noise level. Apart from the biomedical applications which are dominated by large multi-channel systems in combination with more or less heavily magnetically shielded rooms, SQUID setups for material research at very low temperatures require very sophisticated sensors tailored to the particular experiment. It is, for example, not straightforward to utilize a sensor operating in liquid helium at 4 K for an experiment installed in a millikelvin-refrigerator. Especially, the novel cryogen-free millikelvin refrigerators employing pulse-tube pre-cooling require robust SQUID sensor systems including careful SQUID wiring and filtering. We are developing and manufacturing ultra-sensitive SQUID sensors for various applications at low or high frequencies.

SQUID arrays for the fast read-out of superconducting radiation detectors, e.g. super-conducting single photon detectors, have been made available. With our two-stage SQUID current sensors for experiments where a high energy resolution is required, as e.g. in NMR experiments, a coupled energy resolution of 40 h at 4 K and 4 h below 300 mK can be obtained (h is Planck's constant). Integrated micro-coil input coils can be used as local probes for quantum matter and systems in the micro or nano scale. Nevertheless, contrary to the predicted decrease of flux-noise spectral density with decreasing temperature, we observe an increase of the low-frequency flux noise even in the kHz range when operating our devices at mK temperatures. This behaviour, which is generally observed, is currently under investigation.

The thermal noise limited SQUID sensitivity can be reduced by shrinking the SQUID dimensions, resulting in lower SQUID inductance and capacitance. Whereas micro-sized SQUIDs and SQUID susceptometers can be designed and manufactured employing conventional Nb/AlOx/Nb junctions, for real nanoSQUIDs another junction technology has to be developed. Even so the readout of those nanoSQUIDs is complicated. Above-mentioned SQUID current sensors can be utilized for this purpose.

QUANTUM CRITICALITY AND SUPERCONDUCTIVITY IN SPIN AND CHARGE SYSTEMS

Siddharth S Saxena

Cavendish Laboratory, University of Cambridge, Cambridge, UK. &
Centre for Materials and Microsystems, Fondazione Bruno Kessler, Trento, Italy.

This talk will focus on experimental search and discovery of novel forms of quantum order in metallic and insulating magnets, intercalated compounds, ferroelectric systems and multi-ferroic materials. Particularly discussed will be the pressure-induced superconductivity and critical phenomena in the vicinity of quantum phase transitions.

Materials tuned to the neighbourhood of a zero temperature phase transition often show the emergence of novel quantum phenomena. Much of the effort to study these new emergent effects, like the breakdown of the conventional Fermi-liquid theory in metals has been focused in narrow band electronic systems. But Spin or Charge ordered phases in insulating systems can also be tuned to absolute zero using hydrostatic pressure. Close to such a zero temperature phase transition, physical quantities like resistivity, magnetisation and dielectrics constant change into radically unconventional forms due to the fluctuations experienced in this region giving rise to new kinds ordered states including superconductivity in the metallic systems.

BAND TOPOLOGY IN CORRELATED SOLIDS

Ashvin Vishwanath

University of California, USA
Email: ashvinv@socrates.berkeley.edu

I discuss the prospects for realizing topological insulators in correlated systems, particularly in 5d based transition metal oxides. In addition to topological band insulators, other interesting phases such as magnetic topological insulators, with a large 'theta' parameter may be realized. In the pyrochlore iridates, we predict a novel topological phase with magnetical order and a semi-metallic Dirac spectrum in the bulk. Here, surface states in the form of Fermi arcs appear that cannot be realized in any two dimensional band structure.

KONODO EFFECT AND RKKY INTERACTIONS IN THE KITAEV MODEL

Vikram Tripathi

Tata Institute of Fundamental Research, Mumbai
Email: vtripathi@theory.tifr.res.in

We study the effect of coupling magnetic impurities to the spin ½ Kitaev model in its gapless spin liquid phase. We show that a spin-S impurity coupled to the Kitaev model is associated with an unusual Kondo effect with an intermediate coupling unstable fixed point $K_ {c}\sim J/S$ separating topologically distinct sectors of the Kitaev model. We also show that the massless spinons in the spin liquid mediate a nondipolar interaction noted in various 2D impurity problems with a pseudogapped density of state of the spin bath.

Furthermore, this long-range interaction is possible only if the impurities (a) couple to more than one neighboring spin on the host lattice and (b) the impurity spin $S/ne1 ½.$.

QUANTUM HALL STATES IN NON-ROTATING OPTICAL LATTICES

Syed Hassan

Institute of Mathematical Sciences, Chennai
Email: shassan@imsc.res.in

We analyse the physics of cold atoms in honeycomb optical lattices with spin dependent hopping and onsite repulsion. We note the spin dependent hopping terms are not time-reversal invariant. For a region in space of hopping parameters, the four bands do not overlap and carry non zero Chern numbers. Consequently, the non-interacting system has a quantized anomalous Hall conductivity at ¼ and ¾ filling. We have investigated the effects of the interactions using the Variational cluster perturbation theory (VCPT) and conclude that the quantum Hall state exists in finite region of the interaction and hopping parameter space. The chiral edge states may provide an experimental signature of these states.

SUPERFLUID INSULATOR TRANSITION FOR ULTRACOLD BOSONS IN A SYNTHETIC MAGNETIC FIELD

K. Sengupta

Indian Association for the Cultivation of Science, Jadavpur, Kolkata
Email: ksengupta1@gmail.com

In this talk, I am going to discuss the physics of the superfluid-insulator (S) transition of ultracold neutral bosonic atoms in a square 2D optical lattice and in the presence of a synthetic magnetic field created using Raman coupling of suitably tuned lasers with these bosons. We provide analytical expressions for a)momentum distribution in the Mott phase and b) collective modes in the superfluid phase of the bosons near the quantum critical point. We also construct an effective field Landau-Ginzburg theory for the SI transition and show that it necessarily involves q bosonic fields for a flux of 2\pi/q through the placquette of the lattice. The analysis of this action is shown to lead to a q periodic condensate density in the SF phase.

ROW FORMATION IN WEAKLY CONFINED QUANTUM WIRES

K.J. Thomas

Cavendish Laboratory, University of Cambridge, UK

When Coulomb repulsion between electrons is sufficiently strong to overcome the confinement potential of a one-dimensional quantum wire, the electrons adjust their positions to minimize energy by forming a zigzag lattice. Both quantum and classical calculations suggest that the zigzag will divide as the electron density increases or confinement weakens further, leading to the formation of two and then of progressively more rows of electrons, until the system approaches a regular two-dimensional lattice. I shall present experimental results on the formation of double rows in a weakly confined quantum wire[1].

REFERENCES

1. W. K. Hew, K. J. Thomas, M. Pepper, I. Farrer, D. Anderson, G. A. C. Jones and D. A. Ritchie, Incipient Formation of an Electron Lattice in a Weakly Confined Quantum Wire, Phys. Rev. Lett. 102, 056804 (2009).

EXPERIMENTAL DISCOVERY OF TOPOLOGICAL ORDER IN INSULATORS AND SUPERCONDUCTORS IN BULK SOLIDS

M. Zahid Hasan

Princeton University, USA
Email: mzhasan@princeton.edu

Topological insulators in bilk solids are a new phase of matter, which exhibit quantum-Hall like behavior even in the absence of an applied magnetic field and unlike the quantum Hall liquids can be turned into superconductors [1]. In this talk, I will briefly review the basic theory and experimental discovery of topoligcal insulators in bulk solids (3D) and related superconductors. I will then discuss spin-resolved phase-sensitive experimental results that demonstrate all the fundamental properties of topological insulators such as spin-momentum helical locking, non-trivial quantum Berrys phases, absence of spin backscattering or no U-turn, dissipationless spin flow, protection by time-reversal symmetry and the existence of room temperature topological order. I will also report the exotic roles of superconductivity and spin-order in doped topological insulators, electrodynamics and their potential applications.

REFERENCE

1. Topological Insulators M.Z. Hasan and C.L. Kan E;arXiv:1002.3895 [Rev.of Mod.Phys. {2010}].

REVISITING INSULATOR – METAL TRANSITION IN CORRELATED OXIDES: FERROMAGNETIC INSULATING STATE OF MANGANITES

A.K. Raychaudhuri

Department of Materials Science
S.N. Bose National Centre for Basic Sciences, JD Block,
Sector-III, Salt Lake, Kolkata-700 089
Email: arup@bose.res.in

The issue of insulator-metal transition in complex and correlated oxides have been a recurring theme of the physics of condensed matter physics for a long time. The fact different oxides which are seemingly different can show rather unifying behaviour when they show insulator metal transition which can be by correlation, disorder and band width, carrier concentration and other such parameters.

In this study we present investigation of a rather complex system where a ferromagnetic state co-exist with an insulating state which can be made metallic by agents like pressure. Such a state exists in Perovskite oxide manganites, generally known for their pressure. Such a state exists in Perovskite oxide manganites, generally known for their Colossal Magnetoresistance (CMR), at low hole concentration. This talk is an investigation into the ferromagnetic insulating (FMI) state to answer fundamental questions about the nature of the insulating state using a number of experimental investigations on single crystals of lightly hole doped manganites (that include non-linear conductance, high pressure experiments as well as noise measurements), it has been suggested that the insulating state is likely an electron glass.

ANOMALOUS MAGNETORESISTANCE IN Tb_5Si_3

E.V. Sampathkumaran

Tata Institute of Fundamental Research, Homi Bhabha Road, Mumbai-400 005
Email: sampathev@gmail.com

It is a well recognized fact that the sign of magnetoresistance (MR) is egative at the field-induced magnetic transitions. In contrast to this traditional belief, in a rare-earth based intermetallic compound, Tb_5Si_3, crystallizing in Mn_5Si_3 – type hexagonal structure, MR is found to be interestingly positive, irrespective of whether the transition is first-order or second order (with varying temperature). We invoke the concept of 'inverse metamagnetism' (in which magnetic fluctuations are introduced beyond the transition-field) to explain this. There are observations attributable to an unusual magnetic-phase-coexistence phenomenon, in which the transport interestingly is apparently dominated by high-resistive phase.

Sudden increase in positive MR at the "meta" magnetic transition in Tb_5Si_3 in the entire T-range below magnetic ordering (<69K), irrespective of whether the transition is first order or second order.

Mn_5Si_3 – type hexagonal structure

Poster Presentations

STUDY OF STRUCTURAL AND ELECTRICAL PROPERTIES OF SR DOPED $LaMnO_3$

HILAL AHMED, SHAKEEL KHAN

Department of Applied Physics, Aligarh Muslim University, Aligarh - 202002, India
Email: hilal.alig@gmail.com

We report the results of structural and electrical properties of $La_{0.67}Sr_{0.33}MnO_3$ prepared by solid-state reaction route and sol-gel methods respectively. The structural properties reveal that all the samples exhibit orthorhombic crystal symmetry. The average crystallite size for the samples prepared by both routes is found to be in the range of 21-22 nm. The resistivity data shows a metal-insulator phase transition for both the samples.

The rare earth manganites of the general formula $R_{1-x}A_xMnO_3$ (R = La, Nd, etc. and A = Sr, Ca, etc) have been widely investigated owing to their remarkable electrical and magnetic properties like metal-insulator transition (MIT), colossal magnetoresistance (CMR) and charge ordering (CO) etc. The parent compound RMnO3 is an antiferromagnetic (AFM) insulator. When parent compound is doped with one of the divalent cation such as Sr, Ca or Ba etc, a proportionate number of Mn^{3+} ions with electronic configuration $t_{2g}^3 e_g^1$ are replaced with Mn^{4+} ions having electronic configuration t_2g_3. This creates holes in the e_g band near Fermi energy. This behavior has been interpreted on the basis of Jahn-Teller (JT) effect [1]. The electrical properties have been examined on the basis of Double-Exchange (DE) model [2]. The samples of $La_{0.67}Sr_{0.33}MnO_3$ have been synthesized by two methods i.e. solid state (SS) reaction route [3] and sol-gel (SG) methods. The samples were characterized by x-ray diffraction (XRD) using Cu-Kα radiation of wavelength 1.5406Å. The resistivity of samples was measured by using standard four-probe technique in the temperature range 70-300K in a close cycle refrigerator.

The XRD patterns of $La_{0.67}Sr_{0.33}MnO_3$ samples have been taken at room temperature which show that all the samples are in single phase with orthorhombic crystal symmetry. The crystallite size determined from XRD data for both samples is shown in Table (1)

Table (1) Lattice parameters and crystallite size of both samples

Sample	a (Å)	b (Å)	c (Å)	Crystallite size (nm)
$La_{0.67}Sr_{0.33}MnO_3$(SS)	5.440	5.490	7.740	21.60
$La_{0.67}Sr_{0.33}MnO_3$(SG)	5.420	5.480	7.740	22.08

Figure (1) shows the temperature dependence of resistivity for $La_{0.67}Sr_{0.33}MnO_3$ samples. All the samples show metal-insulator transition (MIT) and the values of metal-insulator transition temperatures are respectively 136.39 K and 215.20 K.

where ρ_o arises due to the grain boundary scattering and plays a major role in the conduction process. On the other hand, ρ_2T_2 term explains the contribution of electron-electron scattering process to the resistivity, while the term $\rho_{4.5}T_{4.5}$ may be attributed to two-magnon scattering process in the ferromagnetic region. The typical plots by using eqn. (1) for both samples are shown in Fig. (2).

In the adiabatic approximation a small polaron hopping theory was proposed according to which the activated conduction follows the relation:

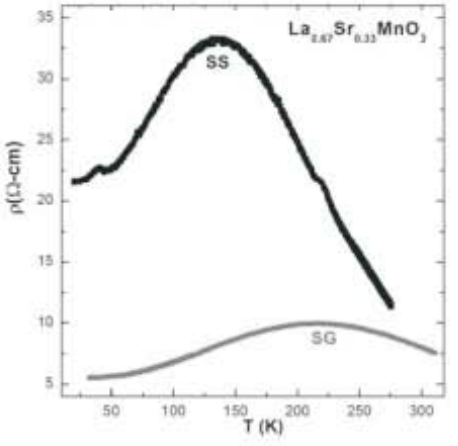

Fig. 1: Temperature dependence of resistivity for $La_{0.67}Sr_{0.33}MnO_3$

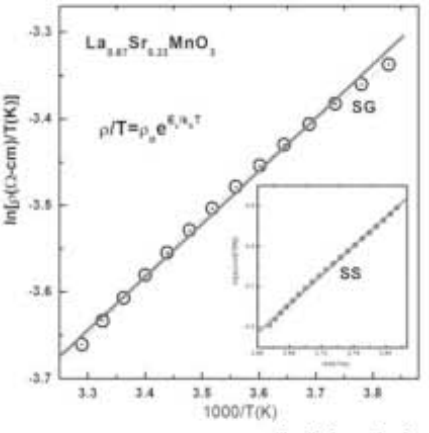

Fig.2: Low Temperature resistivity fitting

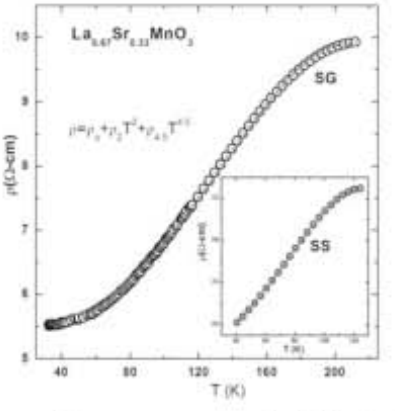

Fig. 3: High temperature resistivity fitting

$$\rho(T) = \rho\alpha T \exp(Ea/k_B T) \qquad (2)$$

where k_B is Boltzmann constant, ñá is the resistivity coefficient and Ea is the activation energy.

We fitted the high temperature resistivity data using the above relation for $La_{0.67}Sr_{0.33}MnO_3$. The typical plots for both samples are shown in Fig. 3.

REFERENCES

1. Millis A.J., Littlewood P.B. and Shrainman B.I., Phy. Rev. Lett. 74 (1995) 5144.
2. Zener C., Phys. Rev. 82 (1951) 403.
3. G.H. Jonker and J.H. van Santen, Physica 16 (1950) 337.

RAMAN STUDY OF PHASE TRANSITION IN SN DOPED $GE_2SB_2TE_5$ FILMS DEPOSITED BY RF MAGNETRON SPUTTERING

ANURAG, SANGEETA SEMWAL, A.K. SHUKLA, P. SRIVASTAVA, V.D. VANKAR

Department of Physics, IIT Delhi-110016, India
Email: pankajs@physics.iitd.ac.in

Phase transition from amorphous to crystalline or vice-versa is the basic principle of writing and erasing the data in phase change memory devices. Generally chalcogenide materials ($Ge_xSb_yTe_z$, and AgInSbTe) are used for phase change memory applications. The $Ge_2Sb_2Te_5$ (GST) alloy is one of the frequently used materials in phase change recording technology. GST films are of great interest because of their high reflectivity contrast between amorphous and crystalline state, high crystallization speed and cyclability [1]. This alloy exhibits two crystalline states, namely a metastable (NaCl-type) phase and a stable hexagonal phase [2]. Doping is considered to be one efficient way to tune the properties of phase change materials. So far, various dopants such as Bi, Sn, O and N have been studied in literature [5-9]. However, no work has been reported so far on Raman study of Sn doped GST thin films.

In present work, we have studied the phase transition phenomenon in Sn doped GST thin films deposited by rf magnetron co-sputtering technique from a composite target of GST and a Sn target. The thin films of Sn doped GST phase change material were deposited on glass substrates for 50 minute at an Ar pressure of 1.2 × 10-3 torr. The thickness of the film was found to be ~100 nm. The as-deposited films were annealed in Ar ambient at 250 and 350°C for 1 hour each in a horizontal furnace.

Figure 1 shows Raman spectra obtained from as-deposited as well as annealed samples. A broad peak is observed in as deposited film around 150 cm^{-1}, which confirms the amorphous nature of Sn doped GST films [3]. An additional peak also appeared around 250 cm^{-1}, which can be attributed to the presence of Sn in GST thin films.

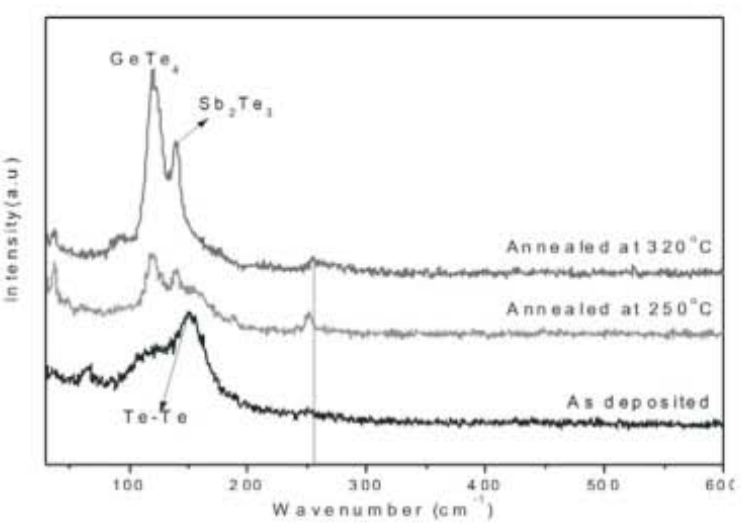

Fig. 1: Raman spectra of as-deposited and annealed thin films of Sn doped GST

Raman spectra of GST films annealed at 250°C showed a broad peak at about 150cm^{-1}, which can be splitted in to two peaks. Further annealing of these films at 350°C showed the presence of two sharp peaks at about 120 and 140 cm^{-1}, which confirms that the material has been crystallized [4].These results were further confirmed by X-ray diffraction (XRD).

REFERENCES

1. M. H. R. Lankhorst, B. W. S. M. M. Ketelaars, and R. A. M. Wolters 2005 Nat.Mater. 4, 347
2. N.Yamada, and T Matsuyama 2000 J. Appl. Phys. 88, 7020
3. Tominaga J, and Atoda N 1999 Jpn. J. Appl. Phys. 38, L322.
4. Ichiro W, Shigeru N, and Tatsuo S 1983 J. non-Crystalline solids 95&96, 509.
5. T.-J. Park, S.-Y. Choi, and M.J. Kang, 2007 Thin Solid Films 515, 5049.
6. Y. Kim, K. Jeong, M.-H. Cho, U. Hwang, H.S. Jeong, and K. Kim, 2007 Appl. Phys. Lett. 90, 171920.
7. J. González-Hernádez, P. Herrera-Fierro, B. Chao, Y. Kovalenko, E. Morales-Sánchez, and E. Prokhorov, 2006 Thin Solid Films 503, 13.
8. K. Wang, D. Wamwangi, S. Ziegler, C. Steimer, M.J. Kang, S.Y. Choi, and M. Wuttig, 2004
9. Phys. Stat. Solidi A 201, 3087.
10. B. Liu, Z. Song, T. Zhang, J. Xia, S. Feng, and B. Chen, 2005 Thin Solid Films 478, 49.

TEMPERATURE DEPENDENT MICRO RAMAN STUDY OF $Ga_{2-x}Fe_xO_3$ (X ~ 1.08-1.10)

Somdutta Mukherjee [1], Rajeev Gupta [1, 2], Ashish Garg [3]

[1]*Department of Physics*
[2]*Materials Science Programme*
[3] *Department of Materials Science and Engineering*
Indian Institute of Technology, Kanpur, U.P- 208016, India

Multiferroic $Ga_{2-x}Fe_xO_3$ ($0.8 \leq x \leq 1.4$) or GFO exhibits ferrimagnetism and piezoelectricity [1] simultaneously in the same phase. Its ferrimagnetic to paramagnetic transition temperature (T_c), varies between ~ 200 K to 400 K. [2,3] The transition temperature (T_c) depends upon the Fe content (x) and processing history. [3] The observed ferrimagnetism at low temperature is attributed to the site disorder of the cations. [3,4] In the present study, we synthesized GFO (x ~ 1.08-1.10) single crystals using flux growth method. [1] Reitveld refinement of room temperature XRD pattern of the crushed single crystals showed orthorhombic $Pc2_1n$ symmetry. Partial occupancies of the cationic sites obtained using Reitveld refinement were used to calculate the lattice magnetic moment which was in reasonable agreement with experimental value of bulk magnetic moment of 0.67 μ_B/ Fe site. Temperature dependent magnetization measurement predicted a T_c ~ 300 K which is in accordance with the previous reports of compositional dependence of magnetic data. [2,3] We also carried out Raman scattering as a function of temperature from 18 K to 450 K.. We observed 30 Raman active modes in the frequency range, 100-800 cm^{-1}. Temperature evolution of the peak positions of most of these modes can be adequately described using an anharmonic model suggesting absence of any lattice anomaly across the phase transitions. This observation was found to be consistent with the XRD data. However, the temperature dependence of the line width of a number of modes exhibited a change in slope across the phase transition boundary. In order to understand and quantify this change in the line width as a function of temperature we calculated the product of electron-phonon coupling strength and the density of states at the Fermi level using Allen's formula. [5] We compared these results with those obtained using transport measurements. The deviation from anharmonicity was qualitatively explained as a consequence of a weak magneto-elastic effect in the low temperature phase.

REFERENCES

1. J. P. Remeika, Journal of Applied Physics **31,** S263-S264 (1960).
2. C. H. Nowlin and R. V. Jones, Journal of Applied Physics **34,** 1262-1263 (1963).
3. T. Arima, D. Higashiyama, Y. Kaneko, J. P. He, T. Goto, S. Miyasaka, T. Kimura, K. Oikawa, T. Kamiyama, R. Kumai, and Y. Tokura, Physical Review B **70,** 064426 (2004).
4. M. J. Han, T. Ozaki, and J. Yu, Physical Review B (Condensed Matter and Materials Physics) **75,** 060404-4 (2007).
5. P. B. Allen, Solid State Communications **14,** 937-940 (1974).

NANO DIMENSIONAL EFFECT ON MAGNETIC AND ELECTRONIC-TRANSPORT PROPERTIES OF UNDER DOPED $Pr_{0.8}Sr_{0.2}MnO_3$

P.T. Das, A. Taraphder, T. K. Nath

Department of Physics and Meteorology, Indian Institute of Technology-Kharagpur, Kharagpur-721 302, India.
Email: dasproloy@phy.iitkgp.ernet.in

The hole doped CMR manganites with general formula $Ln_xR_{1-x}MnO_3$, where Ln is trivalent rare earth metal (e.g. La, Nd, Pr, Sm) and R is divalent alkaline metal (e.g. Sr, Ca, Ba), are strongly correlated electron system where spin, charge, orbital and lattice degrees of freedom play very important role in their transport and magnetic behavior. Among the variety of doping concentrations in manganese perovskites $Pr_{0.8}Sr_{0.2}MnO_3$ (PSMO) is of special interest as bulk material shows ferromagnetic-insulator behavior due to weak DE interaction, whereas in nano regime it shows metal-insulator transition at low temperature. It also exhibits two magnetic phase transitions. It was found that grain boundary effects are significant for a wide temperature range as observed for polycrystalline thin films and bulk materials [1]. The aim of this paper is to report how the nanometric size affects the electronic-, magneto-transport and magnetic properties of ferromagnetic insulating $Pr_{0.8}Sr_{0.2}MnO_3$ (PSMO) samples. It is also useful to find out the average strain inside the grains induced by the nano dimension as this may affect the electronic transport and magnetic properties of the PSMO grains. All the nanometric granular polycrystalline PSMO samples were synthesized by chemical pyrophoric reaction process [2]. We have calcined the as-prepared powder at four different temperatures (850, 950, 1050, and 1350°C) to get the series of PSMO sample with different particle size ranging from nm to mm dimension.

The microstructural, electronic-transport and magnetic properties of all samples have been thoroughly studied by HRXRD with Rietveld refinement fitting, HRTEM, FESEM, high field and low temperature CRYOGENICS CFM VTI system and SQUID magnetometer.

Rietveld refinement of HRXRD pattern for $Pr_{0.8}Sr_{0.2}MnO_3$, sintered at different temperatures confirms that our samples are single phase orthorhombic with Pbnm space group as shown in Fig.1 (a). Using Debye-Scherrer formula ($\varphi = n\lambda/d_{eff}\cos\theta$) the average crystallite sizes of the PSMO samples are estimated to be ~ 40 , 50 and 58 nm for the sintering temperatures of 850°C, 950° C and 1050° C, respectively. FESEM, HRTEM images and selected area diffraction (SAD) pattern for the PSMO sample (Fig. 1(b), 1(c) and 1(d)) show that samples are granular nanocrystalline and polycrystalline in nature. The lattice constants, unit cell volume and the rms-microstrain in the grains are not found to change appreciably with the particle/grain size. From DC magnetization study it is observed that Tc increases with the decrease of particle size (Tc = 190K) compared to its bulk counterpart (Tc = 108 K) [Fig.2(a)]. It is also observed that there are two magnetic phase transitions [PM to FM at ~ 108 K and FM to AFM at ~ 45 K] in bulk sample. Moreover the nanometric 950 PSMO sample shows ferromagnetic behavior [hysteretic M(H) loop and saturation] at low temperature as shown in Fig.2 (b) and its inset. The bulk counterpart shows AFM ordering in the low temperature regime. Fig.2 (c) shows the field dependent MR at different temperatures of 850 PSMO. At lowest temperature (2 K) the maximum MR is ~ 85% for the sample at a field of 8T for 40 nm particle size. For the bulk sample the MR is ~ 50% at 150 K at 8T magnetic field. Figure 2(d) shows the temperature-dependent resistivity plots of PSMO samples of different particle sizes. At

low doping Pr based manganite shows ferromagnetic insulating phase for single crystalline system [3]. Bulk PSMO shows insulating behavior throughout the temperature range. Surprisingly, in the case of nanometric 850 and 950 PSMO, both of them show metal-insulator transition at around ~ 150 K. This transition is absolutely absent in the bulk counterpart. The inset of Fig. 2(d) shows the temperature-dependent insulating behavior of the bulk PSMO for the entire temperature range.

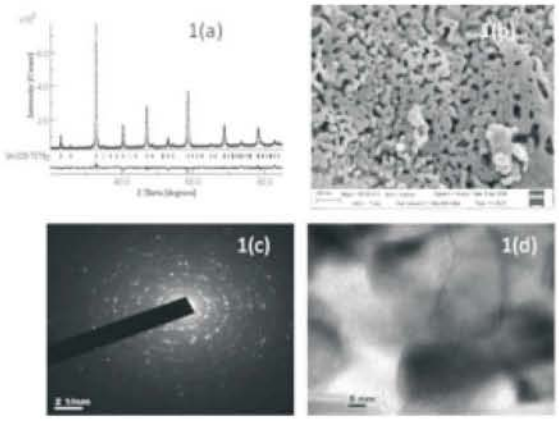

Fig. 1. (a) Rietveld refinement of HRXRD PSMO 950 sample, (b) FESEM micrograph, (c) SAD pattern and (d) HRTEM image of nanometric PSMO sample.

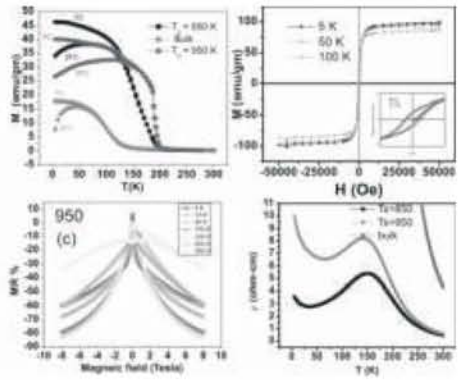

Fig. 2. (a) M(T) of PSMO 40 nm, 50 nm and bulk samples showing drastic change of T**c.** (b) M (H) of 950 PSMO. **(c)** HFMR of nanometric 850 PSMO at different temperatures (d) Resistivity plot with temperature for three different particle sizes; inset shows resistivity vs. T plot of insulating bulk sample.

The observed drastically contrasting behavior in nanometric grains compared to its bulk counterpart is most clearly explained by enhanced surface disorder [4]. The destabilization of the ferromagnetic insulating state at the surface grain boundary is primarily attributed to the surface reconstruction of the electronic states resulting in an increase in DE. The hugely enhanced surface to volume ratio in nano-grains adds up to the sizabale change in electronic transport (metallicity), enhanced magneto-transport and magnetic properties. In summary, we have thoroughly studied the effect of nano size on the electronic-, magneto-transport and magnetic properties of PSMO samples. The contrasting behavior in nanometric grains is attributed to the enhanced surface disorder at the grain surfaces.

REFERENCES

1. H. Y. Hwang, S.-W. Cheong, N. P. Ong, and B. Batlogg, Phys. Rev. Lett. **77**, 2041 (1996).
2. P. Dey, T. K. Nath, Phys. Rev. B, **73**, 214425 (2006).
3. C. Martin, A. Maignan, M. Hervieu, and B. Raveau, Phys. Rev. B **60**, 12191 (1999).
4. S. Kundu et al, arXiv : 1006.2943 ,[cond-mat.str-el],15 Jun 2010.

KO_2: REALIZATION OF ORBITAL ORDERING IN A p-SHELL SYSTEM

Ashis Kumar Nandy[1,2], Priya Mahadevan[2], Prasenjit Sen[3], D. D. Sarma[4]

[1]*Centre for Advanced Materials, Indian Association For the Cultivation of Science, Jadavpur, Kolkata-700 032, India*

[2]*S. N. Bose National Centre for Basic Sciences, Block-JD, Sector-III, Salt Lake City, Kolkata-700 098, India*

[3]*Harish-Chandra Research Institute, Chhatnag Road, Jhusi, Allahabad-211 019, India*

[4]*Solid State and Structural Chemistry Unit, Indian Institute of Science,Bangalore-560 012, India.*

Email: camakn@iacs.res.in

Most of the experimental efforts probing magnetism, charge and orbital ordering have concentrated on transition metal compounds [1]. Possible examples among p band systems have not been explored. The first step in this direction would be to search for narrow band materials in which Coulomb interactions should be important. If one could engineer magnetism in these materials, one could generate a new class of compounds with a rich phase diagram as earlier discussed transition metal counterparts. Our search for stoichiometric materials with p shell magnetism led us to an unusual set of compounds formed by the alkali metal atoms (A) [2]. Here we have considered the prototypical example of KO_2 and explore its properties in great detail [3].

KO_2 is a molecular solid consisting of oxygen dimers aligned parallel in a body centred tetragonal lattice at high temperatures. K present in the lattice donates an electron which goes on to occupy the O p levels. As the basic electronic structure is similar to that of an oxygen molecule, except for broadening due to solid state effects, KO_2 represents the realization of the doping of oxygen molecules arranged in a lattice. These considerations alone result in magnetism with high ordering temperatures as our calculations reveal. However, we find that the high temperature structure is unstable to an orbital ordering (OO) transition. The microscopic considerations driving the OO transition, however, are electrostatic interactions instead of the often encountered super-exchange driven ordering within the Kugel-Khomskii model [4] often used to describe the OO. This OO transition is also found to preclude any possibility of high magnetic ordering temperatures, which otherwise seemed possible.

REFERENCES

1. T. Hotta Rep. Prog. Phys. 69 (2006) 2061
2. W. Hesse, M. Jansen and W. Schnick Prog. Solid. St. Chem. 19 (1989) 47
3. A. K. Nandy, Priya Mahadevan, P. Sen and D. D. Sarma. Phys. Rev. Lett. 105 (2010) 056403
4. K. I. Kugel and D. I. Khomskii Sov. Phys. JETP 37 (1973) 725

RARE EARTH OXIDE BASED DILUTED MAGNETIC DIELECTRICS

NATHAN W. GRAY, PAUL K. SLUSSER, ASHUTOSH TIWARI

Nanostructured Materials Research Laboratory, Department of Materials Science and Engineering, University of Utah, Salt Lake City, Utah 84112, USA
E-mail: tiwari@eng.utah.edu

It is widely believed that the successful integration of spin functionality into present semiconductor based electronic devices will improve their processing speed, storage capacity and power requirement. The above notion has led to the discovery of several new and exotic spintronic materials which in many cases exhibit phenomena that can't be adequately explained by current physical models. One such example is the discovery of diluted magnetic dielectrics (DMD). Specifically a number of highly insulating oxides such as TiO_2 (anatase), HfO_2, GaN and SnO_2 have been reported to show room temperature ferromagnetism when doped with small amounts of transition metal elements. Such systems exhibit ferromagnetic long range ordering even though the magnetic dopant level is far below the percolation threshold for dipole exchange interaction. In these insulating systems, carrier mediated RKKY magnetic exchange cannot be applied to explain the observed ferromagnetism, and other mechanisms such as super-exchange or double exchange also fall short.

In this presentation we will report our recent results and the discovery of a new DMD system based on Rare Earth oxides (REO). Specifically, we found that when a small amount of transition metal elements are doped in certain REO thin films, the system exhibits a unique magnetic phenomenon which cannot be accounted for by conventional models. Though the observed magnetic properties appear quite similar to those observed in superparamagnetic systems, the origin of these properties is entirely different. Careful atomic-scale structural analysis showed no secondary phases or compositional variation which could account for the observed magnetic response. A model, based on the widely accepted bound polaron theory for insulating ferromagnets, is proposed to explain the unique magnetic behavior of these materials. In this model, exchange mediating defects form magnetically active regions which behave in some ways like superparamagnetic clusters; however, unlike superparamagnetic systems the size of magnetically active regions is not static but changes dynamically with temperature.

REFERENCES

1. G. A. Prinz, "Device physics – Magnetoelectronics", Science **282**, 1660 (1998).
2. S. Das Sarma, "Spintronics", American Scientist **89**, 516-523 (2001).
3. S. A. Chambers, "A Potential Role in Spintronics", Materials Today **4,** 34-39 (2002).
4. P.K. Slusser, D. Kumar and A. Tiwari, "Unexpected Magnetic Behavior of Cu-doped CeO_2", Applied Physics Letters **96**, 142506(2010)

EFFECT OF SINTERING TEMPERATURE ON MAGNETIC PROPERTIES OF $Zn_{0.95}Mn_{0.05}O$

Umesh Kr. Gaur[1,3], A. Gaur[1], P. Chand[1], A. Kumar[1], G.D. Varma[2]

[1] *Department of Physics, National Institute of Technology, Kurukshetra-136119, India*
[2] *Department of Physics, Indian Institute of Technology Roorkee, Roorkee-247667, India*
[3] *Presently working at Centre of Nanotechnology, Indian Institute of Technology Roorkee, India*
Email: anuragdph@gmail.com

Researchers all over the world have recently been looking for new kind of semiconductors in which both the charge and spin of carriers can be exploited to provide new functionality for spintronic devices [1]. The primary requirement of such devices is to have room temperature ferromagnetism (RTFM) and high spin transport, so that it can be used in spin transistors, ultra dense non-volatile memory devices (e.g. MRAMs) and optical emitters. Following the prediction of RTFM in the otherwise nonmagnetic II–VI and III–V semiconductor compounds, by Dietl et al. [2] in 2000, researchers started re-investigating transition metal (TM) doped II–VI semiconductor oxides (e.g. ZnO, SnO_2 and TiO_2), and III–V compounds (e.g. GaN, GaAs, InAs, etc.) [3,4]. Manganese substituted ZnO has attracted significant attention not only due to technological advantages but also due to the prevailing disagreement in both the existence as well as the origin of room temperature ferromagnetic behavior. The present study aims at systematic investigations on $Zn_{1-x}Mn_xO$ (x= 5%) sintered successively at different temperatures to understand the origin of room temperature ferromagnetic behaviour.

We have synthesized the $Zn_{0.95}Mn_{0.05}O$ nanoparticles by sol-gel method. The sintering temperature has been varied from 400 to 800 °C to vary the particle size. X-ray diffraction (XRD), scanning electron microscopy (SEM), and Vibrating Sample magnetometer (VSM) have been used in present investigations to characterize the samples. The phase formation, crystalline size determination and magnetic properties have been studied successfully. X-ray diffraction pattern of $Zn_{0.95}Mn_{0.05}O$ samples sintered at 400, 500, 600 and 800 °C have been shown in Fig. 1.The XRD results show that the phase formation of ZnO starts at 400 °C and particle size varies between 19 to 72 nm as sintering temperature varies from 400 to 800 °C. However, grain size, observed from SEM, varies from 20 to 150 nm.

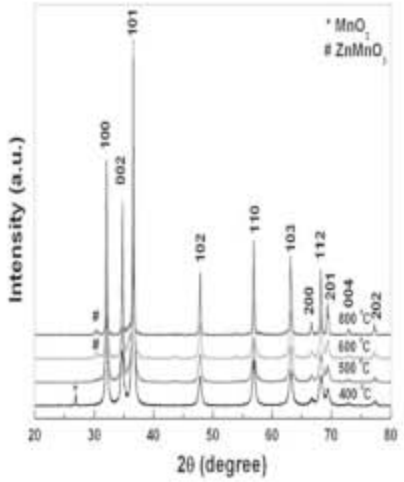

Fig: 1: X-ray diffraction pattern of $Zn_{0.95}Mn_{0.05}O$ samples sintered at 400, 500, 600 and 800 °C.

The most interesting feature of present investigations is the observations of room temperature ferromagnetism (RTFM) in 5% Mn doped ZnO samples sintered at 400 and 500 ^{0}C. The observation of room temperature ferromagnetism makes this material a possible candidate for spintronics devices.

REFERENCES

1. S.A. Wolf, D.D. Awschalom, R.A. Buhrman, J.M. Daughton, S. von Molnar, M.L. Raukes, A.Y. Chiehelkanova, D.M. Treger, Science 294 (2001) 1488.
2. T. Dietl, H. Ohno, F. Matsukur, J. Cibert, D. Ferrad, Science 287 (2000) 1019.
3. S.S. Yan, C. Ren, X. Wang, Y. Xin, Z.X. Zhou, L.M. Mei, M.J. Ren, Y.X. Chen, Y.H. Liu, Appl. Phys. Lett. 84 (2004) 2376.
4. K.P. Bhatti, S. Chaudhary, D.K. Pandya, S.C. Kashyap, Solid State Commun. 140 (2006) 23.

MAGNETOELECTRIC COUPLING IN NOVEL SPIN FRUSTRATED MULTIFERROICS

A.K. Singh, S. Patnaik

School of Physical Sciences, Jawaharlal Nehru University, New Delhi-110067
Email: kumaranil83@gmail.com

Multiferroic magnetoelectric materials, which simultaneously display ferroelectricity and ferromagnetism, have recently stimulated a sharply increasing number of research activities for their great fundamental and technological interest. As a consequence, the magnetic (electric) domains can be tuned by the application of an external electric (magnetic) field and/or strain, suggesting tremendous potential for innovative device applications and exploration of the fundamental physics of coupled phenomena. In order to achieve these potential applications, the microscopic origin of the coupling between electric and magnetic order parameters should be known. Ferroelectricity and magnetism tend to be mutually exclusive and interact weakly with each other when they coexist. But in a certain class of materials large magnetodielectric effects were discovered due to magnetic origin of ferroelectricity. In these multiferroics, ferroelectric order develops upon a magnetic phase transition into a spiral or noncollinear magnetic ordered phase.

I will review some of my recent key experimental findings in spin frustrated multiferroics systems. The focus will be on recently discovered magnetoelectric compound $Bi_2Fe_4O_9$, competing magnetic interaction in $Ni_3V_2O_8$, role of strain on multiferroic properties, and microscopic origin of multiferroicity in hexagonal $YMnO_3$. Novel inverse Dzyaloshinskii-Moriya (DM) effect which explains magnetoelectric coupling in this class of compounds, and the key scientific challenges in this field will also be discussed.

REFERENCES

1. K. Singh *et al.*, Appl. Phys. Lett. **92**, 132910 (2008).
2. K. Singh *et al.*, Euro. Phys. Lett. **86**, 57001 (2009).
3. K. Singh *et al.*, J. Appl. Phys. **106**, 014109 (2009).
4. K. Singh *et al.*, Phys. Rev B **81**, 184406 (2010).

ELECTRON SPIN RESONANCE STUDIES OF $Bi_{0.5}Ca_{0.5}Mn_{0.95}TM_{0.05}O_3$ (TM = Cr, Fe, Ni)

D.Vijayan, Joji Kurian, R. Singh

School of Physics, University of Hyderabad, Central University, P.O. Hyderabad-500046, India
E-mail:vijayanphysics@gmail.com

Perovskite structured manganites of the form $A_{(1-x)}B_xMnO_3$ (A = La, Bi, Pr, Sm etc and B = Sr, Ca, Pb, Ce etc) exhibit interesting phenomena like charge/orbital – ordering (CO/OO), metal – insulator (M – I) transitions, colossal magnetoresistance (CMR) effect etc[1]. These exotic phenomena are defined by altering the Mn^{3+}/Mn^{4+} ratio in the materials. Desired properties can be infused in these materials using different A and B – site elements and/or by substituting Mn by multi valent elements like transition metals (TM)[2,3]. In this work the effect of substituting transition metals at the Mn site of $Bi_{0.5}Ca_{0.5}Mn_{0.95}TM_{0.05}O_3$ (TM = Fe, Cr, Ni) on the magnetic properties is presented. Electron Spin Resonance (ESR) is known to be a highly sensitive technique for understanding the spin structure and its dynamics in a sample. Temperature dependent ESR studies in the temperature range 120 – 470K are undertaken to understand the evolution of micro/nano magnetic phases and its effects on the magnetic properties of the samples. The ESR signals are assigned to the contribution of ferromagnetic (FM) double exchange (DE) interactions involving the Mn^{3+} – O – Mn^{4+} network[4]. In the present study the electronic structure of the substituants play a role in deciding the FM DE interactions and in turn the properties of the samples. Nickle can exist as Ni^{2+} and/or Ni^{3+}, substituting for Mn^{3+} and/or Mn^{4+} respectively, enhancing FM correlations. Chromium exists predominantly as

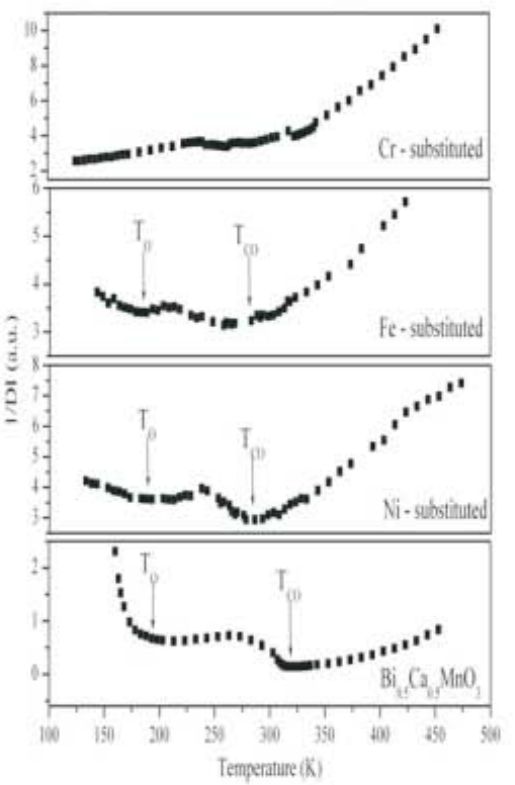

Figure 1: 1/DI v T plots for $Bi_{0.5}Ca_{0.5}MnO_3$ and $Bi_{0.5}Ca_{0.5}Mn_{0.95}TM_{0.05}O_3$ (TM = Fe, Cr, Ni)

Cr^{3+}, which is isoelectronic with Mn^{4+}, thereby contributing to Mn^{3+} – O – Cr^{3+} mediated FM correlations[3]. Fe^{3+} substitutes Mn^{3+} due to the similar ionic radii. The higher effective magnetic moment of Fe^{3+} compared to that of Mn^{3+} increases the net magnetic moment of the material. From the ESR studies the variation of the double integrated intensity of the resonance lines (DI), which is proportional to χ_{ESR}, with temperature (T) is plotted as 1/DI v T plots for the samples (fig.1). Two minima, one at high temperature and the other at low temperature, depicted as the charge ordering and onset of long range antiferromagnetic (AFM) ordering, T_{CO} and T_O, respectively, of the undoped, Ni and Fe substituted samples are shown in fig 1. For $T > T_{CO}$ 1/DI decreases with decreasing temperature. On decreasing temperature, for $T_{CO} > T > T_O$, 1/DI increases initially for a short temperature range, remains constant and decreases again till T_O. Below T_O, 1/DI increases rapidly. The 1/DI decreases continuously with decreasing temperature for the Cr substituted sample, with only a change in slope indicating variation in the strength of contributions of FM and AFM phases. The ESR studies are analysed in view of the phase separation model[4]. For $T > T_{CO}$ decrease in 1/DI indicates contributions of evolving FM correlations, which melt the CO state, evidenced as a broad transition peaks of T_{CO}. An increase of 1/DI below T_{CO} is attributed to the residual effect of AFM correlations, which gives rise to the CO state. The coexistence of evolving competing FM and AFM phases is observed at the temperature range $T_{CO} > T > T_O$. For $T < T_O$ the samples enter the long range AFM ordered phase.

REFERENCES

1. M. R. Ibarra and J. M de Teresa *Colossal Magnetoresistance, Charge Ordering and Related Properties of Manganese Oxides* (1998)
2. O. Toulemonde, F. Studer, A. Barnabe, A. Maignan, C. Martin and B Raveau Eur. Phys. J. B **4**, 159 (1998).
3. Joji Kurian and R. Singh J. Phys.: Confer.Ser. **200**, 012100 (2010).
4. Joji Kurian and R. Singh J. Phys. D: Appl. Phys. **41**, 215006 (2008).

A FIRST PRINCIPLES STUDY OF STRONGLY CORRELATED ErSb:

Subhra Kulshrestha, Pooja Rana, S.K. Sngh, Dinesh C. Gupta

Condensed Matter Theory Group, School of Studies in Physics,
Jiwaji University,Gwalior – 474 011 (M.P.) INDIA
Email: subhrafizix@yahoo.co.in

The magnetic, electronic, structural and mechanical properties of ErSb in the stable Fm m and high-pressure $pm\bar{3}m$ phases have been analyzed *ab-initio* employing the full potential method within the framework of density functional theory. The Local Spin Density Approximation along with Hubbard U based on exchange-correlation energy optimization has been used for calculating the total energy. The magnetic phase stability has been determined from the total energy calculations for both the non-magnetic and magnetic phases which show that it is ferromagnetically stable at ambient and high pressures. Under compression, ErSb undergoes first-order structural transition from B1 to B2 phase at 24.56 GPa which show good agreement with the experimental value of 25 GPa. The structural properties *viz*, equilibrium lattice constant, bulk modulus and its pressure derivative, transition pressure, volume collapse and elastic moduli agree well with the experimental data. The electronic structure at different volumes is obtained with the LSDA+U approach. The LSDA+U strategy shows significant impact on the energy levels of the occupied and unoccupied 4*f* states of ErSb.

STRUCTURAL AND MAGNETIC PROPERTIES OF SPUTTERED $Co_2Cr_{0.6}Fe_{0.4}Al$ HEUSLER ALLOY THIN FILMS

ANJALI YADAV, SUJEET CHAUDHARY

Thin Film Laboratory, Department of Physics, Indian Institute of Technology Delhi, New Delhi 110016, India
Email: sujeetc@physics.iitd.ac.in

Highly spin polarized materials are required to develop and realize novel spintronic devices such as efficient spin injectors, spin filters, tunnel junctions or GMR [1]. The ferromagnetic full Heusler alloy $Co_2Cr_{0.6}Fe_{0.4}Al$ (CCFA) have a high Curie temperature (T_C) ~750K, and are theoretically predicted to possess a high value of saturation magnetization of $3.8\mu_B$ per formula unit. Their expected half metallicity makes them a good candidate for a number of applications in spintronic devices [2]. Experimentally, high magnetoresistance ~80% at room temperature and in small fields ~10 mT has been reported [3]. In the present work, we deposited CCFA (~50 nm) on MgO *(100)* and Si *(100)* at room temperature and 550°C by using pulsed DC – sputtering technique with an Argon flow of 15 sccm. The working pressure is maintained at 5.5×10^{-3} torr and base pressure at 7.5×10^{-6} torr. The magnetron sputtering is a novel method for preparing thin films of CCFA due to its high deposition rate, ease of sputtering any metal, alloy or compound, high purity films, extremely high adhesion of films and excellent uniformity on large area substrates [4]. We studied the effect of substrate-type and growth-temperature on the structural and magnetic properties of CCFA film using X-ray diffraction (XRD) and Magneto Optical Kerr Effect (MOKE) measurements. The Magneto Optical Kerr Effect (MOKE) is a qualitative and surface-sensitive method to provide a very quick magnetic M-H behaviour

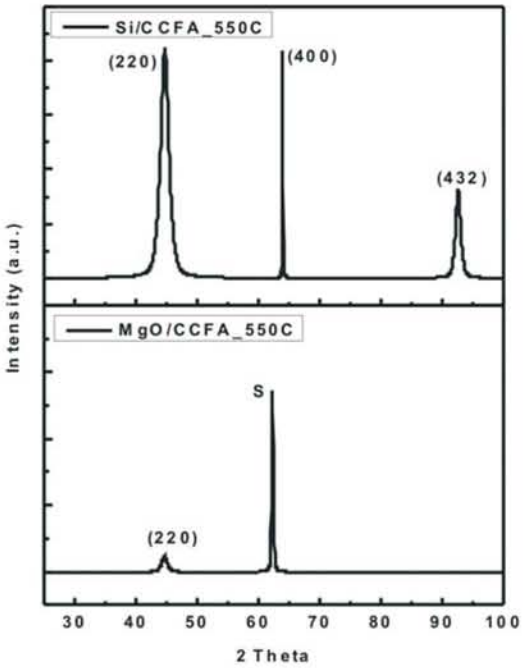

Fig. 1 XRD patterns of CCFA films on Si (top panel) and MgO (bottom panel) substrates. 'S' refers to the peak appearing due to substrate.

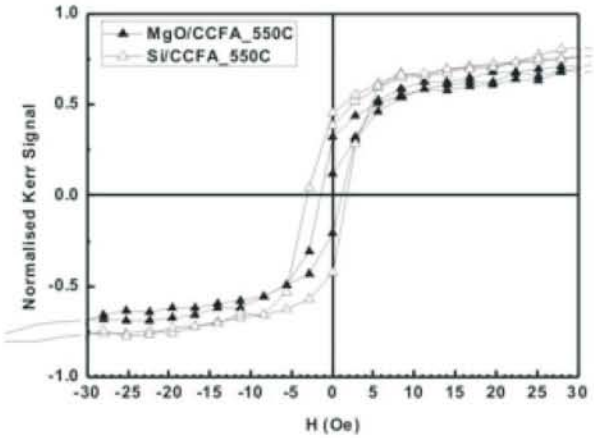

Fig 2. Normalised magnetic hysteresis curves measured by MOKE at RT of the as-grown CCFA films on MgO and Si (see text for details).

of the films. The hysteresis loop of the sample can be taken in a normalised manner, where the information concerning the coercivity can correctly be extracted. While Fig.1 shows the XRD patterns of CCFA films grown on MgO and Si substrates at 550°C temperature, Fig. 2 shows the MOKE M-H loops of these CCFA films. The coercivity of CCFA film grown on MgO was ~1.5 Oe and on Silicon was ~3.0 Oe. Detailed result will be presented during the conference.

REFERENCES

1. D. Rata et al., Eur. Phys. J. B. 52, 445-451 (2006)
2. Andres Conca et al. J. Phys. D: A. Phys 40, 1534, (2010)
3. E. Clifford et al. Solid State Commun. 131, 61(2004)
4. S. Swann, Phys. Technol. 19 (1988)

GROUND STATE PHASE DIAGRAM OF SPINLESS FALICOV-KIMBALL MODEL AWAY FROM HALF FILLING

Monika Dhariwal*, Umesh K. Yadav, Tulika Maitra, Ishwar Singh

Department of Physics, I. I. T Roorkee, Roorkee – 247667, Uttarakhand, India
Email: monikadhariwal9@gmail.com

Layered systems like colossal magnetoresistance (CMR) materials e.g. La1-xMxMnO3, M= [Ca, Sr] and Pr1-xCa1+xMnO4 [1] have attracted considerable attention recently, as they exhibit remarkable cooperative phenomena such as metal-insulator transition, charge and magnetic order, excitonic instability etc. These materials also show drastic change in the above mentioned phenomena with variation in temperature, hole doping and also by the application of pressure and magnetic field. Recently it is proposed that these systems very effectively can be explained by two dimensional Falicov Kimball model [FKM] [2] on square lattice [3]. We have studied the ground state phase diagram of the spin independent FKM on square lattice using Monte Carlo simulation algorithm, described in details in [4] as function of Coulomb repulsion (U) between itinerant (d) and localized (f) electrons and different fillings of localized electrons (nf). Our calculations are mainly focused on away from half filling (nd + nf =n ; n away from 1; where nd, nf and n are density of d-, f- and total number of electrons respectively) case. Ordered and disordered ground state configurations of f-electrons are observed for small U-values. Phase segregation in the f-electron configuration is observed for large values of U. We have also studied Metal-insulator transition and density of d-electrons as function of U and nf.

REFERENCES

1. X. Z. Yu, R. Mathieu, T. Arima. Y. Kaneko, J. P. He, M. Uchida, T. Asaka, T. Nagai, K.Kimoto, A. Asamitsu, Y. Matsui, and Y. Tokura, Phy. Rev. B. 75, 174441 (2007).
2. L. M. Falicov and J. C. Kimball, Phys. Rev. Lett. 22, 997 (1969).
3. R. Lemanski, J. K. Freericks, and G. banach, J. Stat. Phy. 116, 699 (2004).
4. Umesh K Yadav, T. Maitra, Ishwar Singh and A. Taraphder, J. Phys.: Condens. Matter 22, 295602 (2010), Umesh K Yadav, T. Maitra and Ishwar Singh, Proc., DAE-SSPS 54, 1065 (2009).

PHONON DYNAMICS OF A MULTIFERROIC $BiFeO_3$ IN CUBIC PHASE

M. M. Sinha, Ruby

Department of Physics, Sant Longowal Institute of Engineering and Technology, Longowal, Sangrur (Punjab) – 148106, India
Email: mm_sinha@rediffmail.com

Multiferroic (MF) materials exhibit a highly coupled, spontaneous ferroelectric polarization and magnetization. Intriguingly, these novel properties of multiferroics enable the magnetization to be switched by applying external electric fields and, vice versa, for applications such as memories and sensors. Coupling between electrical and magnetic properties in multiferroic materials makes them a promising material for the design of multifunctional device applications, but also because of the interesting physics found in this class of materials. The coexistence of ferroelectricity and anti ferromagnetism at room temperature makes $BiFeO_3$ one of the most interesting multiferroic materials. Optical spectroscopy is a very powerful tool to understand the driving mechanism of the ferroelectric transition and, eventually, its coupling to magnetic ordering. Nevertheless, only a few Raman and infrared IR studies on $BiFeO_3$ are known to date. The role or absence of phonon softening in order to explain ferroelectric transition and the phonon modes symmetry in $BiFeO_3$ are some important questions still needs to be answered. Very little is known about the behaviour of phonons in magnetoelectric multiferroics, and this although investigations of phonons have in the past played a crucial role in the understanding of classic ferroelectrics. Motivated to determine and understand the role of phonons in multiferroics, we have undertaken the theoretical investigation on the phonon properties of $BiFeO_3$ in its cubic phase by applying lattice dynamical simulation method based on de Launey angular force (DAF) constant model. The calculated zone centre phonon frequencies agree well with available results. The phonon spectrum of $BiFeO_3$ is calculated along the three symmetry directions. Some modes of $BiFeO_3$ are coming out to be negative, representing the soft modes. The imaginary frequencies are associated with unstable mode and are in agreement with other calculations. The soft modes are interpreted in terms of transition of phase and other related properties in these materials.

SURFACE SPINS INVESTIGATIONS OF KEROSENE BASED Fe_3O_4 FERROFLUID

Manju Arora, R.P. Pant

CSIR, National Physical Laboratory, Dr. K.S. Krishnan Road, New Delhi
Email: marora@nplindia.org

We have investigated temperature dependence (10-300K) magnetic properties of Fe_3O_4 base ferrofluids using EPR technique. A single, strong and relatively broad resonance signal was observed at ambient temperature with effective g-value of ~ 2.25 along with a weak kink of effective g-values ~ 4.00 in 10K to 70K range and ~ 2.00, 3.200 in 100 K to 300 K. The intensity, line width and resonance field are strongly temperature dependent. The decrease in magnetic interaction between the particles leads to the increase in line width and resonance field values at low temperatures. This reduces the total effective magnetic moment originating from the non-collinear spin structure formed by the pinning of surface spins and surfactant at the interface of nanoparticles.

Nanoscale magnetic materials have been a field of intense study due to their quantum dimension in the transition region between atom and the bulk. In order to understand the transition from quantum to classical behavior in spin system, electron paramagnetic resonance (EPR) is a very versatile technique [1-3]. The finite size effect and the large surface area of magnetic nanoparticles dramatically change the magnetic properties and exhibit superparamagnetic (SP) phenomena when particle size is smaller than a single domain. These features are observed in quantum systems and not expected in classical case.

The SP size particles were prepared by the chemical co-precipitation route. These fine particles were coated with oleic acid and dispersed in kerosene. Magnetic properties of this resulted ferrofluid were investigated by X-band EPR spectrometer (Make: Bruker Biospin, Model: A300) at different low temperatures i.e. from 10K to 300 K.

The SP size Fe_3O_4 particles are considered as single domain ferromagnetic state where all the spins are strongly coupled, giving rise to a total magnetic moment. As the particle size is less than the critical size. The superparamagnetic behavior is exhibited which means when magnetic energy is of the order of thermal energy k_T or less. In this regime, the direction of magnetic moment fluctuates significantly from the equilibrium position while their amplitude remains same.

In these investigations, EPR spectra of the ferrofluid exhibits the coexistence of two different resonance modes: (i) a broad line due to ferrimagnetic resonance and (ii) a kink at g ~2 due to superparamangetic particles. Dipole-dipole interaction between the particles causing the broadening of the signal due to spin disorder arising mainly from the antiferromagnetic interactions between the neighboring spins in magnetic nanoparticles. At low temperatures the spectra broadens and shifts to lower resonance field as shown in Fig. 1 and 2.

As seen from the Fig. 3 represents peak to peak linewidth (ΔHpp) and g-value are strongly temperature dependent The This can be explained in terms the temperature related behavior of narrow component and uniaxial nature of the ferrofluid anisotropy. The peak-to-peak linewidth variation with higher temperature indicates the weakening of the magnetic moment due to pinning of the surface spins and coated surfactant at the interface of nanoparticles is responsible for the observed reduction in the line width fig 2. The ~ g at 4.2 is due to the

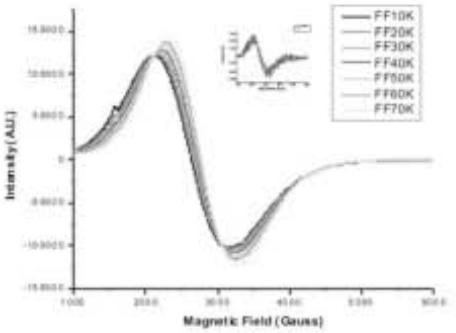

Fig. 1: EPR spectra of Fe_3O_4 ferrofluid from 10 K to 70K

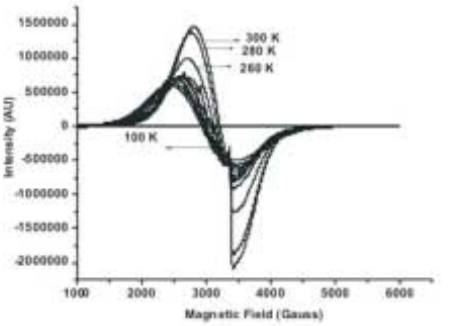

Fig. 2: EPR spectra of Fe_3O_4 ferrofluid from 100K to 300K

Isolated spin of Fe^{3+} becomes prominent with decrease in temperature(10K) and shows the stability. The spin concentration increases with increasing temperature and the values from 10K to 70K is listed in Table 1.

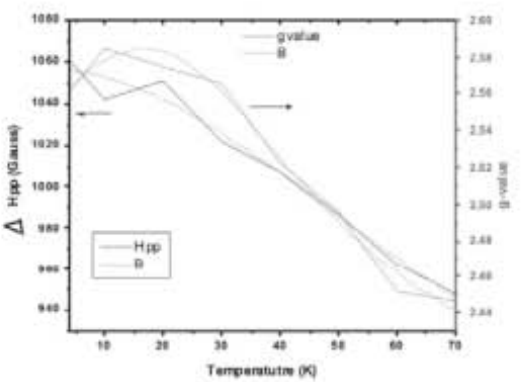

Fig. 3: ΔHpp and g-value vs. temperature

Table 1: Spin Concentration with temperature

Temperature (K)	Spin concentration (Spins/gm)
4	1.82×10^{18}
10	2.33×10^{18}
20	2.96×10^{18}
30	3.41×10^{18}
40	3.98×10^{18}
50	4.32×10^{18}
60	4.65×10^{18}
70	5.33×10^{18}

CONCLUSION

EPR spectroscopy technique has been successfully used for the investigations of surface spin and their behavior at low temperatures. Fe^{3+} ions isolated spins becomes prominent at low temperatures due to weakening of magnetic moment and spin disorder. This leads to the transition from spin glass to cluster glass state. The super exchange interactions among fluid dominates at higher temperature.

REFERENCE

1. Batlle X and Labarta A 2002 *J. Phys. D: Appl. Phys.* **35** R15.
2. Bulte J W, Douglas T, Mann S, Frankel R B, Moskowitz B M, Brooks R A, Baumgarner C D, Vymazal J, Strub M P and Frank J A 1994 *J. Magn. Reson. Imaging* **4** 49.
3. Bell A T 2003 *Science* **299** 1688.

COMPARATIVE STUDY OF Cr & Fe DOPED $La_{0.7}Ca_{0.3}MnO_3$

Neeraj Kumar[1,2], Ashok Rao[2], V.P.S. Awana[1]

[1]*Quantum Phenomenon and Applications Division, National Physical Laboratory, New Delhi-12, India*

[2]*Department of Physics, Manipal Institute of Technology, Manipal Karnataka*

E-mail: awana@mail.nplindia.ernet.in

Manganites with general formula $RE_{1-x}A_xMnO_3$ (RE = trivalent rare earth and A = alkali metal) has attracted a lot of attention in last over one and half decades due to their complex magnetic phase diagram and novel magneto-resistive properties, for example see review article [1]. The transport properties of the manganite materials are explained by the double-exchange and electron-phonon coupling arising from Jahn-Teller distortion [2]. The lack of data at close intervals for Fe and Cr substitutions in manganites materials motivated us to study the effect of Cr^{+3}, Fe^{3+} ion doping in $La_{0.7}Ca_{0.3}MnO_3$ manganite at close intervals. We studied complete phase diagram and ensuing transformation from double-exchange (DE) to super exchange (SE) interactions with increasing content of Fe and Cr in $La_{0.7}Ca_{0.3}MnO_3$ manganites [3,4].

Samples with nominal composition $La_{0.7}Ca_{0.3}Mn_{1-x}Cr_xO_3$ and $La_{0.7}Ca_{0.3}Mn_{1-x}Fe_xO_3$ ($0 \leq x \leq 1$) have been prepared by conventional solid state reaction method. The single phased x-ray patterns of $La_{0.7}Ca_{0.3}Mn_{1-x}Cr_xO_3$ and $La_{0.7}Ca_{0.3}Mn_{1-x}Fe_xO_3$ ($0 \leq x \leq 1$) series powders are indexed with orthorhombic structure in *Pbnm* space group. Decrease in lattice volume with the Cr doping can be attributed to the smaller ionic size of Cr^{+3} (0.62 Å) than that of Mn^{+3} ion (0.64 Å). However, a regular shift towards lower angle is noticed on increasing Fe content even though Mn^{3+} ion and Fe^{3+} ion have same ionic radii (0.0645 *nm*). Although, volume is a complex quantity as in $La_{1-x}SrxMnO_3$ there is a decrease in volume except Sr ion has larger ionic radii [6]. One possibility may be the formation of magnetic polaron (self trapping of carrier along with lattice distortion) that can affect Mn-O bond length results a change in volume.

Figure 1 shows the electrical resistivity behavior of the nominal series. As Cr^{3+} ion has same electronic structure ($3d^3$, t_{2g}^3 e_g^0) as Mn^{4+} and can be connected to Mn^{3+} ion via oxygen in a similar way as for Mn^{4+}. Therefore, the double-exchange interaction between Mn^{3+} /Cr^{3+} and Mn^{3+}/Mn^{4+} pairs may be thought responsible for the high temperature peak and a small sensitivity about transition temperature in the Cr-doped samples. The second peak may result from the competition between DE and anti-ferromagnetic (AFM) interaction due to super-exchange mechanisms between Cr^{3+}/Cr^{3+} and/or Cr^{3+}/Mn^{4+} ions. At higher doping concentrations there is an absolute reduction in Mn^{3+} ion in comparison to both Cr^{3+} and Mn^{4+} ions as a result increases AFM correlations between Cr^{3+}/Mn^{4+} and Cr^{3+}/Cr^{3+} via super-exchange (SE) interactions. With increase in Cr doping other magnetic states like mixed FM and AFM are observed. The co-existence of FM and AFM states is supported by M-T and M-H curves. For 10% Cr doping the ZFC and FC curves is very well bifurcated at low temperatures and there is a sudden drop in magnetic moment at around 40*K*. This sudden drop represents some sort of magnetic anisotropy or magnetic frustration in the sample. Also from M-H curves it can be seen that the magnetization is not saturated and thus supports canted anti-ferromagnetic state that arises due to random distribution of Cr^{3+} ions with random oriented spin. With increase in Cr doping, the SE driven AFM interactions become more prominent than the DE based FM. The AFM-FM phase transition is seen clearly for Cr = 0.50. Though still there is canted spin state behavior generated by

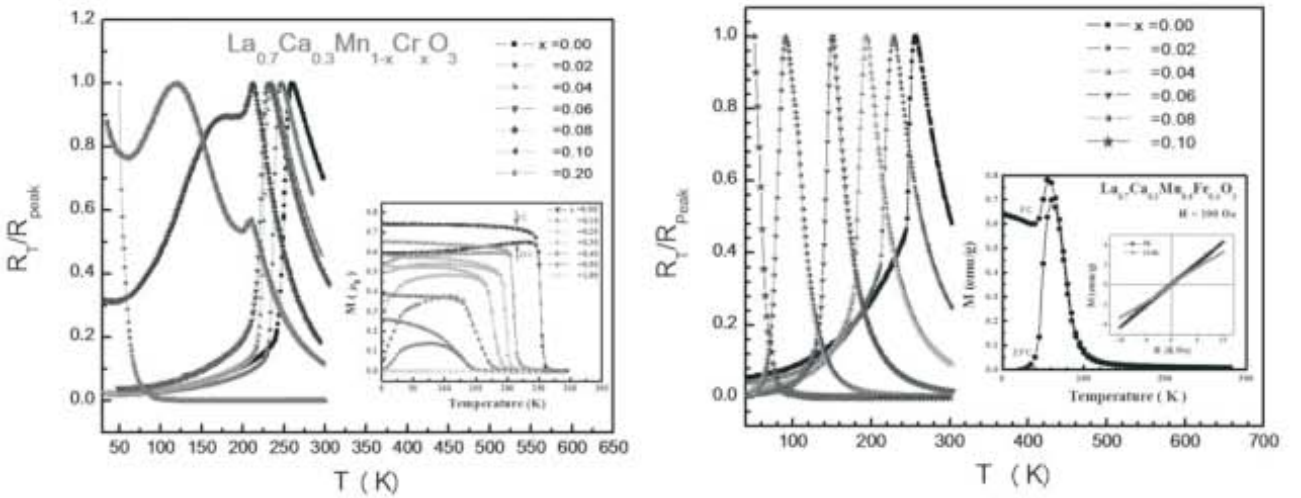

Fig 1: Temperature (K) variation of resistivity, Magnetization (M) vs. Temperature (K) and Magnetization (M) for the nominal compounds

the competition between FM and AFM. On the other hand as we increase the Fe doping concentration, T_{MI} temperature shifts towards low temperatures faster than Cr doping. The remarkable influence of Fe doping on electrical transport properties is characterized by the tremendous shift of T_{MI} temperature from 257*K* to 90.4*K* only for x = 0.08 and destruction of conductivity with Fe doping. As XPS study suggests the presence of only Fe^{3+} ions in our system and due to their half filled stable 3d-state ($3d^5$, t^3_{2g} e^2_g), Fe doesn't takes part in DE conduction mechanism. With Fe doping the available hopping sites suppresses and x > 0.08 compound behaves as insulator. With increase in Fe-doping concentration the magnetization moment decreases due to increases in anti-ferromagnetic interaction. For x>0.30 magnetic measurements shows an anti-ferromagnetic nature with Neel temperature below 50 *K*. For all the other doped compounds *M* does not show saturation even under the field of 20 *KOe*. The $La_{0.7}Ca_{0.3}Mn_{1-x}Fe_xO_3$ transforms from pure ferromagnetic (FM) for lower x (x<0.10) values to AFM for higher x (x>0.30) and exhibits spin glass (SG) like character for intermediate x i.e. 0.10 < x < 0.30. The SG reason appears mainly due to competing DE driven FM and SE driven AFM interactions. The competeting nature of both interaction forms magnetic polaron that shows the anomalous structural behavior in the studied $La_{0.7}Ca_{0.3}Mn_{1-x}Fe_xO_3$ system.

REFERENCES

1. Y. Tokura and N. Nagosa, Science 288, 468 (2000)
2. C. Zener, Phys. Rev. 82, 403 (1951)
3. Neeraj Kumar, Ashok Rao, H. Kishan and V. P. S. Awana, J. Appl. Phys. 107, 083905 (2010)
4. eeraj Kumar, H. Kishan and V. P. S. Awana, J. Alloys and compounds 502, 283-288 (2010)

TUNING Ce-OXYPNICTIDES SUPERCONDUCTORS WITH DOPING

S. J. Singh[1], S. Patnaik[1], J. Prakash[2], A. K. Ganguli[2]

[1]*School of Physical Sciences, Jawaharlal Nehru University, New Delhi 110067 India*
[2]*Department of Chemistry, Indian Institute of Technology, New Delhi 110016 India*
Email: spatnaik@mail.jnu.ac.in, shivjees@gmail.com

The parent compound of newly discovered FeAs based oxypnictides shows anomalous behaviour around 150 K due to structural phase transition followed by long-range antiferromagnetic (AFM) ordering. This anomaly disappears when the compounds become superconducting through electron or hole doping. Here we have taken Ce-based oxypnictides and studied the effect on superconducting properties by substitution with fluorine (F), cobalt (Co), yttrium (Y) and antimony (Sb) at different sites of CeOFeAs. All samples were synthesized by two step solid state reaction method and phase purity is confirmed by X-ray diffraction (XRD) technique. The transition temperature (T_c) and upper critical field (H_{c2}) reached maximum of 48.6 K and 146 T respectively.

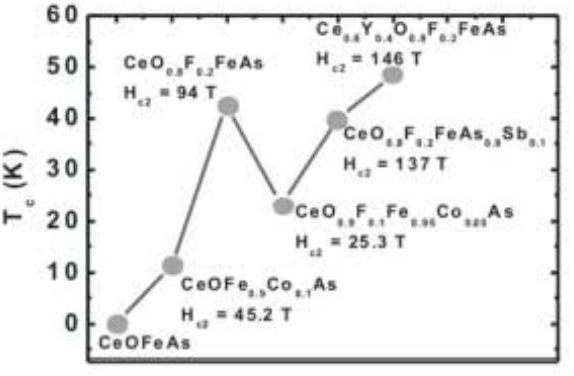

The magnetization curve of all samples showed very little hysteresis indicating weak link behaviour or an imperfectly connected superconducting state. The remanent magnetization showed one major peak that confirmed substantial electromagnetic granularity. The magnetization critical current density increased by an order of magnitude at 30 K and 1 T magnetic field with yttrium substitution. The thermoelectric power and Hall measurement confirmed the dominant role played by electrons in these multiband superconductors. The rf penetration depth analysis indicated s-wave pairing symmetry with two gap values for all superconducting samples.

REFERENCES

1. Y. Kamihara et al., J. Am. Chem. Soc. 130, 3296 (2008).
2. S. J. Singh et al., Solid State Communications 149, 181 (2009).
3. S. J. Singh et al., Physica C 469, 82 (2009).
4. S. J. Singh et al., J. Phys.: Condens. Matter 21, 175705 (2009).
5. S. J. Singh et al., Applied Physics Letter 95, 262507 (2009).
6. S. J. Singh et al., J. Solid State Chemistry 183, 338 (2010).
7. A.K. Ganguli, S. J. Singh et al., Eur. Phys. J. B. 73, 177 (2010).
8. S. J. Singh et al., Physica C (accepted) (2010).

DYNAMICS OF MAGNETIC FLUIDS IN PRESENCE OF MAGNETIC FIELD STUDIED USING TEM AND SQUID MAGNETOMETRY

Mohini Gupta, Manish Sharma

Center for Applied Research in Electronics, Indian Institute of Technology, Delhi, Hauz Khas, New Delhi-110016
Email: manish@care.iitd.ac.in

Superparamagnetic iron oxide nanoparticles (SPIONs) are a promising material for medical applications as drug delivery system, molecular resonance imaging, cancer therapy etc. Several ferrofluid samples were prepared by precipitation method using ferrous chloride tetra hydroxide and sodium hydroxide as precursors. The reactions were initially carried out at high temperature with different concentration of iron salts. These magnetic nanoparticles then disperse in milli Q-water to measure the dynamics in suspension.

The particle diameter polydispersity profile and crystal structure of iron oxide nanoparticles were measured by transmission electron microscopy (TEM) and X-ray diffraction analysis. The measured particles were confirmed to be crystalline magnetite (cubic spinel structure) with an average size of 9.5 nm. Magnetic measurements done using SQUID predict a magnetic particle size of 7.75 nm, that is smaller than the size measured by TEM. This suggests a "magnetically dead layer" is present on the surface of particles because of its surface anisotropy.

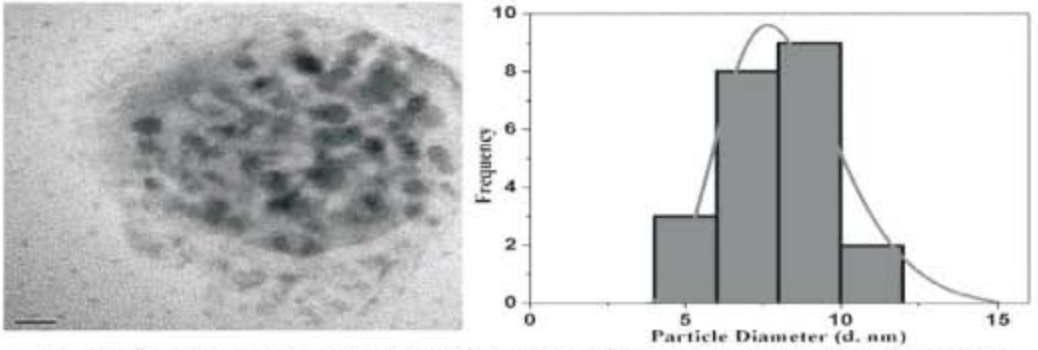

Fig. 1: (a) TEM of Magnetic nanoparticles (b) Particle size distribution (PSD) fitted by log-normal distribution.

REFERENCES

1. R. E. Rosensweig, *Ferrohydrodynamics*, New York : Dover , (1997).
2. H.C. Yang et al. *JAP* 99, 124701, (2006)
3. P. Tartaj et al. *J. Phys. D: Appl. Phys.* 36, R182-R197 (2003)
4. Y. R. Chamla et al. *PANS 97*, 14268-14272, (2000)
5. D. Eberbeck, F. Wiekhorst, U. Steinhoff and L. Trahms, *J. Phys.: Condens.Matter.* 18, S2929, (2006).
6. J. H. E. Promislow, A.P. Gast and M. Fermigier, *J.Chem. Phy.*, 102, 5492, (1995).
7. Q. A. Pankhurst, J. Connolly, S. K. Jones and J. Dobson, *J. Phys. D: Appl. Phys.* 36, R167 (2003).

FERROMAGNETIC NANOWIRES FOR MICROWAVE APPLICATIONS

Monika Sharma, Sachin Pathak, Manish Sharma, Anandan Basu

Center for Applied Research in Electronics, Indian Institute of Technology Delhi, India
Email: manish@care.iitd.ac.in

In recent years, a great deal of attention has been focused on magnetic nanowires embedded in an insulating matrix as a promising candidate for high frequency applications[1-2]. Ferromagnetic nanowires embedded in insulating templates have higher saturation magnetization compared to ferrites so higher operating frequency can be achieved very easily. The small diameter in nanometer limits the eddy current loss and eliminates the skin effect. Microwave devices, such as unbiased circulators, isolators and band stop filters, based on magnetic nanowire array have small size and broad bandwidth. The frequencies in these devices can be tuned using external magnetic field[3].

Our group is presently working on the fabrication of such kind of nanostructures in different insulating matrix like polycarbonate membrane and anodic alumina template as shown in Figure 1. Scanning electron microscope confirmed the presence of nanowires in these templates Figure 2. Structural and compositional analysis was done using X-ray diffraction and energy dispersive X-ray spectroscopy as shown in Figure 3. For microwave measurement, the FMR technique is used which can provide valuable information about the properties of material as well as microwave properties for device application.

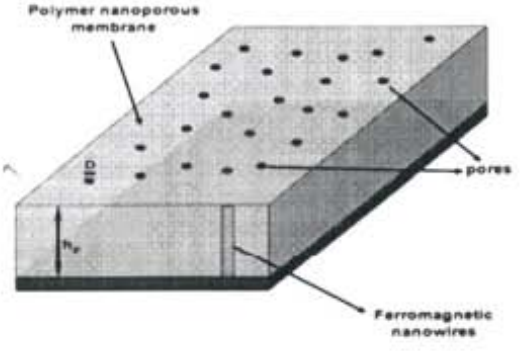

Figure 1: Ferromagnetic nanowires in PCT

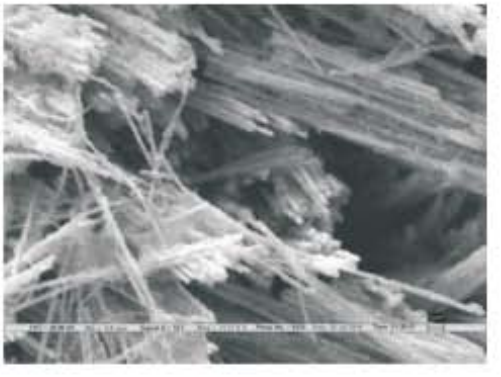

Figure 2: SEM image of Co nanowires

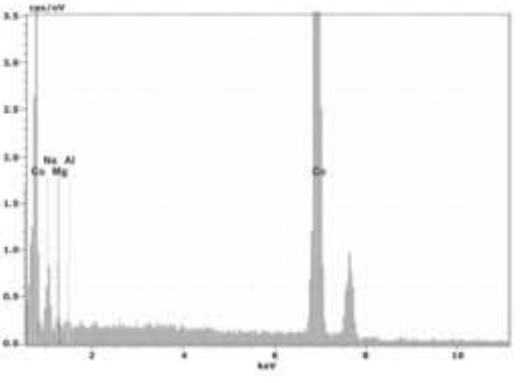

Figure 3: EDX spectrum of Co nanowires

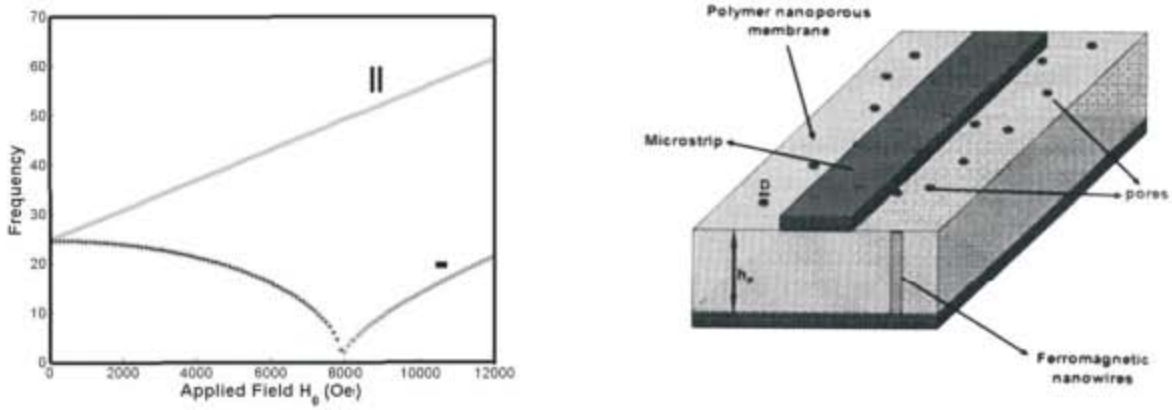

Figure 4: (a) Simulated plot of field dependence of resonance frequency (b) microstrip geometry over ferromagnetic nanowire embedded polycarbonate membrane

Figure 4(a) shows the simulated plot of field dependence of ferromagnetic nanowires along parallel and perpendicular axis. It revealed that with increase of external magnetic field resonance frequency increases. Figure 4(b) shows the model of microwave device on which we are working. It consists of a transmission line over the polycarbonate template containing ferromagnetic nanowires.

REFERENCES

1. Sklyuyev et al., Microwave studies of magnetic anisotropy of Co nanowire arrays, Journal of Applied Physics **105**, 023914 (2009).
2. G. Goglio et al., Microwave properties of metallic nanowires, Applied Physics Letter **75**, 1769 (1999).
3. G. Kartopu et al., Preparation and FMR analysis of Co nanowires in alumina templates, Journal of Magnetism and Magnetic Materials **321**, 1142 (2009).

ELECTRON-PHONON MECHANISM IN HIGH TEMPERATURE SUPERCONDUCTING PHASE

VINOD ASHOKAN[1], B.D. INDU[2]

Department of Physics, Indian Institute of Technology Roorkee, Uttrakhand-247667, India
Email: vamumdph@iitr.ernet.in

An expression for electron-phonon line width is developed for high temperature superconducting materials with the help of double time thermodynamic electron Green's function via an almost complete Hamiltonian which consists of all the contributions of a real system, namely, electrons, phonons, defects, anharmonicities and interaction thereof. The life time for electron-phonon scattering phenomenon, thus obtained is found highly sensitive to temperature and frequency variations and explains well the thermal conductivity data in during the spectacular dip in the vicinity of transition temperature. The sensitivity of this term is described by various calculations for high temperature superconducting solids. This also establishes the importance of electron-phonon coupling to create pairons, responsible for the high temperature superconducting phenomenon.

EXPLORING THE ROLE OF BaO/SrO LAYERS IN DECIDING THE ELECTRONIC STRUCTURE OF $Cu_{0.3}Co_{0.7}Ba_{2-x}Sr_xYCu_2O_{7+\delta}$ x=0, 1 & 2

Shiva Kumar Singh,[1,2] M. Husain,[2] H. Kishan[1], V.P.S Awana[1]

[1]*Quntum Phenomena and Application, National Physical Laboratory (CSIR), New Delhi-110012, India*

[2]*Department of Physics, Jamia Millia Islamia, New Delhi-110025, India*

Email: awana@mail.nplindia.ernet.in

Here we are studying the change in electronic structure $Cu_{0.3}Co_{0.7}Ba_{2-x}Sr_xYCu_2O_{7-}$ with change in structural pressure. The Rietveld refined X-ray diffraction pattern shows the samples are phase pure. The XPS measurements are done to find out the variation in ionic state Co and Cu with ionic size variation in BaO/SrO layers.

The samples are synthesized in air by solid-state reaction route. The samples have been characterized by X-ray photoelectron spectroscopy (XPS), working at a base pressure of $5x10^{-10}$ torr. We have used Mg-Kα (1253.6 eV) X-ray source for our analysis. The calibration of the binding energy scale has done with the C (1s) line at 284.6 eV. The $CoSr_2YCu_2O_{7+\delta}$ (Co-1212) is crystallize in orthorhombic *Ima2* phase [1] whereas with Ba ion on Sr ion site ($Cu_{1-x}Co_xBa_2YCu_2O_{7+\delta}$, x=0.84 composition) was reported to crystallize in tetragonal *P4/mmm* space group [2].

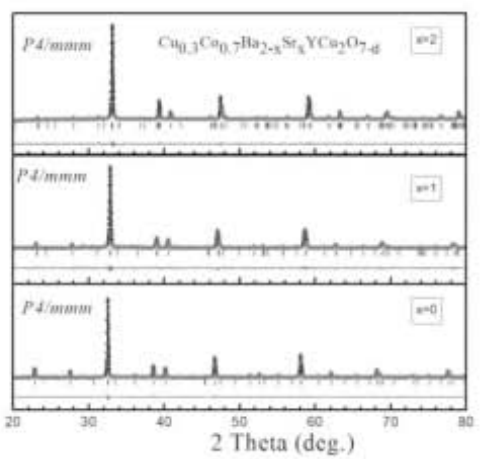

Fig.1 Rietveld fitted XRD pattern of $Cu_{0.3}Co_{0.7}Ba_{1-x}Sr_xYCu_2O_{7+\delta}$ (x=0, 1 & 2) samples with space group *P4/mmm*.

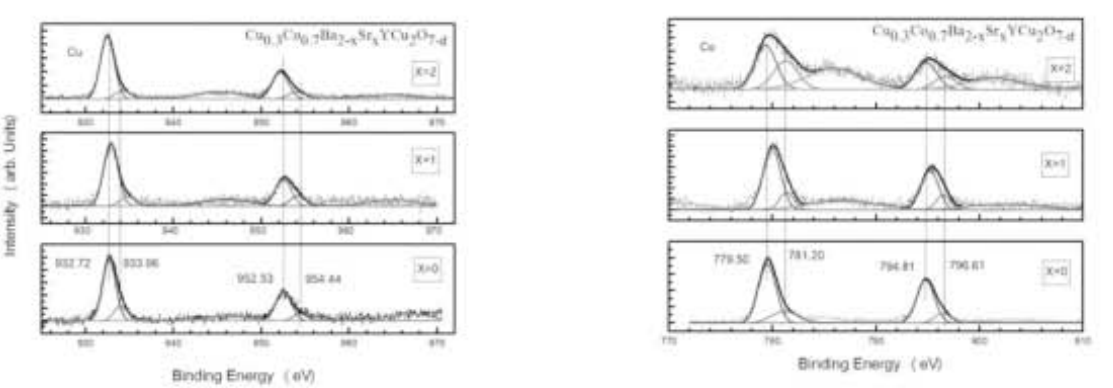

Fig2. (a) The Cu2*p* XPS spectra. (b) The Co2*p* XPS spectra for the sample *x*=0, 1 & 2.

All the compositions (x=0, 1 & 2) are fitted in tetragonal *P4/mmm* space group [Fig.1]. The monotonic decrease in lattice parameter clearly indicates that Sr^{2+} ion with lower ionic radii (1.18 Å CN VI) replacing Ba^{2+} with higher ionic radii (1.35Å CN VI). To find out the oxidation state of Cu & Co the XPS study has been carried out. The Cu (2p) & Co (2p) core level spectra have been deconvoluted in to the different Gaussian component to find out the contribution of different ionic states [Fig. 2a, 2b]. The deconvoluted Cu (2p) core level spectra for all samples are shown in Fig. 2a. Deconvolution of Cu (2p) core level spectra shows the presence of Cu^{2+} and Cu^{3+} with a satellite peak, at the binding energy of 932.72 eV & 933.96 eV for Cu ($2p_{3/2}$) and 952.53 eV & 954.44 eV for Cu ($2p_{1/2}$) in all compositions. Similar results have also been reported in literature regarding binding energy of $Cu^{2+/3+}$ [3]. Comparing to the spectrum of x=0.0, the binding energy of two main component of Cu ($2p_{3/2}$ and $2p_{1/2}$), in the spectrum for the sample x=1, shifts towards higher binding energy. But there is decrease in valence state of Cu ion in x=2 sample. The concentration of Cu^{3+} contribution is very less in comparison of Cu^{2+}. The deconvoluted Co (2p) core level spectra for all samples are shown in Fig. 2b. Comparing to the spectrum of x=0.0, the binding energy of two main component of Co ($2p_{3/2}$ and Co $2p_{1/2}$), in the spectrum for the sample x=1 & 2, shifts towards higher binding energy. We have observed peak broadening in the x=2 in comparison to x=0.0. Deconvolution of Co (2p) core level spectra shows the presence of Co^{3+} and Co^{4+} with a satellite peak, at the binding energy of 779.50 eV & 781.20 eV for Co ($2p_{3/2}$) and 794.81 eV & 796.61 eV for Co($2p_{1/2}$) respectively in all compositions. The similar kinds of results have also been reported in literature regarding concentration and binding energy of $Co^{3+/4+}$ [4]. Curve shows the domination of Co^{3+} state over Co^{4+} state for x=0 & 1 sample, but for x=2 both states are almost equal. The corresponding variation in the valence state of Co is can be observed i.e. it is increasing monotonically. The observed behaviour can be explained as; in x=1 the small increase in valance of Cu is due to the chemical pressure (smaller ionic radii of Sr ion). In x=2 the decrease in valance state of Cu may be due to structural changes. Since $CoSr_2YCu_2O_{7+\delta}$ is crystallize in orthorhombic *Ima2* [1, 4] and it our x=2 sample has 30% Cu at Co site hence it may have the in between structure of orthorhombic *Ima2* and tetragonal *P4/mmm* space group. For further confirmation we fitted it in orthorhombic *Ima2* space group and it shows a good fit. Since in *Ima2* space group the unit cell got doubled than *P4/mmm* space group hence it may have some impact on carrier doping in CuO_2 planes.

REFERENCES

1. T. Nagai et. al. Journal of Solid State Chemistry 176 213 (2003)
2. P. Zolliker et. el. Phy. Rev. B 38, 6575 (1988)
3. J. Ghijsen, et. al. Phy. Rev. B 38, 11322 (1988)
4. Shiva Kumar, et. al. J. Appl. Phy 107, 063905 (2010)

SUPPRESSION OF SPIN DENSITY WAVE TRANSITION BY Ni DOPING IN $EuFe_2As_2$

ANUPAM[1], P. L. PAULOSE[2], S. RAMAKRISHNAN[2], Z. HOSSAIN[1]

[1]*Department of Physics, Indian Institute of Technology Kanpur, Kanpur - 208016, India*

[2]*Tata Institute of Fundamental Research, Homi Bhabha Road, Mumbai - 400005, India*

E-mail: anupam@iitk.ac.in

The recent discovery of high temperature superconductivity in FeAs based compounds has generated tremendous interest among scientific community. The parent compounds of these iron-based systems exhibit spin density wave (SDW) transition (in the temperature range of 140 – 200 K), which can be suppressed either by hydrostatic pressure, chemical pressure or electron/hole doping to induce superconductivity (SC) [1]. Among the AFe_2As_2 (A = Sr, Ba, Eu and Ca) series, $EuFe_2As_2$ is of particular interest to study the effect of large magnetic moment on Eu^{2+} ions, on its magnetic and superconducting properties. $EuFe_2As_2$ exhibits two magnetic transitions at T_{SDW} = 190 K and T_N = 19 K corresponding to SDW anomaly accompanied or followed by a structural transition and the antiferromagnetic ordering of Eu^{2+} ions, respectively [2]. The doping of Ni at Fe site does not lead to superconductivity down to 2 K by [3]. We have prepared and investigated the polycrystalline samples of $EuFe_{2-x}Ni_xAs_2$ (x = 0, 0.1) using magnetic susceptibility and electrical resistivity measurements. We found that the Ni doping at iron site destroys the spin density wave and antiferromagnetic (AFM) transition completely and give rise to ferromagnetism (FM) below 17 K. This behavior is in contrast to what has been observed for $BaFe_2As_2$ and $SrFe_2As_2$, where Ni doping gives rise to superconductivity below 20 K [4, 5]. The suppression of SDW transition is further confirmed by ^{57}Fe Mössbauer studies.

In addition to FM transition in our sample, two more transitions are observed at T_{peak} = 11.5 K and T_g = 3.5 K. The broad transition at T_{peak} could be due to the transition from FM to AFM state,

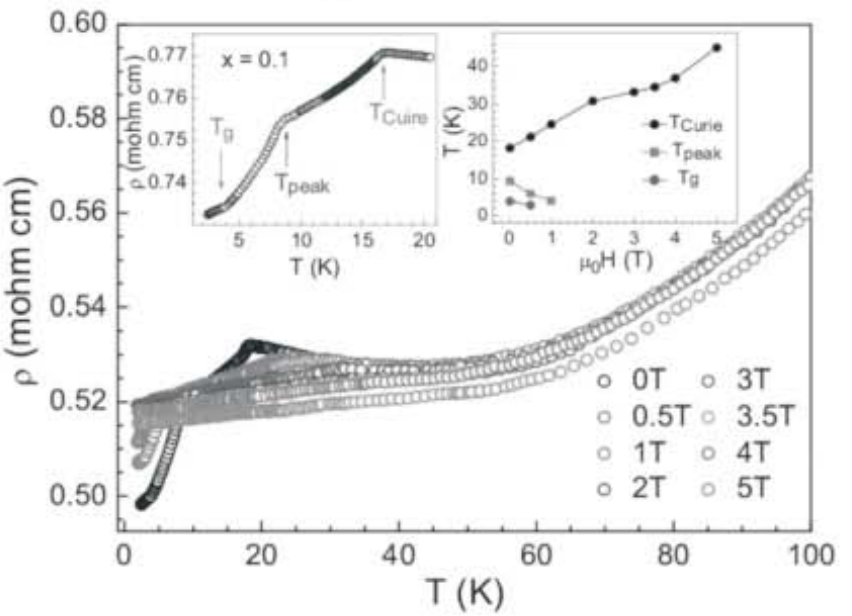

Figure 1: The temperature dependence of electrical resistivity for $EuFe_{1.9}Ni_{0.1}As_2$ at different magnetic fields. The left inset shows the resistivity in the temperature range of 2-20 K. The three anomalies are marked by the arrows. The right inset shows the *H-T* phase diagram.

while the origin of the transition at 3.5 K is not clear. We have done some frequency dependent ac susceptibility measurements and found that this transition shifts towards higher temperature with increase in frequency. This suggests that it could be due to the spin glass ordering, which might arise due to the competition between FM and AFM ordering. Figure 1 shows the temperature dependence of electrical resistivity at different magnetic fields. The insets show the resistivity at low temperature range of 2-20 K. At lower temperature, three kinks are present which corresponds to FM ordering (T_{Curie}), the transition from FM to AFM state (T_{peak}) and spin glass ordering (T_g). An upturn followed by a hump is observed below 50 K, which can be suppressed completely with increase in the Ni doping. With increase in magnetic field the transition at low temperatures T_{peak} and T_g get suppressed while the T_{Curie} increases. The *H-T* phase diagram obtained from the electrical resistivity data is shown as inset in Fig 1.

REFEERENCES

1. Y. A. Izyumov and E. Z. Kurmaev, Physics-Uspekhi **51** (12), 1261 (2008) and the references therein.
2. H. S. Jeevan, Z. Hossain, D. Kasinathan, H. Rosner, C. Geibel, and P. Gegenwart, Phys. Rev. B **78**, 052502 (2008).
3. Z. Ren, X. Lin, Q. Tao, S. Jiang, Z. W. Zhu, C. Wang, G. H. Cao, and Z. A. Xu, Phys. Rev. B **79**, 094426 (2009).
4. L. J. Li, Y. K. Luo, Q. B. Wang, H. Chen, Z. Ren, Q. Tao, Y. K. Li, X. Lin, M. He, Z. W. Zhu, G. H. Cao, and Z. A. Xu, New J. Phys. **11**, 025008 (2009).
5. S. R. Saha, N. P. Butch, K. Kirshenbaum, and J. Paglione, Phys. Rev. B **79**, 224519 (2009).

STRAINED TUNED MAGNETISM IN NONMAGNETIC $LaCoO_3$

Kapil Gupta, Priya Mahadevan

S. N. Bose National Centre for Basic Sciences,
Block-JD, Sector-III, Salt Lake City, Kolkata-700 098, INDIA.
Email: kapil@bose.res.in

A variety of electronic and magnetic properties are observed in 3d transition metal oxides as a result of the strongly coupled spin, orbital and charge degrees of freedom. Thin films represent a means of tuning the ground state properties externally. $LaCoO_3$(LCO) is one of the materials that has been studied in this context. Bulk LCO shows interesting temperature dependent properties, and the aim has been to explore the possible modifications in these properties externally.

Bulk $LaCoO_3$ at low temperature is found to exhibit a low spin state with an electronic configuration of $t^6_{2g}e^0_g$ on Co. It shows anomalous temperature dependence of its susceptibility as well as spectral features in x-ray absorption experiments. These have been interpreted as a spin state transition. However the nature of the transition is still a matter of debate being whether it is a low to high or low to intermediate spin state transition. This crossover takes place as a result of a delicate interplay between the crystal-field splitting and the intra-atomic exchange interaction.

Recent work on thin films of $LaCoO_3$ [1] grown on different substrates, found that the strained films exhibited ferromagnetism with a Curie temperature as large as 85 K for films grown on $(LaAlO_3)_{0.3}(SrAlTaO6)_{0.7}$ (LSAT). A possible explanation that was offered was that the rotation of the CoO_6 octahedra was smaller in the strained films. It was speculated that this led to a near 180^0 Co-O-Co angle which was responsible for the stabilization of the ferromagnetic state.

To address this issue[2] we have considered tetragonal unit cells of LCO where the in-plane and out-of-plane lattice constants have been kept fixed to the experimental values. We however allowed for a rotation of the CoO_6 octahedra which is a commonly observed lattice distortion in perovskite oxides, and optimized the total energy as a function of the. Contrary to earlier speculations we find that there is a very slight angle dependence of the strained films. This therefore cannot be the reason for the spin state transition observed by us in our calculations. The in-plane angle changes are small and cannot explain the stabilization of the ferromagnetic state for finite strain. The out-of- plane Co-O-Co angles are found to decrease with strain in contrast to earlier speculations where angles were expected to approach 180° for films of LCO on LSAT/STO. Hence it is primarily the change in bond lengths as a result of substrate strain which drives the system into the ferromagnetic state. Examining the total energies from our calculations we find that ferromagnetic state is the ground state for the strained films while all nonmagnetic and magnetic solutions lie quite close to each other for unstrained LCO films on LCO.

Further, as support to the model proposed by us, we are able to explain the temperature dependence of the x-ray absorption spectra within our calculations. Experimentally it was found that the films of LCO grown on LCO showed a strong temperature dependence of the O K edge as well as the Co L edge x-ray absorption spectra. LCO films grown on LSAT substrate however did not show any significant temperature dependence. Comparing the total energies obtained by us from calculations for different magnetic states, we find that for LCO on LCO the nonmagnetic solution as well as the other magnetic solutions lie very close in energy. The magnetic solutions correspond to an intermediate spin state. We show that temperature effects change the relative concentrations of

low spin and intermediate spin states, hence explaining the temperature dependence of the spectra. However as the substrate strain is varied, the intermediate spin state gets frozen in as the ground state; the low spin state lies much higher in energy and hence there is no temperature dependence.

REFERENCES

1. D. Fuchs, E. Arac, C. Pinta, S. Schuppler, R. Schneider, and H. v. Löhneysen Phys. Rev. B **77**, 014434 (2008).
2. Kapil Gupta and Priya Mahadevan , Phys. Rev. B **79**, 020406(R) (2009).

FIRST-PRINCIPLES PREDICTION OF Mn-BASED SUPERCONDUCTING PARENT COMPOUND

U.B. Paramanik, Z. Hossain, R. Prasad, S. Auluck

Department of Physics, Indian institute of Technology- Kanpur 208016 India
Email: puday@iitk.ac.in

Here we present electronic band structure, magnetic properties and valence charge density of a hypothetical compound LaOMnSe by first-principles density-functional calculations. The electronic structures were determined by the Full- Potential LAPW method implemented in WIEN2K101. Fermi surfaces were visualized with XcrysDen[1]. The results show that LaOMnSe has similar properties as that of LaOFeAs, the newly discovered parent compound of Fe-As based superconductor. If we replace Fe by Mn and As by Se, its electronic structure will be similar to that of LaOFeAs because the electron number in MnSe-layer is same as that in FeAs-layer. The calculated Manganese moment is close to 2.53 μ_B in LaOMnSe compared to the Iron magnetic moment of 2.03 μ_B in LaOFeAs. The bands around the Fermi level for the compound are primarily formed by Mn-d states similar to Fe-d states for LaOFeAs Ref. [2]. The calculated Fermi surface (FS) in the non-magnetic phase consists of three hole-like sheets around Γ -point and two electron-like surfaces around M-point, similar to the Fermi surface of LaOFeAs. The FS sheets around Γ and M points are nearly parallel, suggesting that significant nesting effect can occur by a wave vector q = (π,π0), giving rise to a certain kinds of ordering, such as charge density wave (CDW) or spin density wave (SDW) at low temperature in the undoped compound, just like LaOFeAs [3,4]. It should be possible then to suppress the CDW/SDW phase and induce superconductivity. We, thus, predict LaOMnSe to be a parent compound of a new type of superconductor.

REFERENCES

1. Karlheinz Schwarz Computational Materials Science 28 (2003) 259–273
2. JETP Letters, 2008, Vol. 88, No. 2, pp. 144–149.
3. D.J. Singh, M.H. Du, Phys. Rev. Lett. 100 (2008) 237003
4. J. Dong, et al., Europhys. Lett. 83 (2008) 27006

SUPERCONDUCTIVITY IN THE VICINITY OF FERROMAGNETISM IN OXYGEN FREE PEROVSKITE $MgCNi_3$

V.P.S. Awana, R. Jha, A. Vajpaye, H. Kishan, R.C. Budhani

Quantum Phenomena and Applications, National Physical Laboratory (CSIR), New Delhi-12, India
Email: awana@mail.nplindia.ernet.in

Superconductivity in the inter-metallic system $MgCNi_3$ was discovered in 2001 with transition temperature near 8 K [1]. The compound has the classical cubic perovskite structure with space group *Pm*3*m*. In addition, $MgCNi_3$ is the only known non-oxide perovskite that superconducts. Because of the large content of Ni in $MgCNi_3$, this material lies in close proximity to ferro-magnetism [2]. The occurrence of superconductivity in $MgCNi_3$ is unusual and a border line case between the conventional nonmagnetic and ferromagnetic superconductors [3]. The conduction electrons of $MgCNi_3$ are derived predominantly from Ni which is ferromagnetic (FM) [2,3]. Carbon atom in $MgCNi_3$ plays a critical role in its superconductivity. Single-phase superconducting compound (MgC_xNi_3) is formed in a narrow range of Carbon content ($0.85<x<1.0$) [4]. In brief, $MgCNi_3$ is a superconductor equipped with its rich physics and hence of tremendous interest to both experimentalists and theoreticians.

Here, we report synthesis, structural analysis and magnetization studies of $MgCNi_3$ compound. Polycrystalline $MgCNi_3$ samples were synthesized by double step solid-state reaction route. The stoichiometric amounts of ingredients were ground thoroughly and palletized using hydraulic press. These pallets were encapsulated in iron tube and heated at 600°C for 2 hours in the continuous flow of argon gas followed by heating at higher temperatures i.e. 900, 930, 950, 975 & 1000 °C for 3 hours and finally cooled to room temperature in the same atmosphere. Magnetic measurements were carried out using a vibrating sample magnetometer.

The crystal structure of these $MgCNi_3$ compounds was determined by Rietveld analysis of room temperature X- ray powder diffraction (XRD) patterns. The observed and Rietveld calculated powder diffraction patterns for 930, 950, and 975 °C synthesized samples are shown in Figure 1. All the samples have the cubic perovskite structure with space group *Pm*3*m*. The coordinate positions for the atoms are: Mg: 1a (0,0,0), C: 1b (0.5,0.5,0.5) and Ni: 3c (0,0.5,0.5). We observed an extra peak due to the presence of unreacted carbon at around 44.5 degree in XRD pattern for all the sintering temperatures. It is found that 950°C is the optimum sintering temperature with least amount of (Please see Figure 1) impurity Carbon. Lattice parameters of the studied $MgCNi_3$ (sintered at 950°C) is found to be around 3.796(6)Å, with only little variations with sintering temperature. Figure 2 shows the DC magnetization of the $MgCNi_3$ sample (sintered at 950°C) in FC and ZFC situations in 10 Oe field. Sample shows bulk superconductivity with an onset temperature (T_c^{onset}) of 7.5 K. Figure 3 represents the AC magnetization of the same sample which also confirms the bulk superconductivity at around 7.5 K in the present compound. A positive background is seen in the normal state magnetization of the compound due to ferromagnetic contribution from ordered Ni atoms. The magnetization $M(H)$ loops of $MgCNi_3$ at 2 and 4K are shown in figure 4, which are typical for any FM superconductor, i.e. positive FM signal is riding over the superconducting diamagnetic response. The FM response is seen clearly when the $M(H)$ loop of $MgCNi_3$ is recorded at 10 K (normal state), see upper inset in Fig.4. The saturation moment is $0.76\mu_B$/Ni atom. The lower inset of Fig.4 shows the lower critical field (H_{c1}) of the compound which is around 500 Oe at 2 K. In conclusion

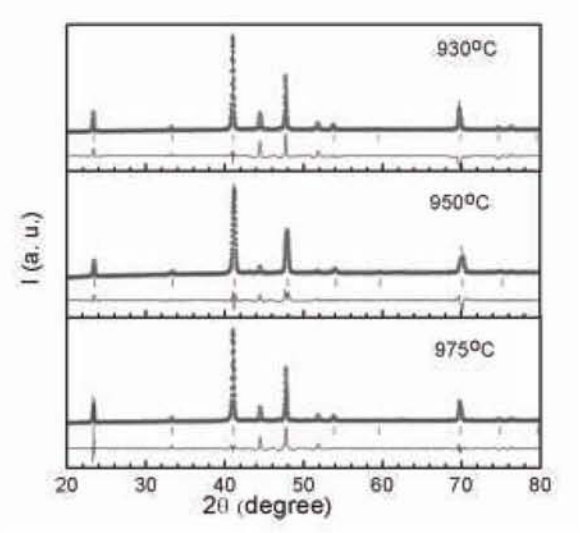

Fig 1: Rietveld analysis of room temperature XRD

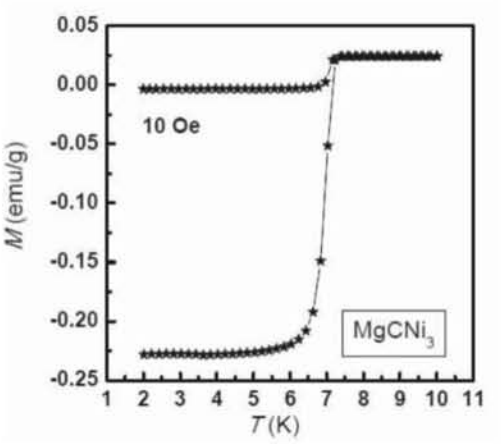

Fig 2: DC magnetization of $MgCNi_3$ in FC and ZFC

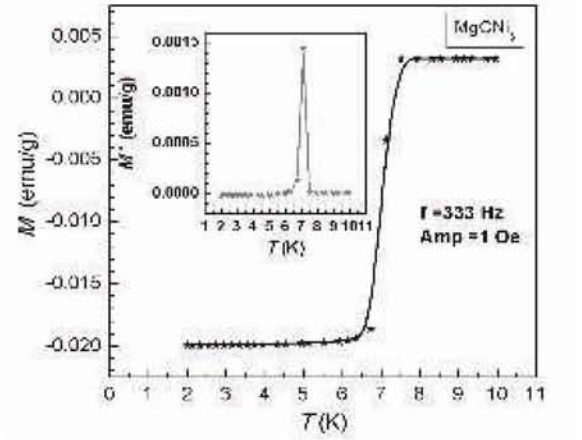

Fig 3: AC magnetization of $MgCNi_3$

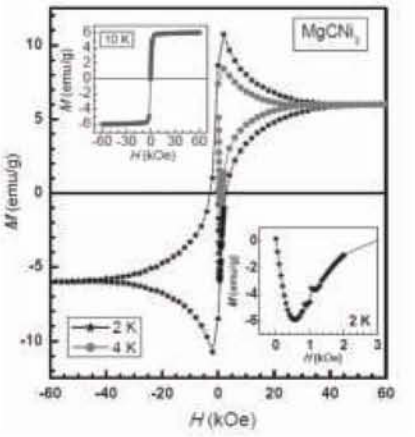

Fig.4: $M(H)$ loop of $MgCNi_3$ at 2, 4 & 10 K

we have optimized the synthesis temperatures for phase pure bulk superconducting and FM $MgCNi_3$ compound with transition temperature (T_c) of 7.5 K. More physical property measurements including magneto-transport, thermo-electric power and heat capacity will be carried out and presented.

REFERENCES

1. T. He, Q. Huang, A. P. Ramirez, H. W. Zandbergen, N. P. Ong and R. J. Cava, Nature, 411 (2001) 54
2. H. Rosner, R. Weht, M.D. Johannes, W.E. Pickett and E. Tosatti, Phys. Rev. Lett. 88 (2002) 27001
3. A.L. Ivanovskii, Phys. Solid state 45 (2003) 1829
4. Y. X. Yao, Z. A. Ren, G. C. Che, H. H. Wen, and Z. X. Zhao Supercond. Sci. Technol. 17 (2004) 608

ANHARMONICITY AND DISORDER EFFECTS ON ELECTRON DENSITY OF STATES OF HIGH TEMPERATURE SUPERCONDUCTORS

VINOD ASHOKAN[1], B.D. INDU[2], ANU SINGH[3], H. P. SINGH[4]

Department of Physics, Indian Institute of Technology Roorkee, Uttrakhand-247667, India
[1]vamumdph@iitr.ernet.in, [2]drbdindu@gmail.com, [3]anuiiser@gmail.com,
[4]singh_hempal@rediffmail.com

The expression for the electron density of states (EDOS) of high temperature superconductors (HTS) has been investigated taking the disorder and anharmonicity effects as a central problem. This has been dealt with the help of double time thermodynamic Green's function theory for electrons via a newly formulated Hamiltonian which consists of the contribution from (i) unperturbed electrons, (ii) unperturbed phonons, (iii) isotopic impurities and (iv) anharmonicities (no BCS type Hamiltonian has been taken up in the formulation). The renormalization effects and emergence of pairons, which is appears as a unique feature of the theory dependence of EDOS on impurity concentration and temperature have been discussed in details with special reference to the HTS.

REFERENCES

1. J. C. K. Hui and P. B. Allen, J.Phys. F4, (1974) L42.
2. G. D. Mahan and J. O. Sofo, Phys. Rev. B 47 (1993) 8050.
3. S. Fujita and S. Godoy, Theory of High Temperature Superconductivity (Kluwer Academic Publishers, New York), (2003).
4. A. A. Maradudin, P. A. Flinn and R. A. Coldwell-Horsefall, Ann. Phys. 15 (1961) 337; ibid. 15 (1961) 360; ibid. 22 (1963) 223.
5. A. A. Maradudin, Solid State Physics, Vols. 18 and 19, Eds., F. Seitz and D. Turnbull, Academic Press, New York, (1966) 273 Pg. 1.
6. R. W. H. Stevenson, Phonons in Perfect Lattice and Lattices with Point Imperfections, Oliver and Boyd, London, (1966).
7. L. R. Testardi, W. G. Moulton, H. Matials,H. K. Ng,C. M. Rey, Phys. Rev.B 37 (1988) 2324.
8. D. Feinburg, S. Ciouchi and F. Pasquale de, Int. J. Mod. Phys. B 1 (1990) 1317.
9. S. N. Behra and S. G. Mishra, Phys. Rev. B 31 (1985) 2773.
10. K. N. Pathak, Phys. Rev. 139 (1965) A1569.
11. B. D. Indu, In. J. Mod. Phys. B 4 (1990) 1379.
12. B. D. Indu, Mod. Phys. Lett. B 6 (1992) 1665.
13. P. K. Sharma and Rita Bahadur, Phys. Rev. B 12 (1975) 1522.
14. D. N. Zubarev, Usp. Fiz. Nauk. 71 (1960) 71 [English Transl: Sov. Phys. Uspehki 3 (1960) 320].
15. P. H. Dederichs, New concepts in the physics of phonons, (1977).
16. M. Arai, K. Yamada, Y. Hidaka, S. Itosh, Z. A. Bowden, A. D. Taylor, and Y. Endoh, Phys. Rev. Lett. 69 (1992) 359.

SUPPRESSION OF LONG RANGE FERROMAGNETIC ORDERING IN HIGHLY DISORDERED $La_{0.5-y}Y_ySr_{0.5}MnO_3$ MANGANITE SYSTEM: EVIDENCE OF METAMAGNETISM

SUBHRANGSU TARAN[1], ARIJIT GHOSH[1], B K CHAUDHURI [1], C. P. SUN[2], H. D.YANG[2], SANDIP CHATTERJEE[3]

[1]Solid State Physics Department, Indian Association for the Cultivation of Science, Jadavpur, Kolkata-700032, India.

[2]National Sun Yat-Sen university, Kaohsiung 804, Taiwan

[3]Institute of Technology, Beneras Hindu University, Varanasi – 221005 (UP), India

Email: sspbkc@rediffmail.com

The yttrium (Y) doped $La_{0.5"y}Y_ySr_{0.5}MnO_3$ ($0 \leq y \leq 0.25$) manganite system, even with higher A site ionic radii ($<r_A>$), possesses relatively much greater value of A-site variance σ^2 ($= \Sigma y_i^2 r_i^2 - <r_A>^2$) and as a consequence, the end members of this system (with y = 0 and 0.25) are found to be structurally different (rhombohedral and orthorhombic, respectively). Increase of *A*-site disorder (and hence σ^2), enhances random local radial distortion of the MnO_6 octahedra giving rise to the suppression of long-range ferromagnetic order (LRFO) in the present system. With further increase of σ^2, LRFO is further melted into the short-range magnetically ordered clusters which, at low temperature, invoking metastability within the ferromagnetic state, with no resemblance to spin glass or cluster glass phase. Structural disorder with ion doping is found to be a crucial factor for controlling the magnetic ordering in such colossal magnetoresistive system.

THE STUDY OF UPPER CRITICAL FIELD (H_{c2}) AND IRREVERSIBILITY FIELD (H_{irr}) OF TE DOPED α-FeSe

SUDESH[1], STUTI RANI[1], SAIKAT DAS[2], C. BERNHARD[2] G.D. VARMA[1]

[1]Indian Institute of Technology Roorkee, Roorkee-247667, India
[2]Department of Physics and Fribourg Centre for Nanomaterials-FriMat, University of Fribourg, Chemin du Musee, CH-1700 Fribourg, Switzerland
Email: gdvarfph@iitr.ernet.in

The pnictides containing FeAs layers has attracted much attention since the discovery of superconductive transition of 26-43K in Fluorine doped LaFeAsO[1]. These materials show an increase in superconductive transition temperature with the application of pressure. One way to look into the pressure effect is by chemically doping the sample with appropriate element at the appropriate site/s of the compound. Superconductivity is now discovered in various pnictide families as, e.g., the single layer $ReO_{1-x}F_xFeAs$ (Re=La, Ce, Pr, Nd, Sm, Tb, Dy, Ho, and Y), the double layer MFe_2As_2(M= Ba, Sr, and Ca), the oxygen free single-layer LiFeAs, etc.Recently, superconductivity with Tc = 8K was discovered in α-$FeSe_{1-x}$ with the PbO structure [2]. Similar to the FeAs compound this compound also has a Fe square lattice with Fe atoms tetrahedrally coordinated by Se. For a complete understanding of superconductivity in iron-based superconductors and for their technological applications, it is important to study the upper critical field H_{c2} because it provides information on coherent length, anisotropy, and the pair-breaking mechanism. In the present work we report the temperature dependence of H_{c2} and H_{irr} for the Te substituted and pure $FeSe_{0.93}$ samples.With the aid of linear interpolation, we find out the value of $H_{c2}(0)$ for all the samples.

The samples were prepared using solid state reaction route [3]. Selenium shots(99.99%), Te powder(99.99%) andiron powder (99%) were used to synthesize the samples with the composition $FeSe_{1-x}Te_x$(x=0, 0.5 and 0.75). The grinding process was carried out in glove box in Ar atmosphere. The ground powder was cold pressed into pellets. The pellets were sealed in an evacuated quartz tube (in 10^{-5}torr vacuum). The pellets were first sintered at 600°C for 20hrs, and then after regrinding they were sintered at 700°C for 30 hrs and slowly cooled down and annealed at 400°C for 30 hrs. The phase identification was done using XRD (Cu-Kα). The phase obtained with x-ray diffraction is tetragonal α-FeSe with the p4/nmm space group symmetry. The sample resistance was measured by using the standard four-probe method using silver paste for contact. Measurements were carried out with a Quantum Design PPMS. Fig. 1(a) shows the temperature dependence of resistance R(T) of the $FeSe_{0.93}$ in different fields.Critical temperature has increased with Te doping at the Se site. In order to determine the upper critical field of the samples, the R(T) curves are measured under different magnetic fields up to 8T. The superconducting transition temperature decreases with an increase in applied magnetic field. For calculating $H_{c2}(T)$ we have used 90% of normal state resistance (Rn) valuesand to calculate H_{irr} we have used 10% of Rn values[Fig1(b)]. In Fig.1(b)we show the $H_{C2}(0)$ values calculated using linear interpolation of $H_{c2}(T)$-T_C curves. These arefound to be 74T, 172T and 99T for x=0, 0.5 and 0.75, respectively.

As usual TChas been found to decrease with increasing magnetic field. We observe that the zero resistance temperature shifts towards lower temperatures more than the onset temperature. As it is known that the zero resistance temperature depends on the weak links between the grains as well as on the vortex flow behavior, while the onset is largely determined by the upper critical field of the

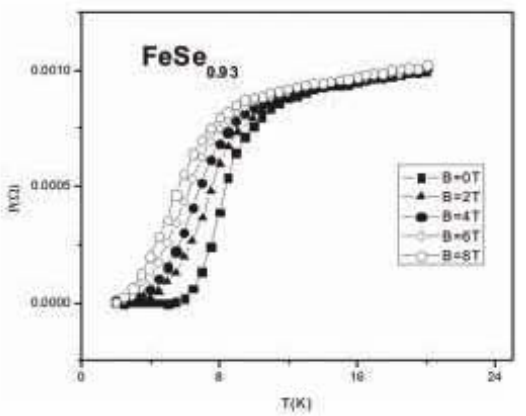

Fig1(a). Variation of resistance, R(T) with temperature for different fields values.

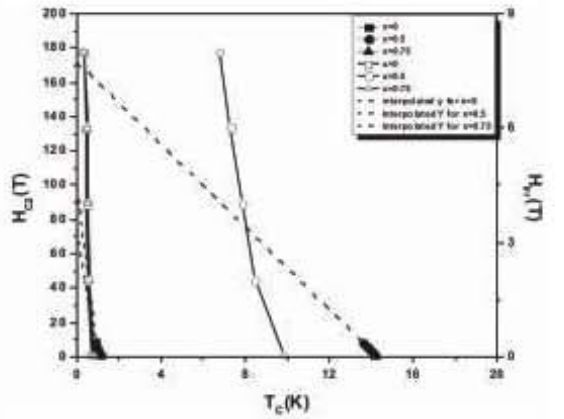

Fig1(b). $H_{c2}(0)$ values by linear interpolation of H_{c2}-T curves, $H_{c2}(T)$ (*solid lines*) and Hirr(T) (*dashed lines*) are obtained taking the onset (90%Rn) and zero(10%Rn) transition temperatures versus magnetic fields.

individual grains. So we conclude that the enhancement of H_{c2} and H_{irr} is mainly attributed to the impurity scattering centers doped into the sample. Decrease in H_{c2} and H_{irr} at further doping(x=0.75) may be due to the decreased fraction of superconducting grains as FeTe is non-superconducting.

REFERENCES

1. Kamihara et.al, J. Am. Chem. Soc., 128,(2006) 10012
2. F.C. Hsu et.al., ProcNatlAcad Sci. 105.,(2008) 14262
3. K. W. Yeh et.al., J. Phys. Soc. Jpn. 77, (2008) 19
4. Bhoi D. et. al., Supercond. Sci. Technol. 22 (2009)095015

THE EFFECT OF GASEOUS ENVIRONMENT ON THE MAGNETIC PROPERTIES OF Al Co-DOPED ZnCoO

NAGESH KUMAR, G.D. VARMA

Department of Physics and Centre of Nanotechnology, Indian Institute of Technology Roorkee, Roorkee-247667, India
Email: gdvarfph@iitr.ernet.in

Soon after the theoretical prediction of room temperature ferromagnetism (RTFM) in transition metal doped ZnO by Dietl et al. [1] lot of research work started on ZnO based DMS. The origin of FM in these materials is still an issue of debate. The currently accepted picture for DMS's FM is that the presence of carriers is essential to mediate the interaction between the magnetic ions. Therefore, some work has been done with additional dopants to enhance ferromagnetism [2]. ZnO doped with B, Al and Ga etc shows n-type conductivity. A high temperature FM has been observed in (Co,Al) codoped ZnO after increasing carrier concentration by doping a few percent of Al [3]. Further, it has been reported that defects like oxygen vacancies, Zn interstitial are important for ferromagnetic interactions in Mn and Co-doped ZnO [4]. In the present work polycrystalline Zn0.98-x Co0.02AlxO (x= 0, 0.01& 0.03) samples were prepared by sol-gel method by sintering in air for 12 h at 800°C followed by furnace cooling. Some air sintered pellets of the sample x=0.01 were further annealed at 800°C in different gaseous environment like oxygen, hydrogenated argon (Ar: H2 = 9.5:0.05) for 1 h.

The XRD results of all the samples reveal the presence of wurtzite structure of ZnO in all the samples. No signature of any impurity phase in the as synthesized and annealed samples has been found through XRD results. The XRD patterns (intensity on logarithmic scale) of the as synthesized and annealed samples with x=0 and 0.01 are shown in figure1(a).

From the XRD results it has been found that diffraction peaks shift towards the higher angles with increasing x value (figure 1(b)), suggesting that doped Al (ionic radius of Al3+ ~53 pm) substitute at Zn sites (ionic radius of Zn^{2+} ~74 pm). The M-H plots of all the as synthesized samples, measured at room temperature, show that the samples x=0.0 and 0.01 have weak

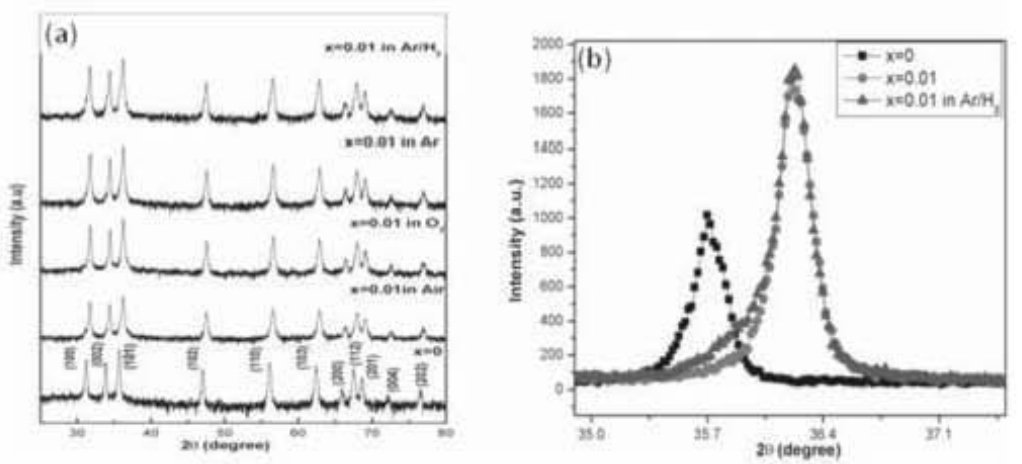

Figure 1: X-ray diffraction patterns (intensity on logarithmic scale) of (a) as synthesized x=0 sample and the x=0.01 samples annealed in different gaseous atmospheres (b) diffraction peak shift when value of x increases from 0 to 0.01.

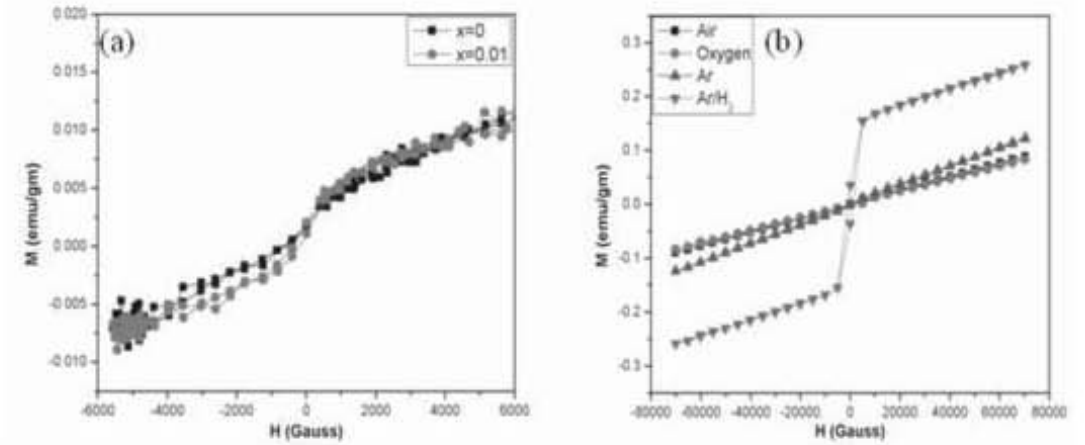

Figure 2: M-H plots at room temperature of (a) as synthesized samples x=0 and 0.01 (b) sample x=0.01 annealed in different gaseous atmospheres.

ferromagnetic interactions. The ferromagnetic interactions, however, decreases for the sample x=0.03 as compared to x=0 and 0.01 samples. The M-H plots (room temperature) of the samples with x=0, 0.01sintered in air and samples x=0.01 annealed in 02, Ar and Ar/H2 atmospheres are shown in figure 2. From this figure it is clear that annealing of sample in oxygen atmosphere reduces the magnetization and sample becomes completely paramagnetic. On the other hand, annealing of the samples in hydrogenated argon (Ar/ H2) enhances the ferromagnetic property and magnetization. This enhancement in the ferromagnetic property of the Ar/H2 annealed samples may be due to increase in the oxygen vacancies in the sample. The oxygen vacancies may cause small changes in the lattice parameters; this however could not be detected by X-ray diffraction studies. The FESEM micrographs (not shown here) of the Ar/H2 annealed sample with elemental mapping show that the granularity of the sample has increased and all the constituent elements are uniformly distributed throughout the sample. In the Ar/H2 annealed samples we found decrease in the oxygen atomic % measured through FESEM-EDAX. Therefore, we conclude that there may be some contribution of oxygen vacancies in the observed RTFM. Further transmission electron microscopic (TEM) investigation is in progress to detect presence of Co-clusters in the hydrogenated samples, which may also be responsible for enhanced ferromagnetic interactions in the sample at room temperature.

In summary, we synthesized the Zn0.98-xCo0.02AlxO (x=0, 0.01, 0.03) samples via sol-gel method and studied the effect of gaseous environments on the structural and magnetic properties of Zn0.97 Co0.02Al0.010 sample. We found that annealing of x=0.01 sample in Ar/H2 atmosphere enhances the RTFM, possibly due to increase in oxygen vacancies in the sample after hydrogenation.

REFERENCES

1. T.Dietl, H.Ohno, F.Matsukura, J.Cibert, D.Ferrand, Science 287 (2000) 1019.
2. H.T.Lin,T.S.Chin,J.C.Shih, S.H.Lin, T.M.Hong, R.T.Huang, F.RChen and J.J.Kai, Appl.Phys.Lett.85, 621(2004)
3. X.C.Liu, E.W.Shi, Z.A.Chen, H.W.Huang, B.Xiao and X.L.Song, Appl.Phys.Lett. 88, 252503 2006.
4. V.K.Sharma and G.D.Varma, J.Appl.Phys.102, 056105 (2007).

SUPERCONDUCTING & MAGNETIC PROPERTIES OF $Y_{1-x}Ca_xBa_2Cu_3O_{7-\delta}$

N.P Liyanawaduge, Anuj Kumar, V.P.S Awana, H.Kishan

Quantum Phenomenon and Applications Division, National Physical Laboratory, New Delhi-12, India

Email: awana@mail.nplindia.ernet.in

We report here the superconducting and magnetic properties of $Y_{1-x}Ca_xBa_2Cu_3O_{7-\delta}$ where x = 0.1, 0.2, 0.3. Calcium is a divalent ion which can be preferentially substituted to Y site [1]. The substitution of nonisovalent cations for the Y site is great interest because it varies the carrier concentration which causes variations in critical temperature, normal state conductivity and lattice parameters. We synthesized $Y_{1-x}Ca_xBa_2Cu_3O_{7-\delta}$ where x = 0.1, 0.2, 0.3 polycrystalline samples in solid state reaction route. High purity powders of Y_2O_3, $CaCO_3$, Ba_2CO_3 and CuO (99.99%) with exact stoichiometric ratio were mixed. After initial grinding calcination was done at 860°C in air for 20 h and cooled to the room temperature over 10h. This calcination procedure was repeated for 890 °C, 900 °C and 915 °C temperatures consecutively. In each calcination cycle cooling procedure was done very slowly and samples were re-ground well before the next cycle. After final calcination the samples were pressed into the pellets form and sintered at 925 °C for 24 h in air and cooled down to the room temperature over 12h. Finally the samples were annealed with flowing oxygen to 900 °C for 12h , 600 °C for 18h and 400 for 12h respectively and finally cooled to room temperature over 6 h.

All the samples were characterized by the X-Ray powder diffraction technique. Subsequently analyzed the data by Reitveld refinement method using Fullprof and calculate the lattice parameters which are given in fig.1.It can be seen that reduction of orthorhombocity with increasing Ca content in the system is in agreement in early studies [2]. The temperature dependency to Resistivity of these samples is given in fig 2. The Normal state conductivity initially increases with increasing Ca content up to x = 0.1(or between 0.1 and 0.2) as substitution of Ca will provide mobile holes to CuO_2 planes [2] and decreases onwards. The critical temperature, T_c reduce with increasing Ca content due to the over doping and disorder which take place in the CuO_2 planes due to the Ca doping as reported in early studies[3]. AC susceptibility measurements (ACMS) of all these samples

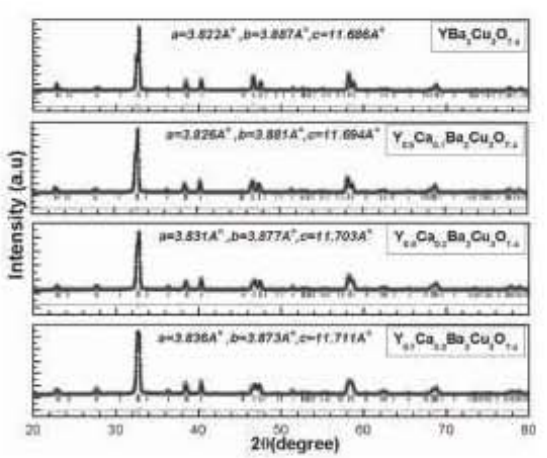

Fig.1 Rietveld fitted XRD pattern

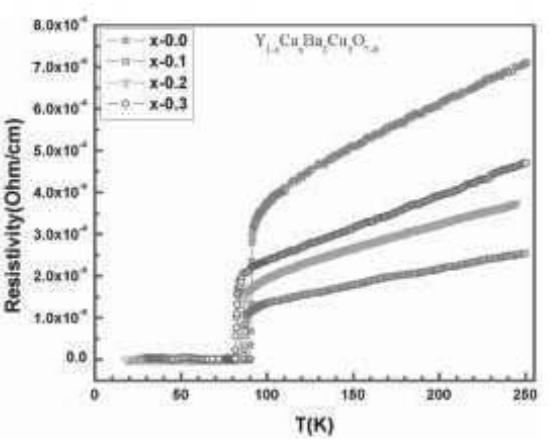

Fig. 2 The Temperature dependency of Resistivity

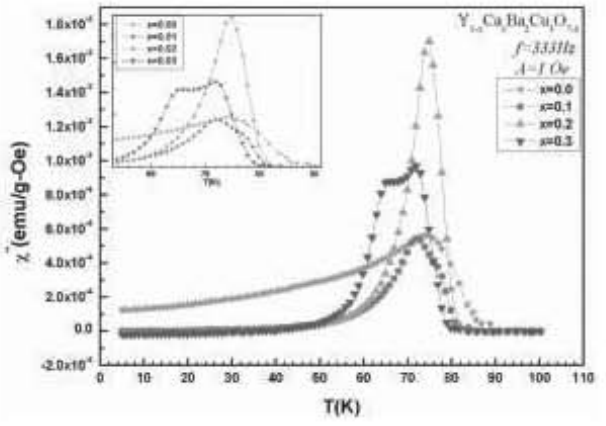

Fig.3 The Imaginary part of the AC Susceptibility

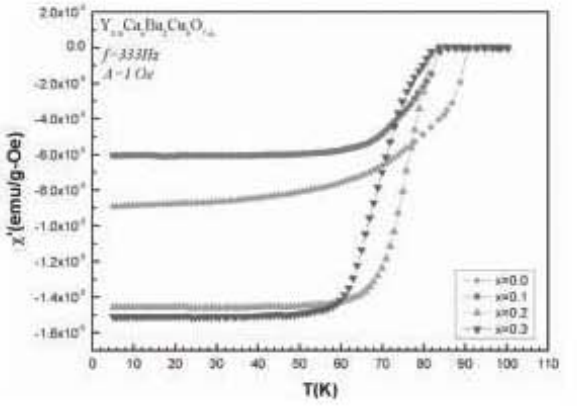

Fig.4 The Real Part of the AC Susceptibility

are given in figure.3 (imaginary part) & figure 4(real Part). In the imaginary curve the inter-grain peak (low temperature peak) shifts to high temperature side when the Ca content is increased up to x = 0.1(or between 0.1 and 0.2) and then the inter-grain peak once again shifts to the low temperature side when further increasing of Ca content. The two peaks have clearly separated in the x = 0.3 curve. This indicates that when the Ca content increases first inter- grain couplings increase and reach maxima near about Ca content x=0.1(or between 0.1 and 0.2) and further increase of Ca causes the activation of grain boundary resistance in agreement of SEM picture study in [4]. We think that this activation of grain boundary resistance around x=0.1 and 0.2 will be the reason for reduction of normal state conductivity in sample x=0.3. The high temperature peak which is responsible for intra-grain properties always improving with increasing of Ca content thus the grain size is increasing with increasing Ca. A systematic reduction of T_c can be seen in fig.4 with increasing Ca content as in agreement with resistivity curves.

REFERENCES

1. B Fisher, J Genossar, C.G Kuper, G.M Reisner and Knizhnik , Phys. Rev. B 47 (1992) 6054.
2. Rajiv Giri, H.K Singh, O.N Srivasatava, V.P.S Awana, Anurag Gupta, and H.Kishan, Physica C 419 (2005) 101.
3. V.P.S Awana, A.V Narlikar Phys. Rev. B 49 (1993) 635
4. J.T Kucera, J.C Bravman, Phys. Rev. B 51 (1994) 8582.

CATION EXCESS EFFECT ON THE TUNNELING MAGNETORESISTANCE OF THE DOUBLE PEROVSKITE Sr_2FeMoO_6

VIBHAV PANDEY, SIJIN KUMAR, VIVEK VERMA, JYOTI SHAH, R P ALOYSIUS, R K KOTNALA

National Physical Laboratory, CSIR, New Delhi, India-110012
Email: rkkotnala@gmail.com

Double perovskite A_2FeMoO_6 systems exhibit large tunneling type magnetoresistance in bulk polycrystalline form. In polycrystalline double perovskites, the grains act as metallic magnetic electrode while grain boundaries provide insulating barriers for tunneling mechanism. The modification of grain boundaries may provide a significant change in tunneling and tunneling type magnetoresistance. In the present study we have studied the modification of grain boundaries using extra amount of reactant powder during synthesis of double perovskite. X- ray diffraction measurement on $Sr_2Fe_{1+x}MoO_6$ (x= 0.0, 0.05, 0.10, 0.15, 0.20) samples showed no significant change in lattice parameters of the compounds. The presence of Fe is confirmed by different measurements. The magnetoresistance value of samples having extra Fe is reduced drastically which is related to presence of metallic magnetic Fe at grain boundaries. Analogous to it we have also prepared the compound $Sr_2FeMo_{1+y}O_6$ (y= 0.0, 0.05, 0.10, 0.15, 0.20) and $Sr_{2+z}FeMoO_6$ (z= 0.0, 0.05, 0.10, 0.15, 0.20). The polycrystalline samples were prepared using solid state sintering method using carbonates and oxides. For creating the excess of cation the extra amount of oxides and carbonates were used. It is expected that the presence of insulating SrO at grain boundaries (which is expected to arise due to extra addition of $SrCO_3$) may strengthen the boundary barrier and shall provide the enhancement in tunnel type magnetoresistance. A similar type of effect is expected for Molybdenum oxide added samples also. The measurements on these samples are in progress.

A NEW MULTIFERROIC Z-type HEXAFERRITE $Sr_3Co_2Fe_{24}O_{41}$ FURTHER MODIFIED TO REALIZE STRONG ROOM TEMPERATURE MAGNETOELECTRIC EFFECT

R. K. Kotnala, Vibhav Pandey, Sijin babu, R.P. Aloysius, Jyoti, Vivek Verma

National Physical Laboratory, CSIR, New Delhi, India-110012
Email: rkkotnala@gmail.com

Multiferroics with sufficient magnetoelectric coupling at room temperature and low magnetic fields are very important for various spintronics as well as sensor applications. Recently a Z-type hexaferrite ($Sr_3Co_2Fe_{24}O_{41}$) has been reported to be one of such important multiferroic materials [1]. Under normal preparation conditions $Sr_3Co_2Fe_{24}O_{41}$ compound cannot be synthesized in single phase, after developing many strategic steps we could prepare pure phase compound in our laboratory. At preliminary stage some of extra ferrite phases (Y-type & others) were also present with Z-type hexaferrite phase. The synthesized samples have been characterized for structural, dielectric and magnetic properties. Further to improve magnetoelectric coupling in $Sr_3Co_2Fe_{24}O_{41}$ some of additives Bi_2O_3, CuO and metallic silver are being tried. The measurements on these samples are in progress.

REFERENCE

1. "Low-field magnetoelectric effect at room temperature"
Y. Kitagawa, Y. Hiraoka, T. Honda, T. Ishikura, H. Nakamura and T. Kimura.
Nature material August 2010 , DOI: 10.1038/NMAT2826.

DIMENSIONALITY STUDY ON Fe BASED SUPERCONDUCTORS

SWATI PANDYA[1], SIYA SHERIF[1,2], L.S. SHARATH CHANDRA[1,3], V. GANESAN [1,3]

[1]*UGC-DAE Consortium for scientific research, University Campus, Khandwa Road, Indore (MP) 452017*

[2]*Department of Studies in Physics, University of Mysore, Manasagangothri, Mysore -570006*

[3]*Presently at Materials, Advanced Accelerator Science Division, Raja Ramanna Centre for Advanced Technology, Indore -452 013*

Email: swatipandya@csr.ernet.in

The dimensionality of the superconductivity is an important aspect to know the potential of system for technological application. Here we are presenting the dimensionality study on new Fe based Chalcogenides systems like FeTe and FeSe. FeTe is non-superconducting but it shows superconductivity for chemical substitution like Sulfur and Selenium, whereas FeSe shows superconductivity around ~ 8K. Derivatives of FeTe and FeSe i.e $FeTe_{1-x}S_x$ (0.1, 0.2), $FeSe_{1-x}Sb_x$ (0.05, 0.1) and $FeSe_{1-x}Si_x$ (0.05, 0.1) are prepared using solid state reaction method and magneto-resistivity is measured down to 2K in presence of magnetic field upto 14T. Onset of superconductivity is seen around ~10K for these samples. Lowest Landau level scaling is applied to study magnetic field dependent fluctuation conductivity [1-3].Representative results of magneto-resistivity and LLL scaling of $FeTe_{1-x}S_x$, $FeSe_{1-x}Sb_x$ and $FeSe_{1-x}Si_x$ samples are shown in figure. It is observed that the 2D scaling is better above $H_{LL} \sim 8T$ for $FeTe_{1-x}S_x$, whereas 3D scaling is better above $H_{LL} \sim 4T$ for $FeSe_{0.8-x}Sb_x$ and $FeSe_{0.9-x}Si_x$. In conclusion, we have observed 2D –LLL scaling in $FeTe_{1-x}S_x$ (0.1, 0.2) indicating two-dimensional nature of superconductivity and 3D –LLL scaling in $FeSe_{1-x}Sb_x$ (0.05, 0.1) and $FeSe_{1-x}Si_x$ (0.05, 0.1) indicating three-dimensional nature of superconductivity. 3D nature of FeSe based superconductors signifies its potential for future technological applications. However there is a bright possibility for FeTe derived system to be a 3D superconductor with proper tuning of chemical substitution, as FeTe and FeSe systems have smaller difference in lattice parameters along c-axis.

ACKNOWLEDGMENT

Authors thank Dr. P. Chaddah and Prof. Ajay Gupta, for their kind support and encouragement, the staff of the low temperature and cryogenics laboratory for their technical support. We acknowledge the support of DST, for the LTHM project and CSIR, New Delhi for a fellowship to SP.

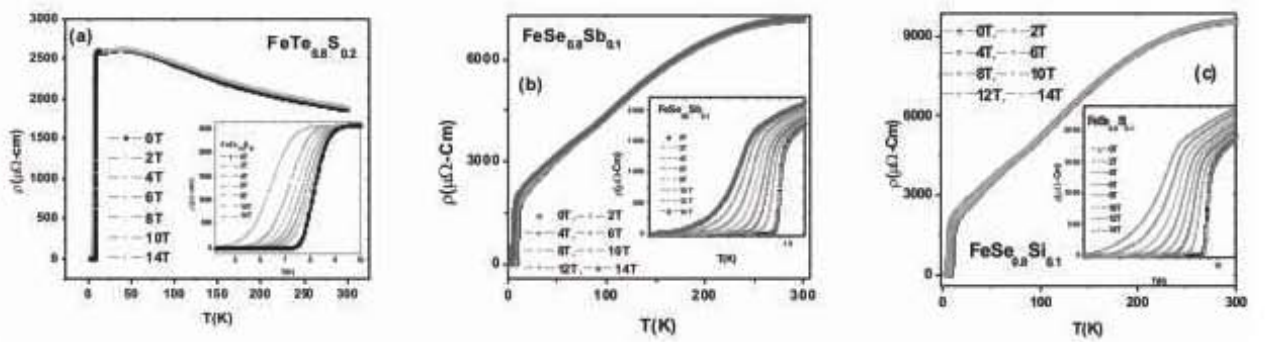

Figure.1 Magneto-resistivity down to 2K in magnetic field upto 14T of (a) $FeTe_{0.8}S_{0.2}$ (b) $FeSe_{0.8}Sb_{0.1}$ and (c) $FeSe_{0.8}Si_{0.1}$. Insets show magneto-resistivity near superconducting transition.

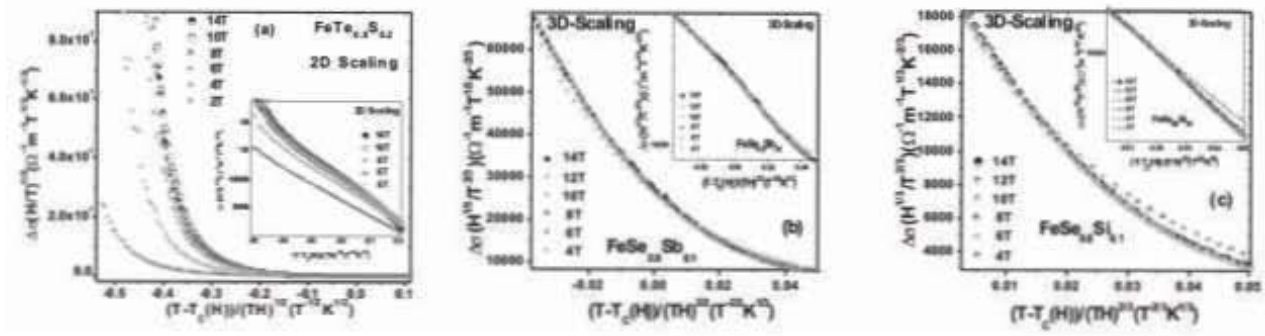

Figure.2 2D LLL scaling of $FeTe_{0.8}S_{0.2}$ (a) and 3D LLL scaling of $FeSe_{0.9}Sb_{0.1}$(b) and $FeSe_{0.9}Si_{0.1}$(c). Insets show same plots in semi-logarithmic scale.

REFERENCES

1. U.Welp et al, Phys.Rev.Lett.67, 3180(1991)
2. I.Pallecchi et al, Phys.Rev.B 79,104515(2009)
3. Swati Pandya et al, Supercond.Sci.Technol. 23, 075015 (2010)

ROLE OF INTER AND INTRA GRAINS CONNECTIVITY ON PHYSICAL PROPERTIES OF Bi-2212 AND Bi-2223 SUPERCONDUCTORS

JAGDISH KUMAR[1, 2], P.K. AHLUWALIA[2], ANURAG GUPTA[1], V.P.S. AWANA[1]

[1]*Quantum Phenomenon and Applications Division, National Physical Laboratory, Krishnan Marg, New Delhi-110012, India*

[2] *Department of Physics, Himachal Pradesh University, Shimla-171005, India*

E-mail: awana@mail.nplindia.ernet.in

We have done magneto-transport studies on intergrowth Bi-2212 and Bi-2223 samples synthesized from solid state route [1]. The XRD analysis shows small amount of Bi-2201 inter-grown in Bi-2212 sample and significant amount of Bi-2212 in Bi-2223 sample. The transition temperature T_c for Bi-2212 sample is found to be around 85K and 100K for Bi-2223 sample as observed in resistivity and magnetization measurements. The magnetization measurements were carried using AC susceptometer at various field amplitudes and frequency values. The real part of susceptibility is observed to be stepwise as a function of temperature, representing transition from near perfect screening to complete penetration of external AC magnetic field into sample. It is observed that there is single step transition in magnetization in real part of Bi-2212 sample whereas double transition is observed in Bi-2223 sample.

In Bi-2212 imaginary part of susceptibility shows a single loss peak that corresponds to intra-granular transition near transition temperature. No peak corresponding to inter-granular transition is observed that shows a good inter-granular coupling (Fig 1). For a given value of frequency the loss peak shift to lower temperature with increasing amplitude that shows a thermally activated phenomenon associated. For increasing frequency the peak shifts to higher temperature that can be interpreted in terms of flux creep. The *R(T)* measurements under magnetic field shows interesting non-linear drop in $T_c^{R=0}$ with applied values of applied field (Fig. 3). For lower values of fields the value of dT_c/dH is as high as 140K/Tesla which drops to 0.4K/Tesla at 14 Tesla applied field. The value of $T_c^{R=0}$ at 14 Tesla is around 30K with a drop rate of 0.4K/Tesla. This ensures its applications at low temperature under relatively high magnetic fields.

In Bi-2223 sample we have observed two peaks in imaginary part of magnetization at 98K and 53K and two steps in real part near 104K and 82K that corresponds to two different phases Bi-2212 and Bi-2223 (Fig. 2). We have observed two peaks in imaginary part of magnetic susceptibility. The first peak corresponds to the intra-granular loss around T_c, second corresponding to inter-granular T_c. The shifting of loss peaks is similar in nature as observed in Bi-2212 sample. The resistance versus temperature plots shows onset temperature of 120K but $T_c^{R=0}$ is attained at around 102K (Fig. 4). Presence of significant amount of Bi-2212 phase in Bi-2223 phase makes inter-granular coupling weak and leads to a broad transition. With application of magnetic field the onset is almost unchanged but the $T_c^{R=0}$ shifts to lower temperatures and transition width increases.

The results can be interpreted according to the flux creep model by Tinkham and Muller [2, 3], when frequency is increased, inter/intra granular vortices have less time to relax and then penetrate the superconductor during each cycle. In order to reach the full penetration, the effective inter granular pinning force density must be weakened. Since the pinning force density is weakened by increasing temperature, the T_{inter}/T_{intra} must increase with increasing frequency. Similarly as the driving field amplitude increases, larger screening currents are required to shield the applied field,

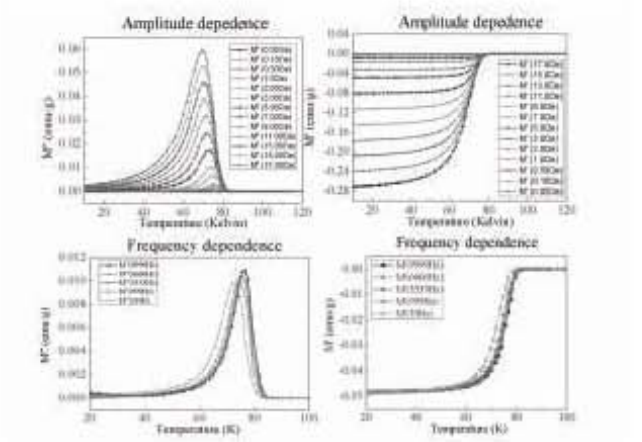

Figure 1: Amplitude and frequency dependence of real and imaginary parts of Magnetization for Bi-2212

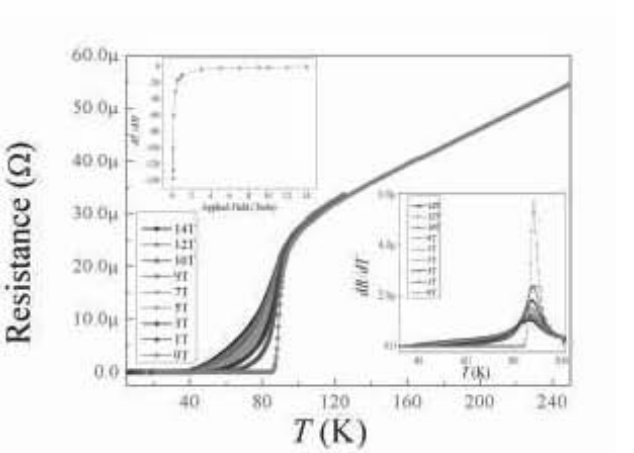

Figure 3: Resistance versus temperature of Bi-2212 sample under magnetic field

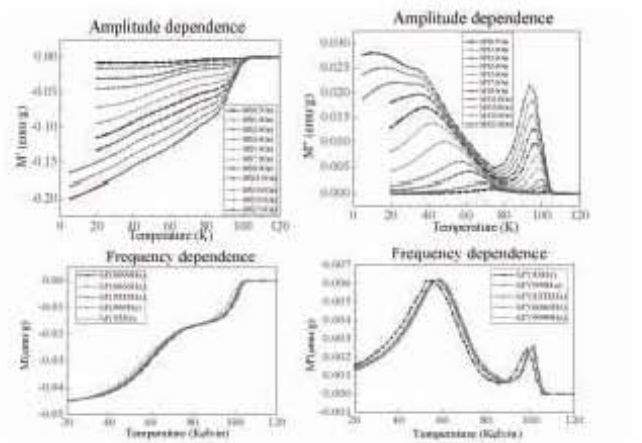

Figure 2: Amplitude and frequency dependence of real and imaginary parts of Magnetization for Bi-2223

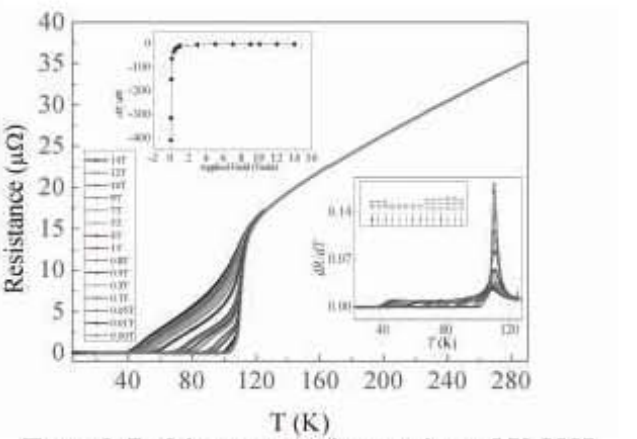

Figure 4: Resistance versus temperature of Bi-2223 sample under magnetic field

hence pinning force density is to be weakened consequently decreasing the T_{irrbar}/T_{irrbar}. The increase in transition width of R-T plots with magnetic field can be interpreted in terms of flux creep model [2, 3].

REFERENCES

1. Jagdish Kumar et al., J Supercond Nov Magn, volume 23, Number 4, 493-499
2. K.H.Muller, physica C, 168 (1990) 585
3. M.Tinkham et al., solid state physics, volume 42, academic press, New York, 1989, p91

ANOMALOUS HEAT CAPACITY AND X-RAY PHOTOELECTRON SPECTROSCOPY OF SUPERCONDUCTING $FeSe_{1/2}Te_{1/2}$

V.P.S. Awana, Govind, Anand Pal, A. Vajpayee, Jagdish Kumar, H. Kishan

Quantum Phenomenon and Applications Division, National Physical Laboratory, New Delhi-12, India

E-mail : awana@mail.nplindia.ernet.in: www.freewebs.com/vpsawana

The bulk polycrystalline sample $FeSe_{1/2}Te_{1/2}$ is synthesized by solid state reaction route in an evacuated sealed quartz tube at 750 ^{o}C. The presence of superconductivity is confirmed through magnetization/thermoelectric/resistivity studies. It is found that the superconducting transition temperature (T_c) is around 12 K. Heat capacity (C_p) of superconducting $FeSe_{1-x}Te_x$ exhibited a hump near T_c, instead of well defined Lambda transition. X-ray Photo electron spectroscopy (*XPS*) studies revealed well defined positions for divalent Fe, Se and Te but with sufficient hybridization of Fe (2p) and Se/Te (3d) core levels. In particular divalent Fe is shifted to higher BE (binding energy) and Se and Te to lower. The situation is similar to that as observed earlier for famous Cu based *HTSc* (High T_c superconductors), where Cu (3d) orbital hybridizes with O (2p). We also found the satellite peak of Fe at 712.00 eV which is be attributed to charge carrier localization induced by Fe at 2c site.

Following the discovery of superconductivity in $LaFeAsO_{1-x}F_x$ ('1111') [1], an important development has been the invention of superconductivity in another class of materials Fe(Se,Te) ('11') [2]. The effect of chemical pressure has been studied in '11' systems by means of Se-site substitution [4]. It is found that superconducting transition temperature increases with Te doping in $FeSe_{1-x}Te_x$ system, reaches a maximum at about 50% substitution, and then decreases with more Te doping [3]. The polycrystalline sample of $FeSe_{1/2}Te_{1/2}$ was synthesized by the solid state reaction route. The stoichiometric ratio of highly pure (> 3N) Fe, Se, and Te are ground, pelletized and then encapsulated in an evacuated (10^{-3} Torr) quartz tube. The encapsulated tube is then heated at 750 ^{o}C for 12 hours and slowly cooled to room temperature. Temperature dependence of AC magnetization of the $FeSe_{1/2}Te_{1/2}$ sample is taken on *PPMS* (physical property measurement system). Heat capacity $C_p(T)$ in zero field is also measured on PPMS. The $FeSe_{1/2}Te_{1/2}$ has been characterized by x-ray photoelectron spectroscopy (*XPS*) Perkin Elmer -PHI Model 1257, working at a base pressure of 5x 10^{-10} torr.

Figure 1 depicts the observed and fitted X-ray diffraction pattern of $FeSe_{1/2}Te_{1/2}$ that corresponds to P4/nmm space group. The lattice parameters a = 3.7926(3) Å and c = 6.015(2) Å. The insets of Figure 1 show the resistivity (ρ) and AC susceptibility (χ) versus temperature (T) plots for the studied $FeSe_{1/2}Te_{1/2}$ compound. Both $\rho(T)$ and $\chi(T)$ demonstrate that the compound is bulk superconducting below 12 K. Detailed physical property characterization of the studied $FeSe_{1/2}Te_{1/2}$ compound is reported by some of us previously [4]. Figure 2 shows the heat capacity (C_p) versus temperature (T) plot for $FeSe_{1/2}Te_{1/2}$. The room temperature (300 K) C_p is around 55 J/mol-K, which is in general agreement with reported values for this compound [9]. The data was fitted to the equation $C_p = \gamma T + BT^3 + CT^5$ from above superconducting transition from 13 K to 16 K. Where, γT and $BT^3 + CT^5$ are electronic and phononic specific heat contributions respectively. The value of g was found to be 57.73 mJ/mol-K^2 which is somewhat higher than other reported values [5]. As far as the entropy contribution due to superconducting condensate is concerned, the superconducting state – normal state is plotted in upper inset of Figure 2. The shape of Lambda transition for

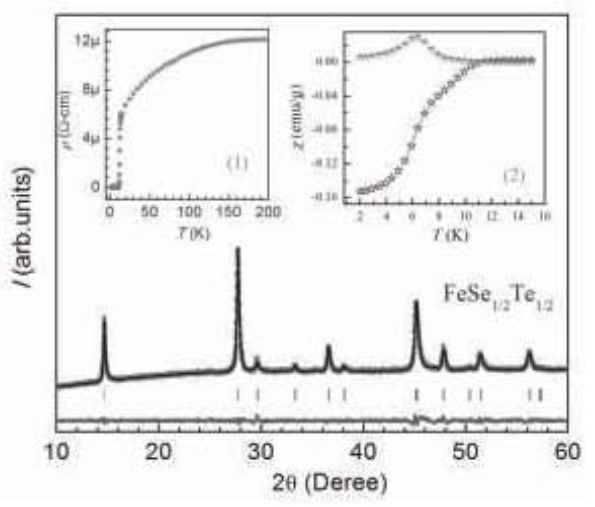

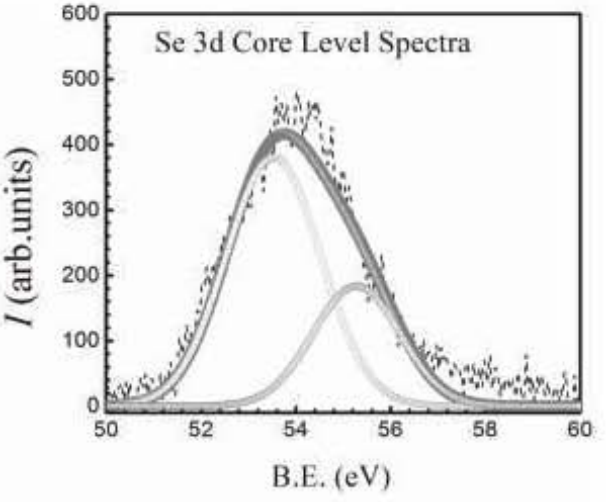

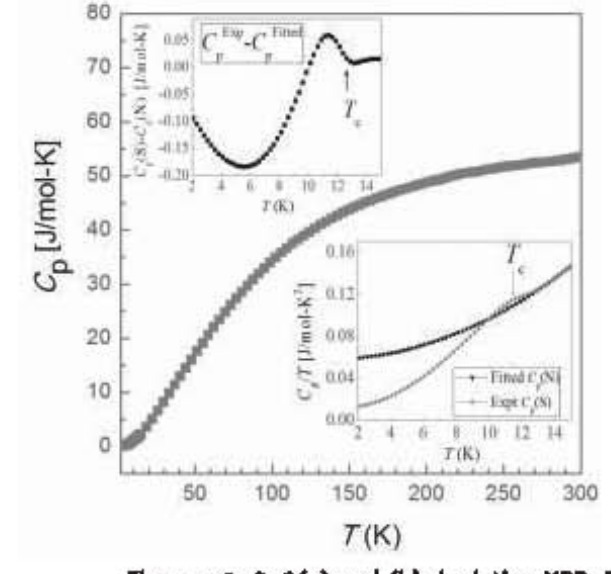

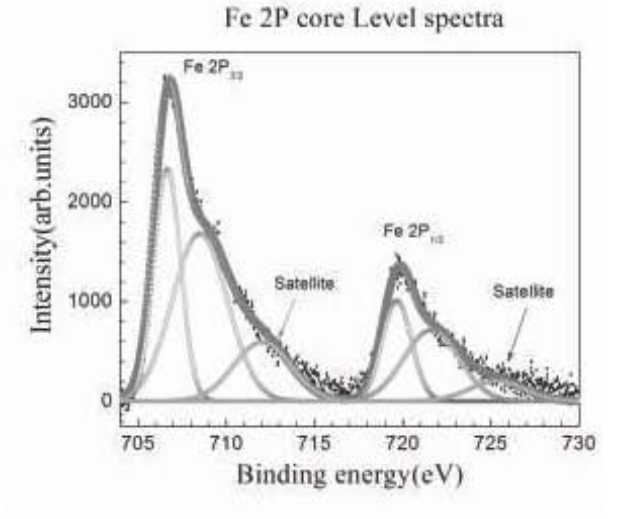

Figures: 1, 2, 3(a) and (b) depicting XRD, R-T, magnetization, Cp(T) and XPS of $FeSe_{1/2}Te_{1/2}$

studied $FeSe_{1/2}Te_{1/2}$ does not exhibit sharp discontinuity at T_c as seen but a broad hump like structure. Figure 3 (a) and 3 (b) show the deconvoluted core level *XPS* spectra of Se (3d) and Fe(2p) respectively for $FeSe_{1/2}Te_{1/2}$ sample. The Fe ($2p_{3/2}$) spectra could be resolved into three spin-orbit components at 706.65 eV, 708.50 eV and 712.00 eV after the carbon correction. A Fe (2p1/2) core level spectrum was also deconvoluted three peaks in similar way. The 3d core level spectrum of Te is deconvoluted into three peaks with binding energy 572.00 eV, 572.65 eV and 573.90 eV. The peak at energy 572.65 eV corresponds to pure Te metal while peak at lower binding energy 572.00 eV may have appeared due to the hybridization. In case of Se, the core level spectra are deconvoluted into two peaks with binding energies 53.52 eV and 55.28 eV. The peak for higher BE corresponds to pure Se while peak at lower BE appeared due to the hybridization.

REFERENCES

1. Y. Kamihara, J. Am.Chem. Soc. 130, 3296 (2008).
2. F. C. Hsu, Proc. Natl. Acad. Sci. U.S.A. 105, 14262 (2008).
3. K. W. Yeh, Europhys. Lett. 84, 37002 (2008).
4. V. P. S. Awana, J. Appl. Phys. 107, 09E128 (2010).
5. B. C. Sales, Phys. Rev. B 79, 094521 (2009).

EFFECT OF 3d METAL (Ni AND Co) DOPING ON THE SUPERCONDUCTIVITY OF $FeTe_{1/2}Se_{1/2}$

Anuj Kumar[1,2], Shahnawaz[2], H. Kishan[1], V.P.S. Awana[1]

[1]Quantum Phenomena Application Division, National Physical Laboratory, New Delhi-110012
[2]Department of Physics and Astrophysics, University of Delhi New Delhi-110007
E-Mail: awana@mail.nplindia.ernet.in

We report the effect of Cobalt (Co) and Nickel (Ni) doping in the $FeTe_{1/2}Se_{1/2}$ superconductor with the nominal composition range $Fe_{1-x}M_xTe_{0.5}Se_{0.5}$ (M = Co, Ni and x = 0.02, 0.05, 0.10). These samples are synthesized by solid state reaction route and they crystallize in single phase with space group *P4nmm*. The lattice parameters 'a', 'c' and volume decrease with increase in Co and Ni content, although not monotonically. In fact the 'a' lattice parameter of Co doped samples is nearly unaffected for Co doped samples. This indicates successful substitution of smaller ion Ni and Co at divalent Fe site in the parent $FeTe_{1/2}Se_{1/2}$ superconductor. The superconducting transition temperature (T_c) is measured from both DC and AC magnetic susceptibility, which decrease with increase in Ni or Co content. Interestingly Ni suppresses the superconductivity much faster than the Co substitution. Fe/Ni 2at% substitution itself decreases the T_c from around 14K to 4K and 5at% doped sample is not superconducting down to 2K. Ni suppresses the T_c of $FeTe_{1/2}Se_{1/2}$ superconductor by ~ 5K/at%. On the other hand the suppression of T_c from Fe/Co substitution is found to be around 2K/at%. As revealed from the lattice parameter variations although they decrease in both Ni and Co substituted samples, the a-parameter is least affected in case of Co doped samples. This indicates less effect on in plane Fe-Se distances and thus reduced disorder in case of Co when compared with Ni substation at Fe site in $FeTe_{1/2}Se_{1/2}$ superconductor. It is concluded that in plane disorder on superconducting Fe-Se/Te planes directly affects superconductivity in $FeTe_{1/2}Se_{1/2}$ superconductor.

Recent invention of high T_c (above 55K) superconductivity in Fe based pnictides with general formula ReFeAsO (Re = rare erath) has taken the scientific community by surprise [1]. Soon after another Fe based chalcegonide compound (FeSe) joined the race, although with a lower T_c of around 8K. [2]. Application of mechanical pressure on this compound increased its T_c to above 27K [3]. Hence soon after chemical pressure was applied by substituting Se/Te and stable compound with T_c above 14K was achieved with chemical formula $FeSe_{1/2}Te_{1/2}$ [4]. We report here the impact of Co and Ni substitution on Fe site of an optimized $FeSe_{1/2}Te_{1/2}$ superconductor and probe the role of disorder on superconductivity of this newest superconducting entrant. Samples of composition $Fe_{1-x}(Co,Ni)_xTe_{1/2}Se_{1/2}$ are synthesized by solid state reaction route via encapsulation of stoichiometric high purity (>3N) Fe, Se, Te, Co and Ni ingredients, details are same as in ref. 6. The X-ray diffraction is done on rigaku Mini Flex diffractometer. The Magnetization (AC and DC) are carried out on a physical property measurement system (PPMS) from Quantum Design USA. Figure 1 depicts the XRD patterns of $Fe_{1-x}M_xTe_{0.5}Se_{0.5}$ (M = Co, Ni and x = 0.02, 0.05) samples. These samples are single phase. The lattice parameters are obtained from respective Reitveld analysis of all the XRD patterns. Decrease in volume of lattice indicates successful substitution of smaller Co^{2+}, Ni^{2+} ions at bigger Fe^{2+} in doped $FeSe_{1/2}Te_{1/2}$. The 'a' lattice parameter is affected relatively more in case of Ni than Co substitution.

The AC and DC magnetic susceptibility plots of $Fe_{1-x}M_xTe_{0.5}Se_{0.5}$ (M = Co, Ni and x = 0.02, 0.05) samples, are given in Figure 2(a) and 2(b) respectively. The Tc for pristine compound is around 14K,

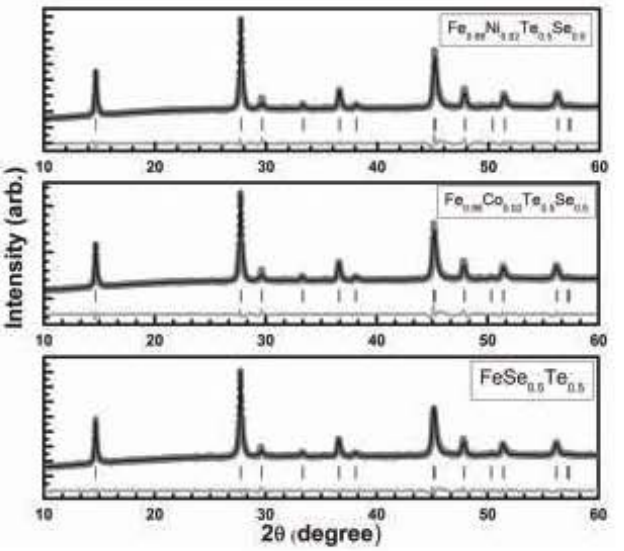

Fig. 1, XRD patterns of $Fe_{1-x}M_xTe_{0.5}Se_{0.5}$ (M = Co, Ni and x = 0.02, 0.05).

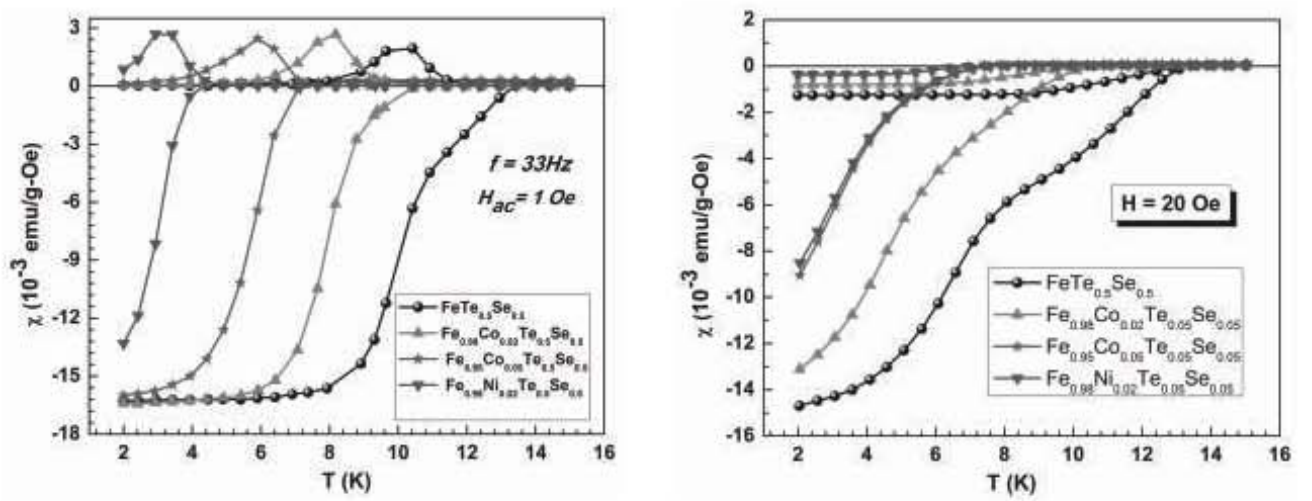

Fig. 2(a), (b) AC and DC magnetic susceptibility of $Fe_{1-x}M_xTe_{0.5}Se_{0.5}$ (M = Co, Ni and x = 0.02, 0.05).

as viewed from diamagnetic onset in both the real part AC (Fig. 2a) and the DC susceptibility (Figure.2b). With an increase in Ni content the Tc suppresses to below 4K for 2at% doping and 5at% Ni doped sample is not superconducting. On the other hand for Co substitution although Tc is decreased to 12K and 6K for 2at% and 5at% samples, the relative depression is much smaller than as for Ni substitution. These results are depicted in Figures. 2(a) and (b). The large suppression of Tc by Ni substitution is directly related to the variation of 'a' lattice parameter of doped system and hence large disorder in case of Ni than for Co doping. Summarily our results indicate that disorder plays an important role in suppression of superconductivity in FeSe1/2Te1/2 superconductor.

REFERENCES

1. Y. Kamihara, T. Watanabe, M. Hirano and H. Hosono, J. Am. Chem. Soc. 130 (2008) 3296
2. F. C. Hsu, L. Y. Luo, K. and P. M. Wu, Proc. Natl. Acad. Sci. USA, 105 (2008) 14262
3. Yoshikazu Mizuguchi and Takahide Yamaguchi, Appl. Phys. Lett. 93 (2008) 152505
4. V.P.S. Awana, Anand Pal, and E. Takayama-Muromachi J. Appl. Phys. 107 (2010) 09E128

IMPACT OF PARTICLE SIZE ON THE MAGNETO-TRANSPORT PROPERTIES OF $La_{1.85}Sr_{0.15}CuO_4$

DEVINA SHARMA[1,2], RANJAN KUMAR[2], V.P.S. AWANA[1*]

[1]*Quantum Phenomenon and Applications, National Physical Laboratory, New Delhi-12, India*
[2]*Department of Physics, Punjab Universiy, Chandigrah, India*
E-mail: awana@mail.nplindia.ernet.in

We study the impact of varying grain size on the magneto-transport properties of bulk $La_{1.85}Sr_{0.15}CuO_4$ superconductor. Polycrystalline samples are synthesized by sol-gel route. Particle size is varied by sintering the samples at three different sintering temperatures (T_s), heated at rate of 10°C/min to 900, 1000 and 1050°C respectively and hold for 12 hours. The samples were then cooled down to room temperature. Phase purity of all the samples is confirmed by X-ray diffraction pattern while the varying particle size is checked from Scanning Electron Microscopy (SEM) images [1]. Resistivity and magnetization measurements are carried out to study the magneto-transport properties of the samples on Quantum Design PPMS.

The most observable effect related to the broadening of the superconducting transition is marked by the existence of three different temperatures labeled as T_{ci}, T_{cj} and T_{co}. T_{ci} corresponds to onset temperature at which Cooper pairs appear inside the grains of the superconductor while T_{cj} is the temperature below which the grains are connected by Josephson Effect and finally at T_{co} resistance becomes zero. In order to obtain more information about the coupling effects, magnetic field effects on the resistivity of the samples are studied (See Fig 1). It is worth observing that T_{cj} and T_{co} vary considerably with the change in the particle size while T_{ci} (onset temperature) is almost constant (See Fig 2). This suggests that with the particle size variation it is inter-granular coupling which is more affected than the intra granular coupling. Also from the resistivity in magnetic field study we find a good systematic decrease in the magneto-resistance with increase in the particle size owing to the reduced grain boundaries (See Fig 3).

In addition to electrical resistivity, ac susceptibility study is carried out to probe the nature of weak links in the sample with different particle sizes as a function of temperature (4-40 K) at various amplitudes (1-17 Oe) and over a wide range of frequency (333-9999 Hz). The complex ac susceptibility ($\chi = \chi' + i\,\chi''$) consists of a real (χ') and an imaginary (χ'') component. The two step transition in real part (χ') depicts diamagnetic shielding to the current in inter and intra granular region. In the imaginary part (χ''), two peaks appearing at temperatures, T^G and T^J ($T^G > T^J$) indicates maximum hysteresis loss due to motion of intra-granular (Arbikosov) and inter-granular (Josephson) vortices respectively. Maximum loss always takes place when the magnetic flux lines just penetrate the centre of the sample. Shift in the peak temperature with a change in applied field amplitude or frequency is related to the pinning force density as per flux creep model given by Tinkham and Muller [2]. When frequency is increased, inter/intra granular vortices have less time to relax and then penetrate the superconductor during each cycle. In order to reach the full penetration, the effective inter granular pinning force density must be weakened. Since the pinning force density is weakened by increasing temperature, the T_{inter}/T_{intra} must increase with increasing frequency. Similarly as the driving field amplitude increases, larger screening currents are required to shield the applied field, hence pinning force density is to be weakened consequently decreasing the $T_{inter}/T_{intra.}$ In both the field and frequency dependence curves for ac susceptibility (See Fig 4 & 5), we find that

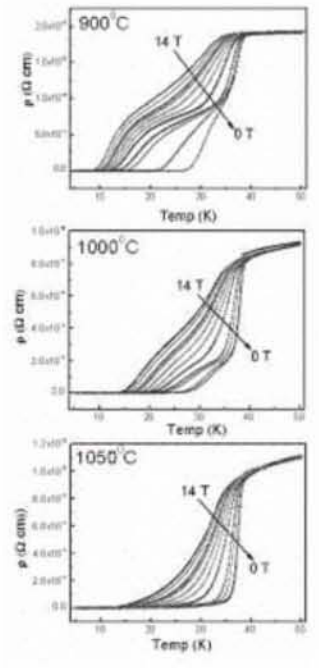

Fig .1: R(T)H plots:

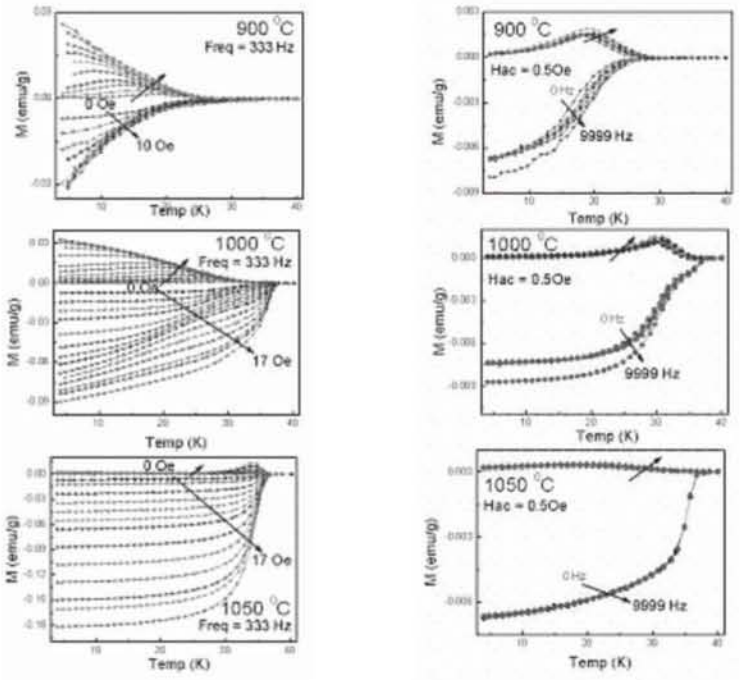

Fig. 4 ACS(Frequency) and Fig. 5 ACS(Field) for various LSCO

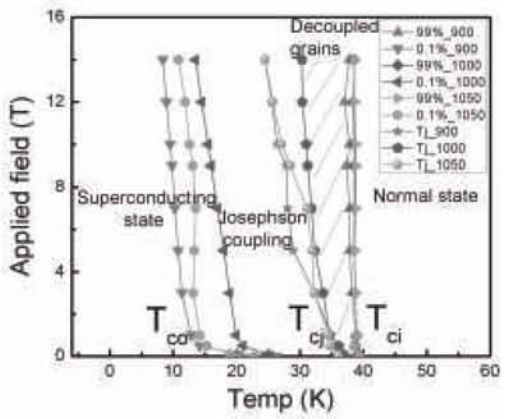

Fig. 2: T_{ci}, T_{cj} and T_{co} Variation of sintered at 900, 1000 & 1050°C with magnetic field

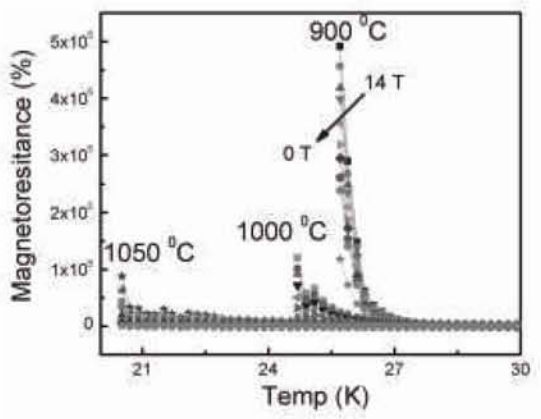

Fig. 3: Magneto-resistance variation for samples sintered at 900, 1000 & 1050°C with magnetic field

as the particle size increases loss peak temperature shifts to higher value suggesting decrease in the pinning force density.

In conclusion magneto-transport measurements suggest that as the particle size is varied inter-granular parameters in general get more affected than the corresponding intra-granular ones.

REFERENCES

1. Devina Sharma et al., J supercond, Nov Magn, doi: 10.1007/s10948-010-0920-8 (2010)
2. K.H.Muller, physica C, 168 (1990) 585

STUDY OF TCR/MR RESPONSES OF $La_{0.7}Ca_{0.2}Ba_{0.1}MnO_3$+Ag AND $La_{0.7}Ca_{0.2}Sr_{0.1}MnO_3$+Ag COMPOUNDS: A PROMISING CANDIDATE FOR INFRARED/ MAGNETIC SENSING DEVICES AT ROOM TEMPERATURE

Rahul Tripathi[1,2], V.P.S. Awana[1], H. Kishan[1], G.L. Bhalla[2]

[1]*National Physical Laboratory, Dr. K. S. Krishnan Marg, New Delhi-110012, India*
[2]*Department of Physics and Astrophysics, University of Delhi, Delhi-110007, India*
E-mail: awana@mail.nplindia.org

Manganites with general formula $A_{1-x}B_xMnO_3$ (where A = rare earth element and B = Alkaline earth metals) had attracted a lot of attention. These compounds are considered to be promising materials for technical applications. Among all other properties, the most outstanding and extensively explored is the magneto-resistance (MR). It is seen that the maximum MR in hole-doped manganites occur near the metal-insulator (MI) transition being accompanied with ferromagnetic-paramagnetic (FM) transition. For Bolometric applications, sudden change in resistivity over a small temperature zone is required. In manganites, MI transition presents itself as a zone of steep transition in resistivity. So, this metal-insulator crossover determines the sensitivity as well as active zone for bolometric sensors. The change or sharpness in resistivity with temperature is described in terms of temperature coefficient of resistance (TCR). TCR is defined as, TCR% = [1/R x (dR / dT)] x 100, where R is the resistance and T is the temperature.

For practical purpose, both high TCR and LFMR at room temperature are required. In this paper we report an enhanced temperature coefficient of resistance (TCR) and high magneto-resistance (MR) close/at room temperature in $La_{0.7}Ca_{0.2}Ba_{0.1}MnO_3$+$Ag_x$ and $La_{0.7}Ca_{0.2}Sr_{0.1}MnO_3$+$Ag_x$ ($0 \leq x \leq 0.4$) doped manganites. In case of $La_{0.7}Ca_{0.2}Ba_{0.1}MnO_3$ + Ag_x, TCR values remains almost unchanged (~11%/K) for all silver content at 284K which is greater than the pristine samples(3%/K).Improved magneto-resistance (19% at 1 Tesla) is observed for silver doped composition at relatively low magnetic field near room temperature.

On the other hand, for $La_{0.70}Ca_{0.20}Sr0_{0.10}MnO_3$+$Ag_x$, the maximum TCR and MR are tuned to room temperature ~300 K with the former being as high as 9% and the later being ~20 % and ~30 % at 5 and 10 k0e magnetic fields respectively. The enhanced TCR and MR at / near room temperature open up the possibility of the use of such materials as infrared bolometric and magnetic field sensors respectively [1-4].

REFERENCES

1. V. P. S. Awana, Rahul Tripathi, S. Balamurugan, H. Kishan and E. Takayama-Muromachi, Sol. Stat. Commu. , **140**, 410(2006).
2. Rahul Tripathi, V. P. S. Awana, S.K. Aggrawal, Neeraj Panwar, G.L. Bhalla, H.U. Habermier and H. Kishan , J. Phys. D: Appl. Phys **42**, 175002(2009).
3. V. P. S. Awana, Rahul Tripathi, Neeraj Kumar, H. Kishan, G.L. Bhalla, R. Zeng, L.S. Sharth Chandra, V. Ganesan, and H.U. Habermeier , J. Applied Physics **107,** 09D723 (2010) .
4. M.Rajewari et.al., Appl. Phys. Lett. **69**, 851 (1996).

HIGH SUPERCONDUCTING PERFORMANCE *n*-SiC DOPED MgB_2 SUPERCONDUCTOR

Arpita Vajpayee, R. Jha, A. K. Srivastava, H. Kishan, V.P.S. Awana

Quantum Phenomena and Application, National Physical Laboratory, New Delhi-12, India
E-mail: awana@mail.nplindia.ernet.in

We study the impact of sintering temperature on the phase formation, lattice parameters, amount of carbon (C) substitution, microstructure, critical temperature (T_c), irreversibility field (H_{irr}), critical current density (J_c), upper critical field (H_{c2}) and flux pinning in *nano*(*n*)-SiC added bulk MgB_2 superconductor. Four batches of samples of MgB_2+$(n\text{-SiC})_x$; x=0.0, 0.05 & 0.10 were prepared at four different sintering temperatures (T_s) i.e. 700, 750, 800 and 850°C with the same heating rate as 10°C/min. We found 750°C (*second batch*) as an optimal sintering temperature for *n*-SiC doping in bulk MgB_2 superconductor in order to get the best superconducting performance in terms of J_c, H_{c2} and H_{irr}. Carbon (C) substitution enhances the H_{c2} while the low temperature sintering is responsible for the improvement in J_c due to the smaller grain size, defects and *nano*-inclusion induced by C incorporation into MgB_2 matrix, which is corroborated by elaborative *HRTEM* (high-resolution transmission electron microscopy) results.

Polycrystalline MgB_2+n-SiCx (x = 0, 5-wt% & 10-wt%) samples were synthesized by solid-state reaction route. the stoichiometric amounts of ingredients were ground thoroughly, palletized using hydraulic press and put in a tubular furnace at four different temperatures 700°C, 750°C, 800°C & 850°C for 2.5 hours in argon atmosphere and finally furnace cooled in the same atmosphere of argon to room temperature.

Powder XRD analysis revealed that single-phase MgB2 bulks containing only a minor fraction of MgO were obtained for all the samples heated at above 700°C, while the samples heated at 700°C showed strong diffraction peaks due to unreacted magnesium in the sample. The volume fraction of unreacted Mg is nearly 24.48% in pure MgB2 sample sintered at 700°C. MgO fraction is almost the same in all the samples irrespective of SiC content and sintering temperature. Samples doped with SiC showed a considerable amount of Mg_2Si and minor quantities of unreacted SiC. At lower doping level (x = 5-wt%) the samples consist of a major phase of MgB2 with minority phase of Mg2Si and as we increase (x = 10-wt%) the doping level of n-SiC, the amount of this non-superconducting phase was increased. The a-axis parameter shows a larger drop for the SiC doped samples sintered at all the temperatures in comparison to pristine MgB_2. The change in 'c' parameter with increasing x (content of n-SiC) is relatively small as compared to 'a' parameter. The decrease in 'a' parameter indicated towards the partial substitution of B by C [1-3]. DC susceptibility measurement χ(T) depicts that for the undoped sample the Tc shows an increase with increasing sintering temperature, which can be attributed to the improvement of crystallinity for samples sintered at higher temperatures. The Tc for the doped samples depends on two opposite factors: C substitution level and crystallinity. An increase in Ts improves crystallinity and hence Tc while an increase in C substitution level should reduce Tc. Figure 1 implies that doping with n-SiC has significantly improved the Hirr for all the sintering temperatures. Among all the sintering temperatures the 750°C gives the best value of Hirr, which is attributed to grain boundary pinning due to smaller grain size at low sintering temperature. The values of H_{irr} for the 10-wt% n-SiC added sample reached 14, 11.8 & 6.5 T compared to 8.9, 7.9, 5.0 T for the pure one at 5, 10 & 20 K respectively.

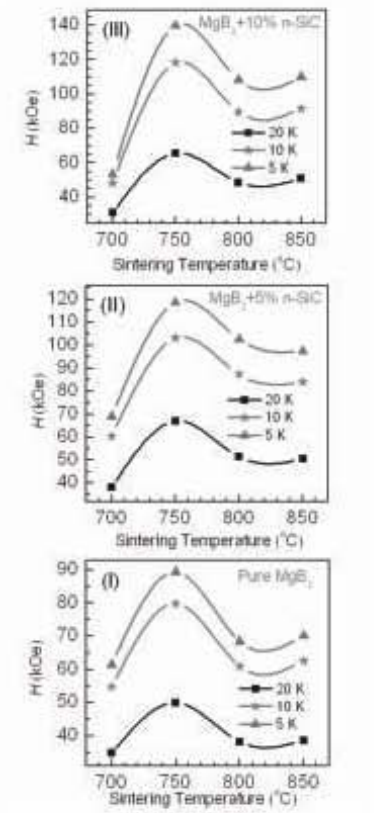

Fig. (1): Effect of sintering temperature (T_s) on H_{irr} for pure and doped samples

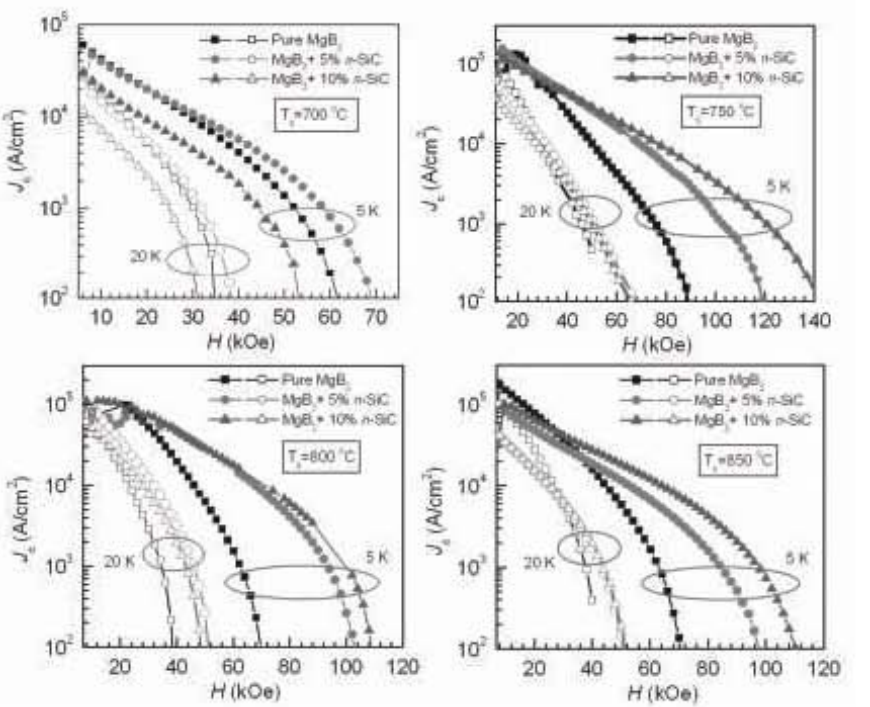

Fig. (2): $J_c(H)$ plots at 20 & 5 K for SiC doped and undoped samples sintered at 700, 750, 800 & 850°C

Some theoretical models are needed to be applied to determine the upper critical field values at low temperatures. By applying Ginzburg-Landau (GL) equation [4]; Hc2(0) for 5-wt% n-SiC doped sample is found to be about 33.2 Tesla while the same is just nearly 16.1 Tesla for the pure MgB_2 sample of second batch (Ts=750°C). Among all the four batches second batch demonstrates the superior Jc(H) performance (see Figure 2). The Jc is 16 times higher than pure one in case of 5-wt% n-SiC doped sample and 30 times higher for the 10-wt% n-SiC doped sample at 5 K in 8.5 Tesla field. The Jc values are 1.08 x 102 A/cm2 and 1.22 x 103 A/cm2 at 5 K in the high field of 12 T for 5-wt% and 10-wt% n-SiC doped samples respectively.

Consequently, we can say that two factors are responsible for the best performance of n-SiC doped samples of low sintering temperature: C substitution for B induces disorder in lattice sites, increase in resistivity and hence improvement in Hc_2; hence in Jc and low temperature processing results in reduction in grain size, extra defects and embedded inclusions such as Mg_2Si and unreacted n-SiC that enhances the flux pinning [1-3].

REFERENCES

1. Arpita Vajpayee, V. P. S. Awana, G. L. Bhalla and H. Kishan, Nanotechnology 19 (2008) 125708
2. S. X. Dou, O. Shcherbakova, W. K. Yeoh, J. H. Kim, S. Soltanian, X. L. Wang, C. Senatore, R. Flukiger, M. Dhalle, O. Husnjak and E. Babic, Phys. Rev. Lett. 98 (2007) 097002
3. S. X. Dou, S. Soltanian, X. L. Wang, P. Munroe, S. H. Zhou, M. Ionescu, H. K. Liu, and M. Tomsic, Appl. Phys. Lett. 81 (2002) 3419
4. I. N. Askerzade, A. Gencer and N. Guclu, Supercond. Sci. Technol. 15 (2002) L13

CONNECTIVITY IN NORMAL AND SUPERCONDUCTING STATE OF EX-SITU BULK MgB_2 WITH DIFFERENT ADDITIVES

ANURAG GUPTA,[1] A.V.NARLIKAR[2]

[1]*National Physical Laboratory (CSIR), Dr.K.S.Krishnan Road, New Delhi -110012, India*
[2]*UGC-DAE Consortium for Scientific Research, University Campus, Khandwa Road, Indore-452017, MP, India*

Variety of ex-situ bulk MgB_2 samples were prepared with additions like excess-Mg, nano-Ag and nano-SiC, and using sintering temperatures varying between 700 ^oC to 950 ^oC. The samples were characterized by XRD, SEM, thermoelectric power S(T), resistivity ρ(T) and magnetization M(B) at 4.2 and 20 K in applied fields B=0 - 8 T. The observed values of ρ(300 K) were typically high (0.12 – 254 mΩcm) and those of critical current density J_c were low ($1.8x10^7$ – $2.8x10^8$ A/m^2 at 4.2 K and 1 Tesla). The large variation in both the quantities, demonstrate a corresponding variation of connectivity in the normal and superconducting state of the different samples. The T dependent part of ρ(T) in the normal state of all samples can be made to scale perfectly by multiplication with different constant factors. Following Rowell's analysis [1], this indicates a difference in connectivity, i.e., effective current carrying cross section in the samples. In the superconducting state, at low fields, the normalized $J_c(B)/J_c(B=1T)$ of all the samples scale perfectly and follows a B^{-1} dependence at both 4.2 K and 20 K. These results apparently reveal that the variation of the low field J_c in different samples has its origin in underlying different effective super-current carrying cross sections. However, we find that the effective cross sections in the normal and superconducting state of the samples do not correlate with each other. This indicates that the electrical connectivity in the normal and superconducting states involve different mechanisms.

REFERENCES

1. J.M. Rowell, Supercond. Sci. Technol. 16 (2003) R17.

PREPARATION AND CHARACTERIZATION OF MICROSTRUCTURE AND MAGNETISM OF Co-NANOPARTICLES

Ashok Kumar Jangir, Renu Pasricha, Anurag Gupta, Hari Kishan, R.C.Budhani

National Physical Laboratory (CSIR), Dr K.S.Krishnan Road, New Delhi-110012, India

The Co-nanoparticles were synthesized by chemical route (thermal decomposition) in the presence of capping agent and surfactant using $Co_2(CO)_5$ inert atmosphere. The nanoparticles were microstructurally characterized by HRTEM and subjected to magnetization (M) measurements in a temperature range T = 5 – 300 K and applied field B = 0 – 1 Tesla. The HRTEM demonstrates monodisperse, homogeneous, polycrystalline spherical nanoparticles with ~ 9 nm diameters. The M(T) curves of the nanoparticles highlight many interesting results: (a) the ZFC and FC branches of M(T) show hysteresis in large T and B region, (b) magnetic upturns at T_M ~ 30 K, below which M(T) rises sharply, (c) T_M does not depend on B, and (d) at T_M both the ZFC and FC branches show shallow minimum that vanishes at B=0.5 T. The measured isothermal M(B) loops at T = 100 – 300 K show similar ferromagnetic behaviour. With change in T, only a small variation in the saturation magnetization M_S ~ 17 - 18 emu/gm, remnant magnetization M_R ~ 4 – 5.5 emu/gm and coercive field B_C ~ 0.014 – 0.015 T was observed. At T < T_M, i.e. 5 K, the M(B) loop at high fields does not saturate fully and shows an increase. Relatively higher values of M_R ~ 12 emu/gm and B_C ~ 0.018 T were observed at 5 K. The nature of magnetism in the Co-nanoparticles, and the effect of capping agent and size will be exhibited.

SYNTHESIS AND MAGNETO TRANSPORT STUDY OF RECoPO (RE=Nd & Sm)

Anand Pal[1,2], Mushahid Hussain[2], V.P.S. Awana[1-]

[1] *Quantum Phenomenon and Applications (QPA) Division, National Physical Laboratory (CSIR) Dr. K.S. Krishnan Marg, New Delhi-110012, India*

[2] *Department of Physics, Jamia, Millia, Islamia, University, New Delhi-110025, India*

E-mail: awana@mail.nplindia.ernet.in

We report the magneto transport and specific heat studies for polycrystalline NdCoPO and SmCoPO samples. These bulk polycrystalline samples are synthesized by solid state reaction route in an evacuated sealed quartz tube.[1] The XRD analysis show that the samples are in single phase, crystallized in a tetragonal structure with space group P4/nmm(fig.1). The lattice parameters a = 3.9072(8)Å, c = 8.1774(6)Å for NdCoPO and a = 3.8794(8)Å, c = 8.0759(0)Å for SmCoPO. The lattice parameters noticeably decrease as the ionic size of trivalent Nd and Sm decrease.

The transport measurements showed that all studied compounds are metallic in nature, and their magnetic ordering in particular the AFM is clearly reflected in magneto-transport studies. These compounds show three magnetic transitions in magneto resistance and specific heat measurement. NdCoPO shows a upward step like transition in $\rho(T)$ measurement under zero field (fig.2) and SmCoPO shows same step under Field(fig.3). The transition of Co spins from ferromagnetic (FM) to anti-ferromagnetic (AFM) for in (Nd/Sm)CoPO is field dependent. The Sm/Nd magnetic moments interact with the ordered Co spins in adjacent layer (RE-O layer) and thus transforms the FM ordered Co spins to AFM.

The $\rho(T)$ measurement plots for NdCoPO at various applied fields shown in Fig. 2. The resistivity of NdCoPO shows an upside step like turn below 20K in Zero field and the temperature of the step like turn decrease with increasing magnetic field, shown in upper inset of Fig.2. The Step like transition is attributed to the ordering of Nd^{4f} moments hybridizing with Co^{3d} moments [2,3]. The isothermal MR with varying magnetic field at various temperatures are depicted in lower inset of Fig. 2. The *MR*% is maximum in the *PM-FM* transformation region and least in both *PM* and saturated *FM* states. The same situation occurs at 2.5K, at higher field of 80kOe and maximum *MR* is yet nearly -12%. The unusual increase of *MR* at lower temperatures possibly the Nd^{4f} moments ordering and their interplay with the *FM* ordered Co^{3d} spins in adjacent Co-P layers.

Figure 3 exhibits the $\rho(T)$ plots for SmCoPO at various applied fields. No, NdCoPO like step transition is observed in zero field resistivity of SmCoPO down to 2.5K. Interestingly in SmCoPO shows the same $\rho(T)$ step like upward transition under magnetic field below 40K, see Fig.3. The step-like upward transition in $\rho(T)$ of NdCoPO is due to *AFM* ordering of Nd spins, the absence of the same transition in SmCoPO keep out the possibility of Sm spins being ordered in field. The step-like transition of SmCoPO under magnetic fields is similar to NdCoPO without field. It's because Sm^{4f} spins order in similar ordered state under field as Nd^{4f} in zero field. The isothermal *MR* data of SmCoPO in various applied fields up to 100kOe at various temperatures is shown in lower inset of Fig. 3. The *MR* is increasing up to -22% as the temperature decrease to 20K at applied field 10kOe and saturates at higher field. Below 50K MR% is increasing due the competition between *FM-AFM* and *FM* state dominates. As temperature goes below 20K the *AFM* state dominate and MR% decrease transitions. Also evident in are the shoulder hysteresis during increase/decrease of field at 10K.

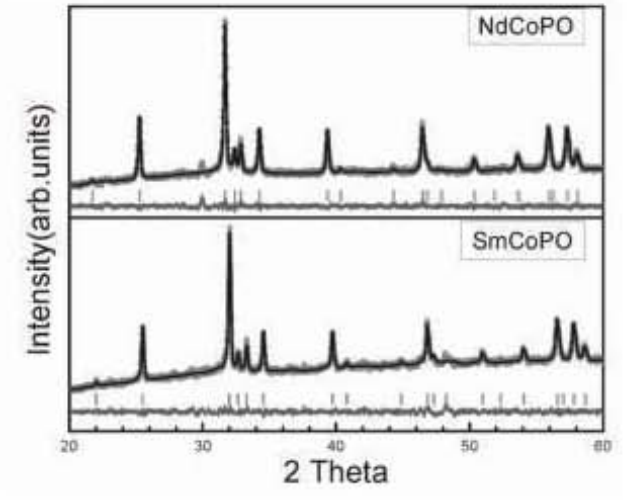

Fig.1 XRD patterns of RECoPO

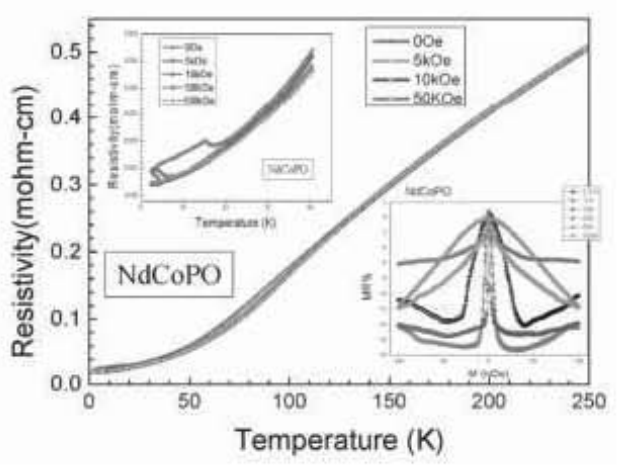

FIG.2 $\tilde{N}(T)$ AND MR% OF NDCOPO

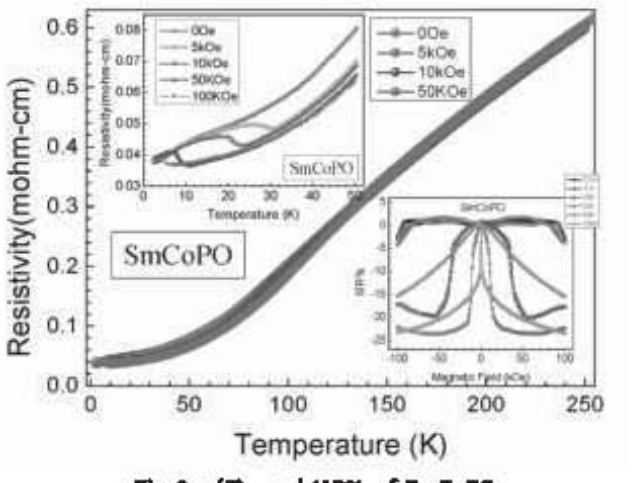

Fig.3 ρ(T) and MR% of SmCoPO

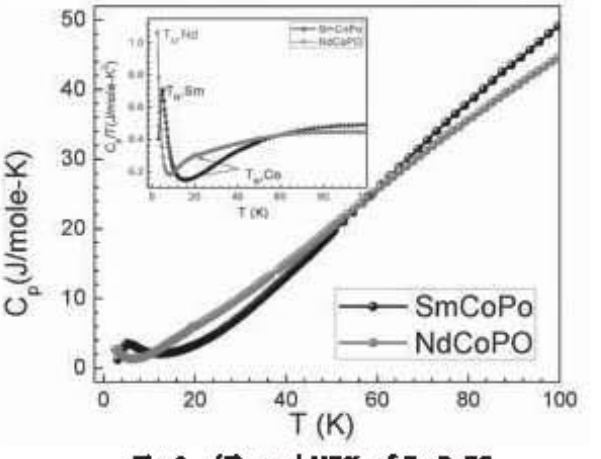

Fig.3 ρ(T) and MR% of SmCoPO

The heat capacity of $C_p(T)$ of the both studied samples NdCoPO and SmCoPO are shown in Figure 4. The expected Sm T_N (AFM) is seen as a peak in $C_p(T)$ at 5.4K, and for Nd the same is below 2K in SmCoPO and NdCoPO respectively. The C_p/T vs T plots slope change first at around 80K, which roughly coincides with the *FM* ordering of Co spins. With further lowering of temperature the C_p/T vs T plots slope change at around 20K and 15K with a shallow broad minimum respectively for SmCoPO and NdCoPO. These temperatures roughly coincide with the complex *AFM* ordering of Sm^{4f}-Co^{3d} and Nd^{4f}-Co^{3d} interplayed matrix. It seems the Sm/NdCoPO undergo three magnetic transitions i.e., T_{Co} (~80K), the Sm^{4f}-Co^{3d} and Nd^{4f}-Co^{3d} interplayed *AFM* below 20K and finally Sm^{3+} and Nd^{3+} spins individual *AFM* at 5.4K and below 2K respectively.

REFERENCES

1. V. P. S. Awana, I. Nowik, Anand Pal, K. Yamaura, E. Takayama-Muromachi, and I. Felner Phys. Rev. B 81, 212501 (2010).
2. M. A. McGuire, D. J. Gout, V. O. Garlea, A. S. Sefat, B. C. Sales, and D. Mandrus, Phys. Rev. B 81, 104405 (2010).
3. Anand Pal, H. Kishan, and V.P.S. Awana arXiv:1008.2593 (2010)

ROLE OF DISORDER IN THE SUPERCONDUCTIVITY OF $FeTe_{1/2}Se_{1/2}$

Anuj Kumar[1,2], Somnath Dey[1], Shahnawaz[2], H. Kishan[1], V.P.S. Awana[1]

[1]*Quantum Phenomena Application Division, National Physical Laboratory, New Delhi-110012*
[2]*Department of Physics and Astrophysics, University of Delhi New Delhi-110007*
E-mail: awana@mail.nplindia.ernet.in

Here we report the effect of quenching on $FeTe_{1/2}Se_{1/2}$ superconductor at various 700°C, 500°C, 300°C and 30°C temperatures, and study the role of disorder on superconductivity of $FeTe_{1/2}Se_{1/2}$. Samples are synthesized by standard solid state reaction route. These samples are quenched to air systematically at 700°C, 500°C, 300°C and RT. We study their structural and magnetic properties. XRD and dc magnetization studies revels that samples quenched at 700°C possess different phase and are not superconducting as well. It is clear quenching introduced disorder in the unit cell of $FeTe_{1/2}Se_{1/2}$ superconductor affects its superconductivity dramatically.

The discovery of new iron-based high T_c superconductors has ignited immense excitement in the material science community from past two years. Oxy-pnictides have general structural formula $REFeAsO_{1-x}F_x$ (RE = rare earth). The parent compounds of the FeAs based superconductors do not exhibit superconductivity but possess stripe type commensurate anti-ferromagnetic spin order accompanied by a structural transition at around 150 K [1]. The highest T_c in these oxypnictide is reported at 56K for $SmFeAsO_{0.85}$ and $Gd_{0.8}Th_{0.2}FeAsO$ [2,3]. Another important series of Iron based same family compounds are chalcogenides (FeSe, $FeSe_{1-\delta}$, $FeSe_{1-x}Te_x$, $FeTe_{1-x}Se_x$) having similer Fe_2Se_2 layers. The self doped anion deficient binary superconductor β-$FeSe_{1-\delta}$ shows a T_c of 8K which increases to 37K by applying a hydrostatic pressure of 8.9 GPa. The compound has similar structure and band filling as that of FeAs layer found in the quaternary iron arsenide and therefore presents a simple suitable model to study the interplay of structure, magnetism and superconductivity within iron based superconducting family. Samples of $FeTe_{1/2}Se_{1/2}$ are synthesized by standard solid state reaction route via encapsulation of stoichiometric high purity (>3N) Fe, Se, Te, details are same as in ref. 4. The X-ray diffraction is done on Rigaku Mini Flex diffractometer. The Magnetization (AC and DC) are carried out on a physical property measurement system (PPMS) from Quantum Design USA.

Figure 1 shows the XRD patterns of various temperatures (700°C, 500°C, 300°C and RT) quenched $FeTe_{1/2}Se_{1/2}$. Samples quenched at 500°C, 300°C and RT have the same XRD patterns, while the 700°C quenched sample has different phase, seemingly Fe_7Se_8. The 500°C, 300°C and RT samples are all crystallized in tetragonal structure with space group P4/nmm. Detailed Reitveld analysis of their XRD patterns showed that though are single phase in nature, their co-ordinate positions and lattice parameters are slightly different. The occupancy and co-ordinates of Se and Te are affected with quenching.

The DC magnetic susceptibility plots of various temperatures (700°C, 500°C, 300°C and RT) quenched $FeTe_{1/2}Se_{1/2}$ sample are given in Figure 2. RT and 300°C quenched samples shows superconducting transition at 13K. Inset of figure 2 shows dc susceptibility behavior of 500°C and 700°C quenched sample. Both samples quenched at 700°C and 500°C are non superconducting even at 2K. Sample quenched at 700°C shows a ZFC and FC branching around temperature 200K due to possible magnetic ordering of Fe. Similar branching of ZFC and FC is seen at around 130K for 500°C

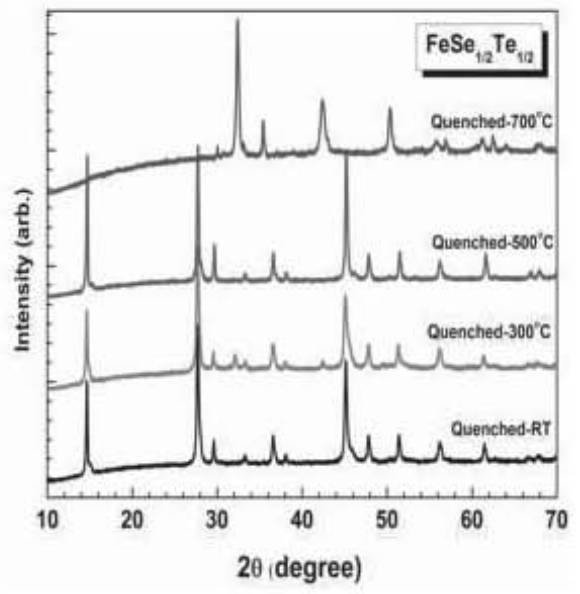

Fig. 1 XRD pattern of various temperatures quenched $FeSe_{1/2}Te_{1/2}$

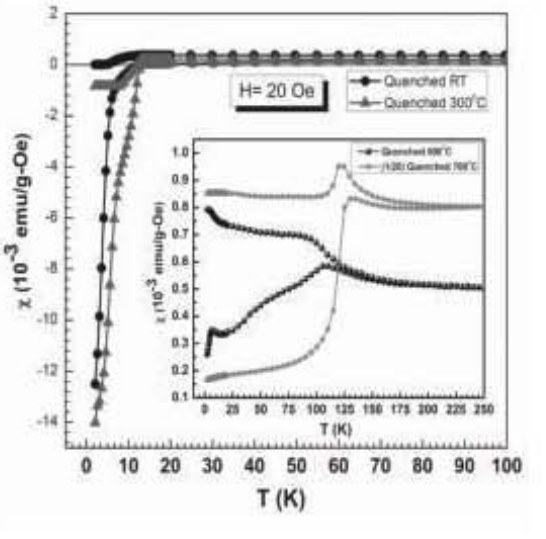

Fig. 2 M-T plots for RT and 300°C quenched $FeSe_{1/2}Te_{1/2}$ at 20 Oe Inset shows same for 500°C and 700°C quenched $FeSe_{1/2}Te_{1/2}$

quenched sample. The 500°C quenched sample though also exhibited some sign of superconductivity in ZFC transition below say 10K, but the diamagnetic volume fraction seems very small.

Detailed Reitveld analysis of the XRD patterns of variously quenched $FeSe_{1/2}Te_{1/2}$ superconductor directly relates the extent of Fe, Se, and Te sites disorder to the appearance/disappearance of superconductivity in this system. In conclusion, our results indicate Fe, Se and Te site disorder dependent superconductivity in $FeSe_{1/2}Te_{1/2}$.

REFERENCES

1. C. R. dela Cruz, H. A. Mook, N. L. Wang and P. Dai, Nature **453** (2008) 899.
2. Z.A. Ren et al., Euro. Phys. Lett. **83** (2008) 17002
3. C. Wang et al., Euro. Phys. Lett. **83** (2008) 67006
4. V.P.S. Awana et al., J. Appl. Phys. **107** (2010) 09E128

SINGLE STEP SYNTHESIS OF $NdFeAsO_{0.80}F_{0.20}$ BULK 50K SUPERCONDUCTOR

V.P.S. Awana, R.S. Meena, H. Kishan

Quantum Phenomenon and Applications Division, National Physical Laboratory, Dr. K.S. Krishnan Marg, New Delhi-110012, India
E-mail: awana@mail.nplindia.ernet.in

We report an easy *single step* synthesis route of title compound $NdFeAsO_{0.80}F_{0.20}$ superconductor having bulk superconductivity below 50 K. The title compound is synthesized via solid-state reaction route by encapsulation in an evacuated (10^{-3} Torr) quartz tube. Rietveld analysis of powder X-ray diffraction data shows that compound crystallized in tetragonal structure with space group *P4/nmm* (Fig.1). *R(T)H* measurements showed superconductivity with T_c (*R*=0) at 48 K (Fig.2) and a very high upper critical field (H_{c2}) of up to 345 Tesla (Fig.3). Magnetic measurements exhibited bulk

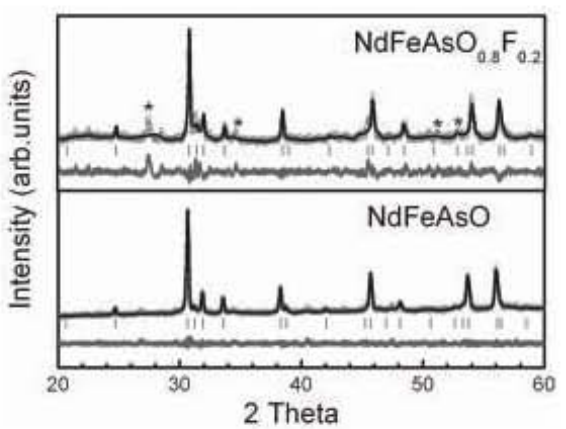

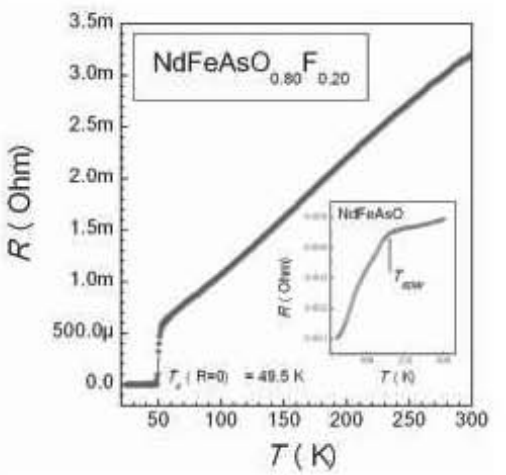

Fig.1 XRD and Fig.2 R(T) of NdFeAsOF and $NdFeAsO_{0.8}F_{0.2}$

superconductivity in terms of diamagnetic onset below 50 K. The lower critical field (H_{c1}) is around 1000 Oe at 5 K. In normal state i.e., above 60 K, the compound exhibited purely paramagnetic behavior and thus ruling out the presence of any ordered FeO_x impurity in the matrix. In specific heat (C_p) measurements a jump is observed in the vicinity of superconducting transition (T_c) along with an uptum at below *T*=4 K due to the AFM ordering of Nd^{+3} ions in the system. The Thermo-electric power (*TEP*) is negative down to T_c, thus indicating dominant carriers to be of n-type in $NdFeAsO_{0.80}F_{0.20}$ superconductor. The granularity of the bulk superconducting $NdFeAsO_{0.8}F_{0.2}$ sample is investigated and the intra and inter grain contributions have been individuated by looking at various amplitude and frequencies of the applied AC drive magnetic field [1].

REFERENCES

1. V.P.S. Awana et al to appear in Euro. Phys. Journal B (2011)/ arxiv (2010).

ENHANCED GRAIN-COUPLING AND TRANSPORT CURRENTS OF BSCCO SUPERCONDUCTOR WITH NANO-SIZE DOPANTS

NITIN KUMAR, SURAJ BHAN, LOVNEET TYAGI AND P.L.UPADHYAY

National Physical Laboratory, Dr.K.S.Krishnan Road, New Delhi 110012
Email: pushpa@mail.nplindia.org

Despite their superior intrinsic characteristics, the high temperature superconductors have not been able to match the widespread utility of conventional Nb-based superconductors in practical devices, particularly those using the long-length wires of these materials such as the high field superconducting magnets. The reason for this limitation is the drastic drop in critical currents at the grain-boundaries. The phenomenon has been extensively investigated, both theoretically [1-3] and experimentally whereby efforts are directed to improve the coupling across mismatched grain-boundaries. In recent years, nano-size dopants have proved extremely beneficial in raising the critical current density of $YBa_2Cu_3O_{7-y}$ by drastically improving the flux-pinning properties [4]. This paper reports the effect of nano-particle inclusions on the properties of the Bi-based Bi-2223 superconductor and a marked increase in transport critical current density Jc, has been observed both at 77K and at 4.2 K when doped with nano-Mo. Samples of Bi-2223 were prepared using the nominal composition of $Bi_{1.8}Pb_{0.4}Sr_2Ca_2Cu_3O_y$ to which nano-Mo (~ 100 nm) was added. The carbonates and oxides were calcinated and sintered at 845 °C for ~ 65 to 100 hours using the standard solid state diffusion process.

In another approach, composites of Bi-2223 with nano-Mo were prepared by adding 1-5 wt.% Mo powder to the pure un-doped $Bi_{1.8}Pb_{0.4}Sr_2Ca_2Cu_3O_y$ and sintering the pellet at 400°C only. The increase in T_c with doping is only marginal (Fig.1), but the enhancement of J_c, both at 77K and 4.2 K (measured on a ~ 1 x 4 x 40 mm sample-strip and I_c defined by the 1 μV/cm criteria), is quite noticeable (Table 1). This is accompanied with an improvement in the inter-grain coupling in the same samples as indicated by the width and positions of C" peaks of the complex part of the a.c. susceptibility (Fig.2). A preliminary analysis suggests that the improved inter-grain coupling could be responsible for the increase in overall transport current density as a result of better flow of super-current across the grains in samples doped with nano-Mo. Whether there is any contribution of the nano-scale dopant on the flux-pinning properties and thereby enhancement of Jc , however, is not very clear and is being investigated.

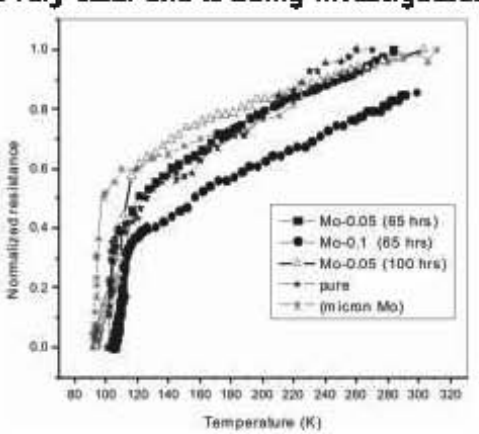

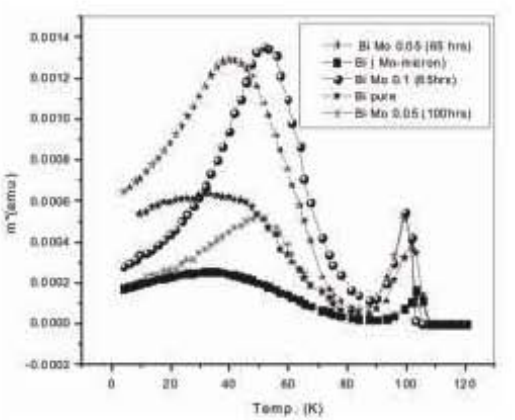

Fig. 1. Resistivity vs. temperature behavior and Fig. 2. a.c.susceptibity (X") versus temperature for various samples of Table 1.

TABLE 1 Tc values from a.c. susceptibility (X') measurements, and Jc values at 4.2 and 77K along with dopant conc. for samples of Fig.(1 & 2)

Dopant Mo in Bi-2223	T_c(on) (K)	J_c(4.2K) A.cm^{-2}	J_c(77K) A.cm^{-2}	XRD (summary)
Nano 0.05 (I)	106	2.2x10^3	0.25x10^3	2223
0.05 (II)	106	2.0x10^3	0.2x10^3	2223+2212
0.1 (I)	108	3.2x10^3	0.36x10^3	2223
0.05(μm)	106	1.2x 10^3	0.08x10^3	2223+2212
pure	104	1.0x10^3	0.06x10^3	2223

REFERENCES

1. Sigrist M.& Rice T.M., J.low temp.Phys,**95**, 589 (1994)
2. Yokoyama T. et al. , Phys.Rev.B **95,** 020502 (2007)
3. Gurevich A. & Pashtishiki E.A, Phys.RevB,**57**, 13878 (1998)
4. Yeoh W.K et al, Trans.on Appl Supercond **3**, L-19 (2009)

STRUCTURAL, MAGNETIC, MAGNETO-TRANSPORT AND CHARGE ORDERING PROPERTIES OF $Bi_{0.6-x}Pr_xCa_{0.4}MnO_3$ ($0 \leq x \leq 0.6$) PEROVSKITE MANGANITES

KAMLESH YADAV, G.D. VARMA

Department of Physics, Indian Institute of Technology, Roorkee-247667, India
Email: gdvarfph@iitr.ernet.in

In the past few years, doped perovskite manganites have been intensively studied to understand their electrical and magnetic properties. In these materials, the magnetoresistance effect, metal-insulator transition, orbital ordering, charge ordering, double exchange interaction, etc. can be changed over a wide range by different doping levels. $Bi_{1-x}Ca_xMnO_3$ (BCMO) constitutes a very interesting but less-studied system. Early experiments showed that the system is insulating over a broad region of Ca doping $0.2<x<1.0$. An interesting property of Bismuth-based manganites ($Bi_{1-x}A_xMnO_3$, A= Ca, Sr) is of a very high charge ordering temperature (T_{CO}). Bi^{+3} ions have been found to push T_{CO} up to 550 K in $Bi_{0.5}Sr_{0.5}MnO_3$ while $Bi_{0.6}Ca_{0.5}MnO_3$ displays T_{CO} = 325 K. In contrast with rare-earth-based manganites, bismuth-based manganites have not been extensively studied due to the lack of an appreciable magnetoresistive property.

In this present work, the effect of Pr-doping on the charge ordering (CO) state in $Bi_{0.6-x}Pr_xCa_{0.4}MnO_3$, where x=0.00, 0.10, 0.20, 0.30, 0.40, 0.50 and 0.60 has been investigated by transport and magnetic measurements. Polycrystalline $Bi_{0.6-x}Pr_xCa_{0.4}MnO_3$ samples are prepared using the standard solid –state reaction route. Stoichiometric precursor powders Bi_2O_3, $CaCO_3$, and Pr_6O_{11} and MnO_2 are mixed and ground to get highly homogenized powder. The resultant powder is then calcined for 12 h at 800°C. This powder is again reground and calcined at 850°C for 12 h and then at 900° C for another 12 h with intermediate grinding. After the final grinding, the powder is pressed into rectangular pellets with the dimension of 12.0 ×7.0× 2.0 mm^3. The pellets are sintered at 1100°C for 24 h. The synthesized samples are examined by x-ray diffraction (XRD, CuK_α) for determination of crystal structure. Resistivity as a function of temperature is measured by a standard four probe method without or with magnetic fields (0–1 T). The DC magnetization measurements are done using a SQUID magnetometer. XRD patterns indicate that all samples are orthorhombic. The unit cell volume decreases with increasing Pr content because smaller Pr^{+3}(1.126 Å) ions substitute larger Bi^{+3} (1.17Å) ions.

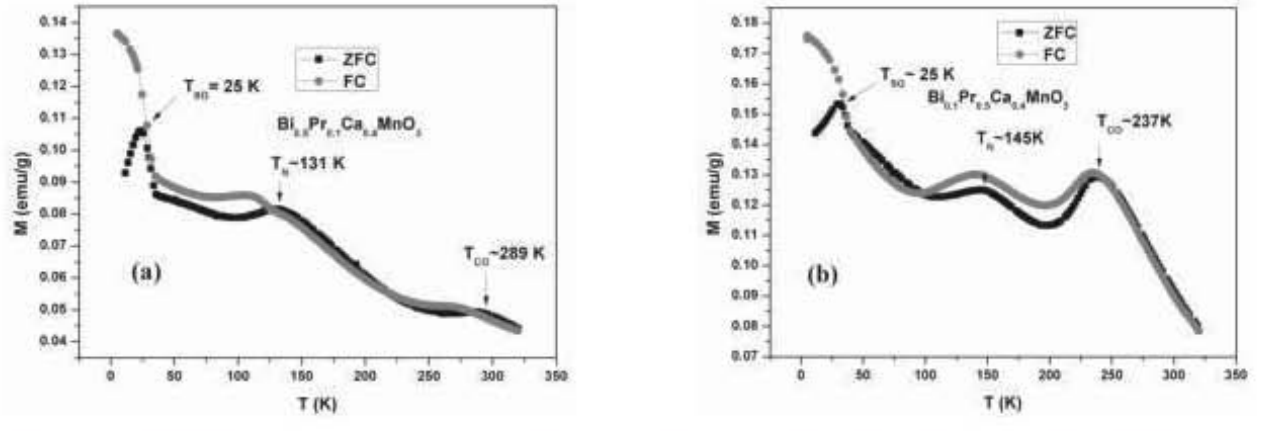

Fig. 1(a-b) Magnetization as a function of temperature under zero field cooling (ZFC) and field cooling (FC) at H= 500 Oe for $Bi_{0.5}Pr_{0.1}Ca_{0.4}MnO_3$ and $Bi_{0.1}Pr_{0.5}Ca_{0.4}MnO_3$ samples

From the magnetization vs temperature plots [Fig.1 (a-b)], the charge ordering temperatures (T_{CO}) are found to be ~ 289 K, 264 K, 256 K, 244 K and 237 K for the samples x= 0.1, 0.2, 0.3, 0.4, and 0.5 respectively. In charge ordered phase, anti-ferromagnetic (AFM) super-exchange interactions dominate and lead to an AFM ordering at the antiferromagnetic transition temperature T_N~ 131 K, 128 K, 125K, 132 K, and 145 K for x= 0.1, 0.2, 0.3, 0.4, and 0.5, respectively. The contribution of AFM interaction indicates inhomogeneity in long range ferromagnetic order. The appearance of a cusp in ZFC curve and irreversibility between ZFC and FC at 25 K indicates that a spin glass (SG) behaviour dominates below this temperature. It is expected that the SG state originates from the competition between the ferromagnetic (FM) double exchange and AFM superexchange interaction [1]. For the temperatures above T_{CO}, Curie-Weiss type behavior is obtained with positive value of θ_P for all samples confirming the ferromagnetic interaction. θ_P is negative for T below T_N indicating the existence of strong AFM interactions in CO state. The T_{CO} decreases gradually with increasing Pr doping level in $Bi_{0.6}Ca_{0.4}MnO_3$. All samples are paramagnetic at 300 K and sample x=0.50, 0.60 are ferromagnetic at 10 K and no saturation in magnetization is observed with the applied magnetic field up to 7 T. The increased magnetizations are observed with increasing the Pr-doping. Magnetization measurements as a function of temperature in a magnetic applied field of 500 Oe shows that $Pr_{0.6}Ca_{0.4}MnO_3$ sample exhibit a sharp transition from paramagnetic to ferromagnetic state at the Curie temperature T_C~103 K.

The temperature-dependent resistivity measurement shows that the conductivity increases with increasing the Pr content. This is due to the delocalisation of charge carriers with Pr doping, which enhances the spatial overlap between Mn e_g and O 2p orbitals and therefore increases the mobility of carriers [2, 3]. We have plotted in ρ-$T^{-1/4}$ curves for all the samples. The resistivity can be best fitted with the Mott's variable range hopping (VRH) model $\rho \sim \exp (T_o/T)^{1/4}$[4]. T_o is related to localization length ξ by the relation $k_B T_o = 24/(\pi N(E_F) \xi^3)$, where $N(E_F)$ represents the density of states at Fermi level. From the fitting of the data, we found that $T_o^{1/4}$ (Mott's parameter) decreases gradually with Pr doping. This suggests that the localization length ξ increases with the increasing Pr-doping content provided $N(E_F)$ does not change. This is to say that the carriers become less localized with the increasing Pr-doping content.

REFERENCES

1. W.J. Lu, Y.P. Sun, X.B. Zhu, W.H. Song, J.J. Du. Solid State Communications, 138 (2006) 200-204.
2. X. Z .Yu, T. Arima, Y. Kaneko, J. P. He, R. Mathieu, T. Asaka, T. Hara, K. Kimoto, Y. Matsui and Y. Tokura, J. Phys.:Condens. Matter 19 (2007) 172203
3. R.R. Zhang, G.L.Kuang, X.Luo, Y.P.Sun, J. Magn. Magn. Mater, 321(2009) 3933-3937
4. N.F. Mott, E.A. Davis, Electronic Processes in Non-crystalline Materials, Clarendon Press, Oxford, 1979.

EFFECT OF Ni^{2+} ON $Ni_xCo_{1-x}Fe_2O_4$ (x= 0.5, 0.75, 0.9) MAGNETIC NANOPARTICLES

AJAY SHANKAR[1], SANDEEP KUMAR[1], MANJU ARORA[1], SANJEEVE THAKUR[2], R.P.PANT[1]

[1]*National Physical Laboratory, Dr. K.S. Krishnan Marg, New Delhi-110012, India*
[2]*Netaji Subhas Institute of Technology (NSIT) University of Delhi, Delhi-110007*

Nanocrystalline materials are in focus of recent research due to their potential applications and interesting physics involved in them. The physical properties of the ferrites are very sensitive to the method of synthesis, size, shape, purity, cation distribution, the type of substitution. The high coercivity of these magnetic particles find applications in the field of high density magnetic media, recording color imaging, high frequency devices, magnetic refrigeration, sensors and materials for biomedical field etc. [1-2]. In the present work, the structural and magnetic properties of different Ni^{2+} ions concentration doped cobalt ferrite were investigated. Nickel cobalt ferrite nanoparticles with chemical composition $Ni_xCo_{1-x}Fe_2O_4$ (a = x = 0.5, b = x= 0.75 and c = x = 0.9) have been synthesized by chemical co-precipitation route by using iron (III) chloride, cobalt (II) chloride and nickel (II) chloride as precursors for iron, cobalt and nickel respectively. The structure and phase confirmation were characterized by Rigaku Japan make powder X-ray Diffractometer using Cu Kα radiation. Magnetic properties. X-band EPR spectrometer model A300, Bruker Biospin, Germany was used for investigating the magnetic resonance phenomena in these particles at ambient temperature. Polytronic search coil magnetic properties measurement setup was used to find saturation magnetization and coercivity of these developed particles with different cobalt content.

The X – ray diffraction patterns confirm the formation of single phase nickel cobalt ferrite nanoparticles. The lattice parameters, strain and crystallite size were calculated using strong (311) plane from the XRD pattern. Crystallite size decreases from 18.39 nm (x=0.5) to 13 nm (0.9). The unit cell parameter 'a' decreases linearly with the increase in nickel concentration due to small ionic radius of nickel which results the reduction in lattice strain are listed in Table 1.The structure of Ni-Co ferrite is known to be normal spinal, where Ni^{2+} ions prefer to occupy tetrahedral site because their 4s,p electrons can form a covalent bond with the six 2p electron of the oxygen ions. As Ni^{2+} increase the magneto crystalline anisotropy decreases and leads to decrease in magnetization.

EPR spectra of the different nickel ions concentration doped cobalt ferrite nanoparticles were recorded in 4000 $\pm$ 4000 scan range at 100 kHz modulation and 1 mW microwave power showed a broad strong resonance signal superimposed by a narrow signal. DPPH was used a standard reference field marker. The broadness of EPR signal arises from Fe^{3+} of g-value ~ 2.24 indicates the ferromagnetic behavior and strong dipolar-dipolar interaction among nanoparticles. While the narrow line signal of g-value ~ 2.00 confirms the presence of superparamagnetic particles. The peak-to-peak line width

Sample	Experimental lattice parameter a(Å)	Experimental interplanar spacing d_n(Å)	Standard interplanar spacing, d_0(Å)	Strain $(d_n - d_0)/ d_n$	Crystallite size (nm)
a	8.411	2.529	2.532	-0.001190	8.535
b	8.386	2.520	2.532	-0.00476	11.375
c	8.372	2.516	2.532	-0.00636	12.407

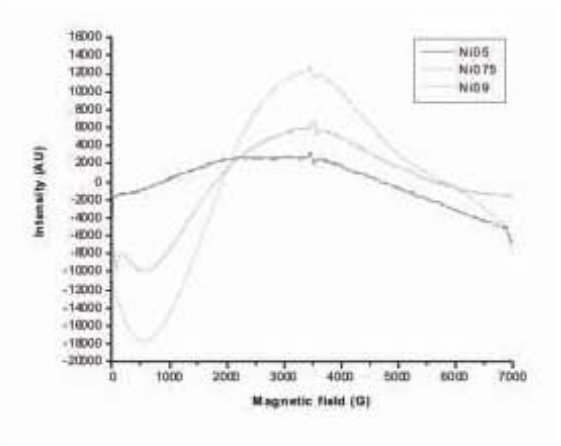

Fig. 1: EPR spectra of $Ni_xCo_{(1-x)}Fe_2O_4$ (x = 0.5, 0.75 and 0.9)

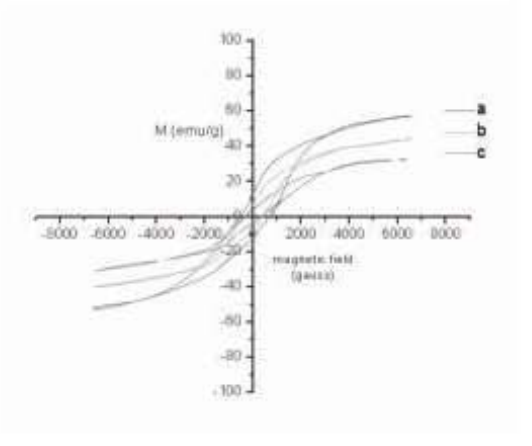

Fig.2: Magnetic measurements of $Ni_xCo_{(1-x)}Fe_2O_4$ (a= x = 0.5, b = x = 0.75 and c = x= 0.9)

and g-value of the narrow signal increases with increasing nickel content due to the strengthening of magnetic interactions among particles which increases the effective magnetic moment originating from the variation in spin structure.

The magnetization hysteresis loops of these samples exhibits strong magnetic nature at room temperature. The coercivity and saturation magnetization were found to decrease with increasing content of Ni^{2+} which was attributed to large magnetocrystalline anisotropy.

REFERENCES

1. H. Lee, J. Ch. Jung, H. Kim, Y.M. Chun, T.J. Kim, S.J. Lee, S.H. Oh, Y.S. Kim, I.K. Song, Catal. Lett. 122 (2008) 281.
2. J.T. Jang, H. Nah, J.H. Lee, S.H. Moon, M.G. Kin, Cheon, J. Angew. Chem. Int. Ed. 48

STRUCTURAL AND MAGNETIC CHARACTERIZATION OF NANOCRYSTALLINE $Pr_{1-x}Sr_xMnO_3$ ($0.40 \leq x \leq 0.60$)

NEELAM MAIKHURI[1], H. K. SINGH[2], ANURAG GAUR[1]

[1]*Department of Physics, National Institute of Technology, Kurukshetra-136119, India*
[2]*National Physical Laboratory, Dr. K.S. Krishnan Marg, New Delhi-110012, India*
Email: anuragdph@gmail.com

Recently several experimental and theoretical studies have focused on the exploration of grain size effect on the structural, magnetic and magnetotransport properties of alkaline earth doped rare earth perovskite manganites, chemically represented by $RE_{1-x}AE_xMnO_3$ (RE=rare earth cation and AE=alkaline earth cation) [1-4]. Since size reduction leads to increased contribution from the surface regions, the broken Mn-O-Mn bonds are indeed expected to have a definite impact on magneto-electrical properties in manganites. It has been shown that in nano-manganites, size reduction below ~100 nm renders the charge and orbitally ordered (CO-OO) ground state with unstable antiferromagnetic (AFM) spin order, giving rise to a ferromagnetic (FM) ground state [3].

In the present work, we have studied the effect of Sr content on structural and magnetic properties of nanocrystalline $Pr_{1-x}Sr_xMnO_3$ (x=0.40, 0.50, 0.55 and 0.60). The nanocrystalline $Pr_{1-x}Sr_xMnO_3$ (PSMO) sample are synthesized by polymeric precursor based sol-gel route. Structural and microstructural characterizations are carried out by powder X-ray diffraction (XRD) and scanning electron microscopy (SEM). Magnetic characterizations are carried out by measuring the temperature dependent ac susceptibility using the lock-in technique.

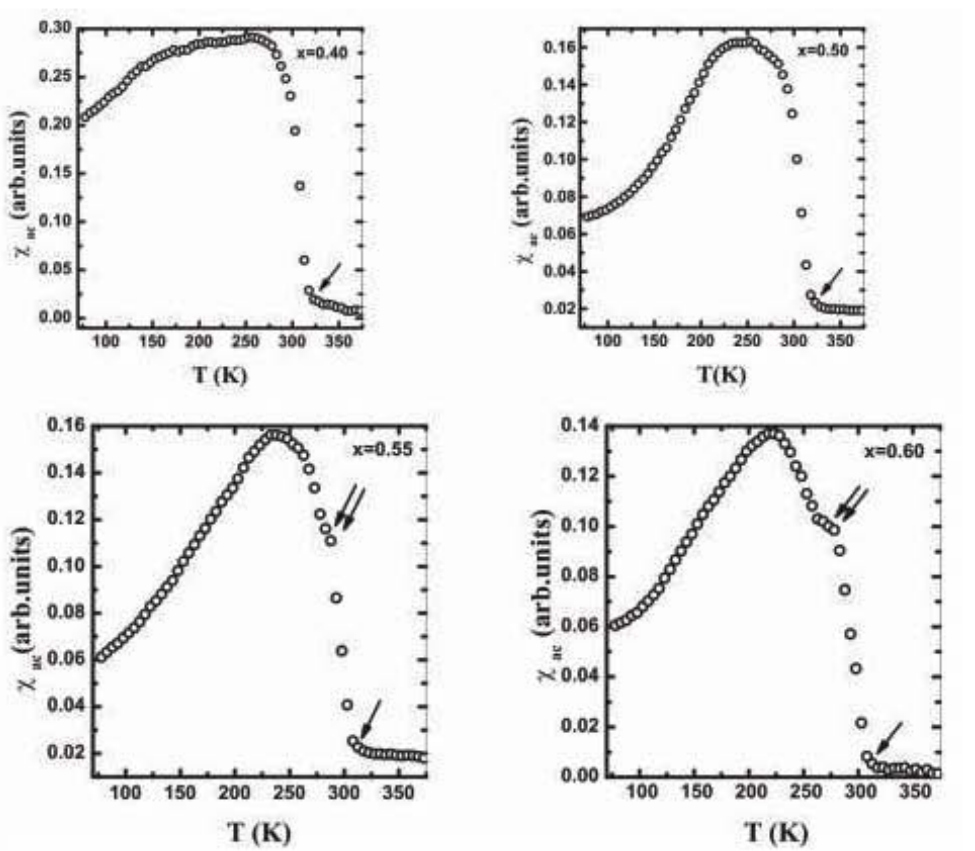

Fig. 1: Temperature dependent ac susceptibility of $Pr_{1-x}Sr_xMnO_3$ (x=0.40, 0.50. 0.55 & 0.60)

XRD results show that all samples have single PSMO phase and possess orthorhombic structure. The surface microstructure of the samples, as revealed by scanning electron microscopy (SEM), is found to consist of nanometric grains. The average grain size is found to be 40-50 nm in all the samples. The temperature dependent AC susceptibility (χ-T), measured through lock-in technique, is shown in Fig. 1. The PSMO samples with x=0.40 and 0.50 show a sharp paramagnetic to ferromagnetic (PM-FM) transition at T_C=308 K. However, In PSMO samples with x=0.55 and 0.60, the FM transition temperature is found to decrease slightly to T_C~300 K and the transition width also increases. The most interesting observation in PSMO samples with x=0.55 and 0.60 is the occurrence of a second transition (marked by double arrow in Fig. 1), which occurs at T~273 and 255 K for x=0.55 and 0.60 samples, respectively. The presence of second AFM phase in PSMO samples with x=0.55 and 0.60 is also evidenced by sharp decrease in their value of susceptibility in the lower temperature range.

REFERENCES

1. Y. Tokura and Y. Tomioka, J. Magn. Magn. Mater. **200**, 1 (1999).
2. F. Chen, et al., J. Phys.: Condens. Matter **17**, L467 (2005).
3. S. S. Rao, K. N. Anuradha, S. Sarangi, and S. V. Bhat, Appl. Phys. Lett. **87**, 182503 (2005).
4. D. Akahoshi, et al, Phys. Rev. B, **77** 054404 (2008).

TEMPERATURE DEPENDENT JUNCTION MAGNETORESISTANCE BEHAVIOR OF THE Ni NANOPARTICLE IN TiN WITH p-Si HETEROJUNCTION

J. Panda, S. Chattopadhyay, T. K. Nath

Department of Physics and Meteorology, Indian Institute of Technology Kharagpur, WestBengal, 721302

Email: panda.phy@gmail.com

Nanocrystalline nickel particles embedded in crystalline titanium nitride (TiN) matrices shows good magnetic properties along with anomalous Hall Effect behavior [1]. As the nanocrystalline nickel particles embedded in crystalline titanium nitride (TiN) matrices have good magnetic behavior as well as good conductivity, this can be a good candidate for magnetic electrode in spintronics device family. In this work, we have presented the temperature dependent junction magnetoresistance (JMR) behavior of nanocrystalline nickel particles embedded in crystalline titanium nitride (TiN) matrices on Si substrate where Ni nanocrystallites are self-assembled and epitaxially grown. This heterojunction of nanocrystalline Ni particles embedded in crystalline TiN matrices with p-Si exhibits diode like excellent rectifying behavior in the temperature range of 77-300 K. The I-V characteristics with and without external magnetic field have been studied in the temperature range of 77-300 K. The good rectifying diode like characterstics has been observed with positive magnetoresistance at 77 and 200 K and negative magnetoresistance at 300 K.

Nanocrystalline nickel particles embedded in a metallic TiN matrix thin film have been grown on p-Si substrate using the pulsed laser deposition technique in a high vacuum environment (~5 $\times 10^{-7}$ Torr) at 600 °C substrate temperature. The energy density and the repetition rate of the laser beam used were 2 J /cm^2 and 10 Hz, respectively. The size distribution of Ni particles and the crystalline quality of both the matrix and the magnetic particles were investigated by cross-sectional high-resolution scanning transmission electron microscopy with atomic number (Z) contrast (STEM-Z) and low temperature I-V properties have been carried out using a source meter (Keithley-2612) and temperature controller (Lakeshore-331).

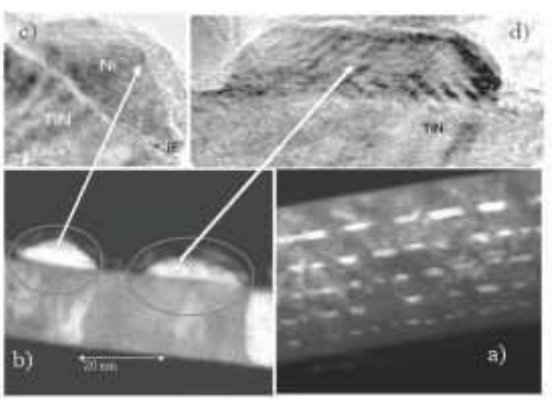

FIG. 1.(a) A cross-sectional STEM-Z image, (b) its expanded view, (c) high-resolution STEM-Z contrast image of textured Ni nanocrystallites with triangular morphology, and (d) with rectangular morphology.

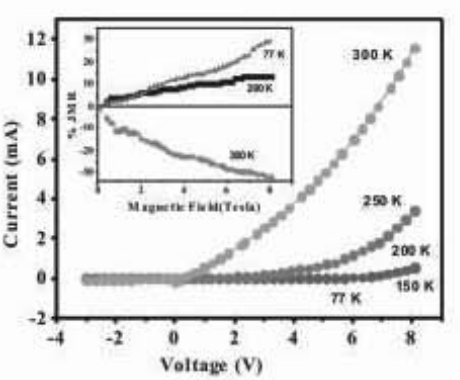

FIG. 2 I-V behavior of TiN(Ni)/p-Si heterojuction at different temperatures without applied magnetic field. Inset shows the variation of magnetoresistance with applied field up to 8 T.

The cross sectional STEM-*Z* image of Ni particles in TiN matrix [Figs. 1(a) and 1(b)] has shown that the metallic particles are well separated (10 nm) from each other. A high-resolution cross sectional STEM-*Z* contrast image of a triangular precipitate in <110> direction is shown in Fig. 1(c). Fig. 1(d) shows the cube-on-cube <001>Ni/ / <001>TiN/Si with dots with rectangular morphology.

The I-V characteristics of the heterojuncton without magnetic field at different temperatures have been shown in Fig 2. In inset of Fig 2, the positive magneto resistance at 77 K (≈ 29%), 200 K (≈ 13%) and negative magneto- resistance at 300 K (31%) have been shown keeping the forward bias voltage at 6 V. The appearance of positive magneto-resistance seems to be due to the spin injection from metallic TiN with Ni side to non-magnetic p-Si side as spin splitting and large population of up-spin electrons dominates at the metallic TiN with Ni electrode at temperatures 77 and 200 K [2]. The spin-up population decreases at higher temperature (300 K) and the spin injection reduces. The appearance of negative magnetoresistance at 300 K is most like due to the negative magnetoresistive behavior of the magnetic electrode.

REFERENCES:

1. P. Khatua, T. K. Nath and A. K. Majumdar, Phys. Rev. B **73**, 064408 (2006)
2. M. Johnson, Magnetoelectronics, (Academic press, Elsevier)

HYSTERESIS IN SUPERCONDUCTING SHORT WEAK LINKS AND μ-SQUIDS

D. Hazra[1], L. Pascal[2], H. Courtois[2], A. K. Gupta[1]

[1]*Department of Physics, Indian Institute of Technology, Kanpur – 208016, India.*
[2]*Institut Ne'el, CNRS and Universite' Joseph Fourier, Grenoble, France.*
Email: dibhaz@iitk.ac.in

A micron-size superconducting quantum interference device (μ-SQUID) consists of two superconducting Dayem bridges or weak links (WL) [1] of dimension of the order of the coherence length, in parallel, forming a loop with area in the μm² range. A superconducting single WL behaves very much like a Josephson junction [1] with the supercurrent approximately given by $I = I_c \sin(\Theta)$, where I_c is the critical current and Θ is the phase difference across the junction. When two such junctions are fabricated in parallel in a SQUID, interference between the two current branches gives an oscillating behavior of the critical current I_c with the external magnetic field [2]. The flux period is equal to the flux quanta $\Phi_0 = 2.05 \times 10^{-15}$ T.m². This makes the SQUID a very sensitive device to measure magnetic field. While the flux sensitivity achieved by conventional SQUIDs is better than $10^{-7}\,\Phi_0/\sqrt{\text{Hz}}$, for a μ-SQUID, it has only been about $10^{-4}\,\Phi_0/\sqrt{\text{Hz}}$ [3]. SQUIDs have been used to study the magnetization reversal [3] of an isolated magnetic nano particle, the persistent current in phase-coherent rings [3, 4] and also in scanning SQUID microscopy [5].

An improved sensitivity of μ-SQUIDs would be useful for probing ferromagnetic particles of smaller size or magnetic nano particles where surface spins of the particles play an important role [6]. Other than the sensitivity, the hysteresis in μ-SQUIDs current-voltage (I-V) characteristic (see e.g. Ref. 5) is a major hurdle as it (1) increases the measurement time, (2) complicates the measurement electronics, (3) changes the temperature of the sample placed in close proximity with

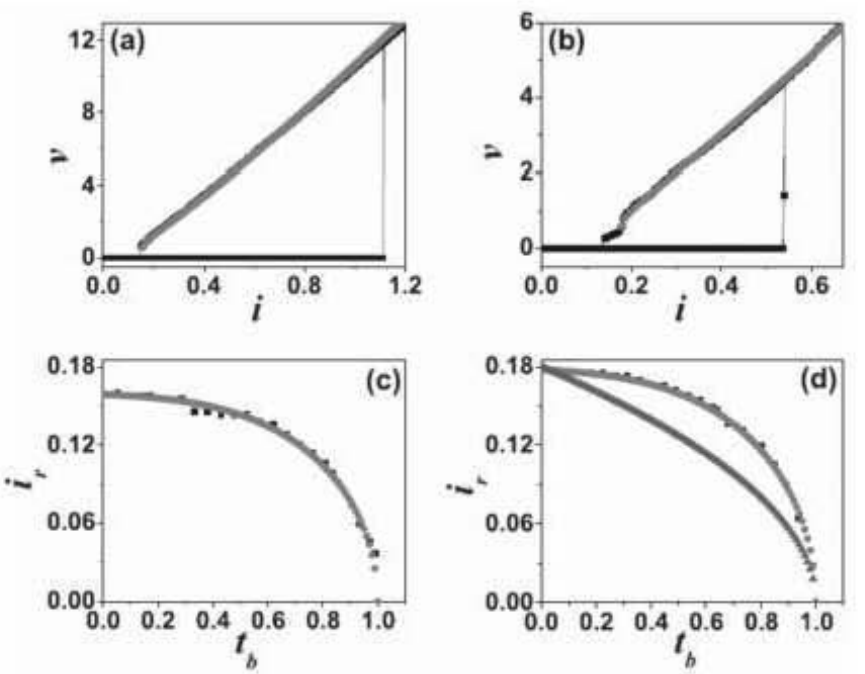

FIG. 1. Experimental (black) and numerical fit (red) of normalized I-V curves for (a) Sample 1 and (b) Sample 2. (c) and (d) correspond to the fitting of the temperature (bath) dependence of the retrapping current of Sample 1 and 2. Blue curve in (d) shows a comparison with earlier model by Skocpol et al. [7].

the μ-SQUID. Thus it is important to understand this hysteresis and devise ways of eliminating it. In this report, following Skocpol et al. [7], we describe a thermal model to understand the hysteresis in the current-voltage characteristics in short superconducting weak links and μ-SQUIDs. We consider a Normal-metal superconductor interface defined by $T= T_c$ for a given current and calculate the resistance and thus voltage. This model enables us to calculate the temperature dependence of the retrapping current, which turns out to be the smallest current which provides the NS interface with $T= T_c$. Using the temperature dependence of the critical current, we also find that above a certain temperature the hysteresis disappears. This model is tested down to 300 mK on Nb based μ-SQUIDs made by the focused ion beam and electron beam lithography. A good agreement between experiment and theory is obtained (Fig.1). We also compare the temperature dependence of the retrapping current with a previous model [7]. We further analyze the current-voltage characteristics and the weak link temperature variation in both the hysteretic and non-hysteretic regimes. We also discuss the effect of the weak link geometry in order to widen the temperature range of hysteresis-free operation.

REFERENCES

1. K. K. Likharev, Rev. Mod. Phys. 51, 101 (1979).
2. M. Tinkham, Introduction to Superconductivity 2nd ed. (Mc Graw-Hill, New York, 1996).
3. W. Wernsdorfer, Adv. Chem. Phys. 118, 99 (2001).
4. W. Rabaud, L. Saminadayar, D. Mailly, K. Hasselbach, A. Benoit, and B. Etienne, Phys. Rev. Lett. 86, 3124 (2001).
5. K. Hasselbach, C. Veauvy, D. Mailly, Physica C 332, 140 (2000).
6. S. A. Makhlouf, F. T. Parker, F. E. Spada, and A. E. Berkowitz, J. Appl. Phys. 81, 5561 (1997); S. D. Tiwari and K. P. Rajeev, Phys. Rev. B 72, 104433 (2005).
7. W. J. Skocpol, M. R. Beasley, and M. Tinkham, J. Appl. Phys. 45, 4054 (1974).

MOKE INVESTIGATIONS ON SPUTTER DEPOSITED FM/AF SYSTEMS GROWN ON DIFFERENT SEED LAYERS FOR BOTTOM PINNED MAGNETIC TUNNEL JUNCTIONS

HIMANSHU FULARA, SUJEET CHAUDHARY, SUBHASH C. KASHYAP, D. K. PANDYA

Thin Film Laboratory, Department of Physics,
Indian institute of Technology Delhi, New Delhi 110016 (India)
Email: sujeetc@physics.iitd.ac.in

Ferromagnet (FM) and an antiferromagnet (AF) layers are integral part of magnetic tunnel junctions (MTJs) employed in spin-electronic devices such as magnetic sensors and non-volatile magnetic random-access memories (MRAMs) [1]. Exchange bias is key to the performance of MTJs [2]. In the present work magnetic properties of IrMn/CoFeB or /CoFe systems (as deposited as well as magnetically annealed) grown on seed layers (CoFe and Cu) [3] are investigated by Magneto-Optic Kerr Effect (MOKE). Bottom pinned Si/seed CoFe(t =7, 10, 15 nm)/IrMn(15 nm)/CoFeB(10 nm) and Si/seed Cu (t =0, 11 nm)/IrMn(15 nm)/CoFe(10 nm) systems were deposited at room temperature by using different sputtering techniques (Pulsed DC magnetron sputtering and Ion beam sputtering). The thicknesses of the layers were estimated by X-ray reflectivity (XRR) measurements.

The ferromagnetic layers are found to be polycrystalline and textured. Also, the grain size is found to increase with thickness of seed CoFe layer. The FM layers of CoFeB and CoFe separated by 15 nm thin IrMn films remained directly coupled in magnetically annealed CoFe (t=7, 10, 15 nm)/ IrMn(15 nm)/CoFeB(10 nm) systems [figure 1 (a)]. The coercivity of CoFeB layers can be tuned by seed layer thickness in the magnetically annealed samples. The nonmagnetic seed layer of Cu in Si/ Cu(11)/IrMn(15)/CoFe(10) has shown strong affect in magnetization reversal mechanism, with a large increase of coercivity of CoFe films [figure 1 (b)]. This study is promising in utilizing the trilayer stack in CoFeB and CoFe based bottom pinned TMR structures.

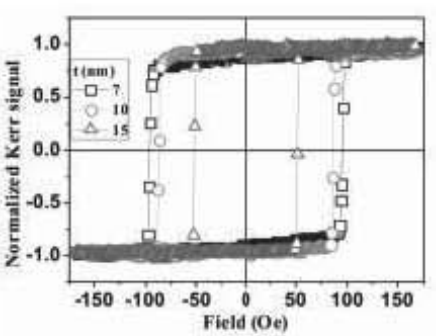

Fig.1(a):MOKE M-H loops of Si/CoFe (t)/ IrMn (15 nm)/CoFeB(10 nm) films magnetically annealed for 60 min.

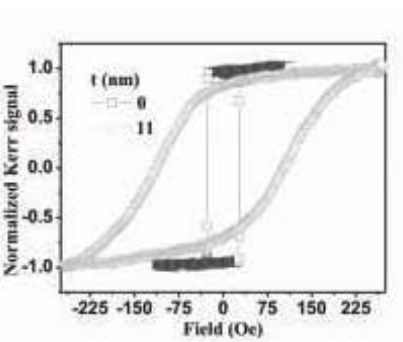

Fig. 1(b):MOKE M-H loops of Si/Cu(t)/ IrMn(15nm)/CoFe(10 nm) films magnetically annealed for 30 min.

REFERENCES

1. J. S. Moodera, L. R. Kinder et. al, Phys. Rev. Lett. 74, 3273 (1995).
2. J. Nogues, Ivan K. Schuller, J. Magn. Magn. Mater. 192, 552 (1999).
3. Himanshu Fulara, M. Raju, Sujeet Chaudhary et al, NSTI -Nanotech 2010 Vol. 1, Ch. 1, Nanoscale Material Characterization, p133-136.

STUDY OF PSEUDOGAP STATE IN NbN USING SCANNING TUNNELING SPECTROSCOPY

Anand Kamlapure, Garima Saraswat, Madhavi Chand, Mintu Mondal, Sanjeev Kumar, John Jesudasan, Vivas Bagwe, Pratap Raychaudhuri

Department of Condensed Matter Physics and Materials Science, Tata Institute of Fundamental Research, Homi Bhabha Road, Colaba, Mumbai 400005
Email: ask@tifr.res.in

We present the scanning tunneling spectroscopy (STS) and transport measurements done on thin films of 3-dimensional NbN films with increasing disorder. NbN samples with different disorder are grown using reactive magnetron sputtering[1] in the chamber attached to STM. Conductance spectra at each temperature are recorded using modulation technique[2,5] and are averaged over 32 points along 150 nm line. Magneto-resistance measurements are done on same samples in a home built cryostat. Figure 1 shows the STS measurement done on the four samples with increasing disorder with T_c~11.9K, 6K, 4.1K and 1.65K. The intensity plot in upper half of each panel shows conductance spectra as a function of temperature, y axis being bias and intensity being normalized conductance while the lower halves of the panels are resistance vs. temperature curves.

Fig. 1a) for the ordered film (T_c=11.9K) shows superconducting band gap in the conductance spectrum at low temperature while the gap vanishes above T_c (see the inset). While Fig.1d) for the most disordered film (T_c=1.65K) shows that gap in the dI/dV spectra associated with superconductivity

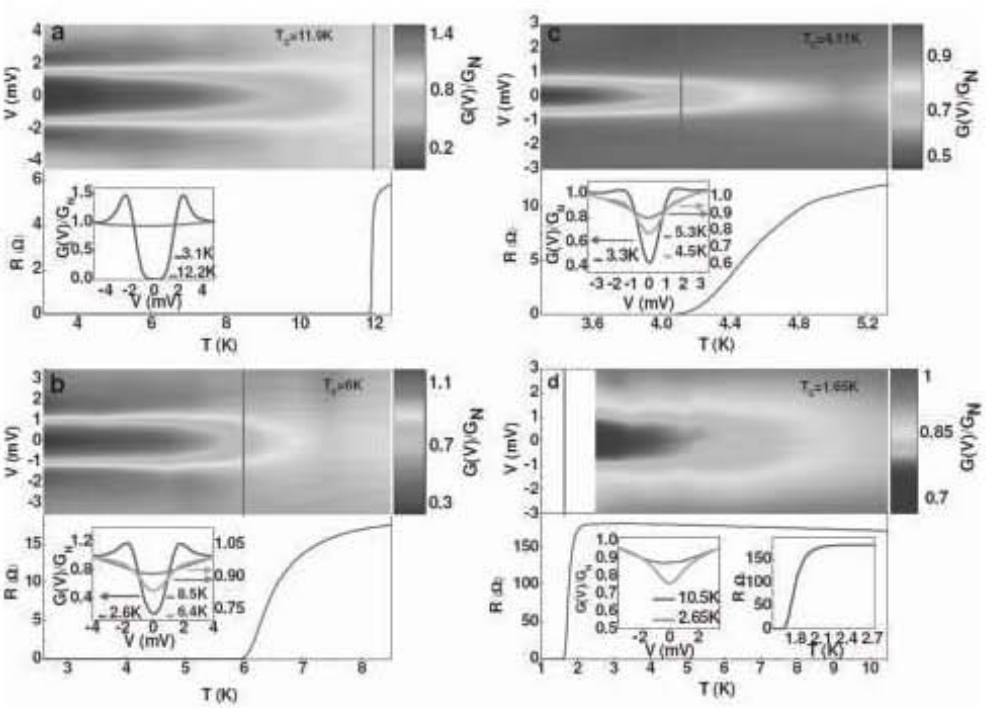

Figure 1: Scanning tunneling spectroscopy data for four samples with T_c 11.9K, 6K, 4.11K, 1.65K. Upper half of each Panels shows normalized conductance spectra as a function of temperature and lower half shows the corresponding resistance Vs temperature data. The Insets in each of the lower panels shows the conductance spectra at different temperatures. Second inset in the panel (d) shows expanded view of the resistance Vs temperature at the transition.

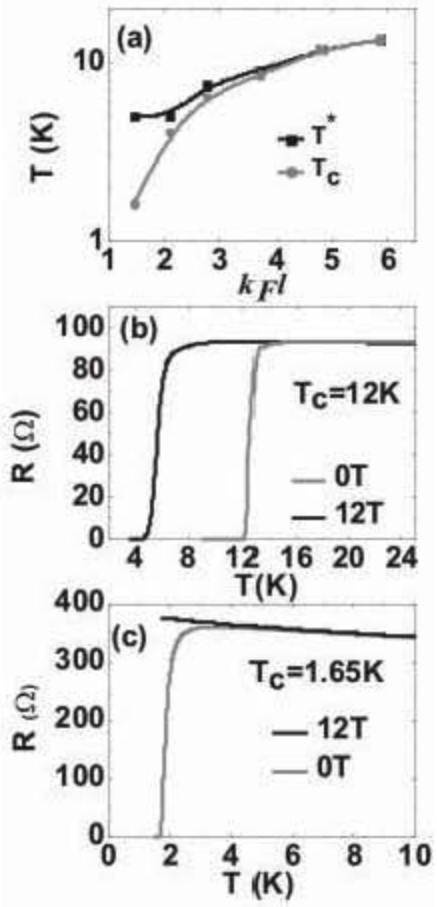

Figure 2: (a) Phenomenological phase diagram showing the two energy scales T and T* as a function of $k_F l$.

(b) and (c) Resistance Vs temperature measured at zero field and 12T for the two samples with T_c 12K and 1.65K respectively

persists even above the T_c. The persistence of superconducting pairing correlation above T_c as well as on the insulating side of the disorder driven superconductor-insulator transition has been observed in the similar systems like TiN [3]. We observe that the samples with high disorder ($k_F l$<2, $k_F l$ being Ioffe Regel Parameter) shows the finite gap in the conductance spectra even above the T_c upto the characteristic temperature T*. The gap observed in the spectra above the T_c is called Pseudogap in the high T_c superconductor literature. Magneto-resistance measurement done on the same samples shows strong MR component upto the temperature T*. These observations strongly suggest that NbN forms psedogap state in the high disorder limit.

The existence of pseudogap state can be attributed to phase fluctuation[4,5] where in the presence of strong disorder system segregates into phase disconnected superconducting puddles hence no global superconductivity. Magneto-transport observation (Fig.2) further support the phase fluctuation scenario where it can be seen that for most disordered film magneto-resistance persists all the way upto T*.

REFERENCES

1. S. P. Chockalingam, M. Chand, J. Jesudasan, V. Tripathi, and P. Raychaudhuri, Phys. Rev. B **70**, 214503 (2008)
2. Anand Kamlapure, Mintu Mondal, Madhavi Chand, Archana Mishra, John Jesudasan, Vivas Bagwe, L. Benfatto, Vikram Tripathi, and Pratap Raychaudhuri, Appl. Phys. Lett. **96**, 072509 (2010)
3. B. Sacépé, C. Chapelier, T. I. Baturina, V. M. Vinokur, M. R. Baklanov, and M. Sanquer, Phys. Rev. Lett. **101**, 157006 (2008)
4. A. Ghosal, M. Randeria, and N. Trivedi, Phys. Rev. Lett. **81**, 3940 (1998); Phys. Rev. B **65**, 014501 (2001); Y. Dubi, Y. Meir, and Y. Avishai, Nature (London) **449**, 876 (2007).
5. arXiv:1006.4143v3 [cond-mat.supr-con]

ANISOTROPIC ANGULAR MAGNETORESISTANCE IN NbN-Fe-NbN JOSEPHSON JUNCTION ARRAYS

S. K. Bose[1] R. C. Budhani[1,2]

[1]*Condensed Matter - Low Dimensional Systems Laboratory, IIT Kanpur, Kanpur-208016, India*
[2]*National Physical Laboratory, Dr. K. S. Krishnan Marg, New Delhi - 110012, India*
Email: skbose@iitk.ac.in

In a recent letter,[1] we reported briefly the successful self-assembly of distributed NbN-Fe-NbN JJs by Volmer-Weber type plaquette growth of Fe on [100] MgO, whose electrical connectivity is then tailored by NbN layers of different thickness (d_{NbN}). Here, in this paper we address how the magnetic flux-closure domains of Fe-plaquette affect Josephson coupling between the NbN layers through careful measurements of the angular dependence of magnetoresistance (MR).

The samples studied here consist of Fe plaquettes (~50 nm high) covered with NbN (d_{NbN} = 10/20/30 nm). In Fig. 1(a), the morphology investigated via scanning electron microscopy (SEM) show formation of ~100 x 100 nm^2 area square Fe plaquettes covered with NbN. The intra- and inter-plaquette NbN form JJs as shown in inset Fig. 1(a). The effect of magnetic field on the SC state of the JJs has been investigated via angular dependence of magneto-resistance measurements. These have been performed by rotating the direction of the magnetic field (H) with respect to the plane of the sample as shown in the inset Fig. 1(c). One typical MR response of 30 nm Fe-NbN sample, obtained at 6 K is presented in Fig. 1(b) along with that of a plain 30 nm NbN film. The data for the JJs plotted for different directions of current (I_+, I_- and I_{av}) shows two characteristic features in stark contrast to the data for the plain NbN.

First, both I_+ and I_- show an enhanced resistance (R) when the field (3.5 kOe) is in-the-plane of the film (θ=90^0 and 270^0), as compared to the resistance for θ = 0^0 and 180^0. Secondly, at θ = 90^0, R_{I-} is much larger than R_{I+}, whereas at θ = 270^0, $R_{I-} << R_{I+}$. In contrast, the MR response of the plain NbN film is independent of the direction of I.

To understand this current polarity dependence, MR measurements with H rotated in the film plane have been performed [Fig. 2(a)]. Here, Φ is the angle of H with direction of I_+. The average

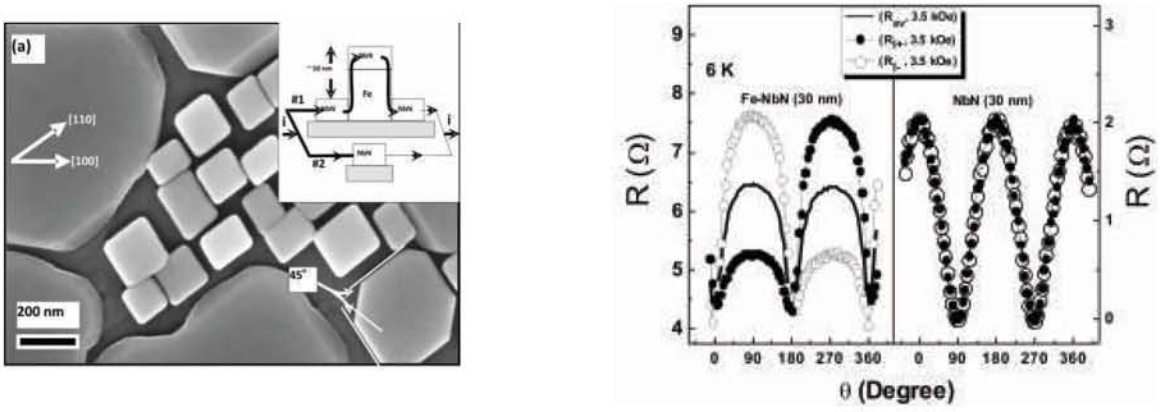

Figure 1. (a) SEM micrograph showing Fe nano-plaquettes covered with NbN. (b) Angular dependence of MR for Fe-NbN (30 nm) and plain NbN (30 nm) sample.

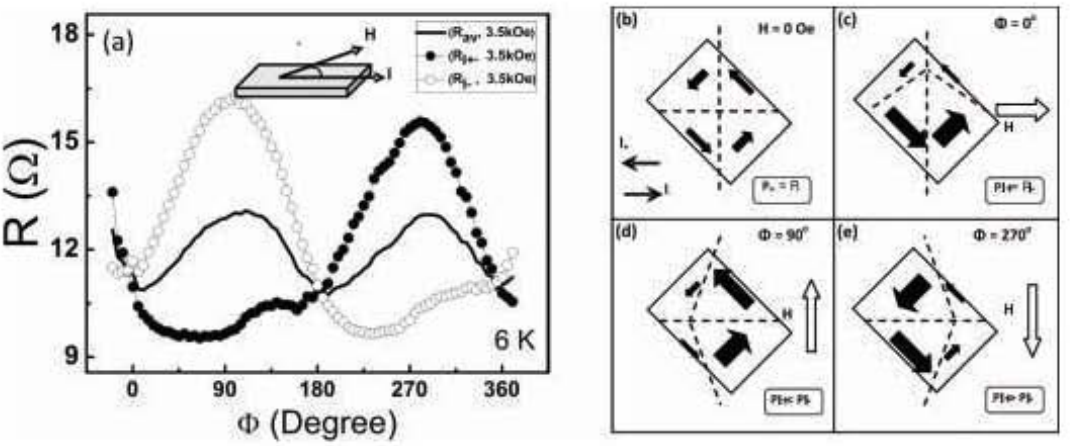

Figure 2. a) Angular dependence of MR with *H* rotated in the film plane. (b-e) Schematic diagram of magnetic flux-closure domains transforming with field *H* rotated in the film plane.

response (bold line) peaks when *H* is perpendicular to *I* ($\Phi = 90^0$ & 270^0). However, the R_{I+} and R_{I-} separately show large asymmetry in response at $\Phi=90^0$ & 270^0. We believe that the reason for this striking behavior lies in magnetic domain structure of the Fe plaquettes.[2] Figure 2(b) shows a schematic view of the magnetic flux-closure domains of one Fe plaquette in zero-field. In the absence of external field, the individual magnetic domains are of equal strength. As the electrons climbs up these areas into the top NbN layer, they get spin polarized. The same is the case for a non-zero field *H* provided $\Phi = 0^0$ as shown in Fig. 2(c). In this case, the current travels equal areas of $\pi/2$ out-of-phase domains while entering and exiting the top NbN. Thus, we expect a fixed value for resistance due to pair-breaking effects in NbN irrespective of the polarity of current. However, when $\Phi = 90^0$ or 270^0 as shown in Fig. 2(d) and 2(e) respectively, the magnetic domains grow in the direction of *H* at the expense of the ones with non-zero anti-parallel component of magnetization. Thus, for Fig. 2(d), we argue that the electrons injected by I_- to be strongly spin polarized ($P_{I+}<P_{I-}$), resulting in enhancement of R_{I-}. Whereas, the ones injected by I_+ in this scenario are weakly spin polarized, therefore the resistance decreases with increasing Φ. At $\Phi = 270^0$ [Fig. 2(e)], the situation is reversed.

REFERENCES

1. S. K. Bose and R. C. Budhani, *Appl. Phys. Lett.* **95**, 042507 (2009).
2. R. P. Cowburn, D. K. Koltsov, A. O. Adeyeye, M. E. Welland, and D. M. Tricker, *Phys. Rev. Lett.* **83**, 1042-1045 (1999).

ENHANCED SUPERCONDUCTIVITY AT $La_{1.48}Nd_{0.4}Sr_{0.12}CuO_4$/ $La_{1.55}Sr_{0.45}CuO_4$ BILAYER INTERFACE

P. K. ROUT[1], R. C. BUDHANI[1,2]

[1]*Condensed Matter– Low Dimensional Systems Laboratory, Department of Physics, Indian Institute of Technology, Kanpur – 208016, India.*
[2]*National Physical Laboratory, New Delhi 110012, India.*
Email: pkrout@iitk.ac.in

A number of recent experiments and theories have provided an insight into completely different electronic properties at the interfaces between correlated electron systems as compared to the properties of the parent systems. One of the unusual realizations of these effects is the interface superconductivity at oxide interfaces [1-3]. In this report, we observe a large enhancement (~ 50 %) of the superconducting transition temperature (T_c) in the bilayers made up of metallic overdoped compound $La_{1.55}Sr_{0.45}CuO_4$ (LSCO) and stripe ordered compound $La_{1.48}Nd_{0.4}Sr_{0.12}CuO_4$ (LNSCO) as compared to that of Nd-doped monolayer film. This enhancement in T_c is due to the superconductivity in the interfacial layer, as confirmed by our experiments. The X-ray diffraction analysis shows a layer-by-layer growth of epitaxial bilayers on SLAO substrate with an interface roughness of ~ 1.7 nm. The four-probe resistivity measurements show a T_c ~ 13.6 K for the bilayer, which is about 4.5 K higher than that of LNSCO, film (Fig. 1).

The temperature dependent critical current data of the bilayer can be assumed to be a combination of two contributions: one from LNSCO layer and the other from the interfacial layer. Further evidence for the interface superconductivity can be found out from ac screening measurements with a two-coil mutual inductance method similar to the one described by Jeanneret *et al.*[4]. The

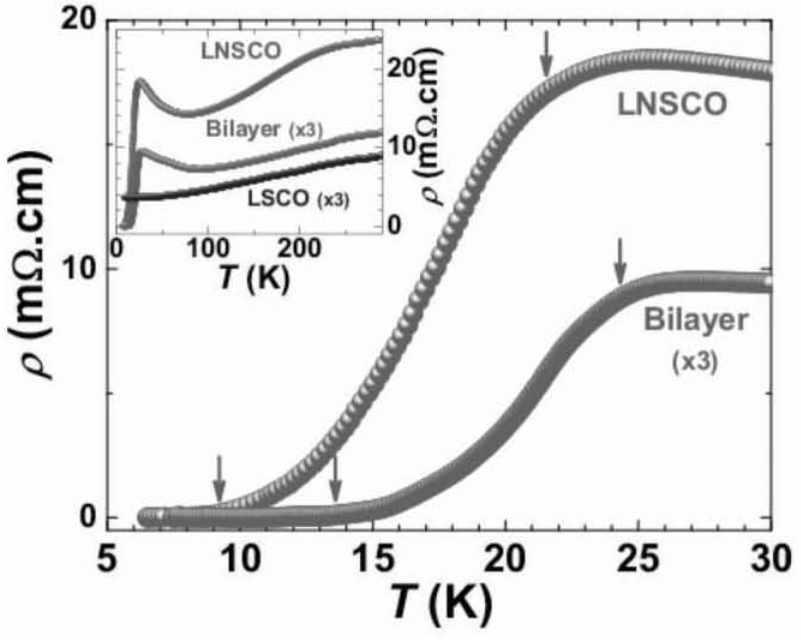

FIG. 1. The in-plane resistivity ρ(*T*) for LNSCO (red) and LNSCO/LSCO (green) films. The inset shows ρ(*T*) for LSCO (blue) film in addition to LNSCO and bilayer films. For clarity, the data for LSCO and bilayer films are multiplied by a factor of 3.

pick-up coil voltage due to screening supercurrent flowing in the bilayer clearly shows a small transition at ~ 13.7 K in addition to the superconducting transition of LNSCO layer at T_c ~ 10.3 K. The enhanced superconductivity in these bilayers can be explained by a simple model based on the Sr^{2+}/Nd^{3+} ion distributions across the interface, taking into account the smearing of charges [5]. This model predicts the interface superconductivity is confined within two unit cells of LNSCO right next to the interface.

REFERENCES

1. Gozar *et al.*, Nature **55**, 782 (2008).
2. N. Reyren *et al.*, Science **317**, 1196 (2007).
3. P. K. Rout and R. C. Budhani, Phys. Rev. B **82**, 024518 (2010).
4. Jeanneret *et al.*, Appl. Phys. Lett. **55**, 2336 (1989).
5. V. M. Loktev and Yu. G. Pogorelov, Phys. Rev. B **78**, 180501(R) (2008).

FIRST PRINCIPLES CALCULATIONS OF STRUCTURAL, ELECTRICAL AND MAGNETIC PROPERTIES OF MULTIFERROIC $SrTiO_3$/ $BiFeO_3$ MULTILAYER STRUCTURE

Amritendu Roy [1], Ashish Garg [1], Rajendra Prasad [2], Sushil Auluck [2]

[1] *Department of Materials Science and Engineering*
[2] *Department of Physics*
Indian Institute of Technology, Kanpur, Uttar Pradesh, India – 208016

Material designing based on artificial layered structures has generated enormous interest lately due to the possibility of evolving extraordinary and novel functional properties which are not necessarily present in the respective bulk systems. In the present work, we report the results of first principles calculations of structural, electrical and magnetic properties for $SrTiO_3$/ $BiFeO_3$ (STO/ BFO) multilayer using generalized gradient approximation (GGA+U) coupled with Hubbard parameter, U = 4.5 eV. We employed the simplified, rotationally invariant approach introduced by Dudarev to include Hubbard parameter in our calculations. We started our calculations with the experimental lattice parameters and symmetry ($Pm\bar{3}m$) of bulk $SrTiO_3$. Keeping the $Pm\bar{3}m$ symmetry of bulk STO, we stacked alternate unit cells of STO and BFO with lattice parameters identical to that of STO. The bottom and top layers are of STO. Fig. 1(a) shows a schematic of such layer structure. For our calculations, we chose a 40 atom $\sqrt{2} \times \sqrt{2} \times 4$ supercell constructed from the layered structure described above. Fig. 1(b) shows the structure of the supercell considered in our calculation. The structures with all possible spin configurations, namely ferromagnetic (FM) and A, C and G type antiferromagnetic (AFM) spin configurations, were further relaxed such that the Hellmann-Feynman forces are less than 0.001 eV/Å and pressure values on structures are almost zero. Our calculations suggest G-type antiferromagnetic structure with in-plane lattice parameters, $a = b = 3.8856$ Å is the ground state

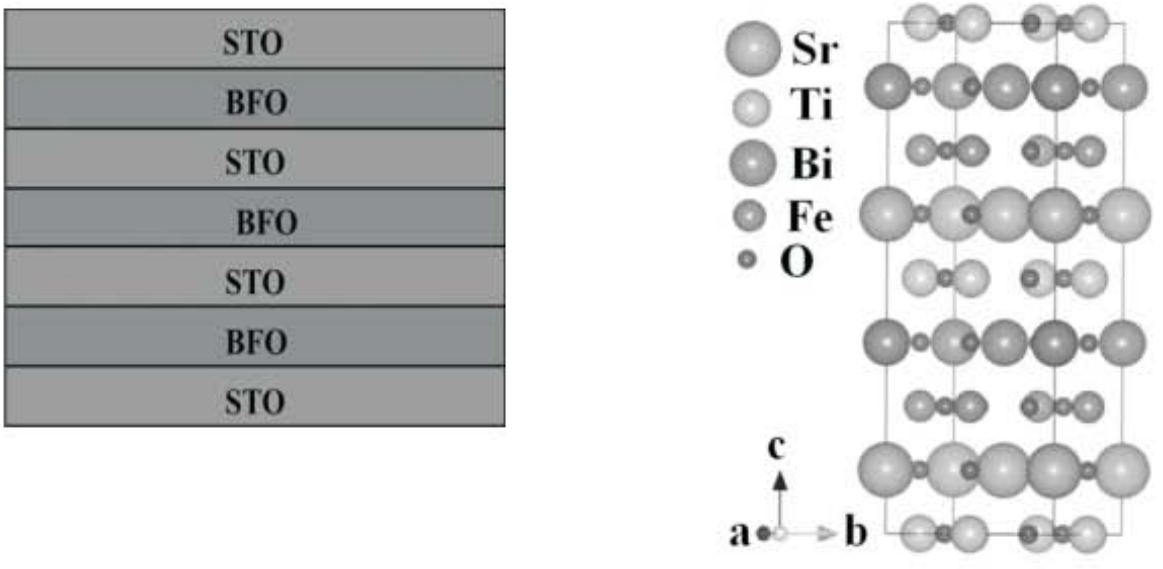

Fig. 1 (a) Schematic diagram of alternate layers of SrTiO3 and BiFeO3 layers. (b) $\sqrt{2} \times \sqrt{2} \times 4$ supercell with lattice parameters and site symmetry of SrTiO3 where TiO2, SrO, FeO2 and BiO layers are stacked sequentially to result in STO-BFO multilayer.

ACOUSTIC PHONON SCATTERING LIMITED MOBILITY IN A BILAYER GRAPHENE

K. S. BHARGAVI, S.S.KUBAKADDI

Department of Physics, Karnatak University, Dharwad-580 003, India
Email:sskubakaddi@gmail.com

The realization of bilayer graphene (BLG), by mechanical exfoliation of graphite, has aroused the great interest in the study of its electronic transport properties because of the tunable energy gap and an unusual quantum Hall effect [1]. Because of the interlayer interaction, the BLG has a quadratic dispersion with finite effective mass m of the carriers with chiral character and zero energy gap [1]. The key property of interest is its carrier mobility for the fast electronic transport devices. Very recently, carrier scattering due to impurity and mobility μ are studied theoretically [2,3] and experimentally [2]. If the impurity concentration can be reduced significantly, then acoustic phonon limited mobility μ_{ac} can be significantly high, particularly around room temperature. μ_{ac} has been studied in detail in monolayer grapheme(MLG) [4]. In the present work we study theoretically $\mu_{ac,}$ employing the Boltzmann transport theory [5] considering the 2D carrier interaction with 2D acoustic phonons (of wave vector **q** and energy $\omega_{q)}$ via deformation potential coupling in BLG [6].

In Bloch-Grüneisen (BG) regime $q << 2k_f$ ($k_f = \sqrt{\pi n}$ is the Fermi wave vector and carrier concentration n) and $\omega_q \approx k_B T$. Then mobility is given by $\mu_{ac}(BG)=[2e\pi^5/2\ ^6\rho v_s n^{3/2}]/[m^2D^2(k_BT)^4 4!\zeta(4)$ where, D is the deformation potential coupling constant, ζ(n) is the Riemann Zeta function. In equipartition (EP) regime, scattering is quasi elastic, $\omega_q << E_f$ (Fermi energy), and the phonon distribution function $N\mathbf{q}H \approx N\mathbf{q}+1\ H \approx k_BT/\ \omega_q$, $\mu_{ac}(EP)=(2.545\pi e\rho\ ^3v_s^2)/(4m^2D^2k_BT)$. For illustration we use the following graphene material parameters: $m=0.033m_o$, $\rho=7.6\times10^{-8}$ cm^{-2}, $v_s=2\times10^6$ cm/s and $D=20$ eV. $\mu_{ac}(BG) \sim T^{-4}$ and $n^{3/2}$ as compared to $\mu_{ac}(MLG) \sim T^{-4}$ and $n^{1/2}$ [4]. $\mu_{ac} \sim T^{-4}$ is a manifestation of 2D nature of acoustic phonons and $\mu_{ac} \sim n^{3/2}$ is the result of parabolic nature of the carriers dispersion. However, in conventional 2DEG $\mu_{ac} \sim T^{-5}$ and $n^{3/2}$. The ratio $\mu_{ac}(BLG)/\mu_{ac}(MLG) = (\pi\ ^2n)/(m^2v_f^2)$ which gives ~ 0.4 for $n=1\times10^{12}$ cm^{-2}.

In EP regime, interestingly, momentum relaxation time $\tau(E_k)$ is independent of energy and it is attributed to the constant density of states of the carriers in BLG. $\mu_{ac} \sim T^{-1}$, which is same as in MLG but it is independent of n in contrast with $n^{1/2}$ in MLG [4]. We calculate Hall mobility μ_H using Eqn. (37) of Ref.[5]. In Fig 1 we compare Hall mobility μ_{ac} vs T with those due to ionized impurity

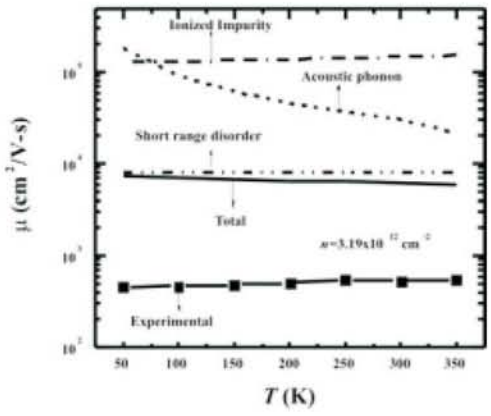

Fig 2. Hall mobility μ vs temperature T.

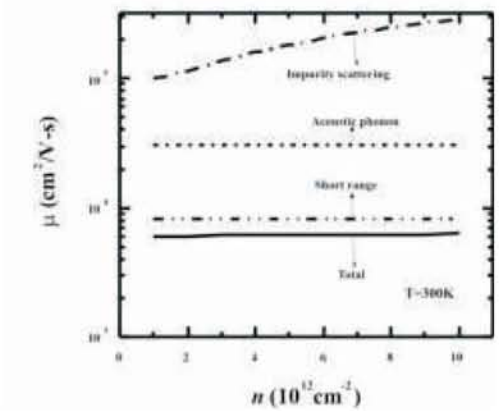

Fig. 2. Mobility μ vs Carrier Concentration

scattering and short-range disorder [3] and experimental data [2] for n=3.19x10^{12} cm^{-2}.It is to be noted that μ_H and μ are same for acoustic phonon and shortrange disorder scattering as their relaxation times are independent of energy. It is found that, the mobility due to disorder dominates. The resultant μ is obtained using Matthiessen's rule. We note that no quantitative agreement is obtained with the chosen reasonable parameters. We also note that, in EP regime, chiral character of the carriers reduces the mobility by factor 2. In Fig.2 we compare our calculated results of μ_{ac} vs n with those due short-range disorder scattering and ionized impurity and at 300 K. Former two are independent of n and short range disorder dominates for the range of n considered.

REFERENCES

1. K.S.Novoselov et al, Nat. Phys. **2**,177 (2006).
2. W.Zhu et al Phys. Rev. B **80**, 235402 (2009).
3. S.Das Sarma et al, Phys. Rev. B **81**, 161407(R) (2010).
4. E.H.Hwang and S.Das Sarma, Phys. Rev. B **77**, 115449 (2008).
5. T.Kawamura and S.Das Sarma , Phys. Rev. B **45**, 3612 (1992).
6. J.K.Viljas and T.T.Heikkila, Phys. Rev. B 81, 245404 (2010).

X-RAY REFLECTIVITY STUDIES ON ION BEAM SPUTTERED Si/ CoFeB(6nm)/MgO(3nm) AND Si/MgO(3nm)/CoFeB(6nm) BILAYERS FOR SPINTRONIC APPLICATIONS

M. Raju, Sujeet Chaudhary, D. K. Pandya

Thin Film Laboratory, Department of Physics, Indian Institute of Technology Delhi
New Delhi 110016 (INDIA)
Email: rajuhcu519@gmail.com

The MgO and CoFeB have emerged important materials in magnetic tunnel junctions(MTJs) [1], with CoFeB acting as ferromagnetic (FM) electrode and MgO as insulating barrier. The tunnel magneto resistance (TMR) in these systems is sensitive to the quality of the insulating barrier, FM electrode, interface between FM electrode and barrier, etc. In the present work, we have deposited bilayers of Si/MgO(~3nm)/CoFeB(~6nm), Si/CoFeB(~6nm)/MgO(~3nm) on n-type silicon at room temperature (RT) using ion beam sputtering technique. The working pressure is maintained at 1.3×10^{-4} torr and the base pressure was 8×10^{-7} torr. The x-ray reflectivity (XRR), being a non-destructive and powerful tool to study the interfaces of buried layers in multi layer thin films have been used to investigate these bilayers.

The oxidation of Mg to form MgO is done in *three* different methods; (a) Ion assisted growth of MgO (SCM-I, SMC-I) (b) Reactive sputtering of Mg (SCM-R, SMC-R), and (c) Post oxidation of ultra thin Mg in oxygen environment (SCM-PO, SMC-PO). Figure 1a and b show simulated and experimental XRR profiles on two ion beam sputtered Si/CoFeB/MgO stacks in which MgO is formed by post oxidation and reactive sputtering, respectively. This simulation yields the insight (at atomic level) to the interface in these nanometric bilayers. Detailed results will be presented during the conference.

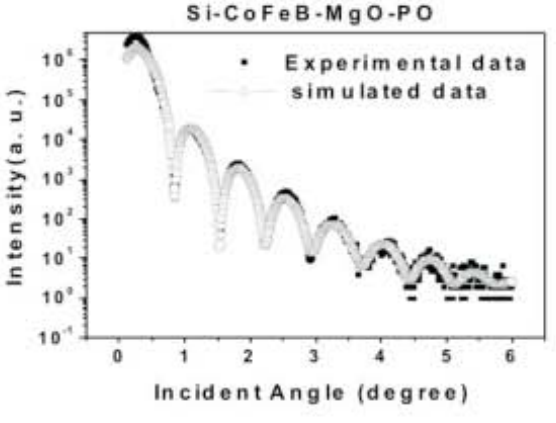

Figure 1a: XRR profile of SCM-PO

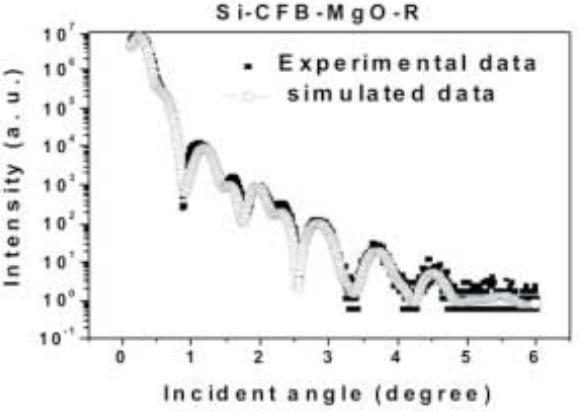

Figure 1b: XRR profile of SCM-R

REFERENCES

1. Y. M. Lee et al. Appl. Phys. Lett. 89, 042506 (2006); S. Isogami et al. Appl. Phys. Lett. 93, 192109 (2008). S. Ikeda et al. Appl. Phys. Lett. 93, 082508 (2008).

1/f NOISE AS A PROBE TO INVESTIGATE THE BAND STRUCTURE OF GRAPHENE

Atindra Nath Pal, Arindam Ghosh

Department of Physics, Indian Institute of Science, Bangalore-560012, India
Email: atin@physics.iisc.ernet.in

Graphene, single atomic layer of hexagonal carbon atoms, has become a potential candidate for future electronics because of its unusual electronic properties. In particular, extensive research on single and bilayer graphene (BLG) has led to significant improvement in both material properties, as well as fundamental understanding, for nanoelectronic applications. A distinctive feature of single layer graphene is the linearly dispersive energy bands, which in case of multilayer graphene become parabolic. Other than the quantum Hall effect, this distinction has been hard to capture in electron transport. Carrier mobility of graphene has been scrutinized, but many parallel scattering mechanisms often obscure its sensitivity to band structure. The flicker noise in graphene depends explicitly on its ability to screen local potential fluctuations. Here we show that the flicker noise is a sensitive probe to the band structure of graphene that vary differently with the carrier density for the linear and parabolic bands. We have used seven different types of graphene field effect devices in our experiments which include exfoliated single and multilayer graphene on oxide substrate, freely suspended single layer graphene, and chemical vapor deposition (CVD)-grown graphene on SiO_2. We find this difference to be robust against disorder in the presence or absence of substrate. Also, an analytical model has been developed to understand the mechanism of graphene field effect transistors. Our results reveal the microscopic mechanism of noise in Graphene Field Effect Transistors (GraFET), and outline a simple portable method to separate the single from multi layered devices.

REFERENCES

1. "Resistance noise in electrically biased bilayer graphene", Atindra Nath Pal and Arindam Ghosh, Physical Review Letters 102, 126805 (2009).
2. "Ultralow noise field-effect transistor from multilayer graphene", Atindra Nath Pal and Arindam Ghosh, Appl. Phys. Lett., 95, 082105 (2009).
3. "Large Low frequency noise in chemical vapor deposited graphene", Atindra Nath Pal, Ageeth A. Bol, and Arindam Ghosh, Applied Physics Letter (2010) (in press).
4. "1/f noise as a probe for investigating band structure in graphene", Atindra Nath Pal, Subhamoy Ghatak, Vidya Kochat, Sneha E. S., Arjun B.S., Srinivasan Raghaban, and Arindam Ghosh, Physical Review Letters (under review).

EMERGENCE OF EXOTIC PHENOMENA IN THE STUDY OF SUPERCONDUCTOR/ FERROMAGNET HETEROSTRUCTURES

D. Samal, P. S. Anil Kumar

Department of Physics, Indian Institute of Science, Bangalore, 560012, India
E-mail: debphy@physics.iisc.ernet.in

The study of co-existence of singlet superconductivity and ferromagnetism is one of the most fascinating and challenging area of resaerch since both the phenomenon are antagonistic to eachother. However, the coexistence can be easily achieved in artificially fabricated superconductor–ferromagnet heterostructures and these systems offer unique opportunities to study the interplay beteween two competing order parameters and to conceive novel quantum states. Our investigations on different superconducting(S)/ferromagnetic(F) heterostructures fabricated by pulsed laser deposition reveal an intense suppression of superconductivity due to the magnetic proximity effect and the injection of spin polarised quasiparticles from the F electrode. The current dependent transport studies exhibit a significant reduction of the superconducting T_c in the S/F bilayers as compared to single S layer and strictly adhers in accord to $I^{2/3}$ de-pairing effect. Surprisingly, the superconducting T_c in $YBa_2Cu_3O_{7-\delta}$/ $La_{0.5}Sr_{0.5}CoO_3$ bilayers is observed to be much lower as compared to $YBa_2Cu_3O_{7-\delta}$/ $La_{0.7}Sr_{0.3}MnO_3$ ones. This point to the fact that in addition to the spin polarisation of the ferromagnetic electrode, other factors such as (a) interfce transparency (b) magnetic domain state and (c) the stray field associated with the F layer might play important role in tuning the S order parameter. Magnetotransport studies reveal a remarakable reduction of activation energy (U) and a logarithmic dependence of "U" on the applied magnetic field in S/F heterostrctures. This signifies the signature of the existence of decoupled 2D pancake vortices that can arise from the weakening of the S coherence length (ξ_c) due to the presence of F layers and the dominance of intralayer vortex-vortex interaction over the interlayer one. In contrast, the low field ac susceptibility study on $YBa_2Cu_3O_{7-\delta}$/$La_{0.7}Sr_{0.3}MnO_3$ bilayers reveals stronger pinning and the temperature dependent critical current is found to be less susceptible to temperature. Moreover, we also observe an enhancement of H_{c1} in $YBa_2Cu_3O_{7-\delta}$/$La_{0.7}Sr_{0.3}MnO_3$ bilayer as compared to single $Ba_2Cu_3O_{7-\delta}$ layer.

REFERENCES

1. A.I. Buzdin, *Rev.Mod. Phys*. **77**, 935-976 (2005).
2. D. Samal, C. Shivakumara and P.S. Anil Kumar, *Phys. Rev.B* **77**, 094510 (2008)
3. D. Samal, and P.S. Anil Kumar, *J. Phys.: Condens. Matter*. **21**, 492203 (2009) (IOP Select)
4. D. Samal, Chanchal Sow and P.S. Anil Kumar, *J. Phys.:Condens. Matter.* **22,** 295701(2010)
5. D. Samal and P. S. Anil Kumar (*J. Supercond. Nov. Magn. in press)*

EXCHANGE INTERACTION PARAMETERS IN Co/Pd MULTILAYERS

P. Manchanda, A. Kashyap

The LNM Institute of Information Technology, Jaipur-302031, Rajasthan, INDIA
Email: priyanka.manchanda0@gmail.com

Magnetic structures with artificially created periodicity have attracted much attention because of their interesting magnetic properties and applications. Interlayer exchange coupling in magnetic multilayers has also attracted much interest since its discovery [1]. In particular, Co/Pt and Co/Pd multilayers have been extensively used for high-density magneto-optical storage media because of their high interface-induced perpendicular anisotropy, high coercivity, and high squareness [2]. Several groups have been reported that Co initially grows in face-centered cubic (*fcc*) structure on Pd(111), which facilitates the coherent growth of the Co/Pd(111) multilayers [3]. We present the magnetization and exchange interactions of dense-packed Co/Pd(111) multilayers. The calculations of electronic structure, magnetic moments and exchange interaction are based on *ab-intio* spin-polarized electronic structure calculations using the linear muffin-tin orbital (LMTO) method within atomic sphere approximation. A striking feature of the calculations is the large magnetic moment of Co atom compared to the bulk Co atom. The Pd atom couples ferromagnetically to the Co atom at the interface and has a moment of about ~0.25μ_B per atom. The reason for large Co magnetic moment at the interface is due to strong 3*d*-4*d* hybridization. The interatomic exchange interaction between nearest and next-nearest neighbor (J_{ij}) are calculated in the Heisenberg approximation. — This research is supported by DST (India) through the India-EU collaborative project “DYNAMAG”, INT/EC/CMS(24/233552), and through Nano Mission, SR/NM/NS-20/2008.

REFERENCES

1. P. Grünberg, R. Schreiber, Y. Pang, M. B. Brodsky, and H. Sowers, Phys. Rev. Lett. **57**, 2442 (1986).
2. J. I. Hong, S. Sankar, A. E. Berkowitz, and W. F. Egelhoff Jr., J. Magn. Magn. Mat., **285**, 359 (2005).
3. M. Enrech, R. Skomski, J. M. D. Coey, and J. G. Lunney, J. Appl. Phys. **73**, 6421 (1993).

In-Situ GROWTH OF QUANTUM DOTS IN POLYMER TEMPLATE: PHOTOPHYSICS OF ORGANIC/INORGANIC HYBRID SOLAR CELLS

Mohd Taukeer Khan[1,2], Amarjeet Kaur[2], S K Dhawan[1], Suresh Chand[1]

[1]*Polymeric & Soft Materials Section, National Physical Laboratory, (CSIR), Dr. K. S. Krishnan Road, New Delhi-110 012, India*

[2]*Department of Physics & Astrophysics, University of Delhi, Delhi-110 007, India*

E-mail: khanmtk@mail.nplindia.ernet.in

Organic-inorganic hybrid nanocomposites are attracting extensive interest for electronic and optoelectronic device applications. In-situ synthesis of nanoparticles in polymer without the involvement of any surfactants improves the polymer-nanoparticles interface, which facilitates efficient electronic interaction between them. In the present study nanoparticles of cadmium telluride (CdTe) were directly synthesized in poly(3-hexylthiophene) (P3HT) matrix without use of any surfactant. The success of the formation of nanocomposites was confirmed by the optical and structural analysis. Optical studies suggest that CdTe improves the interchain-interchain interaction in P3HT. Photoluminescence (PL) quenching has been observed for the nanocomposite films, which suggests CdTe nanocrystals, are bound with P3HT via dipole-dipole interaction and form a charge transfer complex (CTC). The nanoparticles of CdTe works as transport bridge between two polymer chains, which facilitate percolation pathways for electron transport. Therefore, enhancement in current density was observed for the bulk heterojunction (BHJ) device of P3HT-CdTe nanocomposites blended with PCBM. A noticeably high open circuit voltage (V_{OC}) of 0.80 V was obtained from the BHJ device due to the increase in the energy level offset between the lowest unoccupied molecular orbital (LUMO) of the acceptor and the highest occupied molecular orbital (HOMO) of the donor. However, the Fill Factor (FF) was significantly lower, which limited the observed efficiency to 0.79%.

EXPERIMENTAL OBSERVATION OF NEUTRAL MODES IN THE FRACTIONAL QUANTUM HALL EFFECT REGIME

Aveek Bid[1], N. Ofek[2], H. Inoue[2], M. Heiblum[2], C. L. Kane[3], V. Umansky[2], D. Mahalu[2]

[1]*Department of Physics, Indian Institute of Science, Bangalore – 560012, India*
[2]*Braun Center for Submicron Research, Department of Condensed Matter Physics, Weizmann Institute of Science, Rehovot 76100, Israel*
[3]*Department of Physics and Astronomy, University of Pennsylvania, Philadelphia, Pennsylvania 19104, USA*
Email:aveek.bid@physics.iisc.ernet.in

In the fractional quantum Hall effect (FQHE) [1] regime current propagates along the edges of the two-dimensional-electron gas (2DEG) via chiral edge modes with a chirality dictated by the applied magnetic field [2]. For some fractional states (the so called holes-conjugate states), such as $\frac{1}{2}<\nu_b<1$ of the lowest Landau level and in particular $\nu_b=2/3$ (where ν_b is the filling factor) early predictions suggested the presence of counter propagating modes on each edge of the device [3,4] - a downstream mode with the expected chirality, and an upstream mode with an opposite chirality. Since experiments could not find the upstream propagating edge modes [5], Kane & Fisher suggested [6] that in the presence of disorder and interactions edge reconstruction may take place resulting in charge modes accompanied by neutral modes - with the latter carrying only energy. Moreover, a neutral upstream Majorana mode was also expected for selected wavefunctions proposed for the even denominator state $\nu_b=5/2$ [7,8].

Here we report on the direct observation of upstream neutral modes in bulk filling factors $\nu_b=2/3$, $\nu_b=3/5$, $\nu_b=5/3$ & $\nu_b=5/2$ [9]. This was done by allowing these modes to be partitioned by a quantum point contact (QPC) constriction and by measuring the resulting shot noise. We observed the following effects: (a) When only the neutral mode was partitioned, no net current was detected at the measuring amplifier, however shot noise proportionate to the voltage applied on the injecting contact was detected. (b) When simultaneously partitioning a charge mode and a neutral mode, the presence of the neutral mode affected significantly the charge and the temperature of the tunneling quasiparticles of the partitioned charged mode.

These observations unambiguously point towards the existence of upstream neutral modes. In particular, for the $\nu_b=5/2$ fractional state, this observation may single out the non-abelian wavefunctions for the quasiparticles.

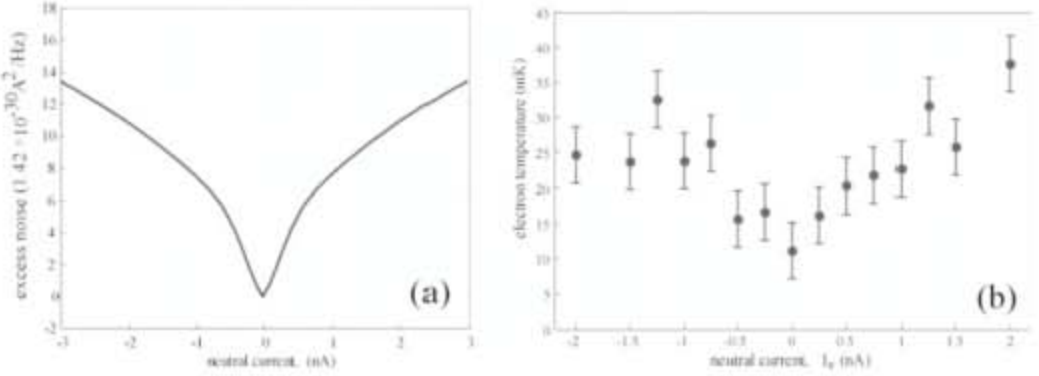

Fig1. (a) Excess noise and (b) electron temperature of quasiparticles of charge mode as a function of neutral mode current in filling factor n=2/3.

REFERENCES

1. Das Sarma, S. & Pinczuk, A., *Perspective in Quantum Hall effects: Novel Quantum Liquid in Low-Dimensional Semiconductor Structures*. (New York, Wiley), 1997.
2. X. G. Wen, Phys. Rev. B **41**, 12838-12844 (1990).
3. A. H. MacDonald Phys. Rev. Lett. **64**, 220-223 (1990).
4. M. D. Johnson *et. al.* Phys. Rev. Lett. **67**, 2060-2063 (1991).
5. R. C. Ashoori et.al. Phys. Rev. B **45**, 3894-3897 (1992).
6. C. L. Kane *et.al.* Phys. Rev. B. **55**, 15832 (1997).
7. M. Levin *et. al.* B. Phys. Rev. Lett. **99**, 236806 (2007).
8. S-S.Lee *et. al.* Phys. Rev. Lett. **99**, 236807 (2007).
9. Aveek Bid, N. Ofek, H. Inoue, M.Heiblum, V. Umansky and D. Mahalu *Nature* **466** 585 (2010).

EFFECT OF CHARGE CARRIER INHOMOGENEITIES ON QUANTUM HALL EFFECT IN GRAPHENE UNDER HIGH MAGNETIC FIELD

Amit Kumar*, J. M. Poumirol, W. Escoffier M. Goiran, B. Raquet

Laboratoire National des Champs Magnétiques Intenses, CNRS UPR 3228, Université de Toulouse, 143 Avenue de Rangueil, F-31400 Toulouse, France
Email: amit.kumar@lncmi.cnrs.fr

Quantum Hall effect (QHE) is one of the most fascinating quantum phenomena in condensed matter physics that occur on truly macroscopic scale in two dimensional electronic systems (2DES). A very unusual QHE was discovered in one atomic thick sheet of carbon atoms called graphene. It provides an unambiguous evidence for the existence of Dirac fermions in such a system, as well as for an additional zero-energy Landau Level, in contrast to conventional 2DES [1]. Understanding the electronic properties of graphene near the charge neutrality point (i.e. within a Fermi energy range where both electron and hole coexist) in high magnetic field is topic of current interest [2]. In this talk, I will first discuss our recent high field magneto transport measurements in disordered graphene, where the presence of electron and hole puddles leads to a mesoscopic inhomogeneous local doping of the sample [3]. Away from the charge neutrality point, Hall resistance plateaus at filling factors í = 2; 6; 10 etc. as well as a vanishing longitudinal resistance is observed, which constitute the hallmark of the QHE in graphene. In the close vicinity of the charge neutrality point, the system breaks up into many small hole-doped or electron-doped pools, leading to an overall vanishing Hall resistance. Large resistance fluctuations are observed, with maximum amplitude when the magnetic length is comparable with the mean size of the electron-hole puddles. I will then discuss transport measurements of annealed graphene and address the role of disorder on QHE in high magnetic field. In contrast to clean graphene devices, high field transport studies reveal a non conventional behavior, namely a decrease of the Hall resistance from the quantized Hall resistance value at $\nu = \pm 2$ [4]. Fading of QHE at $\nu < |\pm 2|$ has been studied for different carrier densities and disorder levels. It is noticed that the disorder rate drives the magnetic field induced modification of the relative electron and hole densities by providing occupied electronic (hole) states below (above) the Fermi level. These states are formed due to the local potential fluctuations in the sample and are responsible for the unexpected transport properties in high magnetic field. In the last part of my talk, I will briefly discuss first experimental observation QHE in trilayer graphene.

REFERENCE

1. K.S. Novoselov et al, *Nature* **438**, 197 (2005).
2. Y. Zhang. *Phys. Rev. Lett.*, **96**, 136806 (2006).
3. J. M. Poumirol et al., *New J. Phys.* **12** 083006 (2010).
4. J. M. Poumirol et al., *Phy. Rev. B (R)* ***82*** *121401 (2010)*.

ELECTRON TRANSPORT IN BILAYER GRAPHENE IN PRESENCE OF ELECTROMAGNETIC POTENTIAL BARRIERS AND ITS POTENTIAL APPLICATIONS

Neetu Garg, Sankalpa Ghosh, Manish Sharma

Centre for Applied Research in Electronics, Indian Institute of Technology Delhi, Hauz Khas, New Delhi 110016, India
Email: neetu2803@gmail.com

The dispersion relation for electrons near the fermi level for a graphene bilayer is very different from that of a monolayer graphene. Moreover, by applying a bias voltage it is possible to create and tune a gap at the fermi level for such bilayers. This control over the gap near the fermi level allows us the flexibility to block/allow Klein tunnelling or tune conductance in different ways. Given this context, we evaluate the transmission and conductance through combinations of magnetic barrier structures and electrostatic potential barriers in biased bilayer graphene as well as in monolayer graphene and compare the two cases. The results contrast sharply for the two cases. We shall particularly show how an optical analogy can be used to understand various transport regimes in bilayer graphene. By exploiting this analogy, we also suggest practical devices akin to optical structures such as waveguides, resonant cavities and Bragg reflectors.

REFERENCES

1. Sankalpa Ghosh and Manish Sharma - J. Phys. Cond. Matt 21, (2009)
2. Manish Sharma and Sankalpa Ghosh - arxiv 0907.... (Submitted)
3. Neetu Garg, Manish Sharma, Sankalpa Ghosh (In preparation).

THICKNESS DEPENDENT PROPERTIES OF $La_{0.35}Pr_{0.275}Ca_{0.375}MnO_3$ THIN FILMS

A.Rastogi[1], A. K. Kushwaha[1], R. C. Budhani[1,2]

[1]*Condensed Matter - Low Dimensional Systems Laboratory, Department of Physics, Indian Institute of Technology, Kanpur - 208016, India and*
[2]*National Physical Laboratory, Dr. K. S. Krishnan Road, New Delhi - 110012, India*
Email: ankurr@iitk.ac.in

We present the structural, transport and magnetic properties of phase separated manganite $La_{0.625-y}Pr_yCa_{0.375}MnO_3$ (LPCMO) with y = 0.275 epitaxial films of 30, 50 and 100 nm thickness grown on (110) orientated $SrTiO_3$ substrate with 20 nm of $NdGaO_3$ as a buffer layer. The relaxation behavior of LPCMO has been investigated through resistivity and magnetization measurements, which shows a slow relaxation. This relaxation follows a logarithmic dependence and decrease in the resistance indicates the evolution of the sample to a more ordered state with time. Above the metal to insulator transition (T_{MI}) the magnetization is decreasing with time while it increases below the T_{MI}. As the film thickness is increased, the strain relaxes (~ 1.0% for 100 nm thick film) and the lattice parameter of the film approaches to the bulk value of 0.384 nm [1]. In resistivity ρ(*T*) plots the effect of this strain can be seen as a shift in the metal to insulator transition, as the thicker films have higher value of T_{MI}.

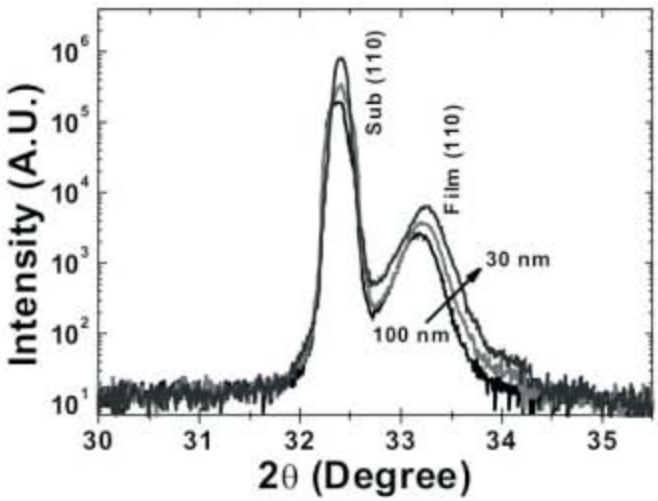

Fig.1: The θ-2θ x-ray diffraction pattern for varying thickness of LPCMO film, which clearly shows the 30 nm thin film has the smallest *c*-axis lattice parameter (~0.372 nm) and as the thickness is increased, it approaches close to bulk lattice parameter (~0.384 nm).

REFERENCES

1. Dane Gillaspie, J. X. Ma, Hong-Ying Zhai, T. Z. Ward, Hans M. Christen, E. W. Plummer, and J. Shen, *J. Appl. Phys.* **99**, 08S901 (2006).

SUCCESSIVE PHASE TRANSITIONS IN NH_4HSO_4

Papia Chowdhury[1], Diptikanta Swain[2], Venkata Srinu Bhadram[2], Chandrabhas Narayana[2], C. N. R. Rao[2]

[1]*Department of Physics & Material Science, Jaypee Institute of Information Technology, Noida, Uttar Pradesh, India*

[2]*Chemistry and Physics of Materials Unit Jawaharlal Nehru Centre for Advanced Scientific Research, Bangalore, India*

Email: papia.chowdhury@jiit.ac.in

Temperature dependent Raman spectroscopic studies on NH_4HSO_4 single crystal were carried out in the temperature range 298-77K. A phase transition from paraelectric to ferroelectric phase was observed around 263K which is second order in nature. The second phase transition from ferroelectric to piezoelectric phase was observed around 143 K which is first order in nature. The spectral data are used for describing the nature of structural disorder to order transition across the transition point leading to phase transition in NH_4HSO_4. NH_4HSO_4 is an acid sulfate which exhibits phase transition at low temperature [1]. The room temperature crystal structure of NH_4HSO_4 is monoclinic. The structure contains two types of chains of crystallographic NH_4HSO_4 units where HSO_4 ions are connected with short O-H...O hydrogen bonds and forming one dimensional long polymeric chain. One chain contains disordered structure of HSO_4 ion with disorderness in oxygen position and other chain with ordered HSO_4 chain structure. Interestingly, after phase transition the disorder chain structure becomes ordered with lower triclinic symmetry. Since one of the HSO_4 ion which involved in polymeric hydrogen bond chain is disordered at O and H crystallographic sites so it is of interest to study the internal vibrations of various molecular units as a function of temperature in order to understand the mechanism of change in polarization and the dynamics of structural phase transition [2,3]. Good quality single crystals of NH_4HSO_4 were grown by slow evaporation from aqueous solution containing equimolar quantities of the $(NH_4)_2SO_4$ and H_2SO_4 at 313K.

The temperature evolution of the Raman spectra of NH_4HSO_4 were recorded in the 180°C backscattering geometry, using a 532 nm excitation from a diode pumped frequency doubled Nd-YAG solid state laser. Laser power at the sample was ~8 mW, and a typical spectral acquisition time

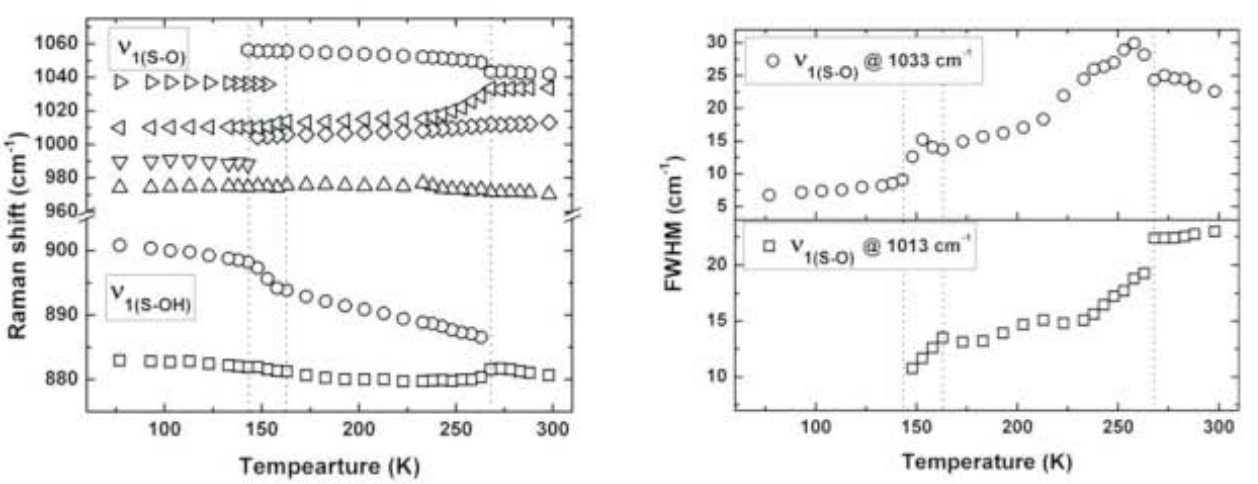

Figure.1: (a) Temperature evolution of $\upsilon_{S\text{-}O}$ and $\upsilon_{S\text{-}OH}$ mode frequencies in the range 300K-77K, (b) Temperature dependent fwhm of $\upsilon_{S\text{-}O}$ modes in the temperature range 300-77 K.

was 1 min. The spectral profile was fitted using Lorentzian functions with the appropriate background. Here we report the dynamics of HSO_4 and the motion of crystal lattice during the phase transition using low temperature Raman spectroscopy which gives an insight into the structural changes, anomaly in polarization and disorder associated with NH_4HSO_4 crystal. To elucidate we are presenting here some of the characteristic changes observed in the Raman spectra.

The phonon mode at 1033 cm^{-1} corresponds to symmetric S-O stretching of ordered HSO_4 unit and its disordered counterpart at 1014 cm^{-1} and at 1028 cm^{-1}. Disordered mode weaken with decrease of temperature up to first transition temperature T_{C1} (263K) and show disappearance at second transition temperature Tc_2 (143K). Similarly phonon modes at 880 cm^{-1} and 887cm^{-1} which are assigned as symmetric S-OH stretching (υSOH), show anomalies in frequency at Tc_2. These changes are shown in Figure 1(a) and (b). In the case of υS-O modes we observe a strong anomaly associated with the disorder in the chain. There is a large increase in the full width at half maxima (FWHM) of the mode [see Fig.1(b)] associated with S-O stretching showing a large disorder across the transition. Along with the above remarkable changes we also observed the splitting of bending modes around 450 cm^{-1} and 580 cm^{-1}. These changes in Raman spectra and their implication will be discussed.

REFERENCES

1. R. Pepinsky, K. Vedam, S. Hosihino, Y. Okaya; Physical Review, **111**, 6, (1956), 1508-1510.
2. V. Verma, N, Rangavittal, C. N. R. Rao; J. Solid State Chem, **106**, (1993), 164.
3. G. K. Pradhan, D. Swain, T. N.Guru Row, C. Narayana, J.Phys.Chem.A. **113**, 8, (2009**)**, 150.

SYNTHESIS OF COBALT NANOPARTICLES BY PULSE LASER ABLATION

BISHNU K. PANDEY, R. GOPAL

Laser Spectroscopy & Nanomaterials Lab, Department of Physics (UGC-CAS), University of Allahabad, Allahabad-211002, INDIA
Email: spectra2@rediffmail.com

Magnetic nanoparticles offer some attractive possibilities in biomedicine. Firstly, They have controllable sizes ranging from a few nanometer up to tens of nanometers, which places them at dimensions that are smaller than or comparable to those of a cell (10-100μm),a virus (20-450nm), a protein (5-50nm) or a gene (2nm wide and 10nm long) . In the present study, cobalt nanoparticles have been synthesized by PLA of highly pure cobalt slice in aqueous medium of 5 mM sodium dodecyl sulfate (SDS). The focused output of 1064 nm wavelength of pulsed Nd: YAG laser operating at 40 mJ/ pulse, 10 Hz was used for ablation. The optical property of the magnetic colloids was studied by UV-visible absorption spectroscopy and magnetic characterization by vibrating sample magnetometer (VSM).

Fig. 1 represents the absorption spectrum of colloidal nanoparticles. The spectrum reveals a peak at 289 nm and another peak at 230 nm.

Fig. 2 represents tauc plot of as synthesized colloidal cobalt nanoparticles in SDS.It has observed that band gap of colloidal cobalt nanoparticles is 4.77eV.

Magnetic measurements of the cobalt nanoparticles were performed using VSM at room temperature in the field range from -1500 to 1500 Oe. The typical M-H loop is presented in Fig. 3. The inset of Fig. 2 shows the value coercivity is ~92 Oe and the saturation magnetization is ~ 0.40 emu/g, are much smaller than that of bulk. Similar types of results reported by Chen et al[1]. The low value of coercivity may be partially induced by small cobalt nanoparticles under the critical size of superparamagnetism. A material with a low coercivity is useful in microwave devices, magnetic shielding, transformers, and recording heads.

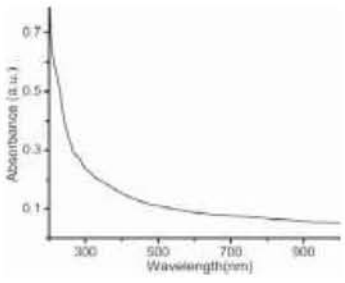

Figure 1 UV-visible absorption spectrum of as synthesize cobalt nanoparticles in 5 mM SDS

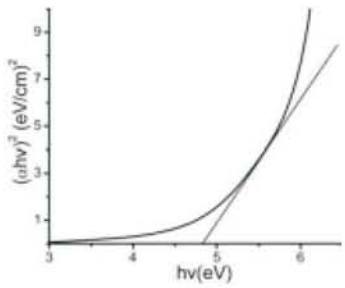

Figure 2 Tauc plot for of as synthesized Cobalt nanoparticles

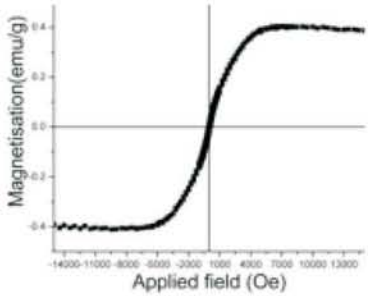

Figure 3: Room temperature M-H curve of as synthesize cobalt nanoparticles in SDS

REFERENCE

1. G. X. Chen et al. Appl. Surf. Sci. 228 (2004) 169.

THICKNESS DEPENDENT SURFACE PLASMON RESONANCE STUDY ON NANOSCALE Ag FILMS

R.Boruah, D.Mohanta, G.A.Ahmed and A.Choudhury

Department of Physics, Tezpur University, PO. Napaam, Assam-784028
Email: rboruah@tezu.ernet.in

We describe a simple experiment, along with theoretical justification on thickness dependent surface plasmon resonance study on Ag nanostructured films of varying thickness (20-100 nm). Using a catalyst-free thermal evaporation method, different thicknesses of Ag films were deposited on the hypotenuse face of a right angle prism. A plane polarized light beam (obtained from a 2 mW He-Ne laser, λ=632.8 nm) was incident through the prism on the back of the metal film. At an angle of incidence, a few degree greater than the critical angle for the total internal reflection, a sharp minimum in the reflected light intensity is observed owing to the excitation of surface plasmons. The minimum reflectivity pattern is assigned to the strong absorption response of the surface plasmons excited in the Ag films. A correlation between the full width at half maxima (FWHM) along with thickness variation will be discussed.

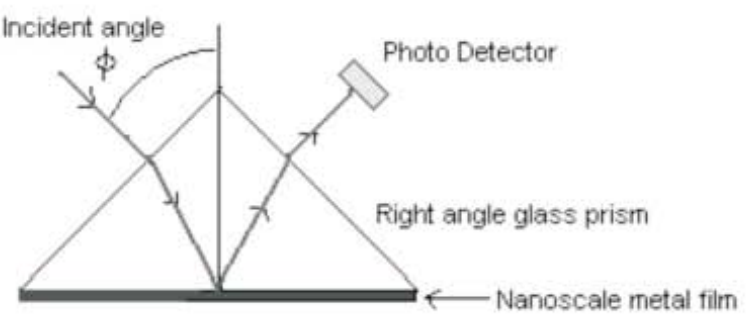

Fig. : A scheme of plasmon resonance using right angle prism.

REFERENCES

1. H. J. Simon, D.E. Mitchell, and J. G. Watson, *Am. J. Phys.* 43 (7) (1975) 630.
2. J. Homola, S.S Yee, and G. Gauglitz, *Sensors and Actuators* B 54 (1999) 3.

ANOMALOUS ELECTRONIC TRANSPORT IN NANODIAMOND-LIKE CARBON FILMS

Soma Mukherjee[1,2], B. K. Chaudhuri[1], H. Sakata[3], M. Wakaki[3]

[1]*Department of Solid State Physics, Indian Association for the Cultivation of Science, Jadavpur, Kolkata –700 032, India*

[2]*Department of Engineering Physics, Guru Nanak Institute of Technology, Panihati, Sodepur, Kolkata – 700 114*

[3]*Department of Optical and Imaging Science & Technology, Tokai University, 1117, Kitakaname, Hiratsuka, Kanagawa 259-1292, Japan*

Email : somamb@rediffmail.com

Thickness dependent electronic transport properties of amorphous diamond-like-carbon (DLC) films prepared by plasma-beam ion-injection deposition (PBIID) method has been reported. The thinner film, DLC1 (90nm thick) shows metallic behavior above 200K and a metal- insulator transition occurs below this temperature. The thicker film DLC2 is, however, a semiconductor over the temperature range 80-300K showing large increase of resistivity below 150K. The scanning electron micrographs and Raman spectroscopic studies revealed the presence of nanometer size diamond-like crystals embedded in the amorphous matrix. Presence of larger number of such nanodiamonds in DLC2 along with larger sp^3/sp^2 ratio observed from XPS study can be attributed to the higher resistivity ($\sim 10^{10}$ ohm cm) of DLC2 compared to that of thinner DLC1($\sim 10^4$ ohm cm). Low temperature semiconducting behavior of the thinner film can be explained by Mott variable range hopping (VRH) model while the resistivity of the thicker film is found to follow Mott small polaron hopping (SPH) model in the high temperature range.

BISMUTH AND ANTIMONY BASED SEMICONDUCTING COMPOUNDS AND THIN FILMS, THEIR GROWTH AND CHARACTERIZATION.

Sandeep Kr. Pundir, Sukhvir Singh, A.K.Srivastava

National Physical Lab., New Delhi-12
Email: skpnagali@gmail.com

In the present study bulk compound of Bi_2Te_3 has been grown by vertical directional solidification (VDS) technique using high purity Bi and Te (99.999%pure) materials. Thin films of Bismuth telluride have been deposited on to single crystal of NaCl and glass substrates at different deposition conditions using thermal evaporation technique under high vacuum technique. The thickness of the thin films was maintained between 55nm–65nm. X-ray diffractrometry technique was utilized to identify the phases present in the as deposited films. Surface morphology of these films has been investigated by using scanning electron microscope (SEM). Compositional elemental analysis of the films was determined by energy dispersive spectrometer (EDS) in order to identify the stoichiometry of the films. Electron diffraction technique was used to confirm the presence of phases and the nature of the films. The Van der Pauw and Hall measurement technique were use to calculate the resistivity, mobility, conductivity, carrier concentration and charge carrier type in the films. Thin films deposited onto glass substrates have been utilized to study the electrical parameters. In the present investigations efforts have been made to study the microstructural features associated with bismuth telluride films prepared at different deposition conditions and correlated these structural details with the electrical properties.

STUDY OF NANOSTRUCTURED $Zn_{0.75}Cd_{0.25}O$ THIN FILMS

Nisha Singhania[1,3], Anurag Gaur[1], Rajendra Singh[2]

[1]*Department of Physics, National Institute of Technology, Kurukshetra-136119, India*
[2]*Department of Physics, Indian Institute of Technology, New Delhi-110016, India*
[3]*Material Research Centre, Indian Institute of Science, Bangalore-560012, India*
Email: n4nishasinghania2@gmail.com

Zinc oxide (ZnO) is one of the most promising materials for the fabrication of optoelectronic devices operating in the blue and ultra-violet (UV) region, owing to its direct wide band gap (3.37 eV) and large exciton binding energy (60 meV). On the other hand, ZnO is a commercially available material with advantages of low cost, nontoxicity and high chemical stability. Ternary ZnCdO semiconductor has great potential applications in short-wavelength optoelectronic devices. To fabricate optical devices such as laser diodes, band gap engineering is necessary and ZnCdO is regarded as an ideal material for ZnO-based devices. By alloying ZnO with CdO, which has a cubic structure and a narrower direct band gap of 2.3 eV, the band gap of ZnO can be red-shifted to blue, or even green light spectra range. Moreover, the incorporation of Cd into ZnO is very useful for the fabrication of $ZnO/Zn_{1-x}Cd_xO$ heterojunctions and superlattices, which are the key elements in ZnO based light emitters and detectors [1-3].

In this work, we have successfully deposited the $Zn_{0.75}Cd_{0.25}O$ thin films by electro deposition method on ITO substrate and to characterize them for structural, morphological and optical properties. X-ray diffraction pattern of $Zn_{0.75}Cd_{0.25}O$ thin films in as grown state and annealed at 400°C, 500°C and 600°C are shown in Fig. 1. The X-ray diffraction study revealed that $Zn_{1-x}Cd_xO$ films exhibit a wurtzite structure with a strongly (002) preferred orientation of their crystallites. The effect of annealing temperature was studied on these films and it has been found that decrease in crystalline size results increase in cadmium concentration indicating the incorporation of cadmium in zinc oxide lattice. Nanoflakes, entangled nanorods, and hexagonal faced nano pellets type nanostructures are synthesized by this electrodeposition method as shown in SEM images (Fig. 2). The presence of cadmium is confirmed by EDX analysis and effect of annealing is observed for the $Zn_{0.75}Cd_{0.25}O$ films.

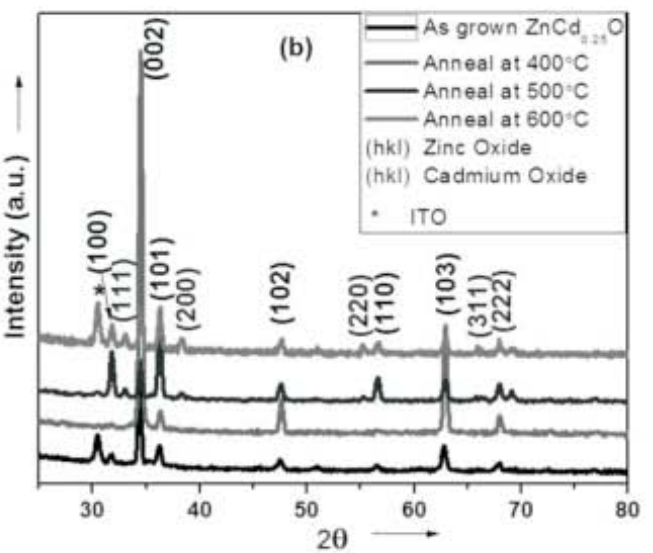

Fig. 1: XRD pattern of Zn0.75Cd0.250 thin films in as grown state and annealed at 400°C, 500°C and 600°C

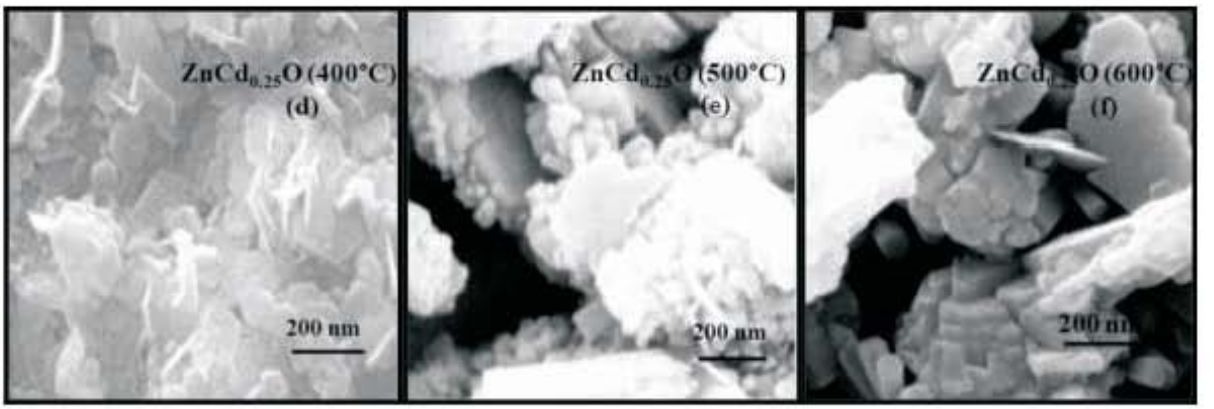

Fig. 2: SEM images of $Zn_{0.75}Cd_{0.25}O$ thin films annealed in air at 400, 500 and 600°C.

Moreover, the optical band gap of the films, determined from UV-Vis spectroscopy data, are found to be 2.38, 3.67 and 3.43 eV for 400, 500 and 600°C annealed films.

REFERENCES

1. J. Jie, G. Wang, X. Han, Q. Yu, Y. Liao, G. Li, J.G. Hou, Chem. Phys. Lett. 387 (2004) 466.
2. H.P. Tang, L.P. Zhu, H.P. He, Z.Z. Ye, Y. Zhang, M.J. Zhi, Z.X. Yang, B.H. Zhao, T.X. Li, J. Phys. D Appl. Phys. 39 (2006) 2696.
3. H.P. He, H.P. Tang, Z.Z. Ye, L.P. Zhu, B.H. Zhao, L. Wang, X.H. Li, Appl. Phys. Lett. 90 (2007) 023104.

STRUCTURAL CHARACTERIZATION OF Zn-Ni FERRITE NANOPARTICLES PREPARED BY SOL-GEL METHOD

PARMOD KUMAR, VIPIN AMOLI, ANURAG GAUR, B.K. KAUSHIK

Department of Physics, National Institute of Technology, Kurukshetra-136119, India
Email: parmodphysics@gmail.com

In the recent past, the nanomagnetic materials have gained remarkable scientific interest owing to their interesting properties and a variety of applications [1]. The high coercivity of these magnetic nanoparticles makes them interesting for applications in the fields of high-density magnetic media, recording color imaging, ferrofluids, high-frequency devices and magnetic refrigeration [2, 3]. The surface to volume ratio of these nano-magnetic materials is very large as compared to the bulk due to which they exhibit unique properties such as spin canting, surface anisotropy, superparamagnetism, etc. [4]. Nickel and zinc are known to have strong preference for the tetrahedral and octahedral sites, respectively, making nickel ferrite a model inverse ferrite and zinc ferrite a model normal ferrite. However, the composite Ni–Zn ferrites are known to exist as mixed spinel structure. The compositional variation in these ferrites results in the redistribution of metal ions over the tetrahedral and octahedral sites, which can modify the properties of ferrites.

The properties of ferrite materials are known to be strongly influenced by their composition and microstructure that in turn are sensitive to the processing methods used to synthesize them. In an attempt to prepare high performance ferrites with reproducible stoichiometric compositions and desired microstructure, the present work aimed at preparing Zn-Ni ferrites using the sol–gel method. The sol–gel techniques for ferrite synthesis have been proved to be more convenient, since the ferrite powders with nano-sized particles can be formed directly from combustion of dried in air [5]. In the present study, we use the sol–gel method to synthesize the reactive nano-sized powder in order to lower the sintering temperature of Zn-Ni ferrite. In this paper, we report on the synthesis and structural characterization of $Zn_{1-x}Ni_xFe_2O_4$ ferrites (x = 0.2, 0.5, 0.6 & 1.0).

To synthesis the Zn-Ni ferrite powders with compositions of $Zn_{1-x}Ni_xFe_2O_4$ (x = 0.2, 0.5, 0.6 & 1.0) via by sol–gel method, the appropriate amount of nitrates was first dissolved into ethylene glycol to form a mixed solution. Then, the mixed solution was poured into a dish and heated firstly

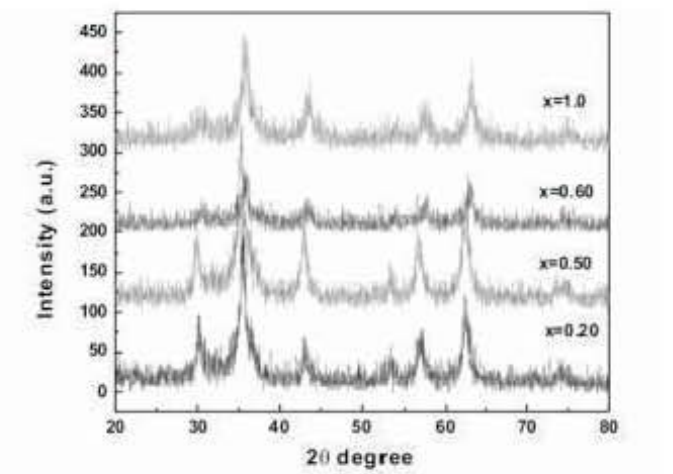

Fig.: X-ray diffraction pattern of $Zn_{1-x}Ni_xFe_2O_4$ (x = 0.2, 0.5, 0.6 & 1.0) nanoparticles.

at 70°C under constant stirring to transform into a dried gel and then finally heated at 100°C to get brown color ferrite powder. The phase identification was characterized by Rigaku X-ray diffractometer (XRD).

By the XRD analysis, it has been found that all the samples are formed in pure phase corresponding to $Zn_{1-x}Ni_xFe_2O_4$. Moreover, the shifting in the XRD peaks indicates that the lattice parameters change with the Ni concentration. We have calculated the lattice parameters for all the samples and it has been found that lattice parameters decrease with increase in Ni concentration. The particle size, calculated by Schreer formula using X-ray data, is found to be ~ 12 nm. Furthermore, the magnetic studies of these samples are under progress.

REFERENCES

1. Schultz, K. Schnitzke, J. Welker, Appl. Phys. Lett. 56 (1990) 868–870.
2. M. Kishimoto, Y. Sakurai, T. Ajima, J. Appl. Phys. 76 (1994) 7506–7509.
3. L. Lu, M.L. Sui, K. Lu, Science 287 (2000) 1463–1466.
4. D. Caruntu, G. Caruntu, C.J.O Connor, J. Phys. D: Appl. Phys. 40 (2007) 5801.
5. G.S. Shahane, A. Kumar, M. Arora, R.P. Pant, K. Lal, J. Magn. Magn. Mater. 322 (2010) 1015.

EVOLUTION OF KOSTERLITZ THOULESS BEREZINSKII (KTB) TRANSITION AND LABUSH PARAMETER IN ULTRA THIN NBN FILMS

Mintu Mondal[1], Sanjeev Kumar[1], Anand Kamlapure[1], Madhavi Chand[1], John Jesudasan[1], Vivas C. Bagwe[1], Garima Saraswat[1], Vikram Tripathi[2], Pratap Raychaudhuri[1]

[1]*Department of Condensed Matter Physics and Materials Science, Tata Institute of Fundamental Research, Homi Bhabha Road, Mumbai 400005, India*
[2]*Department of Theoretical Physics, Tata Institute of Fundamental Research, Homi Bhabha Road, Mumbai 400005, India*
E-mail: mondal@tifr.res.in

We will present detailed experimental study on Kosterlitz Thouless Berezinskii (KTB) transition and vortex pinning by measuring Labush Parameter in presence of magnetic field in ultra thin superconducting NbN films[1]. To explore the KTB transition we have measured the superfluid density, normal carrier density and resistivity of a set of ultrathin NbN films and performed I-V measurents on a set of strip lines of NbN films. Our results show that while the ground state values of $\Delta(0)$ and $\lambda(0)$ are well described by Bardeen-Cooper-Schrieffer (BCS) theory, at elevated temperatures, films with thickness <10nm show sudden drop in superfluid density associated with the Kosterlitz-Thouless-Berezinski (KTB) transition close to T_c. Although the sudden drop started at higher superfluid density expected from 2-D XY model, the nature of transition is well describe by considering the low vortex core energy [2] and slight inhomogeneity in the system. We have measured the Labusch parameter, the average vortex pinning force (L_{exp}) for another set of ultrathin films. The observed change in L_{exp} *with* increasing vortex density and temperature will be discussed in details.

REFERENCES

1. Anand Kamlapure, Mintu Mondal, Madhavi Chand, Archana Mishra, John Jesudasan, Vivas Bagwe, L. Benfatto, Vikram Tripathi, Pratap Raychaudhuri, Appl. Phys. Lett. 96, 072509 (2010).
2. L. Benfatto, C. Castelani, and T. Giamarchi, Phys. Rev. Lett. **98**, 117008 (2007); Phys. Rev. B **77**, 100506 (R) (2008).

LOW TEMPERATURE SUPERSPIN GLASS LIKE MEMORY EFFECTS IN $La_{0.7}Ca_{0.3}MnO_3$ NANOMANGANITE

SHILPI KARMAKAR[1], B K CHAUDHURI[1,2], C CHANG[2], H D YANG[2]

[1]*Department of Solid State Physics, Indian Association for the Cultivation of Science, Kolkata 700032, India*

[2]*Department of Physics, Center for Nanoscience and Nanotechnology, National Sun Yat-Sen University, Kaohsiung 804, Taiwan*

Email: sspbkc@iacs.res.in, sspbkc@rediffmail.com

Interesting low temperature memory phenomena have been observed from equilibrium and out of equilibrium magnetic measurements on the $La_{0.7}Ca_{0.3}MnO_3$ type nano-manganite system. The observed phenomenon were screened for atomic spin glass (SG), super spin glass (SSG), cluster glass (CG) and superparamagnetic (SPM) behavior. The result shows evidences of superspin glass like behavior at low temperature (<40K) in this manganite system consisting of ferromagnetic nanoparticles. Between 40K and ferromagnetic Curie point T_c~238K, a ferromagnetic cluster glass state emerges with a weaker interparticle interaction than the SSG phase. The dynamic susceptibility shows both chaos and memory effects, first reported in this system. Moreover, we have also noticed asymmetric response with respect to temperature change protocol. The origin and nature of the low-temperature superspin glass state for the present system are discussed within the framework of hierarchical organization of metastable states.

MICRO STRUCTURAL FEATURES ASSOCIATED WITH THE THIN FILM OF TIN OXIDE SYNTHESIZED BY THERMAL EVAPORATION TECHNIQUE AT DIFFERENT DEPOSITION CONDITIONS.

P. Jain[1], A.M.Siddiqui[2], S. Singh[1], A.K.Srivastava[1]

[1] NPL, NewDelhi, India;
[2] Jamia Millia Islamia, New Delhi, India
Email: parveenjain21@gmail.com

In the present study thin films of tin oxide have been deposited on to single crystal of KCl and glass substrates at different vacuum conditions using thermal evaporation technique. The thickness of thin films was maintained between 90nm – 100nm. As deposited films were annealed at different temperatures and for different time periods. X-ray diffraction technique was utilized to identify the phases present in the deposited as well as annealed films. Surface morphology of these films has been characterized by using scanning electron microscope (SEM). Compositional elemental analysis of the films was determined by energy dispersive spectrometer (EDS) in order to identify the stoichiometry in the films. Micro structural features present in the deposited as well as annealed films were recorded under high resolution transmission electron microscope (HRTEM). Electron diffraction technique was used to confirm the presence of phases and the nature of the films. Thin films deposited onto glass substrates have been utilized to study the electrical parameters. In the present investigations, a structure property correlation has been established.

CMOS COMPATIBLE SILICON NANOWIRE ARRAYS FOR CHEMFET AND BIOFET

AJAY AGARWAL*, V K KHANNA, CHANDRA SHEKHAR

Central Electronics Engineering Research Institute, Pilani, Rajasthan INDIA 333031
**Email: dr_ajay123@yahoo.com*

Nanotechnologies are creating new nano-dimensional materials and devices that find diverse applications in the fields like medicine, electronics, and energy production. With the increasing spread of knowledge, healthcare is in focus which includes early disease diagnosis, drugs discovery, etc. For these applications specific and sensitive detection of various biological and chemical species becomes crucial. Among various nano-materials, nanowire (NW) based bio-chemical sensors are most exploited for the purpose. The NW sensors work on the principle of Field Effect Transistor (FET) where charge associated with the chemical and biological species attached on the nanowire surface acts as the chemical or bio-gate, hence the devices are also termed as CHEM-FET or BIOFET. For such sensing applications different metallic (Pd, Cd, Mo, Au, Ag, Cu) [1], metal oxides [2] and semiconductors nanowires [3-5] have been realized using various techniques. These processes can be categorized in two categories, one is "bottom-up" approach where, the self-assembly of small sized structures forms larger structures [3] using chemical vapour deposition (CVD), electro-deposition and other techniques. The other is "top-down" approach where, the large systems are reduced to smaller sizes to produce multi-functional nano-structures [4, 5].

This paper presents CMOS compatible silicon process technology to realize silicon nanowires in array format, with cross-sectional dimensions ≤ 50nm and length in tens to hundreds of microns. The devices have thin silicon oxide cover on nanowires as the gate dielectric. The two ends of Si NW are integrated with silicon pads which are connected to metallic inter-connects and pads that allow interface to macroscopic instruments. The chips can be built with integrated fluidic channels or open reserviours for the easy dispensing of analytes. A typical SEM image of a nanowire chip is depicted in Fig 1. The sensitivity of such devices depends on various facts like cross-sectional dimensions of the nanowires, conductivity/ doping of the NW, dielectric thickness and surface modification to attach the analytes under investigations.

Various bio-chemical applications results using these sensors like DNA sensing [6] for Single Nucleotide Polymorphisms (SNP) and Heterozygous SNPs detection; analysis various ions like H^+

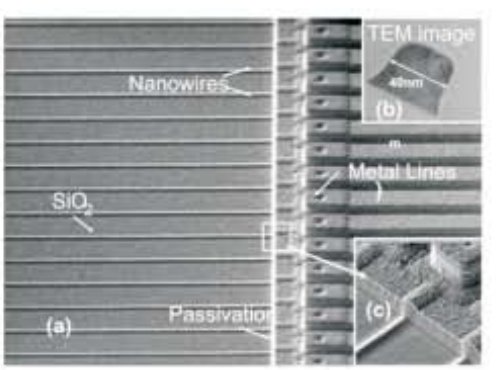

Figure1: (a) SEM image of the sensor chip showing silicon nanowires in an array spaced at 2μm and with individual contacts (b) TEM image suggesting rectangular cross-section of the nanowire (c) Magnified angular SEM image of the array.

(pH), alkali metal ions (Ca^{2+}, Mg^{2+}, Na^{+}, K^{+}) [7]; Cu^{2+}, Zn^{2+}; bio-electricity detection from cells and organs [8], etc. will be presented. The process technologies used to realize such devices are reproducible and are suitable for mass production. Details will be discussed.

REFERENCES

1. E C Walter, et al., Electronic devices from electro deposited metal nanowires, Microelectronic Eng. 61-62, 2002, pp. 555
2. C S Rout, et al., Hydrogen and Ethanol sensors based on ZnO nanorods, nanowires and nanotubes, Chem. Phy. Lett. 418, 2006, pp. 586
3. Y Cui, et al., Nanowire Nanosensors for Highly sensitive and selective detection of biological and chemical species, Science, 293, 2001, pp. 1289
4. Ajay Agarwal, et al., Silicon nanowire sensor array using top-down CMOS technology, Sensors and Actuators A: Physical, 145-146, 2008, pp. 207
5. N. Singh, A Agarwal, et al., Si, SiGe Nanowire Devices by Top-Down Technology and Their Applications, IEEE Transactions on Electron Devices, 55, 2008, pp. 3107
6. Z Gao, Ajay Agarwal, et al., Silicon nanowire arrays for label-free detection of DNA, Anal. Chem., 79 (9), 2007, pp. 3291
7. X Bi, Ajay Agarwal, et al., Development of electrochemical calcium sensors by using silicon nanowires modified with phosphotyrosine, Biosensors Bio-electronics, 23, 2008, pp. 1442
8. T-S Pui, Ajay Agarwal, et al., CMOS-compatible nanowire sensor arrays for detection of cellular bioelectricity, Small, 5, 2009, pp. 208

IMPACT OF OXYGEN VACANCY INDUCED QUENCHED DISORDER ON MAGNETISM AND MAGNETOTRANSPORT IN POLYCRYSTALLINE $Sm_{0.55}Sr_{0.45}MnO_3$ THIN FILMS

M. K. Srivastava[1,2] , R. Prasad[1], P. K. Siwach[1], A. Kaur[2], H. K. Singh[1]

[1]*National Physical Laboratory (CSIR), Dr. K. S. Krishnan Marg, New Delhi-110012, India*
[2]*Department of Physics and Astrophysics, University of Delhi, Delhi-110007, India*
Email: manojk.sri2006@gmail.com

We report the effect of oxygen vacancy and substrate induced inhomogeneous compressive strain which leads to quenched disorder, on the magneto-electrical properties of polycrystalline $Sm_{0.55}Sr_{0.45}MnO_3$ (SSMO) thin films. Polycrystalline SSMO thin films (~100 nm) was prepared on single crystal LAO (001) substarte at ~200 °C by spray pyrolysis technique with post deposition annealing at 1000°C for 12 hrs. Quenched disorder was controlled by varying the annealing conditions. One set of films was annealed in air and slowly cooled to room temperature. The second set was quenched after air annealing and the third one was slowly cooled after annealing in flowing oxygen. All the films are highly textured and are under mild compressive strain. The paramagnetic-ferromagnetic (PM-FM) and insulator-metal (IM) transition occurs at T_C/T_{IM} ~164 K in the air annealed-slow cooled films, which is higher than that for the corresponding single crystals (T_C/T_{IM}~130 K). In contrast, T_C/T_{IM} of films annealed in oxygen is reduced to ~135 K. The films annealed in air and quenched shows the lowest T_C/T_{IM}. The variation of the magneto-electrical properties is attributed to the coupled interplay between the substrate induced strain and oxygen vacancies. The first order IM transition observed in SSMO single crystals is transformed into non-hysteretic and continuous one in the oxygen vacancy ordered films. The large enhancement in T_C/T_{IM} observed in films annealed in air has been explained as a consequence of correlated quenched disorder caused by the coupled effect of spatially nonunifrom strain and ordered oxygen vacancies. Correlated quenched disorder leads to enhanced PM-FM and IM transitions, while uncorrelated quenched disorder results in a decrease in T_C/T_{IM}. The electrical transport mechanism also confirms the influence of quenched disorder in these films.

IMPACT OF THICKNESS ON MAGNETIC PHASE COEXISTENCE AND ELECTRICAL TRANSPORT IN THE VICINITY OF MULTICRITICAL POINTS IN $Nd_{1-x}Sr_xMnO_3$ THIN FILMS

R. Prasad[1,2], M. P. Singh[3], P. K. Siwach[1], V. Agarwal[1], P. Kumar[1], A. Kaur[2] H. K. Singh[1]

[1]*National Physical Laboratory (Council of Scientific and Industrial Research), Dr. K. S. Krishnan Marg, New Delhi-110012, India*

[2]*Department of Physics and Astrophysics, University of Delhi, Delhi-110007, India*

[3]*Département de Physique and RQMP, Université de Sherbrooke, Sherbrooke, Quebec J1K 2R1, Canada*

$Nd_{1-x}Sr_xMnO_3$ (NSMO) possesses several boundaries on the χ-T phase diagram separating paramagnetic (PM), ferromagnetic (FM), antiferromagnetic (AFM) and charge/orbital ordered (CO/OO) phases. NSMO possesses strong phase coexistence in hole as well as electron doped regions of the phase diagram and there are two important regions in the vicinity of χ≈0.5 and χ≈0.63 that contain multicritical points. At χ~0.5, NSMO undergoes simultaneous PM-FM and insulator metal transition (IMT) at T_C≈250 K that is followed by transition to a charge ordered insulating (COI) phase at T_{CO}≈150 K, which is accompanied by a real-space ordering of the $d(3x^2-r^2)$ and $d(3y^2-r^2)$ orbitals and the Mn^{3+} and Mn^{4+} ions in a checkerboard pattern referred to as the correlated electronic (CE) state. The CE-type AFM-CO phase is observed only in the vicinity of χ≈ *0.5* and at slightly higher values of *x* it coexists with the *A*-type *AFM* state. In the vicinity of χ≈0.63, the competing magnetic orders are A- and C-type AFM, of which the former is metallic and the latter insulating. We have studied the influence of thickness on the functional properties, especially a correlation between magnetic phase coexistence and magnetoresistance, of $Nd_{0.50}Sr_{0.50}MnO_3$ and $Nd_{0.37}Sr_{0.63}MnO_3$ thin films. Our study demonstrates that film thickness that controls the degree of compressive strain can have significant impact on the magnetic phase landscape and magnetotransport properties of these films. Films of thickness (~25-120 nm) were deposited on $LaAlO_3$ (001) substrates by DC magnetron sputtering. Hereafter, the χ≈0.50 and χ≈0.63 films will be denoted by N50 and N63, respectively.

The N50 films exhibit multiple magnetic transitions controlled by strong electron correlations and phase coexistence. The dimensionality and the fraction of the coexisting magnetic phases are strongly correlated to the film thickness and hence substrate induced strain. At smaller film thickness, that is, in films which are fully under in-plane compressive strain stronger phase competition and fluctuation are observed. Increase in the film thickness results in relaxation of strain, which favors the FMM phase at the cost of the soft A-AFM and COI phases hence reducing the phase fluctuation. A strong phase fluctuation/coexistence has a strong bearing on the electrical transport in these films and causes a sharp decrease in the resistivity at $T<T_{IM}$. At smaller film thickness, IM transition occurs at $T<T_C$ and the resistivity drops by four orders of magnitude, while in thicker films $T_{IM} \sim T_C$ and the resistivity decrease in less pronounced. These results are well corroborated by the temperature-dependent small polaron activation energy. Near T_C/T_{IM} huge MR (60–80%), is achieved in such films even at moderate magnetic fields ~10–20 kOe.

All the N63 films (in thickness range 25-120 nm) show a weak PM-FM transition. The T_C (≈260 K) remains nearly independent of the film thickness but magnetic moment is reduced considerably at higher film thickness. It must be noted that in bulk poly- and single crystals of similar composition

no such transition is observed at $\chi \approx 0.63$. At lower film thickness these films show insulator like temperature dependences but an external magnetic field induces a drastic decrease in resistivity in the lower temperature range. This results in large *MR*~85 % at T = 30 K and H = 70 kOe. An IMT is observed at higher film thicknesses ($\geq$60 nm) and the magnetic-field independence of the observed T_{IM} (~125 K) distinguishes it from the same observed in prototype manganites ($\chi \sim 0.2–0.4$). The observed phenomena in the overdoped films have been explained in terms of orbital-fluctuation–induced phase separation.

STUDY OF ELECTRONIC TRANSPORT BEHAVIOUR OF LAYERED GRAPHENE NANO-STRUCTURES

Sanjay Kumar, Ajay

Department of Paper Technology, Indian Institute of Technology Roorkee, Saharanpur campus- 247001 India
E-mail: sanjaybharatiy@gmail.com, ajay_phys@yahoo.co.in

After the experimental isolation of graphene in 2004 [1], there have been a wide spectrum of research work based on experimental and theoretical aspects of electronic properties of these systems to underline the technological potential of graphene based systems. The electronic properties of monolayer graphene are interesting due to its unique linear gapless electronic band structure [2]. In bilayer graphene, two graphene monolayers are weakly coupled by interlayer carbon hopping and there are four atoms per unit cell. Bilayer graphene has parabolic band dispersion with an effective band gap of the order of 0.25 eV near the Dirac points [3]. The trilayer graphene shows flat band dispersion and a finite band gap near Dirac points [4]. Due to interlayer asymmetry and interlayer interactions, these bands in trilayer graphene hybridized to produce an increase in density of states at Fermi level [5]. Therefore, the graphene based layered nanomaterials are promising candidates for nano- electronic applications. One need to attempt theoretical studies related to electronic structure and transport in monolayer, bilayer, and trilayer graphene with different stacking as a lot of experimental data on transport properties of graphene and related multilayer system is now available. In the present work therefore, we have planned to attempt theoretical modeling of electronic structure and calculate conductivity within Kubo formalism as a function of temperature and carrier concentration [6] in graphene bilayer and trilayer nanostructures and compare the result with existing experimental results.

REFERENCES

1. K.S. Novoselov et al. “Electric Field Effect in Atomically Thin Carbon Films” Science 306, 666 (2004).
2. K. Geim, et al. “Graphene: Status and Prospects” Science 324, 1530 (2009).
3. Y. B. Zhang et al., “Direct observation of a widely tunable bandgap in bilayer graphene” Nature 459(7248), 820-823, (2009).
4. M. F. Craciun et al., “Trilayer graphene is a semimetal with a gate tunable band overlap” Nature Nanotechnology. Vol. 4 (2009).
5. T. Ohta et al., “Interlayer interaction and electronic screening in multilayer graphene” Phys. Rev. Lett. 98, 206802 (2007).
6. B.S. Tewari et al., “Influence of inter cell resonant tunneling on the out-of-plane electronic transport behavior in layered high Tc cuprates” Eur. Phys. J. B 66, 67–74 (2008).

STATISTICAL THERMODYNAMICS OF RELATIVISTIC FERMIONS IN GRAPHENE

Reena Gupta, G. S. Singh*

Department of Physics, Indian Institute of Technology Roorkee, Roorkee 247667
E-mail: *gss.phy@iitr.ernet.in*

An ideal graphene [1] is a monatomic layer of carbon atoms arranged on a honeycomb lattice and is, therefore, a perfect two-dimensional (2D) system. The electrons moving around carbon atoms interact with the periodic potential of honeycomb lattice giving rise to new quasiparticles with negligibly small rest mass m_0 and effective speed for small wave vectors about $v_F=10^6$ m s^{-1} whence the dispersion relation becomes linear near the symmetry points K and K′ located at the corners of the first Brillouin zone. Hence these quasiparticles, called massless Dirac fermions, accurately describe those physical properties which involve wave vectors close the symmetry points. However, in general, the exact dispersion relation applicable to massive particles should be considered and we have derived exact analytical expressions for the study of the thermodynamic properties of this unusual 2D system with Dirac-like electronic excitations.

Understanding properties of quantum matter confined in 2D has been at the forefront of theoretical physics [2]. The lowered dimensionality is believed to increase the role of interactions, and together with quantum statistics, lead to anomalies in various physical observables [3-5]. Anomalous specific heat of Coulomb-interacting massless Dirac fermions in 2D has been studied in Ref. [6] but the study in Ref. [7] shows that some of the basic thermodynamic features of massive fermions in graphene might be captured considering fermions to be noninteracting.

We consider the grand canonical ensemble and start with the logarithm of the grand potential, $ln\ Z_G$, of an ideal Fermi gas developed as the Mellin transform of the single-particle partition function $Z_1(\beta)$, where $\beta=1/k_BT$. Exact analytical expression has been obtained for $Z_1(\beta)$ in terms of modified Bessel function of the second kind and has been substituted in the Mellin transform. The application of Cauchy's theorem has helped in evaluation of the resulting integral to get an analytical form for $ln\ Z_G$. The grand potential is related to $ln\ Z_G$, and pressure, entropy and average numbers of particles in the system are given by the partial derivatives of the grand potential. Hence exact analytical expressions have been derived for the thermodynamic parameters and the thermodynamic functions. These exact expressions get reduced to the known corresponding quantities for nonrelativistic and ultrarelativistic particles. We have evaluated our expressions and compared with the known results.

REFERENCES

1. See, for example, Neto *et al.*, Rev. Mod. Phys. **81**, 109 (2009).
2. S. Kivelson, D. –H. Lee, and S. –C. Zhang, Sci. Am. **274**, 64 (1996).
3. D. A. Bohm, Nature Phys. **2**, 159 (2006).
4. E. Abraham, S. V. Kravchenko, and M. P. Sarachik, Rev. Mod. Phys. **73**, 251 (2001).
5. Casey et al., Phys. Rev. Lett. **90**, 115301 (2003).
6. O. Vafek, Phys. Rev. Lett. **98**, 216401 (2007).
7. M. K. Lee, S. J. Lee, and T. W. Kang, Current Applied Physics **9**, 769 (2009).

EXISTENCE OF TOPOLOGICAL PHASE IN THALLIUM BASED III-V-VI TERNARY CHALCOGENIDES

Ashutosh Sharma[1], B. Singh[1], R. Prasad[1], H. Lin[2], L.A. Wray[3], S.Y. Xu[3], M.Z. Hasan[3], A. Bansil[2]

[1] *Department of Physics, Indian Institute of Technology Kanpur, Kanpur, India*
[2] *Department of Physics, Northeastern University, Boston, Massachusetts 02115 USA*
[3] *Department of Physics, Princeton University, Princeton, NJ08544 USA*
Email: atsharma@iitk.ac.in, bhrsingh@iitk.ac.in

Topological Insulators are a new class of compounds having a well defined bandgap in the bulk separating the conduction band from the valence band and are characterized by conducting surface states which are immune to non-magnetic impurities. We present the electronic structure of Thallium based ternary chalcogenides $TlAB_2$ where A can be Bi, Sb and B can be S, Se, Te. All calculations are done using PAW pseudopotential and PBE exchange-correlation scheme with plane wave basis set implemented in VASP(Vienna Ab-initio Simulation Package) code. Before calculating properties structure was fully optimized including volume and ionic optimizations. A cut-off energy of 350 eV was used along with a k-mesh of 6 × 6 × 6 centred around gamma. This class of compounds belongs to 166 space group. For bulk calculations, with and without spin-orbit, rhombohedral structure was used and for surface calculations corresponding hexagonal structure was used. We shall present the results of the bulk and surface state calculations for these compounds and examine whether these are trivial or non-trivial topological insulators. We compare and constrast our findings with earlier theoretical computations [1,2] and recent experimental work [3-5] on this series of compounds.

REFRENCES

1. H. Lin, R. S. Markiewicz, L.A. Wray, L. Fu, M.Z. Hasan, A. Bansil Phys. Rev. Lett. 105, 036404(2010).
2. B. Yan, C.-X. Liu, H-J Zhang, C.-Y. Yam, X. L. Qi, T. Frauenheim and S.-C. Zhang EPL 90, 37002 (2010).
3. T. Sato, K. Segawa, H. Guo, K. Sugawara, S. Souma, T. Takahashi and Y. Ando arXiv:1006.2437v1.
4. Y. Chen, Z. Liu, J.G. Analytis, J.-H. Chu, H. Zhang, S.-K. Mo, R. G. Moore, D. Lu, I. Fisher, S. Zhang, Z. Hussain and Z.-X. Shen arXiv:1006.3843v1.
5. S.-Y. Xu, L.A. Wray, Y. Xia, R. Shankar, S. Jia, A. Fedorov, J.H. Dil, F. Meier, B. Slomski, J. Osterwalder, R. J. Cava and M. Z. Hasan, arXiv:1008.3557v1.

GROUND STATE PHASE DIAGRAM OF SPIN-1/2 FALICOV-KIMBALL MODEL ON THE TRIANGULAR LATTICE

Umesh K. Yadav, T. Maitra, Ishwar Singh

Department of Physics, I. I. T Roorkee, Roorkee – 247667, Uttarakhand, India
E-mail: umeshyadav02@gmail.com

Recently systems like transition-metal dichalcogenides, cobaltates, GdI_2 [1] and its doped variant $GdI_2H_{x,}$ have attracted considerable attention as they exhibit remarkable cooperative phenomena like valence and metal insulator transition, charge and magnetic order, excitonic instability etc. They belong to a class of systems where correlation and geometric frustration work in tandem. These systems are characterized by the presence of localized and itinerant electrons confined to the two-dimensional triangular lattice. It has been suggested recently that these correlated systems may very well be described by an effective Falicov-Kimball model (FKM) [1-4] on the triangular lattice. A careful study of the ground states of the spin dependent FKM on a non-bipartite lattice is both interesting and important as this could lead to an understanding of the broken symmetry ground states as well as phase segregations seen in the materials mentioned above. We have studied the spin dependent FKM as a function of Coulomb correlation (U), exchange correlation (J) between itinerant and localized electrons and Coulomb correlations between localized electrons (U_f) using a Monte-Carlo simulation technique, described in details in [3, 4]. Our results indicate various charge and spin ordering of the localized electrons in the ground state. A strong tendency towards the antiferromagnetic coupling between spins of localized electrons is observed close to the half filling. For small fillings the ferromagnetic coupling between localized electrons spin is observed. We have also studied variation of magnetic moments as a function of U, U_f and J.

REFERENCES

1. Taraphder, L. Craco, and M. Laad, Phys. Rev. Lett. 101, 36410 (2008).
2. L. M. Falicov and J. C. Kimball, Phys. Rev. Lett. 22, 997 (1969).
3. Umesh K Yadav, T. Maitra, Ishwar Singh and A. Taraphder, J. Phys.: Condens. Matter 22, 295602 (2010), Umesh K Yadav, T. Maitra and Ishwar Singh, Proc.,DAE- SSPS 54, 1065 (2009).
4. Umesh K Yadav, T. Maitra, Ishwar Singh and A. Taraphder (communicated to EPL).

THIN EPITAXIAL FILMS OF A PROMISING TOPOLOGICAL INSULATOR

Rajni Porwal[1], T. D. Senguttuvan[2], R. C. Budhani[1,2]

[1]*Department of Physics, Indian Institute of Technology Kanpur, Kanpur – 208016, India*
[2]*National Physical Laboratory, New Delhi 110012*

Heavy metal chalcogenides of the type Bi_2Se_3, Bi_2Te_3 and Sb_2Te_3 are well known thermoelectric materials routinely used for power generation and refrigeration in the temperature range of 300 to 600 K. The thermoelectric figure-of-merit (ZT) is defined as ZT = s2σT/KT where s, σ, T and KT are the Seeback coefficient, electrical conductivity, temperature in Kelvin and thermal conductivity, respectively. While the ZT of bulk alloys merit is realized in low dimensional forms such as thin films, superlattices, nanowires of these heavy metal chalcogenides.

The dimensionality has also been found to affect the 3D topological quantum state of these materials. In particular, it has been argued that due to the finite size effects, a gap may open-up in the energy spectrum of the electronic states near the surface in the low dimensional forms of these materials. It is expected that this gap will affect electronic and thermal transport profoundly.

Preparation of high quality thin films of Bi_2Se_3 family of compounds is quite non-trivial due to the volatility of the constituent elements. The other difficulty is the lack of a suitable dielectric substrate which can provide good lattice match to the rhombohedral cell if Bi_2Se_3 for epitaxial is barely above unity, it has been shown that a significant enhancement in the figure-of-growth. Recently, molecular beam epitaxy has been used to grow films of Bi_2Se_3 on 6H–SiC substrates. Angle resolved photoemission shows opening of a gap in the spectrum of surface states in thinner films. Here we present our preliminary results of the growth of highly oriented films of Bi_2Se_3 on (0001) sapphire using the techniques of pulsed laser ablation of a stoichiometric alloy target. Highly oriented c-axis growth is seen in films deposited in the temperature window of 300 to 400^{0}C. Detailed measurements of electronic transport in these films will be presented during the conference.

WARPING OF DIRAC CONE IN TOPOLOGICAL INSULATORS

Paritosh Karnatak, Ashutosh Sharma, R. Prasad

Department of Physics, Indian Institute of Technology Kanpur
Email: karnatak@iitk.ac.in

Topological Insulators possess exotic surface states that are governed by interesting physics and have been extensively studied recently.[1] The surface states are unique due to the presence of a single Dirac cone in the Brillouin zone. Recent ARPES measurements on Bi_2Se_3 show that the Dirac 'cone' is not ideal but distorts at higher energies.[2] This causes higher energy contours to distort from a hexagonal form to a star shape for increasing energies. To understand this phenomenon we propose a representative explanation for the distortion of these surface states due to the boundary and symmetry effects combined. We consider a simple two dimensional s-type tight binding model and show a similar warping of electronic states near the Brillouin zone boundaries by simple calculations. A first principles calculation will be presented, that theoretically demonstrates the warping of Dirac cone in Bi2Se3. Such a calculation may also be performed for other topological insulators to confirm by first principles that it is an effect due to boundary and symmetry effects combined, not limited to the particular structure or stoichiometry.

REFERENCES

1. M. Z. Hasan and C. L. Kane, 2010, arXiv: 1002.3895v1.
2. K. Kuroda, M. Arita, K. Miyamoto, M. Ye, J. Jiang, A. Kimura, E. E. Krasovskii, E. V. Chulkov, H. Iwasawa, T. Okuda, K. Shimada, Y. Ueda, H. Namatame, and M. Taniguchi, Phys. Rev. Lett. 105, 076802 (2010).

SEMICLASSICAL FORMALISM FOR THE DIRAC FERMIONS IN 2+1 DIMENSION

Moitri Maiti, R Shankar

The Institute of Mathematical Sciences, CIT Campus, Taramani, Chennai-600113, India
Email: moitri@imsc.res.in

We start with the single particle Dirac hamiltonian which has spin S and has mass Δ. We define the path integral involving the coherent states which are direct product of the usual coherent states [1] and the spin coherent states $|n(t)\rangle$ {[1] , [2]} spanning a spin S representation of the rotation group. The spin path integral involves sum over trajectories weighted by phases. The sum is given by the total area bounded by the trajectories parameterized by $|n(t)\rangle$ and are generally known as the Wess-Zumino terms. When $S >> \hbar$ then the system is said to be in classical regime. We take the appropriate limit by doing a systematic 1/S expansion [3] to find out the corresponding classical equations of motion followed by Bohr-Sommerfeld quantization of the closed orbits and find out the energy spectrum for the particle in the presence of different external fields. For free particle, the energy obtained from this formalism has an exact correspondence with its quantum mechanical counterpart.

REFERENCES

1. Field Theories of Condensed Matter Systems, E. Fradkin, Addison-Wesley (1991).
2. Coherent States, John R. Klauder and Bo-Sture Skagerstam, World Scientific (1985).
3. Interacting Electrons and Quantum Magnetism, Assa Auerbach, Springer Verlag (1994).

EFFECT OF ANNEALING ON LUMINESCENCE FROM DEFECT STATES IN ZnO NANOPARTICLES

Navendu Goswami, Anshuman Sahai

Department of Physics and Material Science and Engineering, Jaypee Institute of Information Technology, A-10, Sector-62, Noida-201307, India
Email: navendugoswami@gmail.com

The significant properties of condensed bulk material are often observed at low temperatures. Interestingly similar vital properties can be achieved at room temperature for nanomaterials. For example, the excitonic emission in various group II-VI semiconductor quantum dots can be observed at room temperature. The dominant reason behind such advantageous properties of nanostructured materials is the quantum size confinement. Surface states is yet another manifestation of quantum size confinement as these new energy states appear in the semiconductor nanoparticles due to anharmonic potential near the surface. In this paper we study the effect of annealing on the structural and optical properties of ZnO nanoparticles and more importantly the crucial role of defect states in the luminescence of pre- and post-annealed ZnO nanoparticles.

We synthesized ZnO nanoparticles by a chemical precipitation technique without using any capping agent. In this method, growth of nanoparticles is controlled by their pH concentration. The annealing of nanoparticles assists in removing the carbonate impurities and moisture so as to obtain pure ZnO nanocrystals. The wurtzite phase of ZnO particles remains unaffected by annealing. The size estimated by XRD, TEM and AFM are in agreement. Furthermore, shape and size-distribution of nanoparticles is also identical in TEM and AFM analysis. The formation of pure ZnO nanoparticles is also confirmed by metal-oxygen vibration reflected in the FTIR spectrum. The quantum size confinement in ZnO nanocrystals is evident through blue shift of band gap energy, as observed in the UV-visible spectrum [1]. The size confinement and surface effects of nanoparticles not only cause the increase in band gap but also influence the various optical transitions, such as luminescence.

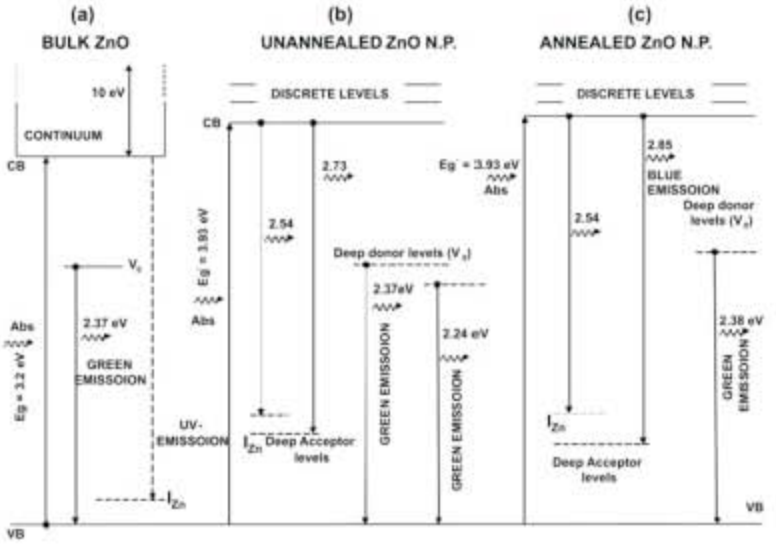

Figure 1: A schematic depiction of band structure, defect states and radiative transitions in (a) bulk ZnO, (b) unannealed ZnO Nanoparticles and (c) annealed ZnO nanoparticles.

In order to probe the origin of typically reported green photoemission (~521nm) in ZnO and to explore the possible effect of annealing on fluorescence of ZnO nanoparticles prepared by our synthesis method, we performed fluorescence spectroscopy. Among the various luminescence properties of ZnO nanoparticles, the green emission around 521nm is usually reported. Vanheusden *et al.* elucidated that oxygen vacancies are responsible for the green luminescence in ZnO [2]. However, Thareja *et al.* observed that luminescence due to defects, in particular, oxygen vacancy, is not observed in ZnO nanoclusters formed in vapor phase [3].

Our extensive fluorescence analysis, as depicted in figure 1, leads to remarkable conclusion that although crystal phase and other structural parameters of ZnO nanoparticles are not influenced by annealing process, fluorescence emissions are affected. This finding paves the way to the process of altering visible luminescence in ZnO nanoparticles without varying their size or shape [1].

REFERENCES

1. N Goswami, D. K. Sharma, *Physica E* **42**, 1675 (2010) and references therein.
2. K. Vanheusden, W. L. Warren, C. H. Seager, D. R. Tallant, J. A. Voigt , B. E. Gnade, *J. Appl. Phys.* **79**, 7983 (1996).
3. A. Mohanta, R. K. Thareja, *J. Appl. Phys.* **104**, 044906 (2008).

EFFECT OF SHELL THICKNESS ON TRANSITION FREQUENCY OF A CdSe/ZnSe CORE/SHELL QUANTUM DOT

SAIKAT CHATTOPADHYAY, PRATIMA SEN., JOSEPH T. ANDREWS, PRANAY K. SEN

Laser Bhawan, School of Physics, Devi Ahilya University, Indore – 452017, India
Department of Applied Physics, Shri G. S. Institute of Technology & Science, Indore-452003, India
Email: the_saikat@yahoo.com

Semiconductor quantum dots (QDs) have drawn significant attention in the last couple of decades as they are the basic elements for modern optoelectronic and spintronic nano-devices. In the semiconductor quantum dots, the electrons and holes are confined within the width of a semiconductor layer of lower energy gap which is encircled by another semiconductor of higher band gap. The confinement of carriers gives rise to novel optical and electronic properties. These nanostructures are popularly known as core–shell quantum dot (CSQD). Such systems are expected to show some improved fundamental properties which are different from a bare quantum dot due to the strong confinement effect in presence of outer most shell.

Present study aims to calculate the transition frequency for ground to exciton state (ω_{0e}) in a CdSe/ZnSe core/shell quantum dot (CSQD). The calculation shows that the transition frequency reduces as the shell thickness increases. This decrease in transition frequency indicates an expected red-shift in optical absorption spectra which is compatible with the experimental observations for different CSQD [1, 2]. To incorporate the core/shell interface effect WKB approximation method is taken into account to find out the exact wave function for the CSQD system [3, 4]. Exciton binding energy (Δ_X) is plotted here which shows an initial increase with increasing shell thickness. The binding energy (Δ_X) saturates after few monolayers of shell (Fig. 1). The red shift in transition frequency can be explained from the equation below.

$$\hbar\omega_{0e}(a,d) = \left[\varepsilon_g - |\Delta_X(a,d)|\right] \tag{1}$$

Here a, d and ε_g are core radius, shell thickness and binding energy respectively. Eq. (1) describes that, as the binding energy increases with shell thickness, the transition frequency reduces and shows red shift in absorption and PL spectra. Biexciton binding energy (Fig.2) confirms the existence of antibonding state in presence of ZnSe shell.

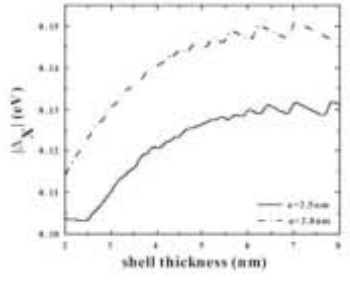

Fig. 1 Dependence of Exciton binding energy on increasing shell thickness in a CdSe/ZnSe CSQD

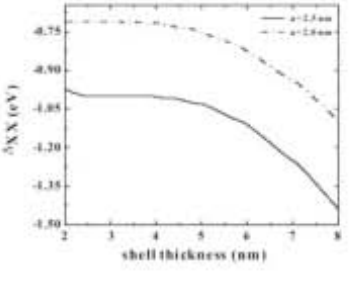

Fig. 2 Dependence of bi-exciton binding energy on increasing shell thickness in a CdSe/ZnSe CSQD

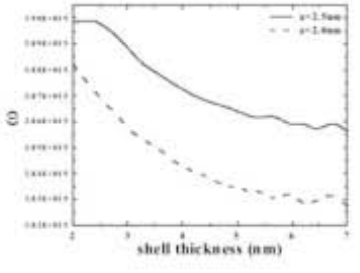

Fig. 3. Dependence of ground to exciton state transition frequency (ω_{0e}) with increasing shell thicknessin a CdSe/ZnSe CSQD

REFERENCES

1. M. Danek, K. F. Jensen, C. B Murray, M. G. Bawendi; Chem Mater **8** 173 – 180 (1996)
2. D. V. Talapin, I. Mekis, S. Gotzinger, A. Kornowski, O. Benson, H. Weller; J. Phys. Chem. B **108** 18826 – 18831 (2004)
3. P. Sen, S. Chattopadhyay, J. T. Andrews, P. K. Sen; J. Phys. Chem. Solids **71** 1201 – 1205 (2010)
4. A. Ghatak, S. Lokanathan, Quantum Mechanics Theory and Applications, 5th ed., Macmillan India Ltd., New Delhi, pp. 380-410 (2004)

QUANTUM SIZE EFFECTS OF Gd^{3+} IONS DOPED NiZn FERRITE

Balwinder Kaur[1], Manju Arora, A.K. Srivastava, R.P. Pant

[1]*G.G.M. Science College, Canal Road, Jammu (J&K) – 180001*
[2]*National Physical Laboratory, Dr. K.S. Krishnan Road, New Delhi – 110012*

Prepared Gd3+ ions substituted Ni0.5Zn0.5GdxFe2-xO4 (where x = 0.1, 0.2, 0.3) ferrites in the size range 15 – 25 nm by co-precipitation method. The effect of Gd3+ ions in spinel structure in correlation to magnetic properties has been studied in detail using XRD, HRTEM and EPR techniques. EPR spectra confirm the ferromagnetic behavior of nanoparticles due to higher order of dipolar interaction. On increasing Gd3+ ions concentrations the narrowing of resonance signal is observed which explains the increase in super exchange interaction among Gd3+ - O - Fe3+ in the core group and spin biasing in the glass layer. The decrease in 'g' value and increase in relaxation time is well correlated with particle size.

The doping of rare earth cations into the spinel structure of Nickel Zinc ferrite results in modification of basic electrical, magnetic and microstructural properties. In the present work, different concentrations of Gd3+ are substituted in the lattice of NiZn ferrite to understand the effect of Gd3+ concentration on structural and the magnetic properties. The Gd3+ substituted NiZn ferrite with composition Ni0.5Zn0.5GdxFe2-xO4 (where x = 0.1, 0.2, 0.3) were synthesized by chemical co-precipitation technique to easily control particle size, chemical homogeneity and degree of agglomeration. The prepared samples were characterized using XRD, HRTEM and EPR spectroscopy to establish the correlation between structural and magnetic properties.

Nanocrystalline samples of gadolinium substituted NiZn ferrite with composition Ni0.5Zn0.5GdxFe2-xO4 (where x = 0.1, 0.2, 0.3) were synthesized by co – precipitation technique. using AR grade Ni(NO3)2.6H2O, Zn(NO3)2.6H2O, Gd(NO3)3.5H2O and Fe(NO3)3.9H2O and annealed at 573K, 773K and 973K temperatures for two hours. The structural parameters are analyzed by using a Rigaku powder X – ray diffractometer 40 kV and 30 mA, using Cu kα (λ=1.54059 Å) radiation in the 2θ range from 200 to 700. High resolution transmission electron microscopy (HRTEM Model Tecnai GZ F30STWIN FEG was used for morphological investigations. X- band EPR Spectrometer Model: A300 Make: Bruker Biospin, Germany at ambient temperature was used for measuring EPR spectra of these particles.. DPPH was used a standard field marker.

X – ray diffraction patterns of as synthesized and annealed Ni0.5Zn0.5GdxFe2-xO4 (where x = 0.1, 0.2, 0.3) recorded at room temperature indicate the poor crystallinity and ultrafine nature. All the peaks match with the cubic spinel structure of nickel zinc ferrite (JCPD Card No. 008 – 0234). In annealed nanoparticles, the peak intensity increase with rise in annealing temperature due to the growth in crystallite size.. In finite size particles, a strain occurs due to the negative pressure. The X–ray density (Dx) and the induced lattice strain due to replacement are calculated.

HRTEM images showed that particles random in shape with normally a facetted morphology with sharp edges and vertices (Fig. 1(a), (b) & (c)). The average size distribution of the particles was about 15, 21 and 25 nm for Gd3+ 0.1, 0.2 and 0.3 concentration nanoparticles respectively.

A single strong EPR resonance signal of g-value ~ 2.00 of as prepared and annealed Gd3+ doped nickel zinc ferrite are presented in Fig. 2 and 3. These spectra were analyzed using Lorentzian distribution for evaluating peak-to-peak line width (ΔHpp), g – value, spin concentration (NS) and

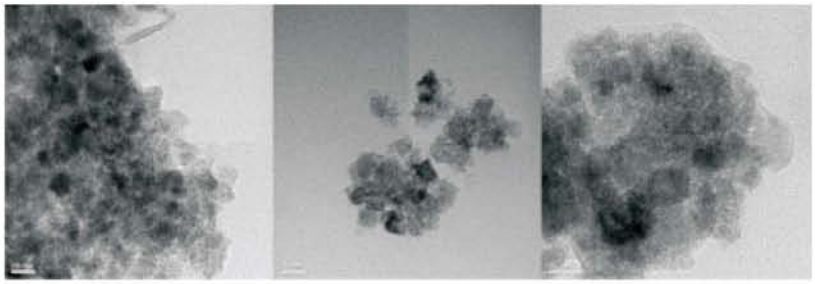

Fig. 1: HRTEM Gd (a) 0.1, (b) 0.2 & (c) 0.3

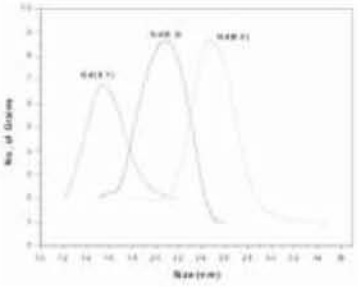

Fig. 2: Particle size distribution

relaxation time (T2) and listed in Table 1 for as prepared nanoparticles. In annealed samples the resonance line width, g-values and spins concentration decreases linearly with annealing temperature. The increase in line width of annealed sample is originating from the glassy behavior and surface anisotropy at higher temperatures.. The spin concentration in as prepared samples with increasing Gd3+ concentration and annealing temperature decreases due to increase in surface anisotropy and spin profile.

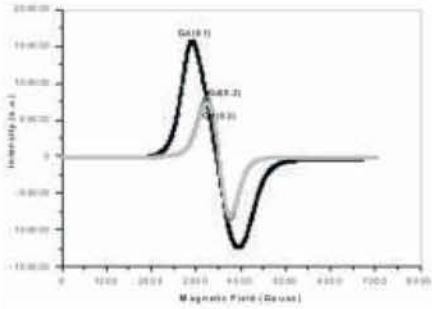

Fig. 2: EPR spectra of Gd doped NiZn ferrite nanoparticles

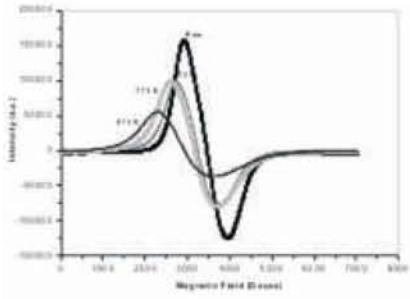

Fig. 3: EPR spectra of annealed analogues

Table 1 : Various parameters calculated from EPR spectra of as synthesized Gd3+ doped NiZn ferrite nanoparticles

Composition	g - value	ΔHpp	Spin Concentration (NS)	Relaxation Time (TS)
Gd(0.1)	2.04507	1050.3	2.17 x 1015	6.116 x 10-15
Gd(0.2)	2.00923	532.6	5.49 x 1014	1.228 x 10-14
Gd(0.3)	2.01635	511.4	4.81 x 1014	1.274 x 10-14

Structural parameters reveal the distortion in the spinel lattice structure induced by large ionic radii of Gd3+ ions and negative pressure at the octahedral Fe3+ ions site in ultrafine nanoparticles of Ni0.5Zn0.5GdxFe2-x04. The crystallite size and particle size data are well in agreement with each other. EPR spectra confirm the ferromagnetic behavior due to higher order of dipolar-dipolar interaction. On increasing Gd3+ ions concentrations the narrowing of signal explains the increase in super exchange interaction i.e. movement of electron among Gd3+-0- Fe3+ in the core group and the spin biasing in the glass layer.

CURRENT CARRIED BY MAGNONS IN COUPLED FERROMAGNETIC QUANTUM DOTS

A. PRATAP

Laser Science and Technology Center, Metcalfe House, Delhi- 110 054, India
Email: amit_drdo@rediffmail.com

We evaluate the magnon transport through magnetic double quantum dots. We consider the two coupled ferromagnetic dots connected to the ferromagnetic reservoirs as shown in Fig1. For these dots, the magnon energy becomes quantized and Hamiltonian may be written as

$$H = \sum_{\xi\lambda} (\varepsilon_{\xi\lambda} + g\mu_B B_\lambda)\, a^\dagger_{\xi\lambda} a_{\xi\lambda} + H_{con} + \sum_{k,n} T_{kL,n} a^\dagger_{kL} \alpha_n + \sum_{k,m} T_{kR,m} a^\dagger_{kR} \beta_m + h.c.$$

with $H_{con} = \sum_n \varepsilon^A_n \alpha^\dagger_n \alpha_n + \sum_m \varepsilon^B_m \beta^\dagger_m \beta_m + \sum_{nm} \varepsilon^{AB}_{nm} \alpha^\dagger_n \beta_m + h.c.$

Applying the non-equilibrium Green's function technique, we obtain the expressions for the magnon mode dispersion, magnon density of states and the current carried by the magnons. In particular, we study the effect of interdot coupling on these properties. As shown in Fig 2, in the presence of the interdot coupling, the magnon mode dispersion shows a splitting and the gap between the modes increases on increasing the strength of interdot coupling. The current carried by the magnons is also significantly affected and shows a nonmonotonic behavior on increasing the interdot coupling. The numerical results show that the coupled dot system acts as resonant tunnel diode and may serve as crucial component for future spintronic applications.

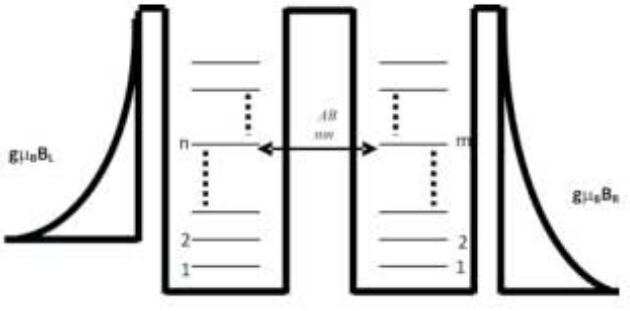

Fig 1

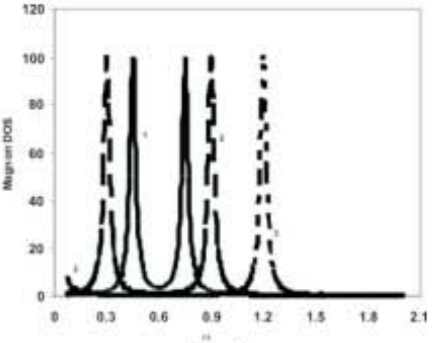

Fig 1

STRUCTURAL AND MAGNETIC INVESTIGATIONS ON QUANTUM SIZE EFFECT OF COBALT FERRITE

SANDEEP KUMAR[1], MAHESH CHAND, M. S. YADAV[2], R. P. PANT[1*]

[1]*National Physical Laboratory, New Delhi-110012, India*
[2]*Kurukshetra University, Haryana, India*

Cobalt ferrite ($CoFe_2O_4$) nanomagnetic particles have synthesized at different reaction temperatures (20°, 40°, 60°, and 80°C) by controlling the temperature of Co^{2+} and Fe^{3+} ions by co-precipitation process. The effect of co-precipitation temperature on structural and magnetic properties have been studied. The reaction temperature affects the particle size of Cobalt ferrite which varies in the range of 5-34 nm. Further, varying the co-precipitation temperature has a direct effect on magnetic parameters (H_c and σ_s), EPR parameters (ΔH_{PP} and T_2). A maximum coercivity of 804.58 Oe and a maximum saturation mass magnetization of 51.37emu/g are obtained for the sample synthesized at 80°C.

The particles synthesized at low temperature (20°C) exhibit large relaxation time ($5.77*10^{-11}$ sec) as compared to particles synthesized at 80°C ($0.88*10^{-11}$ sec). This is due to increase in dipole-dipole interaction with increase particle size.

The synthesis parameters have been optimized for developing suitable ferrofluids for microwave absorption applications in the frequency range 9 to 18 GHz. These materials have applications in recent technological developments (1-3) The material ($CoFe_2O_4$) have been synthesized by taking 1M aqueous solution of high purity salts of $Co(NO_3)_2.6H_2O$ (99%purity) & $Fe(NO_3)_3.9H_2O$ (98%purity). Their homogeneous solutions are well mixed in 1:2 ratio and are homogenized at four temperatures 20°C (sample 'a'), 40°C (sample 'b'), 60°C (sample 'c'), 80°C (sample'd').

The superparamagnetism of the sample is attributed to the size of equiaxial shaped nanoparticles below the SP critical size. According to our experimental results, the critical size is about 5 nm determined by HRTEM, as shown in Table 1. The coercivity increases with increasing average particle size and reaches a maximum value of 804.58 Oe for the sample synthesized at 80°C. The variation of the coercivity with particle size are shown in inset of Fig. 3.The saturation magnetization of as-synthesized samples seems to increase with increasing reaction temperature (Table 1), which also reveals that the average particle size increases. It has been shown that the saturation magnetizations of the samples are significantly lower (51.37 emu/g) than the bulk value of 73 emu/g. This behaviour may be attributed to the surface effects that are aroused by the distortion of the magnetic moments at the nanocrystallite surface. This is due to time gap for the Co^{2+} and Fe^{3+} sole formation in the growth of particle.

Table 1

Precipitation temperature	D (nm)	Average Particle size (nm)	Lattice constant	Strain induced	σ_s(emu/g)	Hc (Or)	(Mr/Ms)
20°C	3	5	8.4600	0.0082	9.88	0.29	0.00009
40°C	6.5	14	8.4322	0.0045	21.05	202.83	0.0898
60°C	8	23	8.4076	0.0015	40.24	435.03	0.2240
80°C	15	34	8.3900	0.0004	51.37	804.58	0.2900

Precipitation temp (°C)	Particle size (nm)	Line width ΔH_{PP} (G)	*g*-factor time (sec) T_2 (*10^{-11})	Relaxation (spins/g)	N_s*10^{22}
20°C	5	1068.5	2.1280	5.77	1.24
40°C	14	1176.6	2.3523	4.74	1.25
60°C	23	4284.2	2.7072	1.13	3.19
80^0C	34	4390.9	3.3874	0.88	3.89

It is distinct that the changes of coercivity and remanence ratio are correlated with the variation of particle size that depends on the reaction temperature. The EPR parameters (ΔH_{PP}, g-factor, NS, and T2) obtained from fig. 3 are given in Table 2. The EPR parameters (i.e., ΔH_{PP}, g-factor, and NS) of the samples increase with increasing reaction temperature (Table 2). These results are due to increase in particle size of Co-ferrite with increasing reaction temperature. This could make the dipole-dipole interactions increase, and then ΔH_{PP}, g-factor increase. The spin-spin relaxation process is the energy difference (ΔE) transferred to neighbouring electrons and the relaxation time (T_2) can be determined from the peak-to-peak linewidth according to:

$$1/T_2 = g\mu_B \Delta H_{1/2} / h, \Delta H_{1/2} = \sqrt{3}\Delta H_{PP} \qquad (2)$$

Where μ_B is the Bohr magneton (9.274*10^{-21} erg /G), $\Delta H_{1/2}$ the linewidth (in Gauss) at half height of the absorption peak, and h is a constant (1.054*10^{-27} erg s) [20].

The spin-spin relaxation time is calculated by equation (2) and shown in table 2. The spin-spin relaxation time T_2 decreases with increasing reaction temperature, indicating that the spin relaxation at high reaction temperature exhibit a fast relaxation and a slow relaxation at low reaction temperature. The calculated spin concentrations of different samples also shown above table .The spin concentration increasing with increases reaction temperature.

PHOTOELECTRIC PROCESS IN Si SEMICONDUCTOR QUANTUM DOT NANOSTRUCTURE

ANCHALA, S.P.PUROHIT, K.C.MATHUR

Department of Physics and Material Science and Engineering
Jaypee Institute of Information Technology
A–10, Sector – 62, Noida, U.P. 201307, India
Email: sppurohitjiit@gmail.com

Silicon is the most abundant and widely used material in semiconductor electronics, optoelectronics and photovoltaics. Advances in experimental techniques have made it possible to fabricate silicon quantum dot nanostructures of different sizes. Recent experimental and theoretical studies on quantum confined effects in silicon nanostructures have been reported by Pavesi [1] and Saar [2].

In this study we investigate the intraband optical transitions in Si nanostructure embedded in SiO2 matrix. We focus on the study of the photoelectric process in spherical Si quantum dot nanostructure for its possible applications in photovoltaics. The process is studied by using effective mass approximation (EMA) [3] and considering singly charged quantum dots.

REFERENCES

1. L.Pavesi, J. Phys.: Condens. Matter 15 (2003) R1169; Adv. Opt. Tech. Volume 2008, (2008) Article ID 416926.
2. A.Saar, J. Nanophotonics, 3, (2009) 032501.
3. S.P.Purohit and K.C.Mathur, J. Computational and Theoretical Nanoscience, 7, (2010), p.1131.

THERMAL PROPERTIES OF ELECTRODEPOSITED BISMUTH TELLURIDE NANOWIRES

Lalat Indu Giri[1], Pramod Kumar Sharma[1], Andleeb Zahra[1], Anwesha Bose[2], Manish Sharma[1]

[1]*Center for Applied Research in Electronics, Indian Institute of Technology Delhi, New Delhi*
[2]*Electronics and Communication Engineering, Delhi Technological University, New Delhi*
Email: manish@care.iitd.ac.in

Bismuth Telluride has always proved itself to be the front runner as a thermoelectric material, all in bulk, thin film and nanostructures forms [1]. For this material, its being widely reported that the thermoelectric dimensionless figure of merit $ZT = S^2\sigma/k$ improves as we move on to the nanostructures, where S is Seebeck coefficient, σ is electrical conductivity, k is thermal conductivity [2,3]. For investigating this fact we prepared AAO template assisted Bismuth Telluride nanowires using electrodeposition method [4,5]. The HRTEM, SEM images showed the presence of nanowires having typical diameter of 130-140nm and the length of the order of 447.86nm. XRD data showed a sharp peak at 37.85° which is very close to the Bi_2Te_3 nanowires. EDX result also supports the existence Bi_2Te_3 nanowires. For realizing a practical solid state thermoelectric device, we also attempted preparing n and p-type nanowires clusters.

A novel approach to establish the enhance ZT value in nanostructures is proposed using the IR thermography technique. Here we use an active thermography using a heating source and measurement of the temperature response. The time constant information of the time temperature curve gives us the thermal conductivity and thermal diffusivity value.

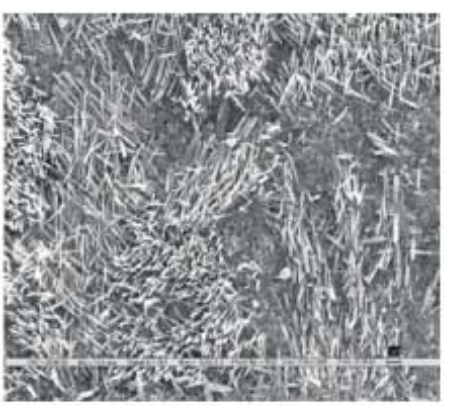

Figure 3: SEM image of Bi_2Te_3 nanowires

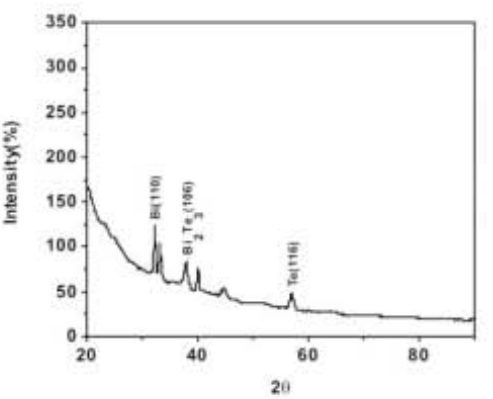

Figure 2: X-ray diffraction pattern

REFERENCES

1. G. S. Nolas et. al. Materials Science, Thermoelectrics: Basic Principles and New Materials Development, Springer Verlag, New York,2001.
2. T. M. Tritt, Science 283, 804 (1999).
3. F. J. DiSalvo, Science 285, 703 (1999).
4. C. R. Martin, Chem. Mater. 1996, 8, 1739.
5. A. Huczko, Appl. Phys. A 2000, 70,365.

DIELECTRIC PROPERTIES OF THE $Ba_{0.5}Sr_{0.5}TiO_3$ / POLY (VINYLIDENE FLUPRIDE) COMPOSITE FILMS

Annapu Reddy.V[1,2, A], Arvind Nautiyal[1], N. P. Pathak[2], R. Nath[1, B]

[1] *Ferroelectric Material and Devices Research Laboratory, Department of Physics, Indian Institute of Technology, Roorkee, India*

[2] *Radio Frequency Integrated Circuits Research Laboratory, Department of Electronics & Computer Engineering, Indian Institute of Technology Roorkee, India.*

Email: [a]venki0001@gmail.com, [b]rnathfph@iitr.ernet.in

Films polymer based material of high dielectric constant and low dissipation factor was prepared by dispersing nanometer size BST particles into PVDF. The homogeneous dispersion of the BST particles in the PVDF has been observed in the composite films. The relative dielectric constant and dissipation factor of the prepared composite films have been measured as a function of temperature by keeping volume ratio fixed. The temperature was varied from 25 ^{0}C-185 ^{0}C at an interval of 2 ^{0}C. The measurement was performed at two different frequencies viz. 100 Hz and 1 kHz. The effect of variation in volume ratio on dielectric properties ware also studied. The dielectric constant of the composite films increases with increase in volume ratio of BST and varies slightly with temperature. The temperature dependence of dielectric constant shows the broad peak in the temperature range 120 ^{0}C - 125 ^{0}C, which is due to the crystallization of the PVDF in the composite films. The highest dielectric constant of 145 and dissipation factor of 0.15 at 100 Hz was obtained for 75 wt % of BST/PVDF composite. Among the dielectric mixing models presented, the modified Lichtenecker model shows the best fit up to 20 % volume fraction, while effective medium theory shows the best fit up to 50 % volume fraction of BST.

FERROMAGNETIC SPIN WAVE RESONANCE IN FULL HEUSLER ALLOY Co_2MnSi

HIMANSHU PANDEY[1,2], P. C. JOSHI[1,2], R. PRASAD[2], R. P. PANT[3], R. C. BUDHANI[1,2,3]

[1]*Condensed Matter-Low Dimensional Systems Laboratory, Department of Physics, Indian Institute of Technology Kanpur, Kanpur – 208016, India*
[2] *Department of Physics, Indian Institute of Technology, Kanpur-208016, India*
[3]*National Physical Laboratory, Dr. K.S. Krishnan Marg, New Delhi – 110012, India*
Email: hp23@iitk.ac.in

Heusler alloys are promising materials for spintronics applications due to their high magnetic ordering temperature and a theoretically predicted half metallic character which makes the conduction band 100% spin polarized. However, in reality it has been difficult to realize full spin polarization due to the factors like atomic disorder, non-stoichiometry, oxidation of constituents and partial crystallization. These problems are acute in thin films and therefore important to study as all spintronics devices will be made using films. We report thin films of full Heusler alloy Co_2MnSi with the $L2_1$ structure on MgO (100) substrate deposited by pulsed laser ablation technique. Our films are deposited at 200°C followed by annealing at different temperatures. By changing the annealing temperature, we observe various degrees of ordering, which results in change of magnetization, spin polarization and other transport properties. Fully epitaxial $L2_1$ ordered films are obtained on annealing at 600°C. The θ-2θ X-ray diffraction combined with □-scan for both (220) and (111) planes show that the epitaxial growth of $L2_1$ ordering is oriented 45° with respect to the substrate. Finally, in the out-of-plane ferromagnetic resonance (FMR) measurements, we observed surface standing modes, which allow evaluation of exchange stiffness constant. We found good agreement between our values to the theoretically calculated one.

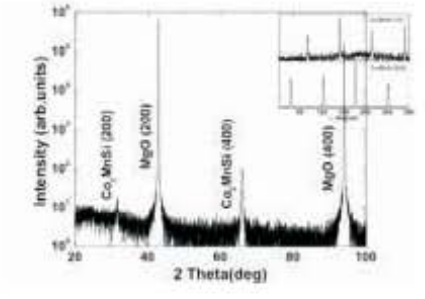

Fig. 1 θ-2θ X-ray diffraction pattern of a (h00) oriented Co_2MnSi (70 nm) film grown on (100) MgO substrate at 200°C and then annealed at 600°C. The inset shows □-scans around (220) and (111) planes of film.

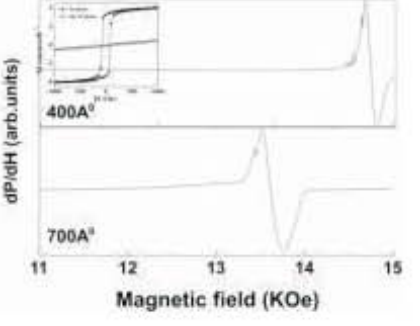

Fig. 2 FMR spectra of thin films of Co_2MnSi annealed at (600°C) for a static magnetic field applied perpendicular to the film plane. The inset is showing in-plane and out-of-plane hysteresis loop at room temperature

SURFACE ANALYSIS OF Ag-ION DOPED NANOSTRUCTURES OF $Cd_{1-x}Zn_xS$ ALLOY BY X-RAY PHOTOELECTRON SPECTROSCOPY

Ruchi Sethi[1], Mahesh Kumar[2], Lokendra Kumar[1]

[1]*Department of Physics , University of Allahabad, Allahabad- 211 002, India*
[2]*National Physical Laboratory, Dr K. S. Krishnan Road, New Delhi 110 012, India Email:*
Email : lkumarau@gmail.com, sethi.ruchi02@gmail.com

We demonstrate the synthesis of Ag-ion doped CdZnS nanostructures by chemical routes for their surface and structural analysis. For this purpose, X-ray photoelectron spectroscopy (XPS), Fourier transform infrared spectroscopy (FTIR), Transmission electron microscopy (TEM), Scanning electron microscopy (SEM) and X-ray diffraction (XRD) were performed. X-ray diffraction analysis reveals that the nanorods were hexagonal while for the quantum dots (QDs) this confirms the cubic structure. XPS was performed to investigate the surface composition and the chemical state of atoms presented. XPS measurement indicated the presence of Cd, Zn, S, C and O elements near the sample surface and no extra impurity phase was detected in the survey scan. Sputtering with Ar^+ ion flow under high vacuum for 10 minutes was also performed to clean the surface contamination and to measure the depth profile of the material under investigation. Furthermore, we have compared the chemical state and the binding energy shift of the elements of these two nanostructures by XPS measurement. Doping of the Ag-ion significantly shift the binding energy of the Zn2p and Cd3d states, which can be explained on the basis on the change in the electro-negativity of the substituent atoms in the alloy. Composition of the element by XPS was measured by measuring the peak area of the individual element and this value is well matched with Energy dispersive X-ray (EDAX) results. Photoluminescence (PL) and absorption measurements were also employed for their optical properties.

Keywords: Alloy, Nanostructures, Photoluminescence, X-ray photoelectron spectroscopy.

THERMOELECTRIC PROPERTIES OF LAYERED-ANTIFERROMAGNET $CuCrS_2$

Girish Chandra Tewari, T. S. Tripathi, A. K. Rastogi

School of Physical Sciences, Jawaharlal Nehru University, New Delhi -110067, India
Email: gctewari2002@gmail.com

We have performed a detailed study of the electrical and thermal conductivities and thermoelectric power behavior of an antiferromagnetic layer compound of chromium, $CuCrS_2$, from 15K to 300K. Unlike previous studies, we find non-insulating properties and a sensitive dependence on the preparation methods, the microstructure and the flaky texture formed in polycrystalline samples after extended sintering at high temperatures. Flakes are found to be metallic with strong localization effects in the conductivity on cooling to low temperatures. The antiferromagnetic transition temperature T_N (=40K) remains essentially unaffected. The Seebeck coefficient is found to be in the range 150-450 μV/K, which is exceptionally large and becomes temperature independent at high temperatures, even for the specimen with a low resistivity value of 5-200 mΩ-cm. We find the thermal conductivity κ to be low, viz. 5-30mW/K-cm. This can be attributed mostly to the dominance of lattice conduction over the electronic. The value of κ is further reduced by the disorder in Cu-occupancy in the quenched phase. We also observe an unusually strong dip in κ at T_N which is probably due to strong magnetocrystalline coupling in these compounds. Finally we discuss the properties of $CuCrS_2$ as a heavily doped Kondo-like insulator in its paramagnetic phase. The combination of the electronic properties observed in $CuCrS_2$ makes it a potential candidate for various thermoelectric applications.

REFERENCES

1. Bongers P.F.; Van Bruggen C. F.; Koopstra J.; Omloo W. P. F. A. M.; Wiegers G. A. and Jellinek F.: J. Phys. Chem. Solids, 29, (1968), 977.
2. Engelsman F. M. R.; Wiegers G. A.; Jellinek F. and Van Laar B.: J. Sol. Stat. Chem, 6, (1973), 574.
3. Le Nagard N.; Collin G. and Gorochov O.: Mat. Res. Bull. 14, (1979), 1411.
4. Tewari Girish C.; Tripathi T. S. and Rastogi A. K.: J. Electronic Mat. 39, Issue-8, (2010), 1133.

INVESTIGATIONS OF SURFACE MORPHOLOGY AND OPTICAL PROPERTIES OF PULSED LASER DEPOSITED (PLD) ZnO FILMS ON STO AND YSZ SUBSTRATES AT DIFFERENT OXYGEN PRESSURE

JAI SINGH, P. K. SRIVASTAVA, R.S.TIWARI, O.N. SRIVASTAVA

Physics Department, Banaras Hindu University, Varanasi 221005, India
Email: jai.bhu@gmail.com

ZnO thin films (TF) and nanostructures (NS) have been intensively investigated due to large direct band gap (~3.37 eV) and free-exciton binding energy (~60 meV), which makes them potentially applicable in electronics, optoelectronics and photonics [1-2]. Properties of ZnO are extremely sensitive to the crystallinity, crystallographic orientation and morphology and hence control over these properties through synthesis is of great interest. ZnO TF and NS are synthesized by various methods such chemical vapor deposition (CVD), metal organic chemical vapor deposition (MOCVD), pulsed laser deposition (PLD) and so on. PLD has advantages over other techniques due to the easy control on the synthesis with good optical and electronic properties [1-2]. Most of the ZnO (TF & NS) have been grown on hexagonal substrates however perovskite substrates which possess various interesting properties such as superconductivity, ferroelectricity and ferromagnetism, can be the most suitable to constitute an active component to define new functionalities.

Thin films of ZnO are deposited by PLD on single crystal $SrTiO_3$ (STO, 001) and Yb stabilized ZrO_2 (YSZ, 001) substrates at ~ 600 °C under varying O_2pressure of ~ 50, 100 and 200 mTorrs. These as deposited ZnO thin films are subjected to structural, microstructural and optical characterization by employing X-ray diffraction (XRD), scanning electron microscopy (SEM) and PL-UV spectroscopy, respectively. XRD reveals that the films are preferentially c-axis i.e. (002) oriented having hexagonal wurtzite structure. The film quality increases with increase in O_2 pressure as evident by enhanced (002) peak intensity at higher O_2 pressure (~ 200 mTorr) on both substrates. SEM investigation results that the density and morphology of film improves at higher O_2 pressure because of increased particle size. PL measurements indicate that all the thin films show intense near band-edge emissions around ~ 380 nm without the presence of any deep level emission at higher wavelength. All the UV

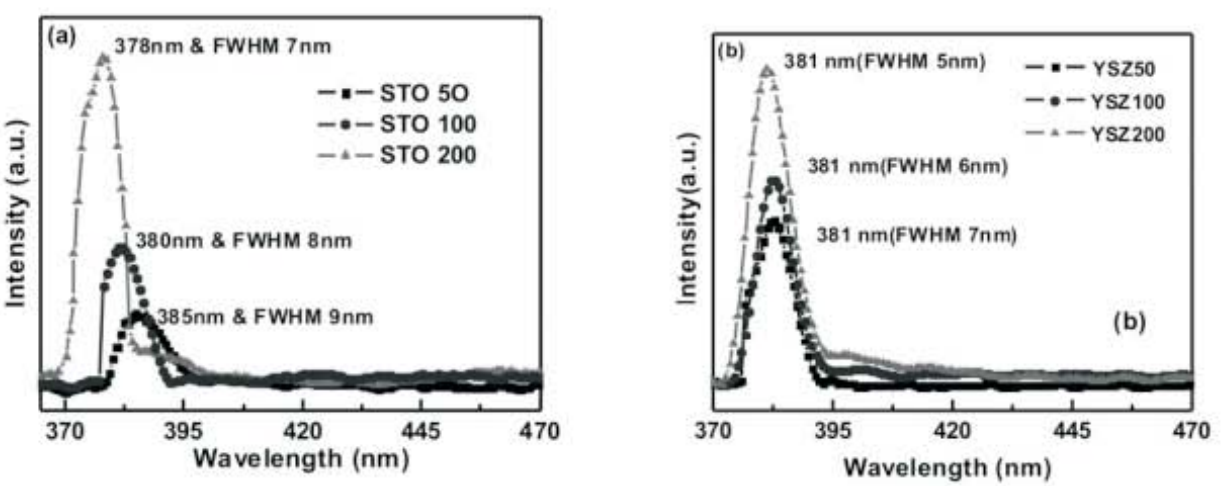

Fig: Room temperature photoluminescence (PL) spectra of ZnO thin films deposited on (a) STO and (b) YSZ substrate by PLD with different oxygen pressure.

peaks on YSZ substrate are located close to ~ 380 nm whereas on STO substrates the UV peaks shifts towards lower wavelength as O_2 pressure increases from 50 mTorr to 200 mTorr (Fig a & b). The optical band gap on YSZ was found to be ~3.28 eV whereas on STO it varies in the range of ~3.28 to 3.30 eV with increasing O_2 pressure. The variation in band gap on STO has been attributed to the compressive strain on ZnO films due to lattice mismatch between ZnO and STO. The improved optical properties at higher O_2 pressure and on different substrate have been discussed in relation to the microstructural variation because of O_2 incorporation and lattice strain arising due to lattice mismatch of substrate (STO &YSZ) with ZnO.

REFERENCES

1. S Singh et al. Structure, Microstructure and Physical Properties of ZnO Based Materials in Various Forms: Bulk, Thin Film and Nano. J. Phys. D: Appl. Phys. 40 6312 (2007).
2. C Jagdish, S Pearton, Zinc Oxide Bulk, Thin Films and Nano Structures Processing, Properties and Applications Elsevier Oxford IX51GB UK (2006).

QUANTUM MECHANICAL ELECTRON TRANSFER THROUGH A METAL ADLAYER

A.V.B. Cruz, A. K. Mishra

Institute of Mathematical Sciences, CIT Campus, Chennai 600113, India

A proper understanding of electron transfer reaction through an adsorbate intermediate constitutes the first step towards modelling the charge transfer across a chemically modified electrode, through a molecular wire, or the phenomenon of the molecular electronics. In fact the indirect heterogeneous electron transfer is a recurring feature in all these processes. In the present communication, the kinetics of an adsorbate mediated electron transfer reaction is considered. The formalism is developed to calculate the current-potential profile corresponding to an arbitrary coverage of the adsorbate, distributed randomally on the electrode surface. The case of weak and strong electrode-adsorbate interaction is modelled in a unified manner. The analysis shows that the current characteristics exhibits Marcus inverted region behaviour, observed in the homogeneous electron transfer reaction, at low coverage, and the traditional direct heterogeneous electron transfer behaviour at high coverage. The localized nature of the adsorbate orbital when the coverage is low, and its getting delocalized due to the metallization of the adlayer in the high coverage regime is the reason behind this behaviour.

GROWTH AND CHARACTERIZATION OF PbTe BULK COMPOUND AND ITS NANOSTRUCTURED THIN FILMS DEPOSITED BY THERMAL EVAPORATION TECHNIQUE

Rajeev Kumar, Sukhvir Singh

Electron and Ion Microscopy, National Physical Laboratory, New delhi-110012
Email: rajphyrk3@gmail.com

PbTe thin films were deposited on KBr and glass substrates using thermal evaporation technique under high vacuum conditions. PbTe bulk compound grown by vertical directional solidification technique was used as the source material to deposited thin films. Thin films were deposited at room temperature, 100°C, 200°C, in the thickness range 100 to 150nm. Powder x-ray diffraction technique was employed to identify the phase of the as grown bulk PbTe compound as well as thin films. Surface morphology and the stoichiometry of the bulk compound and thin films were carried out by using scanning electron microscope (SEM) with attachment of energy dispersive spectrometer (EDS). Micro structural features associated with the as deposited PbTe thin films were studied by using transmission electron microscope (TEM) and HRTEM. In the present study the microstructural details associated with thin films deposited at different temperatures have been analyzed. The prepared PbTe were further characterized by using X-ray photoelectron spectroscopy.

Numerous materials have been investigated for solar cell applications [1]. This lead to the development of new and innovative classes of semiconductor devices: Crystalline silicon, amorphous silicon and thin film polycrystalline materials like cadmium telluride (CdTe), Cadmium zinc Telluride (CZT), Zinc Telluride (ZnTe), etc. are prominent materials. The development of thin film solar cells is an active area of research at this time. Among the II-VI compounds, CdTe is one of the suitable candidates for the production of thin films solar cells due to its ideal band gap, high absorption coefficient and ease of thin film fabrication. Thin film CdTe provides a cost effective solar cell design. CdTe is a very important material for low cost large area photovoltaic solar cells technology, and is of great interest for flexible thin solar cells for integration in building and portable electronics. The choice of the material for solar cells depends upon the potential conversion efficiency expected from the devices made from them. CdTe is found to be promising material [2] for the high efficiency solar cells. CdTe has the flexibility to be deposited by a number of deposition techniques such as screen printing (3), electrodeposition (4,5) etc. Thermal Evaporation technique has been the most productive method owing to the very high deposition rate, low material consumption and low cost of operation. Enormous amount of work has already been reported on structure, optical and electrical properties of CdTe thin films (6,7,8). However it still requires further investigations to optimize structural, optical and electrical parameters.

In the present study, CdTe bulk compound has been grown by vertical directional solidification (VDS) technique. A small piece of CdTe compound taken from the VDS grown bulk compound has been used as the source material to deposit thin films at different depositions conditions using thermal evaporation technique. An effort has been made to study the microstructural details of the thin films deposited at various conditions to correlate the same optical parameters. Thin films we make by thermal evaporation method. The deposition condition will be varied and their effect is to be investigation on the physical property such as macrostructure and optical properties viz transmission and reflection of the transparent material. The thin film will be deposited on different substrates

like as KBr, glass; KCl etc. at different substrate temperature in presence of high vaccum .The thickness of thin film will be nano order. We also make binary and tertiary bulk compound by VDS technique different- different concentration by Vegards law .The effect of various dopants will be investigate on properties of the material. The photolumincence spectra will also be studies. The energy band gap will be determined from transmission spectra of the proposed samples. The" n "and "k" will be determined the complex dielectric constant e=n-k of the material, which is necessary to hone the material for solar applications. The resistivity and conductivity and optical properties will be calculated by deferent method.

The development of newer type of material and better processes for semiconducting and other film is needed by various industries. The cope up the demand of industries basic research in material science is continuously ongoing process. In future plane we also study the nanocomposite films CdTe quantum dots and glucose oxidase used as biosensor [9].

REFRENCES

1. Kestner, J. M.; McElvain, S.; Kelly, S.; Ohno, T.R.; Woods, L. M.;Wolden, C. A. Sol. Energy Mater. Sol. Cells 2004, 83, 55.
2. S.Lalita, R.Sathyamoorthy, Sethilarasu, A.Subbarayan, K.Natarajan "Solar Energy Material & Solar Cells", 82(2004)187-199
3. H.Uda, H. Matumoto, Y. Komatsu A. Nakano, S. Ikegami, Proceedings of the 16th Photovolta specilists conference, San Diego, CA 1982, IEEE New York, 1982 p801
4. Bulent M. Basol, Vijay K Kapoor, Michael L. Ferris J. Appl. Phys. 66 (4) (1989) 15
5. A.E. Rakhshani, J. Appl. Phys. 12(1997) 81
6. N. EL-Kadry, A Ashour, S.A. Mahmoud, Thin Solid films 269 (1995) 112
7. Joel, Pantoja Enrquez, Xavier Mathew, J. Crystal growth 259 (2003) 215-222
8. Xavier Mathew, Solar Energy Mater. Sol. Cells 76 (2003) 225 242
9. Chan, W. C.; Mexwell, D. J.: Gao, X.; Bailey, R. E. Han, M. Nie, S. Curr. Opin. Biotechnol. 2002, 13, 40-46.

EPR INVESTIGATIONS ON CNT-FERROFLUID BASED COMPOSITES

ANNVEER[1,2], SHYAMA RATH[2], MANJU ARORA[1], CHHOTEY LAL[1], R P PANT[1]

[1] *National Physical Laboratory, CSIR, Dr. K.S. Krishnan Road, New Delhi-110012, India*
[2] *Department of Physics & Astrophysics, University of Delhi, Delhi-110007, India*
Email: annveer87@gmail.com

CNTs: ferrofluid based composites have been prepared and investigated for structural and magnetic properties. Such types of composites have unique properties which have not been observed in their bulk state. The CNTs have drawn considerable attention as a promising candidate for versatile applications due to their unique optical, electrical, magnetic, and mechanical properties [1-2]. The Fe_3O_4-CNTs composites have potential applications in the field of magnetic data storage [3-4]. The present work is mainly focused on the synthesis of CNT: Ferrofluid composites and their investigations by EPR and powder X-ray diffraction techniques.

The composites were prepared in two steps i) the preparation of CNT's by CVD technique and then (ii) then three sets of composites were prepared by using different volume % (sample (a) 10%, (b) 20 % and (c) 30%) of CNT's are mixed in the in-situ formation of ferrofluid. To obtain good blend of CNTs, in the composites the samples were annealed at 700 °C in an inert atmosphere, also to see if any change in Fe_3O_4 phase transition and confinement of CNTs.

The X-ray diffraction patterns of three sets of composites are shown in Fig. (1). the characteristic diffraction peaks (220), (311), (400), (422), (511), and (440) are corresponding to cubic Fe_3O_4 phase (JCPDS Card No-019-0629) and peaks (012), (104), (110), (113), (024), (116), (214), and (300) are corresponding to hexagonal Fe_2O_3 phase (JCPDS Card No-080-2377). A comparative study confirms that both Fe_2O_3 and Fe_3O_4 phases are present only in (b), while Fe_3O_4 is the dominant phase in composite (c). With increasing weight fraction of CNTs, the peak intensity of (104) reflection is decreased and for the peak (311) increases. It means that CNTs are playing a role in the protection of Fe_3O_4 from being reduced to Fe_2O_3 phase and thus brings the stability to the Fe_3O_4

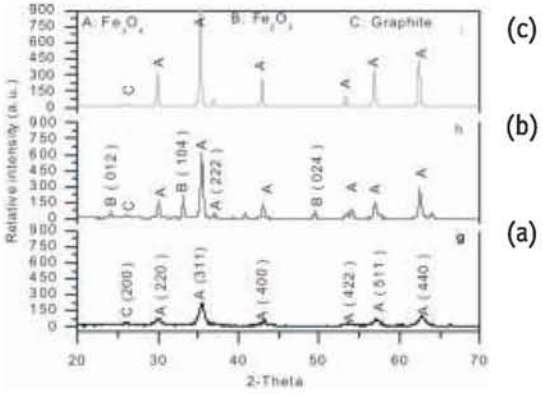

Fig.1: XRD patterns of composite (a), (b) and (c)

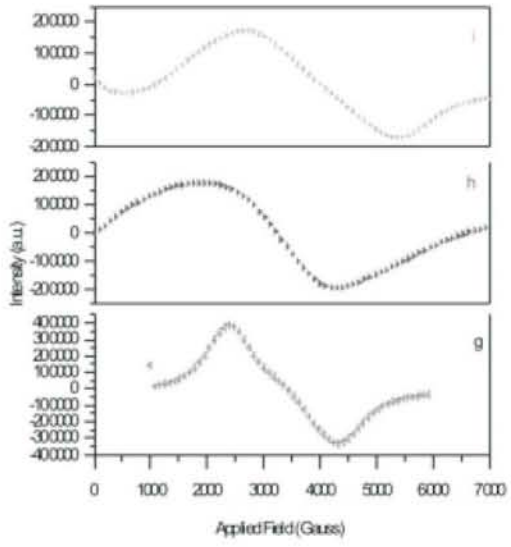

Fig.2: EPR spectra of composite (a), (b) and (c)

Table 1: EPR parameters of composites

S.No.	Material prepared	ΔH(G)	g-value	Spin Conc. (Spin /gram) x 10^{20}
1.	Fe_3O_4 +CNT (10 wt %)	1271	2.19	1.4365
2.	Fe_3O_4 + CNT (20 wt %)	1203	2.228	1.9450
5.	Fe_3O_4 + CNT (30 wt %)	1160	2.235	2.7387

phase in composites (b) and (c). Magnetic properties these composites were studied at ambient temperature by using X-band EPR spectrometer (Make: Bruker Biospin, Germany, Model: A300). The EPR spectra of composites are presented in Fig. 2.

EPR parameters like peak-to-peak linewidth (ΔHpp), g-value and spin concentration are listed in Table 1. These spectra shows broad strong resonance signal having g-value at about 2.20 due to ferromagnetic Fe^{3+} ions in these samples. The small bulge in sample (c) is attributed to the presence SWCNTs which give EPR resonance signal of g-value ~ 2.0. In lower concentration CNT's composites this is submerged within the broad resonance. The decrease in DHpp and increase in g-value and spin concentration is attributed to the ordering of spin through anti ferromagnetic interactions between Fe_3O_4 magnetic particles and CNT's

REFERENCES

1. P.K. Tyagi, M.K. Singh, M. Abha, P. Umesh, D.S. Misra and E.N. Titus, Thin Solid Films, 469–470, 127 (2004).
2. G. Korneva, H.H. Ye, Y. Gogotsi, D. Halverson, G. Friedman and J.C. Bradley, Nano Lett. 5, 879 (2005).
3. L.H. Guan, Z.J. Shi, M.X. Li and Z.N. Gu, Carbon 43, 2780 (2005).
4. C. Tsang, Y.K. Chen, P.J.F. Harris

WIGNER CRYSTALLIZATION IN SPIN-POLARIZED COUPLED ELECTRON QUANTUM LAYERS: FINITE WIDTH EFFECTS

Mukesh G. Nayak, L. K. Saini

Department of Applied Physics, S. V. National Institute of Technology, Surat – 395 007, Gujarat (India)
Email: lks@ashd.svnit.ac.in

We study the effect of finite width on Wigner crystallization in a spin-polarized coupled electron layers. Correlation among carriers are treated beyond the static mean-field theories by using the quantum version of Singwi, Tosi, Land and Sjölander (qSTLS) theory over a wide range of layer parameters *viz.* dimensionless density parameter r_{sl} and interlayer spacing d. Interestingly we find that the inclusion of finite width of layers lowered the critical density, for the onset of Wigner crystal (WC), as compare to the similar recent studies of spin-polarized coupled electron layers without finite width effects.

REFERENCES

1. E. P. Wigner, *Phys. Rev*. **46**, 1002–1011 (1934).
2. D. M. Ceperley and B. J. Alder, *Phys. Rev. Lett.* **45**, 567–569 (1980).
3. B. Tanatar and D. M. Ceperley, *Phys. Rev. B* **39**, 5005–5016 (1989).
4. R. K. Moudgil *et al.*, *Phys. Rev. B* **52**, 11945–11957 (1995).
5. R. K. Moudgil *et al.*, *Phys. Rev. B* **66**, 205316-1–205316-10 (2002).
6. L. K. Saini, *J. Low Temp. Phys.* **158**, 515–522 (2010).
7. F. Rapisarda and G. Senatore, *Aust. J. Phys*. **49**, 161–182 (1996).
8. M. Alatalo *et al.*, *Phys. Rev. B* **52**, 7845–7848 (1995).
9. F. Stern, *Phys. Rev. Lett.* **18**, 546–548, (1967).
10. F. F. Fang and W. E. Howard, *Phys. Rev. Lett*. **16**, 797–799 (1966).
11. T. Ando *et al.*, *Rev. Mod. Phys*. **54**, 437–672 (1982).
12. L. Swierkowski *et al.*, *Phys. Rev. Lett.* **67**, 240–243 (1991).

DIFFERENCE IN MICROSCOPIC PROPERTIES OF MgB_2 AND AlB_2: A DFT STUDY

Jagdish Kumar[1, 2], P K Ahluwalia[1], H Kishan[2] and VPS Awana[2,*], Sushil Auluck[2]

[1] *Department of Physics, Himachal Pradesh University, Summerhill, Shimla-171005*
[2] *Quantum Phenomena and Application Division, National Physical Laboratory, New Delhi-110012*
Email: awana@mail.nplindia.ernet.in

The electronic structure of MgB_2 has received much attention since it was found to be superconducting at a high temperature of 39 K [1]. The observation of boron isotope effect [2] suggested that superconductivity is mediated by phonons. However, the values of the electron-phonon coupling constant [3, 4] indicated that MgB_2 is an intermediate phonon coupled superconductor. There are many results that suggest holes in σ B-2*p* band via which electron-phonon coupling plays important roles in the superconductivity of MgB_2. The reason for such a high value of T_c is still not clear. Despite having a structure AlB_2 does not exhibit any superconductivity [6]. In present study we have studied the electronic properties MgB_2 and AlB_2 using density functional theory. The calculations were performed using *SIESTA* (Spanish Initiative for Electronic Simulations in Thousands of Atoms) code that implements density functional theory using localized atomic orbitals in terms of multiple zeta functions. We used double zeta polarized (DZP) basis set. The pseudopotentials were generated using the *atom* program included in the *SIESTA* package within the general gradient approximation (GGA) of Perdew-Burke-Ernzerhof (PBEsol) exchange-correlation functional. The transferability of pseudopotentials of Al, Mg and B were tested by reproducing ground state bulk properties. The Brillouin zone integrations were performed with a 15 × 15 × 15 special k-grid Monkhorst Pack while calculating lattice parameters and 20 × 20 × 20 for final calculations. The calculated values of lattice parameters for MgB_2 and AlB_2 are compared with the experimental values in Table 1. We find good agreement. We have also calculated the electronic density of states for both MgB_2 and AlB_2 using GGA PBEsol exchange-correlation. For both the diborides spin up and spin down electronic density of state (DOS) overlapped exactly indicating non-magnetic nature as is observed experimentally. The electronic density of state for MgB_2 and AlB_2 is shown in Figure 1 and 2 respectively. The numerical values of total density of states and *l* and *m* resolved for various bands

TABLE 1. Lattice parameters of MgB_2 and AlB_2 using GGA (PBEsol) [5]. The values given in parenthesis are corresponding experimental values[6]

	c/a	a (Å)
MgB_2	1.13(1.14)	3.10(3.08)
AlB_2	1.09	3.02
	(1.08)	(3.01)

TABLE 2. Calculated and experimental values of Sommerfeld constant in ($mJK^{-2}mol^{-1}$) for MgB_2 and AlB_2 and corresponding electron-phonon coupling constant

MgB_2	2.70	1.73	0.56
AlB_2	—	0.86	—

TABLE 3. Percentage contribution to electronic density of states at Fermi level $N(E_F)$ from different orbitals

	Total DOS	B-2p_x	B-2p_y	B-2p_z	Al/Mg-3s	Al/Mg-3p	Al/Mg-3d	B-2$p_{polarised}$
MgB_2	0.3696	0.0689	0.0689	0.1606	0.0155	0.0132	0.0000	0.0403
AlB_2	0.1792	0.0035	0.0035	0.0464	0.0343	0.0142	0.0337	0.0305

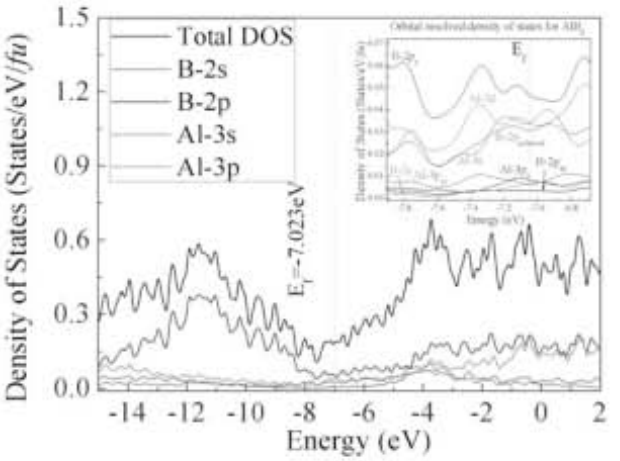

Fig. 8 Calculated partial density of states of AlB_2. Inset shows *l* and *m* resolved values

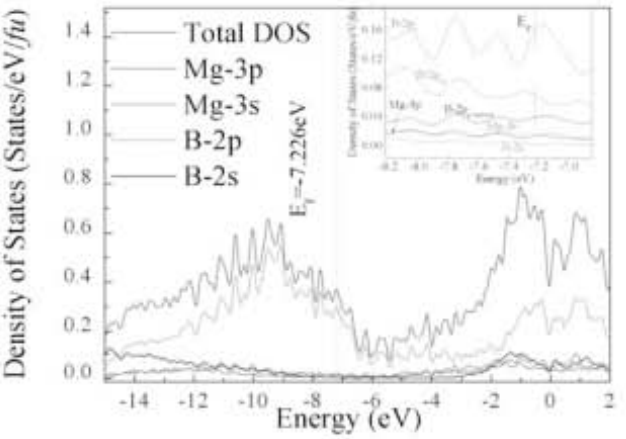

Fig. 7: Calculated partial density of states of MgB_2. Inset shows *l* and *m* resolved value

at Fermi level $N(E_F)$ is summarized in Table 3 and is in good agreement with recent calculations. It can be noticed that for MgB_2 the majority of states come from σ and π 2p states of boron. The δ band consists of B-$2p_x$ and B-$2p_y$ orbitals that overlap quasi-two dimensionally in xy plane to form strong covalent bonds. π bands consists of weaker B-$2p_z$ orbital interactions. $p_{polarised}$, which comes from DZP, is the polarisation of p orbitals in space. The σ bands (holes) are known to play an important role in electron-phonon coupling. In contrast for AlB_2 boron the π $2p_z$ states and Al 3s and 3d states contribute significantly at the Fermi level. It is interesting to note the absence of δ band at Fermi level for AlB_2. This leads to a weak electron phonon coupling and also to hole deficiency as δ bands are known to be of electron type.

From the value of $N(E_F)$ the value of Sommerfeld constant g follows.The value of γ is given by relation $\gamma = \frac{1}{3}\pi^2 N(E_F) K_B^2$. Where K_B is Boltzmann constant. Also electronic specific heat gives direct measurement of γ. From the ratio of $\gamma_{exp}/\gamma_{cal.}$ we have determined the value of electron-phonon coupling constant λ using well known relation $\frac{\gamma_{exp}}{\gamma_{cal}} = (1+\lambda)$. The calculated values are given in Talbe 2. The values agree with values reported by others $\lambda_{MgB2} = 0.61$ and $\lambda_{AlB2} = 0.43$. Our earlier measurements [6] on thermoelectric power have shown that MgB_2 is hole type whereas AlB_2 is electron type. The hole type contribution to MgB_2 comes from σ bands. Our calculated contribution of δ bands supports these measurements. The Al^{3+} substitution at Mg^{2+} site provides extra electrons to fill hole type σ bands and this results in electron type conductivity in AlB_2. The dominance of boron π $2p_z$ states and Al 3s and 3d states at Fermi level do correspond to an increase in the dominance of electron type behaviour.

REFERENCES

1. Nagamatsu J, Nakagawa N, Muranaka T, Zenitani Y and Akimitsu J 2001 *Nature* **410** 63
2. Hinks D G, Claus H and Jorgensen D J 2001 *Nature* **411** 457
3. Kong Y, Dolgov O V, Jepsen O and Andersen O K 2001 *Phys. Rev.* B **64** 0230501
4. Wang Y, Placowski T and Junod A 2001 *Physica* C **355** 179, Bouquet F *et al* 2001 *Phys. Rev. Lett.* **87** 047001
5. Perdew, Burke and Ernzerhof *Phys. Rev. Lett.* **100**, 136406 (2008)
6. V P S Awana, Arpita Vajpayee, Monika Mudgel and H Kishan, *Supercond. Sci. Technol.* **22** (2009) 034015

SUPERPOSITION-MODEL ANALYSIS OF ZERO-FIELD SPLITTING PARAMETERS FOR Mn2+ IN BIS(L-ASPARAGINATO)Zn AND TRICALCIUM PHOSPHATE SINGLE CRSTALS

R.S.BANSAL

A.I.JAT H.M.College, Rohtak-124001, Haryana (India)
Email; rbrsbansal@gmail.com

The Newman superposition-model has been used o investiate the substitution of Mn2+ for Zn2+ site in bis(L-asparaginato)Zn and for Ca2+ in tricalcium phosphate single crstals.The calculated values of the zero-field splitting parameters(ZFS) at room temperature fit the experimental one taken from the literature . The satisfactory reproduction of experimental values of ZFS parameters indicates that Mn2+ substitute in place of Zn2+ and Ca2+ in the lattices and does not causes appreaciable local distortion in the host crystals.The calculations are made with the assumption that the total field experienced at an ion in a crystal is due to close neighbour ions , using power law exponent t= 6 to 8 and the reference distance R=0.22 nm for Mn2+ surrounded by oxygens and R=0.21 nm for Mn2+ surrounded by nitroens.

COLLECTIVE EXCITATIONS OF COMPOSITE FERMIONS ACROSS MULTIPLE Λ LEVELS

Dwipesh Majumder[1,2], Sudhansu S. Mandal[1], Jainendra K. Jain[3]

[1]*Department of Theoretical Physics, Indian Association for the Cultivation of Science, Jadavpur, Kolkata 700 032, India*

[2] *Department of Physics, Santipur College, Santipur, West Bengal, India.*

[3]*104 Davey Laboratory, Physics Department, Pennsylvania State University, University Park, Pennsylvania 168*

The fractional quantum Hall state is a quintessential system for the study of collective quantum behaviour. In such a system, the collective behaviour results in the creation of so-called composite fermions, quasi-particles formed by electrons attached to magnetic flux quanta.Recently, a new collective mode was unexpectedly observed in Raman scattering experiments by Hirjibehedin et.al. on such a system as it was found to split off from the familiar 'fundamental' long-wavelength mode on increase of the wave vector. Here, we shall present the results from extensive theoretical calculations that make a compelling case that this mode corresponds to an excitation of a composite fermion across two three Λ levels-effective kinetic energylevels resembling Landau levels for such particles. In addition to explaining why this excitation merges with the fundamental mode in the long-wavelength limit, our theory also provides a good quantitative account of the amount of splitting, and makes several experimentally verifiable predictions We shall also present the spin-excitations. In this case one of the composite fermions from one of the filled up Λ level to one of the down Λ levels. This results qualitatively explain the experimental facts for several fractional quantum hall effect associate with the higher excitations.

REFERENCE

1. Nature Physics 5, 403 - 406 (2009)

HYDROGENIC EXCITONS IN MAGNETIC FIELD: A TWO-BODY PROBLEM

Bhavtosh Bansal,[1,5] B Karmakar,[2,3] G Doehler,[3,4] S Malzer,[4] B M Arora,[3]
P C M Christianen,[5] J C Maan[5]

[1]*Indian Institute of Science Education and Research-Kolkata, Nadia 741252, India*
[2]*NEST INFM-CNR and Scuola Normale Superiore, Pisa 56126, Italy*
[3]*Tata Institute of Fundamental Research, 1 Homi Bhabha Road, Mumbai 400005, India*
[4]*Max-Planck-Research Group, Institute of Optics, Information, and Photonics, Universitaet Erlangen-Neumberg, 91058 Erlangen, Germany*
[5]*High Field Magnet Laboratory, 6525 ED Nijmegen, The Netherlands*
Email: bhavtosh@iiserkol.ac.in

It has been known since the work of Lamb [1] that a hydrogen atom moving perpendicular to an external magnetic field forms an irreducible two-body system [1-5]. Here contrary to the zero-magnetic field case, the Hamiltonian cannot be cleanly separated into the centre of mass (CoM) and relative co-ordinate frames. This coupling results in the CoM motion manifesting as an effective electric field [Fig.1(c)] in the relative coordinate frame (motional Stark effect) and has been much discussed in atomic physics and astrophysics literature due to its many non-trivial consequences—(i) magnetic field-dependent change in the CoM dispersion (Fig. 2) [4,5], (ii) formation of so-called decentered (or giant-dipole) states [5], and (iii) changes in the selection rules for magneto-

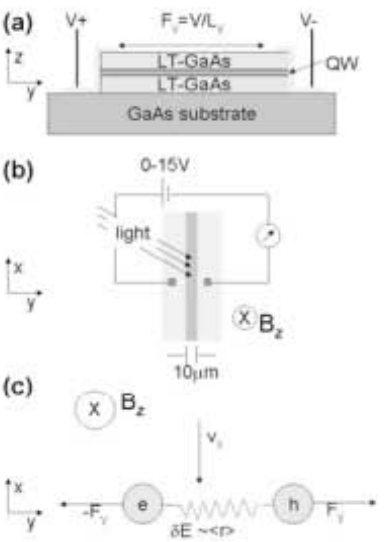

Figure 1: (a) Side view, (b) top view schematic of the special QW structure with additional GaAs layers grown at low-temperature (LT) to ensure uniform electric field. (c) The exciton in magnetic field behaves as a composite entity [3] with the electrons and the holes traveling at the *same* group velocity $v_z = |cF_y/B_z|$, such that the Lorentz force balances the electric field, F_y. The exciton is polarized with stored internal energy δE. This increased internal energy leads to the exciton mass being renormalized (data in Fig 2).

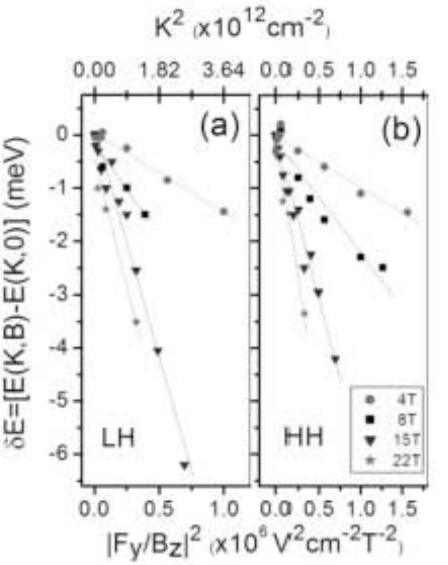

Figure 2: The magneto-Stark shifts of (a) Light hole (LH), and (b) heavy hole (HH) exciton ground states as a function of $|F_y/B_z|^2$ (bottom axes) and the equivalent CoM wave vector K_x^2 (top axes). For the latter, this energy shift is the difference between the exciton dispersion and magneto-exciton dispersions, $E(k,B)-E(k,0)$. The B-dependent slopes prove magneto-exciton mass enhancement. This has so far only been observed for spatially-indirect excitons in coupled-QW using a different experimental technique [4].

optical transitions [6]. The Wannier excitons in semiconductors closely mimic the physics of the hydrogen atoms but with the important difference that the energy scales in the problem are reduced by many orders of magnitude and the laboratory strength electric and magnetic fields can cause significant perturbation on the ground state, B~10T for a typical Wannier exciton is equivalent to ~500,000T for hydrogen atom.

We have performed magneto-optical experiments on a specially designed GaAs quantum well (QW) sample [Fig. 1]. By using an unusual configuration where the sample was under the simultaneous influence of mutually perpendicular electric and magnetic fields of high strengths [Fig.1 (a, b)], we have simulated the situation of the motional Stark effect and observed all the three above mentioned phenomena related to the essential two-body nature of the problem. In particular, we have observed a significant B-dependent enhancement of the mass of both the light-hole (LH) and the heavy-hole (HH) excitons (Fig. 2). We have also inferred the formation of the decentered state [5] for LH excitons at B=4T beyond F~$8 \times 10^3 Vcm^{-1}$. Finally, we have observed the breakdown of the optical selection rules and appearance of an intractably large number of usually forbidden optical transitions (their level spacing distribution indicative of chaos, though not conclusively so) when the QW was in an electric fields of ~$10^4 Vcm^{-1}$ at B=15T.

REFERENCES

1. W. E. Lamb, Jr., Phys. Rev. 85, 259 (1952).
2. B. R. Johnson, J. O. Hirschfelder, and K. H. Yang, Rev. Mod. Phys. 55, 109 (1983).
3. D. Paquet, T. M. Rice, and K. Ueda, Phys. Rev. B 32, 5208 (1985).
4. L. V. Butov et. al, Phys. Rev. Lett. 87, 216804 (2001).
5. Yu. E. Lozovik and S. Yu. Volkov, Phys. Rev. A 70, 023410 (2004).
6. H. Crosswhite, U. Fano, K. T. Lu, and A. R. P. Rau, Phys. Rev. Lett 42, 963 (1979).

IN SEARCH OF QUANTUM FORCE AND ITS PERSPECTIVES IN QUANTUM PHYSICS

Kapil Chandra

Centro de investigaciones energeticas, madioambientales y tecnologicos (CIEMAT)
Ciudad Universitaria of Madrid, Avda. Complutense, 22 – 28040, Madrid, Spain
E-mail:chandra.kapil@ciemat.es

Quantum theory is almost working theory of nature, but up to now we don't have quantized form of force, to bridge this gap I proposed the force in quantum form, the so called the quantum force equation (QF). This article is organized in two parts, in the first part, I empirically proposed the QF and the later part is the conceptual justification and its perspective on quantum physics and I found some interesting results, from the QF, for the first time the wave particle duality equation can be derived apart from the De – Broglie's derivation, the difference is he derived it form the balancing the quantum energy and mass energy but I deducted it by the balancing the so called QF with classical Newtonian force, consequences of it, wave equation can be written in term of force instead of Schrödinger's equation, what is in term of Hamiltonian energy operator. The advantage of this perspective over the past work is its new explanatory view of natural forces and relativistic equation of mass. The QF gives the theoretical foundation of Yukawa's prediction of meson and theoretical equation to calculate the strong nuclear force. The proposed force tells us, there is no relativistic mass as Einstein told, but it is just a form of QF. These finding are very important to understand the Plasmon excitation in metal, quantum computing, quantum information processing, optical particle trapping and entanglements.

QUANTUM EFFECTS AT AMBIENT TEMPERATURES IN SOLIDS

Devinder Gupta

National Physical Laboratory (CSIR)
Dr. K.S. Krishnan Marg, New Delhi-110 012
E-mail: dgupta1952@yahoo.in

Condensed matter systems display a variety of quantum effects at low temperatures and these have been studied extensively. However, quantum effects at ambient temperatures are far less investigated. The present work comprises of infrared studies at ambient temperatures on a variety of solids in the form of metals, semiconductors and dielectrics (insulators); in bulk and film forms; in different crystalline states such as single crystal, poly crystal, amorphous and nano states. Investigations were undertaken at near normal and oblique angles of incidence from 10° to 70° for specular reflection and 0° to 70° for regular transmission spectra in the mid-IR spectral region of 4000-400 cm^{-1}. The incident IR photons interact with material's molecules to create thermal phonons, leading to phonons-photons interactions in solids. It has been observed that with increase in obliquity and wavelength, reflectance values of solids generally decrease whereas their corresponding transmittance values increase. Further, both reflection and transmission bands of solids in general show blue shift with increase in obliquity. However, since reflection phenomena is more sensitive compared to that of transmission, shift in the former case is greater than in the later case. This shift is marginal in case of metal films since there is no band gap in them and practically no change takes place in their carrier's density with variation in obliquity. However, the shift in case of semiconductors is large compared to dielectrics since there is more change in carriers' density (since both electrons and holes contribute) compared to that for dielectrics where only electrons contribute. Further, the band gaps in case of semiconductors are small compared to that of dielectrics. Single and poly crystal have similar behavior with change in obliquity and wavelength. Amorphous solids show large shift compared to single crystals since incident IR radiation induces more changes in isotropic and randomly placed atoms in amorphous solids (with no definate structures) in comparison to anisotropic and well orderly placed atoms in single crystals(with definate structures). Nano solids have behavior like that of corresponding oxides and amorphous solids depending upon the size of nano crystals. The blue shift is caused by strengthening of bonds between atoms of material's molecules, after the energy of incident photons enhance with change in obliquity similar to "anti Stokes lines in Raman Effect". It has also been observed that the transmission bands of solids shift towards the shorter wavelength region (blue shift) at low temperatures. In conclusion, quantum effects on solids at low temperatures are complementary to those observed with IR angular specular reflection and regular transmission studies at ambient temperatures.

THE ZIGZAG SPIN-CHAIN ANTIFERROMAGNET CaV_2O_4 : SYNTHESIS, STRUCTURE AND MAGNETISM

A. Niazi[1]*, O. Pieper[2], B. Lake[2], M. Reehuis[2], A. Doud-Aladine[3], K. Prokeš[2], B. Klemke[2], K. Kiefer[2], J.Q. Yan[1], A. Kreyssig[1], S. Das[1], S. Nandi[1], X. Zong[1], B.J. Suh[1], D.L. Schlagel[1], T.A. Lograsso[1], R.W. McCallum[1], A.I. Goldman[1], S. Budko[1], A. Honecker[4], D.C. Johnston[1]

1. Ames Lab, Ames, USA; 2. HZB & TU, Berlin, Germany; 3. ISIS, Rutherford Appleton Lab, UK; 4. Universität Göttingen, Germany;

**(asad.ph@jmi.ac.in, Dept. of Physics, JMI, New Delhi)*

The compound CaV_2O_4 contains V^{+3} cations with spin S=1 and has an orthorhombic structure at room temperature containing two inequivalent zigzag chains of V atoms running along the *c* axis. The ûrst- and second-neighbor vanadium separations are approximately equal suggesting frustrated antiferromagnetic exchange interactions. We have grown single crystals of CaV_2O_4 and performed crystallography, magnetic susceptibility, O^{17} NMR, heat capacity Cp, and thermal expansion measurements in the temperature T range of 1.8–350 K on the single crystals and on polycrystalline samples. High-temperature susceptibility (300–1000 K) and single-crystal neutron-diffraction measurements have been used to deduce the dominant exchange paths and orbital conûgurations. An orthorhombic-to-monoclinic structural distortion and a long-range antiferromagnetic (AF) transition is found at temperatures $T_S \sim 140$ K and $T_N \sim 51–78$ K, respectively. The magnetic susceptibility $\chi(T)$ shows a broad maximum at ~ 300 K associated with short-range AF ordering and the anisotropy of $\chi(T)$ above T_N is small. The anisotropic $\chi(T) \rightarrow 0$ K data below T_N show that the easy axis of the AF magnetic structure is the b axis. Detailed NMR and neutron diffraction measurements reveal collinear spin order within the chains and canting between chains, with the average spin direction along the b axis. The Cp(T) data indicate strong short-range AF ordering above T_N, consistent with the $\chi(T)$ data. We analyze our data using a J_1-J_2 S=1 Heisenberg chain model, where $J_1(J_2)$ is the (next)-nearest-neighbor exchange interaction. Our results suggest that at high temperatures CaV_2O_4 behaves as a Haldane chain, but at low temperatures, it is a spin-1 ladder. These two magnetic structures are explained by different orbital conûgurations and show how orbital ordering can drive a system from one exotic spin Hamiltonian to another.

REFERENCES

1. X. Zong, et al, Physical Review B 77, 014412 (2008)
2. A. Niazi, et al, Physical Review B 79, 104432 (2009)
3. O. Pieper, et al, Physical Review B 79, 180409R (2009)

MANIPULATING UNPAIRED MAJORANA FERMIONS IN A QUANTUM SPIN CHAIN

Abhinav Saket, S.R. Hassan and R. Shankar

The Institute of Mathematical Sciences, CIT Campus, Chennai 600 113.

We analyze an exactly solvable spin-1/2 chain which is a generalized version of Kitaev's honeycomb model. We show that every state of the system has a N/4-fold degeneracy, where N is the number of sites. We present analytic solutions for the zero energy modes of the Majorana fermions. Localized, unpaired Majorana modes occur even in the bulk of the chain and they are bound to kink antikink Z2 flux configurations. The unpaired Majorana modes can therefore be created and manipulated if the Z2 flux configurations can be controlled. We delineate the regions in parameter space for homogenous chains where the zero modes occur. We further show that there is a large parameter space for inhomogenous chains where the unpaired modes occur and that their wave functions can be tuned if the couplings of the model can be tuned.

QUANTUM CONFINEMENT IN IRIDIUM OXIDE NANOWIRES

Santosh Singh, Manju Arora, K.N. Sood and Sukhvir Singh

National Physical Laboratory, Dr. K.S. Krishnan Road, New Delhi – 110 012 (India)
Email : santoshs@nplindia.org

1D nanostructures, semiconductor nanowires (NWs) have been widely studied as very attractive and versatile building blocks for nanoscale systems due to important electronic and optical properties of the nanowires and the potential for 'bottom-up' assembly of massive number of functional devices. Group IV, III-V and II-VI semiconductor nano-materials have been widely studied as functional device elements and a wide range of nanowire-based devices have been fabricated, including field effect transistors (FETs), photodetectors, light-emitting-diodes (LEDs, lasers, sensors, logic gates and address decoders. In order to build an electronic system, it is very important to have electrically conductive interconnects. There have been efforts in the growth of metallic nanowires such as Ni, NiSi, Au and Pt using either template or after growth metalization methods, and potentials have also been studied in using metallic nanowires as nanoscale interconnects and for field emission devices IrO_2 is conductive metal oxide that has been widely used in dynamic random access memory (DRAM) and FeRAM applications which, as conducting electrodes, are very stable both electrically and chemically at high temperature and in high O_2 ambient environment. IrO_2 has also been studied as a good candidate for field emission cathodes of vacuum microelectronics and field emission displays because of its low work function (4.23 eV) and high chemical stability. The chemical and electrical stability of IrO_2 have also enabled excellent chemical sensing applications, such as pH sensors. IrO_2 thin film, fabricated from either post growth oxidation of Ir thin film and CVD grown IrO_2 thin films, have been reported. Submicron production techniques such as MBE and MOCVD are routinely used to fabricate quantum devices with novel characteristics. As semiconductor technology continues to drive the scaling of electronic device dimensions into the ultrasubmicron and nanodimensional regime, many concepts and phenomena related with ultrasmall and ultrafast devices are being the focus of an intensive research. A principal challenge in the application of quantum-based devices arises from the molecular size considerations The most important feature associated with those small grains, is a quantum size effect, showed as a shift in the excitonic peak of their optical absorption spectra, as the size of the nanocrystal decreases. Metal organic chemical vapor deposition (MOCVD) growth of IrO_2 nanorods has been reported using (methylcyclopentadienyl) (1,5-cyclooctadiene) iridium (I) as precursor.35) But the IrO_2 nanorods are normally polycrystalline structure with high density of point defects and dislocation. In this paper, we have reported the growth of single crystal IrO_2 nanowires with dimension from 10 to 50 nm and 1–2 mm long via s MOCVD method. IrO_2 nanowires growth on Si substrate and thin metal films (such as Au, Ti, Ni, and Co) on Si substrates were tested It was found that thin metal layer facilitates nanowire growth. The nanowires were characterized by XRD, PL, FT Raman and scanning electron microscopy (SEM). X-ray diffraction (XRD) pattern shows a high degree of crystallinity, and all of the peaks match well with Bragg reflections of the standard rutile structure 3.25 Å, *c*) 5.21 Å, JCPDF # 36-1451. Optical studies of the nanowires determine the potentially unique optical properties and observed that quantum confinement effects play an important role in the photoluminescence.

AUTHOR'S INDEX

ADVERTISEMENT

INDO-U.S. SCIENCE AND TECHNOLOGY FORUM

Fulbright House, 12 Hailey Road, New Delhi 110 001, India

Website: www.indousstf.org

The Indo-U.S. Science and Technology Forum (IUSSTF) was established in 2000 under an agreement between the Governments of India and United States of America with a mandate to promote, catalyze and seed bilateral collaboration in science, technology, engineering and biomedical research through substantive interaction amongst government, academia and industry.

As its mandate, IUSSTF provides an enabling platform to the scientific enterprises of the two nations by supporting an S&T program portfolio that is expected to foster sustainable interactions with a potential to forge long term collaborations. IUSSTF program manifests are largely catalytic in nature that helps to create awareness through exchange and dissemination of information and opportunities in promoting bilateral scientific and technological cooperation.

IUSSTF has an evolving program portfolio that is largely conceived and driven by scientific communities of both the countries through extending support for symposia, workshops, conferences on topical and thematic areas of interest; visiting professorships and exchange programs; travel grants; fellowships; advanced training schools; public-private networked centres and knowledge R & D networked centres. IUSSTF also works towards nurturing contacts between young and mid career scientists by convening stimulating flagship events like the Frontiers of Science and Frontiers of Engineering symposium through the U.S. National Academies model. At the same time it reaches out to industries by partnering with business associations to generate high quality events on technology opportunities for business development to foster elements of innovation and enterprise through networking between academia and industry.

IUSSTF maintains a close working relationship with the federal agencies, laboratories, government institutions, and the academia in U.S. and India, cutting across all disciplines. As an autonomous, not-for-profit society, IUSSTF has the ability, agility and flexibility to engage and involve industry, private R&D labs; and non governmental entities in its evolving activity manifold. This operational uniqueness allows the IUSSTF to receive grants and contributions from independent sources both in India and USA, besides the assured core funding from the two governments.

IUSSTF solicits proposals for its activities thrice a year (January, May and September) and awards are made on the basis of peer reviews both in India and USA.

IUSSTF values your interactions and looks forward to work with the S&T community of both countries to implement new ideas that endeavor to promote cutting edge Indo-U.S. Science and Technology collaborations.

The Institute of Mathematical Sciences

The Institute of Mathematical Sciences (IMSc), founded by Alladi Ramakrishnan in 1962, is a national institution for fundamental research in the mathematical and physical sciences. The Institute is governed by a Board and an Academic Council. The present Director of the institute is Prof. R. Balasubramanian.

Research at **IMSc** is supported by the Department of Atomic Energy of the Government of India and by the Government of Tamil Nadu. Institute members work primarily in the areas of Mathematics, Theoretical Computer Science and Theoretical Physics.

The Institute has an active graduate research program to which a select group of students are admitted every year to work towards a Ph.D. degree. IMSc hosts a large number of scientists at the post-doctoral level and supports a vibrant Visiting Scientist Scheme. More information is available under Academic Programmes at IMSc.

IMSc has an outstanding scientific library, a computing facility which contains the fastest academic computer in India (as of mid 2004) and a dedicated high-speed network. The Institute hosts several national and international scientific meetings every year. The Institute Annual Reports summarize past and ongoing research.

A new, centrally air-conditioned office and lecture-hall complex houses academic members of **IMSc**. A 200 seat auditorium, the Ramanujan auditorium, is used for large scientific meetings while smaller lecture halls and classrooms accomodate more modest gatherings. Most public areas in the Institute, including seminar and discussion rooms, lounges and the auditorium are Wi-Fi enabled.

Located in South Chennai, in the Adyar-Taramani area, the Institute is based in the verdant surroundings of the Central Institutes of Technology (CIT) Campus. The Institute campus also contains a student hostel, flatlets for long-term visitors, married students and post-doctoral fellows, and the Institute Guest-House. **IMSc** has its own faculty housing in Tiruvanmiyur near the seashore.

THE INSTITUTE OF MATHEMATICAL SCIENCES

C.I.T. Campus, Taramani, Chennai - 600 113, India.

Telephone: (044) 2254 1856, 2254 2588

Fax: (044) 2254 1586

URL: http://www.imsc.res.in

Retsch®

Solutions in Milling & Sieving

inkarp INSTRUMENTS PVT.LTD.

Retsch GmbH, Germany are known as pioneer and manufacturers for sample preparation systems. They offer a wide range of equipments for size reduction and homogenization through Milling, Sieving & Assisting

Retsch Ball Mills are used for the pulverization of soft, fibrous, hard and brittle materials. These are very much suitable for highest degree of fineness and give a very high final fineness down to the sub micron size range. These ball mills move in planetary motion and the high centrifugal forces of the planetary ball mills result in very high pulverization energy and therefore grinding time is reduced drastically.

PM 100

PM 200

PM 400

Grinding jars are Comfort type – safe , non-slip seating with built –in anti rotation device and conical base centering for excellent grinding with outer lining of stainless steel as a protective jacket for ceramic jars.

Retsch also offers their new Mixer Mills Model MM-200 and MM-400 for grinding, mixing , disrupting small amount of samples. These Mixer Mills are laboratory " all rounders" .They have been developed specially for dry & wet grinding of small sample amounts. They can mix and homogenize powders and suspensions in only few seconds. They are perfectly suitable for the disruption of biological cells.

MM 400

Exceptionally simple , safe handling, dust proof and airtight. Stainless steel protective jacket for Agate , Zirconium Oxide & Tungsten Carbide Jars. Can be used for Cryogenic Grinding also.

Contact for more details:

INKARP INSTRUMENTS PVT LTD.,

1-2-45/1, Street No.2, Kakateeya Nagar Colony, Habsiguda, Hyderabad – 500 007 Tel: 040 27172293 / 27175088, Email: sales@inkarp.co.in, Website: www.inkarp.co.in

EATON

Powering Business Worldwide

- DSP True Online UPS Systems
- 600 VA to 5000 KVA
- Rack Mount UPS (1 KVA to 60 KVA)
- IGBT Rectifier Technology
- Output P.F 0.9
- Wireless Paralleling upto 8 units
- Advance Battery Management

Powerware / Pulsar / E Series

UPS Systems

10 kVA to 160 kVA Tower

1 kVA to 20 kVA
Rack Mount / Tower

1 kVA to 20 kVA
Tower

12 kW to 72 kW
Rack Mount

Katsun
automation

Plugging-Techno Solutions

Katsun Automation Pvt. Ltd

N-161, 203, Thapar House , Gulmohar Enclave Community Center,
New Delhi-110 049. Ph : +91 99588 12299, 4606 6472-73
Email : sales@katsun.in URL : www.katsun.in

DL-28-25950/04-12-08/Manoj (A)

Central Drug Research Institute, Lucknow

(Council of Scientific & Industrial Research)

Formally inaugurated on 17th February, 1951, by India's first Prime Minister, Shri Jawaharlal Nehru, CDRI is a premier centre for drug research in the country. It is equipped with some of the latest research facilities in drug R&D. The institute offers competitive advantage in collaborative research and business opportunities to **academia** and **industry - contract research, product licensing, technical services and human resource development.**

Modern Research Facilities

- **Robotic multiple organic synthesiser for construction of new chemical libraries of several thousand compounds.**
- **Highthroughput screening facility for quick screening of large number of compounds.**
- **Structural biology facility for predicting molecules for structure based design.**
- **Confocal microscope for investigating mechanism of drug action.**
- **DNA-microarray & proteomics facilities and CD-machine for various molecular/cellular biological studies.**
- **State-of-the-art electron microscope facility for better understanding of drug action at molecular level.**

The laboratory through its scientific expertise provides complete facilities for drug discovery and development - synthesis, biological screening, regulatory studies (quality control and standardization, pharmacology, pharmacokinetics, toxicology and clinical trials) conforming with Good Laboratory Practices and International Protocols / Guidelines employing latest testing models / systems, bio-markers, analytical tests and sophisticated instruments.

Technologies Licensed and in Commercial Production

- **Artemether (IPCA Laboratory)**
- **Dextropropoxyphene hydrochloride (Wockhardt)**
- **l-Ephedrine hydrochloride (Malladi)**

Major New Drugs Developed and Marketed

CDRI's Standardised fraction from Bacopa monniera Extract (Memory improvement) Marketed as Memo Plus Gold (Lumen Marketing Co.)

Arteether (Antimalarial) marketed as E-Mal (Themis Ltd.)

Centchroman (Oral contraceptive) Marketed as Saheli (Hindustan Latex)

Bulaquin (Antirelapse antimalarial) Marketed as Aablaquin (Nicholas Piramal)

Mycobacterium tuberculosis Real time PCR based Diagnostic Kit (BIOTRON, Health Care)

CDRI LUCKNOW

For further information please contact:
Director
Central Drug Research Institute
Chattar Manzil Palace, Lucknow-226 001 (India)

Phone: 2612411-18(PABX). **Fax:** 0522-2623405. 2623938
E-mail: director@cdri.res.in

website: www.cdriindia.org

CRYOGENIC

CRYOGENIC LIMITED

Cryogen Free Measurement Systems 5 to 25 Tesla

- **Magnets to 25 Tesla using SuperPower® 2G HTS**
- **Cryogen Free. No liquid helium needed**
- **Room temperature bore or variable temperature sample space**
- **Highly stable magnetic field**
- **High power Pulse Tube cryocoolers with low vibration**
- **No maintenance for 3½ years continuous use**

Cryogen Free 16 Tesla, 50 mm VTI, with option for Dilution Refrigerator Insert for temperatures down to 30 mK

Cryogen Free 5 Tesla Mini Vibrating Sample Magnetometer, with AC Susceptibility and High Temperature Facility to 700 K

Measurement Options:

- Vibrating Sample Magnetometer (VSM) for measurements of DC magnetic moment with sensitivity of 10^{-6}
- AC calorimeter to measure Specific Heat and Thermal conductivity
- Resistivity and Hall effect probe with sample rotation in field
- AC Susceptibility probe
- MFM/AFM and Pressure Cell options

Temperature Ranges:

- High Temperatures Insert with temperatures to 1000 K
- He-3 Insert with temperatures down to 300 mK and 30 hours hold time
- Ultra Low Temperatures down to 10 mK with 17 Tesla shielded coil in a Cryogen Free Dilution Refrigerator

CRYOGENIC LIMITED
30 Acton Park Estate
London W3 7QE, UK
tel: +44 (0)20 8743 6049
email: sales@cryogenic.co.uk
www.cryogenic.co.uk

Pramod Kumar
Vico Scientific Sales Private Limited
tel: +91-11-25871181
fax: +91-11-25872788
email: pkumar@vicosales.com
www.vicosales.com

Cryogen Free Superconducting Magnet Systems

This versatile design features a Room Temperature Bore, which allows for an optional Variable Temperature Insert.

Cryo Industries of America, Inc. has over 25 years of experience in designing and manufacturing Superconductng Magnet Systems.

Cryo ofers Cryogen Free Superconductng Magnet Systems that integrate innovatve design with magnetc felds that range from 2 Tesla up to 15 Tesla (depending on design), you select the magnetc feld. Magnet configuratons available include Vertcal Field Solenoid or Horizontal Field Split Coil magnets.

Cryo ofers Superconductng Magnet designs with a clear vertcal room temperature bore or a top loading variable temperature insert or both. The magnet is cooled through a Giford-McMann cooler or a Pulse Tube cooler for low vibraton experiments.

You select the temperature and cooling power needed!

This innovative design allows for numerous configurations, including a compact design and/or various stand optons.

All complete Superconductng Magnet Systems include:

- Conductvity cooled superconductng magnet
- Removable room temperature bore or variable temperature insert
- Closed cycle refrigerator (G-M or pulse tube)
- Compressor
- Programmable reversing bipolar magnet power supply
- Integral energy absorber
- Temperature controller
- Temperature sensor(s).

Cryo Industries's 'performance by design' Supeconductng Magnet Systems ofers many feld tested and proven designs throughout the scientfc community. Cryo is able to ofer contnued technical support for the life of the system.

The Tinsley Group I Td.
Ph: +91 11 22152150, 22152151
E-Mail: tinsley@ndf.vsnl.net.in
www.cryoindustries.com

SPECIALISE INSTRUMENTS MARKETING COMPANY

305, Kailas Industrial Complex, A-wing 3rd Floor, Building No.2,
Parksite Vikhroli (West), Mumbai-400 079. (INDIA)

INSTRUMENTATION SOLUTIONS FOR ACADEMIA, INDUSTRY AND SCIENTIFIC APPLICATION AND HARDWARE SUPPORT

Quantum Design U. S. A

VSM, SQUID VSM, MPMS & PPMS- Systems

- Versalab Cryo-free VSM , 3 Tesla, 50K to 400K, sensitivity 10 6 emu/rt-H
- MPMS Squid VSM, sensitivity <10 · emu with only 4 second data averaging
- MPMS integrates a SQUID detection system, a precision temperature control unit and a powerful software control operating system.
- PPMS are designed for fields up to 16 Tesla and temperature range in 1.9-400K

PULSED LASERS

Quantel France

- Ylia M20, Ytterbium High Energy Fiber Laser of Pulse Energy 1mJ at 1064 nm
- YG980 series Nanosec. Q-switch Nd:Yag lasers up to 2.4 J Energy at 1064 nm
- Nd:Yag Pumped high resolution Dye Lasers for RIMS application

VIBRATING SAMPLE MAGNETOMETERS

ADE U. S. A

- Resistive Magnet VSM with highest fields and higher sensitivity
- Fastest , most accurate field control in conjunction with temperature control
- Accurate true Torque Magnetometers

CCDs/ICCDs/EMCCDs for Spectroscopy & X-ray imaging

ANDOR U. K TECHNOLOGY

- Special TE cooling down to –100C
- Fastest optical gate for the ICCD
- Slow scan ultra low read noise systems, 16 bit at 1MHz
- Exclusive EMCCD spectroscopy chips with on chip gain, fast readout, spectrographs, Echelle spectrographs for high throughput

Atomic Layer Deposition (ALD) Systems

Picosun Finland

- Deposition of Metal Nitrides and Metal Oxides thin films such as TiN, NbN, ZnO and Al_2O_3
- Uniform and ultra-conformal film deposition on 2-8'' substrates
- Process temperatures up to 500°C
- Precursor sources for gaseous, liquid and solid chemicals
- Heated precursor source temperature up to 200°C

New Delhi office- **Ravi Mohan Garg Mob-98113-75599**
Email-ravimgarg@yahoo.com

Internet Banking

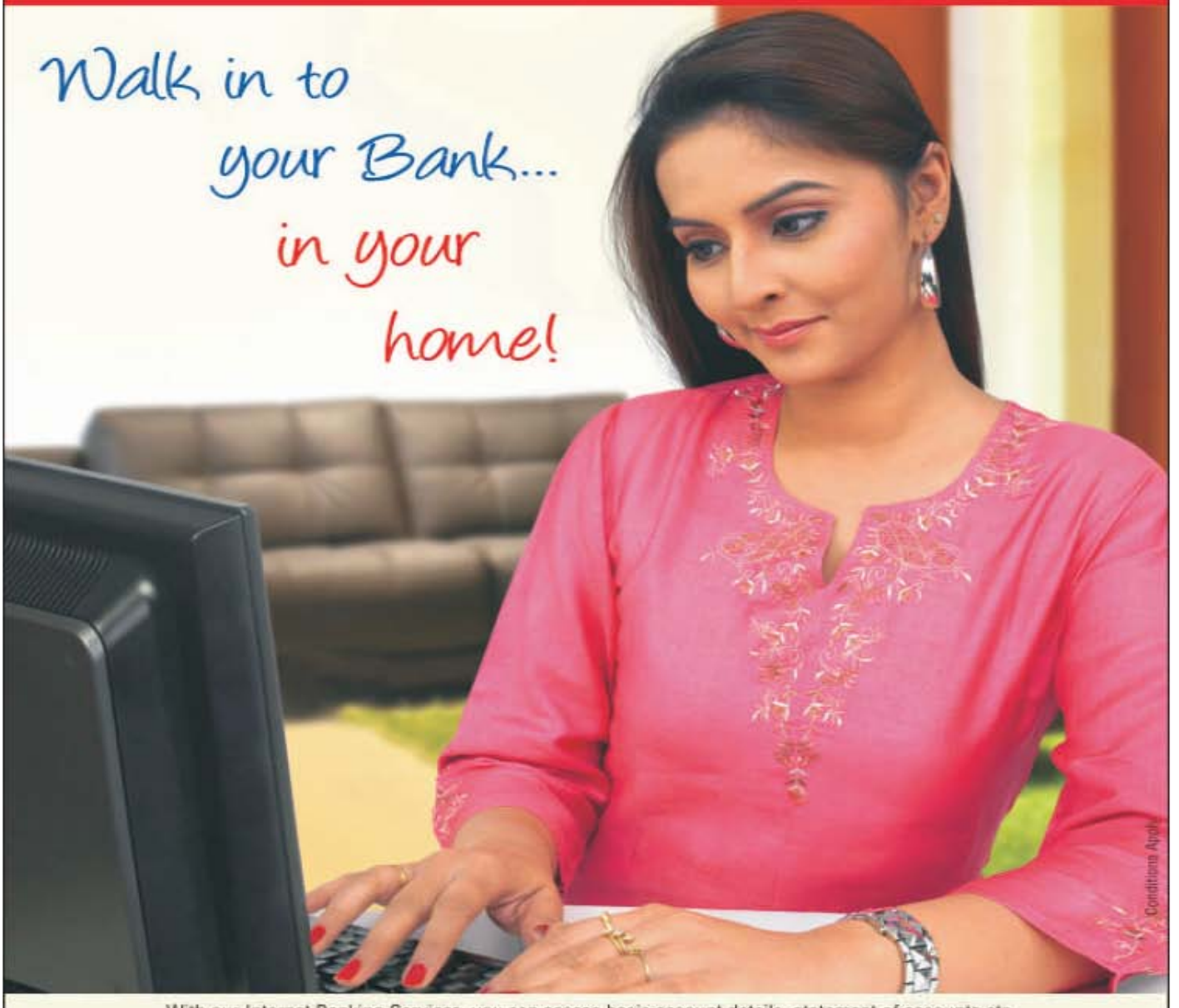

With our Internet Banking Services, you can access basic account details, statement of accounts etc. anytime, anywhere. Ease your life with our enhanced facilities like :

- **Railway e-ticketing**
- **Utility Bill payment**
- **Payment of Direct & Indirect Taxes**

विश्वसनीय. मैत्रीपूर्ण
Faithful. Friendly

सिंडिकेटबैंक
SyndicateBank

भारत सरकार का उपक्रम A Govt. of India Undertaking

www.syndicatebank.in

NORTH-EAST INSTITUTE OF SCIENCE & TECHNOLOGY

JORHAT : ASSAM

NEIST Jorhat

North-East Institute of Science & Technology, Jorhat, Assam, a constituent establishment of Council of Scientific & Industrial Research(CSIR), New Delhi has been engaged in multidisciplinary R&D work relevant to the North Eastern Region in particular and country in general.

MAJOR R&D AREAS

- Bio-sciences
- Chemical Sciences
- Engineering Sciences
- Environmental Sciences
- Earth Sciences
- Materials Sciences
- Agro-technology & Rural Development

WATER TESTING/ANALYSIS

BACTERIOLOGICAL

- Bacteriological test of drinking water.

CHEMICAL

- pH, Total solids, Turbidity, Alkanity, Hardness, Calcium, Magnesium, Sulphate, Cloride & Iron.
- pH, Total solids, Turbidity, Alkanity, Hardness, Calcium, Magnesium, Sulphate, Cloride, Iron, Sodium, Potassium, Manganese and Zinc.
- pH and Iron.
- pH, Iron, Turbidity & Hardness.
- Iron only.
- Iron and pH.
- Silt (Silt of water sample).
- Each element outside above list.

OTHER TESTING/ANALYSIS

- Quality assesment of food products, edible oils, spices.
- Pesticides, fertilizer & soil.
- Building materials, cement, iron & steel, stones, timber.
- Oil & petroleum products, coal, minerals.
- Gems, stones.
- Fibre, paper, boards, garments.

FACILITIES AVAILABLE

- 300 MHz NMR, GC-MS, LCMS, FTIR, CHN & Sulphur Analyser.
- Interfacial Tensiometer for liq-liq and Solid-liq interfacial tension and contact angle.
- Atomic Absorption Spectrophotometer.
- XRD.
- Universal Testing Machine for determining engineering parameters of materials.
- Eirich Mixer R05T suitable for micro-pelletization and mixing.
- High temperature electrical furnace,1600°C, 50 lt cap.
- Laser diffraction particle size analyzer 0.04-2500 micron.
- Zeta Potential Analyser with autotitration.
- Thermal analyser for DTA, TGA & DSC.
- Atomic Emission Spectrophotometer (ICP-AES).
- Petro Minerological Microscope.
- Pilot Plant facility.

CONSULTANCY & TECHNICAL SERVICES

- Cultivation of medicinal and aromatic plants.
- Survey of medicinal, aromatic and economic plants.
- Designing of distillation units and specialised fabrication work.
- Geotechnical study & Foundation Design.
- Seismic survey.
- Hazard & safety analysis.
- Environmental impact assessment & Environmental management.
- Preparation of TEFR, etc.

HUMAN RESOURCE DEVELOPMENT

- Ph D Programmes in Biological, Chemical, Geo & Material sciences, Engineering sciences and Environmental sciences.
- Training programme in R&D areas.
- High skilled welding & fitter.
- Apprentiship in Workshop, Electrical and Electronics.
- Entrepreneurship development.
- Programmes for Science Motivation and CSIR. Youth Leadership in Science for High School students management.

For Details Contact

Director
North-East Institute of Science & Technology
Jorhat - 785006, Assam, India
Phone : (0376) 2370012 Fax : (0376)2370011)
Email : drrljt@csir.res.in & inform@csir.res.in
Website : www.rrljorhat.res.in & www.rrljorhat.com

Bioreactor

Banana fibre products

Mushroom Cultivation

Citronella Oil Distillation Still

Citronella Cultivation

VSK Mini Cement Plant

Connecting Science & Technology for A Brighter Tomorrow

Recognized Centre of Excellence for carrying out R&D, Consultancy, Training of Highway and Transportation Professionals and Documentation




OUR FIELDS OF SPECIALISATION

- Bridges & Structures
- Geotechnical Engineering
- Pavement Engineering & Materials
- Road Development Planning & Management
- Traffic & Transportation Planning

SPECTRUM OF ACTIVITIES

- Contract Research
  - Sponsored Research
  - Collaborative Research
- Consultancy Services / Technical Advices
- Testing and Calibration Services
- Preparation of Standards and Specifications
- Development of Guidelines
- Information Dissemination
- State-of-Art Reports
- Human Resources Development for Highway, Bridges and Transportation Engineering

CRRI

An ISO R&D Institution

For more details, please contact:

Dr. S. Gangopadhyay
Director
Central Road Research Institute
P.O.-CRRI, Mathura Road
New Delhi-110025
India

Ph: 91-11-26848917 / 26823437
Fax: 91-11-26845943 / 26830480
E-mail: director.crri@nic.in
Website: www.crridom.org

CENTRAL ROAD RESEARCH INSTITUTE
NEW DELHI

NATIONAL GEOPHYSICAL RESEARCH INSTITUTE
(Council of Scientific and Industrial Research)
HYDERABAD

An Institute dedicated to research in earth sciences and service to the society

The Institute has state - of - the - art research facilities and capabilities for Geophysical, Geological & Geochemical Investigations with a focus on R&D related to :

- **Exploration of Natural Resources with focus on Energy Security**
- **Shallow sub-surface geophysics for geotechnical applications**
- **Assessment and Management of Groundwater Resources**
- **Earthquake Hazard Assessment**
- **Lithosphere and Earth's Interior**
- **Geo-environment and Climate, Present and Past**

For more information, please contact –

The Director, National Geophysical Research Institute, Hyderabad - 500007

Telephone: +91-40-23434600 & 23434700 : Fax: +91-40-23434651 & 27171564

E-mail: director@ngri.res.in: **Website:** www.ngri.org.in

NIIST

An Institution of CSIR

National Institute for Interdisciplinary Science and Technology

(Council of Scientific & Industrial Research)

Thiruvananthapuram – 695019

An Interdisciplinary R&D Laboratory of CSIR having more than 30 years of reputation, devoted to the areas of Agroprocessing and Natural Products, Biotechnology, Chemical Sciences and Technologies, Materials and Minerals, Process Engineering, Environmental Technology and Computational Modeling.

***Services Offered:* Technical Consultancy, Contract Research, Analysis & Testing, Training and Human Resource Development programmes**

Important Programmes / Expertise

- Natural Products & Bioactive Molecules
- Value-Added Products from Clays / Beach Sand Minerals, Ilmenite beneficiation
- Speciality Polymers (Incl. Photo Polymers)
- Al & Mg Alloys, Composites and Functionally Graded Materials
- Advanced Ceramics and Nanomaterials
- Molecular / Organic / Inorganic Materials
- Technology for Turn-Key Implementation of Palm Oil Processing & Fresh Ginger Oil extraction and refining of rice bran oil
- Neutraceuticals and antioxidants
- Waste Water Technology
- Computational Modelling

Major Achievements / Technologies

- Technologies for Oil Seeds Processing & for Fresh Spice Oils
- Processes for Beneficiation of Clays & Clay Catalysts (Nano Catalysts)
- Technology for Production of High Grade Synthetic Rutile from Ilmenite
- Process for Alumina Sol-Gel Abrasives
- Process for Superconducting Substrates / Tapes
- Building Materials & structural materials Ceramics
- Flame retardant adhesives
- Technology for natural fabric composites
- Process for industrial enzymes
- RRL-T NC Driers
- Virtual Casting Software

For Further Details Please Contact:

The Director, National Institute for Interdisciplinary Science & Technology,Thiruvananthapuram – 695 019, Kerala, India

Telephone (091) 0 471- 2490674 / 2490811, Fax : (0471) 2491712 / 2490186

Email: director@niist.res.in / contact@niist.res.in

राष्ट्रीय पर्यावरण अभियांत्रिकी अनुसंधान संस्थान
नागपुर - 440 020

वर्ष 1958 में वैज्ञानिक तथा औद्योगिक अनुसंधान परिषद के अधीन इस संस्थान की स्थापना केंन्द्रीय जन स्वास्थ्य अभियांत्रिकी अनुसंधान संस्थान (सिफेरी) के रूप में हुई। वर्ष 1974 में तत्कालीन प्रधानमंत्री एवं वैज्ञानिक तथा औद्योगिक अनुसंधान परिषद की अध्यक्षा स्व. श्रीमती इंदिरा गांधी द्वारा इस संस्थान का नाम बदल कर राष्ट्रीय पर्यावरण अभियांत्रिकी अनुसंधान संस्थान (नीरी) रखा गया। वर्तमान में नीरी में लगभग 400 वैज्ञानिक, तकनीकी एवं प्रशासनिक कर्मचारी हैं तथा विभिन्न परियोजनाओं तथा पीएचडी आदि कार्य में लगभग 180 परियोजना एवं अनुसंधान अध्येता कार्यरत हैं।

नीरी का मुख्य परिसर 108 एकड़ में फैला हुआ है, जिसमें प्रयोगशालाएं तथा प्रायोगिक संयंत्र स्थापित हैं। परिसर काफी हरा-भरा है तथा कुल भूमि का लगभग चालीस प्रतिशत पेडों द्वारा आच्छादित है। संस्थान की पांच क्षेत्रीय प्रयोगशालाएं हैं, जो चैन्नई, दिल्ली, हैदराबाद, कोलकाता तथा मुम्बई में स्थित हैं। यह संस्थान विभिन्न साम-आर्थिक विकास कार्यों से उत्पन्न होने वाली पर्यावरणीय समस्याओं के प्रौद्योगिकीय हल उपलब्ध कराता है। तदनुसार इस संस्थान ने सामाजिक कल्याण के अपने अभियान की अपनी वचनबद्धता को पूरा करते हुए अनुसंधान एवं विकास के निम्नलिखित मुख्य क्षेत्रों में उल्लेखनीय योगदान दिया है:-

- पर्यावरणीय अनुवीक्षण
- पर्यावरणीय जैवप्रौद्योगिकी
- जोखिमकारी अपशिष्ट प्रबंधन
- पर्यावरणीय प्रणाली परिरूप एवं प्रतिरूप निर्माण तथा इष्टतमीकरण
- पर्यावरणीय प्रभाव एवं जोखिम मूल्यांकन
- पर्यावरणीय नीती विश्लेषण

संकल्पना

सतत विकास के लिए पर्यावरणीय विज्ञान तथा अभियांत्रिकी में प्रमुखता

लक्ष्य

नीरी एक ऐसे विश्व की कल्पना करता है।

जिसमें

- सभी इस प्रकार कार्य करें कि सतत पर्यावरणीय तथा आर्थिक लक्ष्यों की प्राप्ति सुनिश्चित हो।
- प्राकृतिक संतुलन बना रहे तथा सभी को स्वस्थ पर्यावरण का लाभ प्राप्त हो।

नीरी निरंतर प्रयत्नशील है

- पर्यावरणीय एवं प्राकृतिक स्त्रोत सम्बंधी समस्याओं के नवीन एवं प्रभावी हल उपलब्ध करवाने के माध्यम से मानवीय सेवा के लिए।
- सहभागियों के साथ कंधे से कंधा मिलाकर कार्य करते हुए पर्यावरणीय विज्ञान, प्रौद्योगिकी तथा प्रबंधन में राष्ट्रीय एवं वैश्विक स्तर पर प्रतिनिधित्व के लिए।
- सम्पूर्ण भारत में बेहतर पारिस्थितिकी सुनिश्चितता के लिए अपने साझेदारों के साथ मजबूत एवं प्रभावी कार्य-सम्बंधों के लिए।
- व्यक्तियों तथा संगठनों को समर्थ बनाने के लिए, जिससे कि सम्पूर्ण प्राणि जगत एवं मानवीय कार्यों के आधार पर प्राकृतिक स्त्रोतों का रचनात्मक एवं संयमित उपयोग हो।

पर्यावरणीय प्रौद्योगिकी में अभिनव परिवर्तन

अधिक जानकारी के लिए सम्पर्क करें :

निदेशक
राष्ट्रीय पर्यावरण अभियांत्रिकी अनुसंधान संस्थान
नागपुर - 440 020 (भारत)
फैक्स - 0712-2249900
ई-मेल : director@neeri.res.in
वेबसाईट - www.neeri.res.in

GOODWILL
CRYOGENICS ENT

Sales @ goodwillcryogenics.com

CRYO-CON®

State of the Art,High-Technology

Cryogenic Controllers - (1K to 800K)

(The Highest Standards of Accuracy, Stability & Controllability)

DIGITAL TECHNOLOGY, 32-Bit Processor; PID(Manual and Autotune), 4- Channel Input, 6-Digit Display, RS232, IEEE & USB interface; AC & DC Excitations, Usuable with all Diodes, Resistors & TC Standard sensors of all makes, (Front Panel Selectable, - NO INPUT CARDS), Dual Heater output, and many more features not available in branded controllers

NIST Traceable & CE Certified.

(LOOK FOR BETTER QUALITY AND FORGET BRANDED NAMES !!!)

Mfr. BY: Cryogenic Control Systems - California USA

All India Representatives : GOODWILL Cryogenics Ent. - Vashi (Navi Mumbai)

(Beware of the Impostors)

Sensor Type	Silicon Diode	100Ω Platinum DIN43760	1000Ω Platinum DIN43760	Ruthenium Oxide	Carbon Glass	Cernox	Thermocouple
Temperature Measurement Accuracy	300K: 8.7mK 77K: 12mK 4.2K: 1.6mK	800K: 6.7mK 300K: 6.2mK 77K: 2.8mK 30K: 6.3mK	600K: 10mK 300K: 10mK 77K: 1.1mK 30K: 2.5mK	2.0K: 0.1mK 4.2K: 0.4mK 20K: 7.4mK	4.2K: 0.07mK 77K: 3mK 300K: 31mK	4.2K: 0.1mK 77K: 22mK 300K: 9mK	4.2K: 2.6K* 300K: 60mK* 1500K: 70mK*
Control Stability	300K: 3.0mK 77K: 3.8mK 4.2K: 500µK	800K: 5.1mK 300K: 4.7mK 77K: 1.1mK 30K: 2.4mK	600K: 4mK 300K: 4mK 77K: 0.5mK 30K: 1.0mK	2.0K: 32µK 4.2K: 0.13mK 20K 2.9mK	4.2K: 80µK 77K: 1.2mK 300K: 12mK	4.2K: 80µK 77K: 0.85mK 300K: 3.5mK	4.2K: 0.5K* 300K: 11mK* 1500K: 13mK*

SPECIALISE INSTRUMENTS MARKETING COMPANY

305, Kailas Industrial Complex, A-wing 3rd Floor, Building No.2,
Parksite Vikhroli (West), Mumbai-400 079. (INDIA)

INSTRUMENTATION SOLUTIONS FOR ACADEMIA, INDUSTRY AND SCIENTIFIC APPLICATION AND HARDWARE SUPPORT

Quantum Design U. S. A

VSM, SQUID VSM, MPM & PPM Systems

- Versalab Cryo-free VSM, 3 Tesla, 50 - 400K, sensitivity 10^{-6} emu/rt-H
- MPMS Squid VSM, sensitivity <10^{-8} emu with only 4 second data averaging
- MPMS integrates a SQUID detection system, a precision temperature control unit and a powerful software control operating system.
- PPMS are designed for fields up to 16 Tesla and temperature range in 1.9-400K

MicroSense

VIBRATING SAMPLE MAGNETOMETERS

- Resistive Magnet VSM with highest fields and higher sensitivity
- Accurate true Torque Magnetometers
- Fastest , most accurate field control in conjunction with temperature control

AMI

Superconducting Magnet Systems

- Superconducting magnet sytem upto 16T.
- Cryogen Free superconducting magnet system.
- High field upto 16T and spilt coil system.
- Liquid helium and nitrogen level instruments.

CRYOMECH

Cryogen plants

- Liquid helium Plant ,
- LHeP12 produces ≥ 12 liters/day, Dewar Capacity: 60 liters
- LHeP18 produces ≥ 18 liters/day, Dewar Capacity: 120 liters
- Liquid Nitrogen plant
- 10,20,40,60 and 120 liters per day
- Water or air cooled.
- Cryocoolers: Closed cycle and pulse tube

MONTANA INSTRUMENTS COLD SCIENCE MADE SIMPLE

Cryostation

- Intimate access to the stable sample
- Vary temperature without sample drift
- Vibrations are no longer a concern
- Keep samples and optics clean
- Run on low power

Sample Holders

ATTOCUBE SYSTEMS

Nanopositining and Microscopy

- Atomic force microscope
- Magnetic force Microscope
- Scanning Tunneling Microscopy.
- Scanning Hall Probe Microscope.

Emmtech Calibration

We Introduce our self **Emmtech Calibration Laboratory** is a measuring instruments and Gauges calibration Lab. Our laboratory is accreditated by **"National Accreditation Board for Testing & Calibration Laboratories" (N.A.B.L),** Department of Science & Technology as per IS/ISO/IEC 17025-2005 standard. We have the accreditation in three disciplines, Mechanical (Cert. No. C-0347), (Length, Angle, Flatness, Straightness, Mass, Volume, Density, Pressure, Vacuum, Acoustic & Speed), Thermal (Cert. No. C-0441), (Temperature -40 to 1200°C & Relative Humidity 10 to 95%) and Electro-Technical (Cert. No. C-0510), (AC/DC Voltage, AC/DC Current, Frequency, Power/Energy, Time, Capacitance, Resistance, Inductance & Lux).

Laboratory is committed to total customer satisfaction through reliable, accurate and timely service in the field of calibration which meets their requirements and expectations in terms of quality. The management committed to comply the internal standard IS/ISO/IEC 17025-2005 and continuously improve the effectiveness of the management system.

Our Laboratory is well equipped and skilled engineers are ready to assist our customers at any time. We have a facility of calibration of measuring instruments and gauges as per customer requirements. All staff having training in their relevant field to improve our quality or meet the customer requirements.

Besides calibration we are providing our services in the field;

- Consultancy of IS/ISO/IEC-17025-2005 (Documentary as well as practical as per our resent scope).
- Work shop and desktop trainings.

Contact us:

Emmtech Calibration

D1/90, Sanjay Colony, NIMS Hospital Road, Sector -23, Faridabad. (Haryana)

0129-4124942, 09811787807, 09654373931, 9873837164 & 9999493636

For further details visit our website www.emmtech.in , for any enquiry mail us on our mail I.D. emmtech123@yahoo.co.in , emmtechcalibration@yahoo.co.in & info@emmtech.in

Our Cryogenic Products

DEWAR FLASKS

Refrigeration System

Diode Temperature Sensor

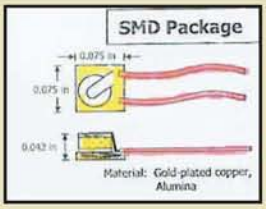

Multifilament

Superconducting Wire
NbTi, Nb_3Sn
Matrix : Cu/Resistive

LIQ. He Transfer Line

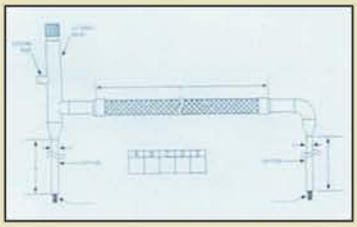

Flexible U Tube with Right Angle Shutoff Valve

Liquid Helium Conainers

CMSH 60-5000 Litre

Self-Pressurizing LN2-Containers

Horizontal Container

Cryogenic Temperature Monitor
Model 18

Hi-Tech, Cryo-Temp. Controller
Operation from <100mK over 1020K

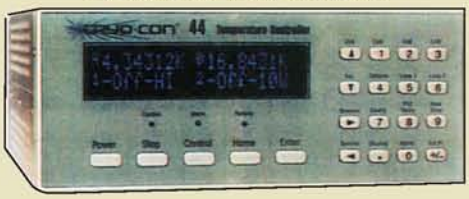

GOODWILL
CRYOGENICS & INSTRUMENTATION

213, Nirmal Vyapar Kendra, Sector-17, Vashi, Navi Mumbai-400 703
Email : sales@goodwillcryogenics. com; gecryo@gmail.com

NATIONAL PHYSICAL LABORATORY

IN SERVICE OF THE NATION

The National Physical Laboratory is a dynamic research institute working in the frontier areas of materials, measurements, radio and atmospheric sciences with the state of the art facilities and highly experienced scientific and technical staff.

MANDATE

The main aim of the laboratory is to strengthen and advance physics-based research and development of science and technology in the country, with specific objectives as listed below:

a) To establish, maintain and improve continuously by research, for the benefit of the nation, the National Standards of Measurements and to realize the Units based on International system.

b) To identify and conduct, after due consideration, research in areas of Physics, which are most appropriate to the needs of the nation and for the advancement of the field.

c) To assist industries, national and other agencies in their developmental tasks by precision measurements, calibration, development of devices, processes and other allied problems related to physics.

MAJOR RESEARCH AREAS

METROLOGY:

- Realization of Base and Derived units.
- Apex level calibration of Physico-mechanical and Electrical & Electronic Standards
- Chemical Metrology including CRM's

MATERIALS:

- Light weight, high strength metallic materials & Composites
- Advanced Carbon Products
- Cryogenics, Superconductivity and Superconducting devices
- Conducting Polymers & Composites
- Organic Electronics – OLEDs, OPVs
- Liquid Crystals & Display Devices
- Luminescent Materials
- Nano materials including nano-composites
- Photovoltaics
- Sensors (Bio, Gas, Chemicals & MEMS)
- Advanced Characterization

RADIO & ATMOSPHERIC SCIENCES:

- Ionosphere & Troposphere
- Global Climate Change
- Antarctica & Arctic Studies
- Radio Propagation
- Communications (Mobile)

THE GLOBAL R& D PLATFORM

- National Metrology Institute
- Academic Research Institute
- Materials Development Institute
- International Collaboration Partner

SOLUTION PROVIDER TO THE INDUSTRY

- Calibration & Testing Services
- Material Characterization Services
- National Time Services
- Consultancy Services
- Contract/Sponsored Research Projects

Director: Prof. R.C. Budhani

NATIONAL PHYSICAL LABORATORY

(Council of Scientific & Industrial Research)

Dr. K.S. Krishnan Marg, New Delhi-110012

Ph. : +91-11-45609201, 45609301; Fax: +91-11-45609310

Email : dnpl@mail.nplindia.ernet.in Visit us at: www.nplindia.org

In service of the nation for 45 years
Our motto –
"Safety to Environment & Health and Service to Industry"

The laboratory through its scientific expertise provides complete facilities for toxicological research, environmental and health risk assessment as well as analysis and testing services conforming to Good Laboratory Practices using NABL and international guidelines employing latest test systems, biomarkers, analytical instruments and mathematical models.

Services offered

- Health and Environmental Monitorng
- Consumer SAfety
- Toxicity Testing
- Analysis
- Information Database
- Environmental Impact Assessment
- Consultancy
- Hazardous Waste Disposal
- Environmental Management Plan
- Health Status of Occupational Workers
- Preparedness of Disaster Management

Technologies Developed/Available

- Water Analysis Kit
- Mobile Laboratory Van for on spot Water quality analysis
- Argemone Detection Kit-For rapid sceeening fo Argemone in mustard Oil
- CD-Strip - For detection of butter yellow an adulterant in edible oils
- Arsenic Detection Kit

INDIAN INSTITUTE OF TOXICOLOGY RESEARCH
(Formerly - Industrial Toxicology Research Centre)
Post Box No. 80, Mahatma Gandhi Marg, Lucknow- 226001
Phone: 0522 - 2627586/ 2613786/ 2611547; Fax:0522-2611547/2628227
E-mail: rpbdiitr@yahoo.com Website: www.iitrindia.org

IR TECH

Rigaku

SmartLab
X-RAY DIFFRACTOMETER

LECO

OLYMPUS

MILESTONE
MICROWAVE
LABORATORY SYSTEMS

CLAISSE

INNOV-X SYSTEMS
Innovative XRF Technologies

Linn High Therm

MOA Instrumentation International

O·I·Analytical

SUGA

Rapiscan systems

IR TECH

I R Technologies Services Pvt. Ltd.

A69, Sector 2, NOIDA 201301, UP

Ph: 0120 4530800 Fax: 0120 4320881 email: sales_del@irtech.in

----------Other Offices ----------

Mumbai	*Bangalore*	*Kolkata*	*Hyderabad*
EL-91, TTC Indl Area, MIDC, Electronic Zone, Mahape, Navi Mumbai, Maharashtra 400710 Ph: 022 41571111 Email: sales_bom@irtech.in	208, Swiss Complex, Race Course Road Bangalore, Karnataka 560001 Ph: 080 22203173 Email: sales_blr@irtech.in	22, Ashutosh Chowdhury Avenue, Flat No. 12, 1st Floor Kolkata, West Bengal 700019 Ph: 033 24615831 Email: sales_cal@irtech.in	406, Agarwal Chambers, 5-9-1121 King Kothi Hyderabad 500001 Ph: 040 66842402 Email: irtech_hyd@vsnl.net

Please visit our Website: www.irtech.in

CLRI – World's Largest Leather Research Body
A Dependable Source for Technologies & Services

Knowledge Basket

- Leather Processing
  - Lime/sulfide free dehairing
  - Bio-processing for leather making
  - Multitone Dyeing
- Leather Chemicals
  - Mineral Syntan
  - Vegetable / Non-mineral /Protein based Syntan
  - Fatliquors
  - Finishing Auxiliaries
- Enzymatic products for application in eco-friendly leather processing
- Environmental technology
  - For removal of TDS, E.Coli., dissolved organics
  - Water/Effluent treatment
  - Secured Landfill
- Devices
  - For Leather Processing
  - 2-D Testing
- Value added products from wastes
  - Parchment like material from Chrome shavings
  - Leather like sheet using buffing dust
  - Dog Chews & Animal Feeds
- Health Care Products
  - Wound healing
  - Bone related
  - Ophthalmic Applications
- Products
  - Novel insole Sheet
  - Carbon Nano Tubes
- Softwares
  - INNOEST-Innovative Footwear Norms Estimator
  - SWAD- a Software for Anaerobic Digester Designer
  - PRETREAT, Design Software for Pretreatment System in Tanneries

Knowledge leads are IP protected in India and Abroad

Range of Consultancy Services

- Waste water Treatment & Environmental Audit
- Industrial Safety & Risk Consequences
- Design of Leather Complex and preparation of Techno Economic Feasibility Reports
- Designing ETPs / CETPS
- Technology Forecasting and Planning
- Survey and Assessment of resource potentials
- Database for Indian Leather Sector
- Creative Leather Product Design & Fashion Forecasting

Education & Training Programmes

- UG and PG Programmes in Leather and Footwear (In association with Anna University, Chennai)
- Vocational Training Programmes in Leather Goods, Garments & Footwear
- Executive Training Programmes
- Specialized Programmes for International Participants

State-of-the-art Testing Facilities

- Testing Eco-Sensitive Chemicals
- SATRA Accredited lab for physical testing of leather / footwear

New Millennium Indian Technology Leadership Initiative (NMITLI)

- Paradigm shift in Leather manufacture from chemical to bio-processing
- CLRI provides expertise in lead selection and coordination
- Ambient preservation, enzyme only processing and microbial reduction of sulfate to sulfur in tannery effluents form themes

CLRI - The Implementing Agency for IDLS / HRD Mission / Global Benchmarking Schemes of Govt. of India

Striving for Excellence and Global Leadership in Leather Technology

For details contact: The Director,
Central Leather Research Institute
(Council of Scientific and Industrial Research)
Adyar, Chennai-600020, India
Phone: 044-24910846 / 24915238 Fax: 044-24912150 / 24911589
E- Mail: bpdclri@yahoo.com / bpd@clri.res.in
URL: www.clri.nic.in

Core Competency :

- Mineral Processing
- Metal Extraction
- Materials Characterisation
- Materials Evaluation
- Materials Forming & Processing
- Corrosion Testing & Prevention
- Waste Utilisation
- Standard Reference Materials & Hall Making
- Intellectural Property Acquisition
- Knowledge Management

NML has been offering its R&D Products, Processes and Expertise to the Industries in the form of Design, Consultancy, Technical and Testing Services.

ISO 9001 : 2000

For further details :
DIRECTOR
NATIONAL METALLURGICAL LABORATORY (NML)
(Council of Scientific & Industrial Research)
Jamshedpur 831 007, India
Phone : 91 657 2345028 / 2345220
Fax : 91 657 2345213
e-mail : director@nmlindia.org
Website : www.nmlindia.org

CSIR - INDUSTRY PARTNERSHIP

BELZ INSTRUMENTS PVT. LTD.

Presents

RELATIVE HUMIDITY GENERATOR / CALIBRATION SYSTEM

CSIR/NPL KNOW-HOW

CSIR THROUGH NPL GRANTED LICENCE OF TECHNICAL KNOW-HOW TO MANUFACTURE & MARKET RELATIVE HUMIDITY GENERATOR/CALIBRATION SYSTEM. THIS IS FIRST INDIGENONSLY DEVELOPED RH GENERATOR & IS A IMPORT SUBSTITUTE

- ★ LOW COST
- ★ NO CONSUMABLE
- ★ HIGH PRECISION

RELATIVE HUMIDITY GENERATOR

RELATIVE HUMIDITY, CALIBRATION SYSTEM

SPECIFICATIONS:		
RH Range	:	15% to 95% RH
Uniformity	:	+/-1% RH
Stability	:	of the order of 20 minutes
Technology	:	Two-Pressure Technique
Carrier Gas	:	Nitrogen or Air

APPLICATION :

Relative Humidity Generator & Calibration

Wide application in Agriculture, Pharmaceutical, Air Conditioning, Calibration Laboratories etc.

Manufactured by:

BELZ INSTRUMENTS PVT. LTD.

132,133, 134A, HSIDC Sec-59, Faridabad-121004 Ph. : 0129-2307994, 2307060
E-mail: belz@airtelmail.in Website : www.belzcallab.com

STIRLING
CRYOGENICS

Liquid N_2
Where you need it, when you need it

Laboratory Gases
Plug and produce
high purity laboratory gases

CRYOZONE
THE CRYO CREATIVES

for special cryogenics needs

L'genie
LN2 transfer pump

Stirling Cryogenics India Pvt. Ltd., 6th Floor Ambadeep Building, 14 Kasturba Gandhi Marg,
New Delhi 110001, India
Tel.: +91 11 435 27000-19, Fax: +91 11 435 27020/21, info@stirlingcryogenics.in www.stirlingcryogenics.in

Central Electronics Engineering Research Institute
Pilani (Rajasthan)

Serving the Country since 1953 through:

- Technology Development
- Sponsored/Contract R&D
- Consultancy
- Specialised Training

In the areas of

- MEMS and Microsensors
- VLSI Design
- LTCC Technology
- Nanoelectronics/Nanostructures
- Agrielectronics & Instrumentation
- Embedded Systems
- Optoelectronic Devices
- Microelectronic Processing & Fabrication
- Microwave Tubes
- Industrial Process Control
- Power Electronics

DEVICES AND TECHNOLOGIES DEVELOPED

- C-band High-power MESFETs and Amplifiers, 980nm Pump Laser diode, InP-InGaAs based PIN Photo Detectors, Bulk Micro-machined Double Ring Capacitive Pressure Sensor, Surface Micro-machined Poly Capacitor Pressure Sensor, P-MOSFET Gamma-ray Dosimeter, 16/32-bit Microprocessor VLSI using VHDL, Application Specific Instruction-set Processor Design, Re-configurable System Design, Hybrid Microcircuits (HMCs) for SROSS and INSAT series of Satellites, ISFET based PH Sensor, Selective Ion sensors, Biosensors, MEMS Acoustic Sensors, MEMS Ultrasonic Transducers, Silicon Carbide Schottky Diode Detectors, MEMS Hotplate, Low Temperature Co-fired Ceramic Technology based Microwave Circuits
- S-band 400 W Carcinotron, S-band 500 kW Magnetron, S-band 1 MW Magnetron, 2 MW S-band Tunable Pulsed Magnetron, 3 MW Pulsed S-Band Magnetron, C-band 75 kW CC-TWT, Broadband 40 W Mini Helix TWT, S-band 30 W Helix TWT, 60 W Space TWT, 6 GHz 20 W Helix TWT, 5 MW Pulsed S-band Klystron, 6 MW Pulse 24 kW Average Power S-Band Klystron, Design and Technology Development for Gyrotron Devices, 25 kV 1 kA Thyratron, 40 kV 3 kA Thyratron, Long-life Dispenser Cathodes, High-power Microwave Window Technology, Related Infrastructure & Technologies, Software packages
- High-power ac and dc Drives, Converters/PWM Actuators, Withering Controls for Tea Processing, Process Control Instrumentation for Sugar Industry, Electronic System for Composting and Cropping Processes of Mushroom, Monitoring and Control System for Paper and Pulp Industry, DIGIMAP, Machine Vision Systems for On-line Sorting and Grading of Fruit, NICAM Receiver, Machine Vision Systems for Bakeries and Steel Mills, Controlled Atmosphere Storage Systems, Electronic Instrumentation for Fresh Water Acqua-culture and RO Systems, NIR-based Instrumentation for Chemometrics, Electronic Tongue, Electronic Nose, Wired and Wireless Communication Network for Underground Mines, Sensor Networks, Specialised Power Supplies and Pulse Power Systems

SERVICES OFFERED

- Mask making, Semiconductor/MEMS Technology Development and Device Prototyping, Unit Process Development and implementation, Consultancy/Industrial Training/Training for Academic Faculty and PG Students in the areas of Semiconductor Technology, VLSI Design (digital, analog and mixed signal), MEMS Technology, Mechatronics and Embedded System Design
- ME/M Tech project work and doctoral thesis work for highly motivated university students in all the above areas of electronics

For further details please contact:

Director, Central Electronics Engineering Research Institute, Pilani (Rajasthan) – 333 031
Tel: 91+1596-242111 Fax: 91+1596-242393 E-mail: director@ceeri.ernet.in www.ceeri.res.in

Tata Institute of Fundamental Research

Homi Bhabha Road, Mumbai 400005, India

About Us

Tata Institute of Fundamental Research is a premier research institute in the country working in areas of basic sciences encompassing most fields in biology, chemistry, computer science, mathematics and physics.

The Science Popularisation and Public Outreach Committee of TIFR develops programmes which will serve the following purposes

- Informing students and general public about the research work being done at TIFR.
- Providing a platform for the teaching community to participate in continuing education and research to improve their professional skills.
- Inspiring students to pursue a career in basic sciences.
- Informing the public about the latest trends and developments in scientific research.
- Conveying the importance of exciting new developments in science and technology.
- Providing authentic information to journalists and science writers etc.

This activity is an important part of TIFR's commitment to the community.

For more details about us Kindly visit our web site

http://www.tifr.res.in

INSTITUTE OF GENOMICS & INTEGRATIVE BIOLOGY

(Council of Scientific & Industrial Research)
Mall Road, Delhi- 110007
Website: http://www.igib.res.in

IGIB
Institute of Genomics & Integrative Biology
Genomics Knowledge Partner

PRINCIPAL AREAS OF R & D
- Allergy & Infectious Diseases
- Functional Genomics
- Molecular Medicine
- Genome Informatics
- Pharmacogenomics
- Proteomics, Structural Biology
- Comparative Genomics
- Gene Expression
- Recombinant DNA products
- Nucleic Acids, peptide Chemistry
- Environmental Biotechnology

KNOW-HOW AVAILABLE
www.igib.res.in/technologies.htm

Healthcare
- Aspergillosis diagnostic kit (antigen & synthetic peptide based)
- Pharmacogenomics leads (Asthma, schizophrenia)
- Novel antibacterial drug targets.

Environmental applications for:
- Bio-neutralization of waste water
- Bio-treatment of palm oil Mill effluent
- Bio-bleaching of wood pulp
- Biosensor for BOD estimation
- BODSEEDS - reference seeding material for BOD analysis
- BODBEADS - reference instant seeding material for BOD analysis

For queries please contact::
Mr. P.Bansal
Convenor, BDMG,
IGIB, Mall Road, Delhi 110 007
email: pbansal@igib.res.in
Phone: 011- 2766 7310
Board : 011-2766 7602/7439, 6156/7
Fax: 011- 2766 7471

SALIENT HIGHLIGHTS
- Largest computing facility (4 Tflop/s) in Asia outside Japan (Ranked 158th among the World's Top 500 Super Computers)
- First CSIR Institute to market bioinformatics software based on in-house R&D
- A Member of the Consortium of Leading Global Players engaged in research related to Functional Genomics
- Involved in the Pan-Asian Initiative - Study Genetic similarities & Diversities in Asia
- Successful track record of PPPs and Business Models

NEW VISTAS IN OFFING
- Setting up bio-incubator facility for scientist entrepreneur and start-up companies to nurture ideas, concepts & provide a platform for commercialisation of products / processes
- Partnering with Leading Agencies to provide Virtual Training Programs in Bioinformatics

GENOME JUNCTION @ IGIB
- A major network program on Disease Genomics with focus on Respiratory, Neurological and Psychiatric Disorders.
- G.N.Ramchandran Knowledge Centre for Genome Informatics for the Development of Novel Bioinformatics Software.

GENOCLUSTER@IGIB

Developed in association with Jubja Technologies, Bangalore Under NMITLI Program of CSIR

Development of High Throughput-SNP, Sequencing & Screening - HT-SSS

Developed with M/s Silicogene, Kolkata

UNVEILING NEW VISTAS THROUGH EXTENDED BIO-SERVICES

National Facility for Biochemical & Genomic Resources (NFBGR) provides:
- Monthly Import Facility (Avail the benefit of consolidated airfreight)
- Buffer Stock Facility (Off-the shelf availability of chemicals on credit)
- Supply of chemicals/ consumables in INR from Leading Global Suppliers

Contact: In-charge, NFBGR, IGIB Email: pbansal@igib.res.in

The Center for Genomics Applications (TCGA) www.tcgaresearch.org
An IGIB-IMM public private partnership Project for providing services in Genomics & Proteomics applications at competitive cost covering:
- High Throughput genotyping and DNA sequencing
- Oligonucleotide synthesis and Micro array services

Contact: Head (Operations), TCGA,
254 Okhla phase III, New Delhi-20

Keep abreast of the latest developments in basic and applied scientific research

NISCAIR, CSIR Journals

Annual Subscription Rates w.e.f. 1st January 2011		Annual Subscription Rates: India [₹]	Annual Subscription Rates: Other Countries [US $]
1. Journal of Scientific & Industrial Research	(Monthly)	3600.00	650.00
2. Indian journal of Chemistry Section A	(Monthly)	4600.00	800.00
3. Indian Journal of Chemistry Section B	(Monthly)	4600.00	800.00
4. Indian Journal of Experimental Biology	(Monthly)	4600.00	800.00
5. Indian Journal of Pure & Applied Physics	(Monthly)	3200.00	550.00
6. Indian Journal of Chemical Technology	(Bimonthly)	1600.00	300.00
7. Indian Journal of Engineering & Material Sciences	(Bimonthly)	1600.00	300.00
8. Indian Journal of Biochemistry & Biophysics	(Bimonthly)	1900.00	330.00
9. Journal of Intellectual Property Rights	(Bimonthly)	3000.00	720.00
10. Medicinal & Aromatic Plants Abstracts	(Bimonthly)	3600.00	720.00
11. Indian Journal of Radio & Space Physics	(Bimonthly)	1600.00	300.00
12. Indian Journal of Biotechnology	(Quarterly)	1200.00	220.00
13. Indian Journal of Fibre & Textile Research	(Quarterly)	1600.00	300.00
14. Indian Journal of Marine Sciences	(Quarterly)	1600.00	300.00
15. Indian Journal of Traditional Knowledge	(Quarterly)	1200.00	220.00
16. Indian Journal of Natural Products and Resources	(Quarterly)	1200.00	270.00
17. Annals of Library & Information Studies	(Quarterly)	1200.00	140.00
18. Indian Science Abstracts	(Fortnightly)	5300.00	1100.00
19. CSIR News	(Fortnightly)	500.00	-
20. भारतीय वैज्ञानिक एवं औद्योगिक अनुसंधान पत्रिका (हिन्दी) *Bhartiya Vaigyanic Evam Audhyogik Anusandhan Patrika (Hindi)*	(अर्ध - वार्षिक) (Half-yearly)	400.00	60.00

Orders may be placed by sending Cheques/DD payable to NISCAIR, New Delhi*

* For inland outstation cheques, please add ₹50/-
For foreign cheques, please add US $10 as Banking charges.

For prompt delivery of publications, please remit payment by Demand Draft

Mailing Address:

Senior Sales & Distribution Officer
National Institute of Science Communication and Information Resources [CSIR]
Dr. K. S. Krishnan Marg, Near Pusa Gate
New Delhi 110 012
India

Phone: 011-25846301-7[extn-291/288/287] ; 011-25843359 Fax: 011-25843359
E-mail: sales@niscair.res.in

Website: www.niscair.res.in

National Accreditation Board for Testing and Calibration Laboratories

Department of Science and Technology (DST), Government of India

The Government of India has authorized NABL as the accreditation body for testing and calibration laboratories. NABL is a registered society under the Societies Registration Act 1860. It operates as an autonomous body under the aegis of In the Department of Science and Technology (DST), Ministry of Science and Technology, Government of India.

NABL Accreditation

NABL has been established with the objective of providing Government, Industry Associations and Industry in general with a scheme of laboratory accreditation which involves third-party assessment of the technical competence of testing and calibration laboratories.

The laboratory accreditation services to testing and calibration laboratories are provided In accordance with ISO/ IEC 17025: 2005 'General Requirements for the Competence of Testing and Calibration Laboratories' and ISO 15189: 2007 'Medical laboratories - Particular requirements for quality and competence'.

Benefits of NABL Accreditation

- Enhanced customer confidence and satisfaction.
- Enhanced business and Improved confidence
- Provides traceability in measurements to national standards
- Reliability of data for R&D
- Insurance companies can rely on test results
- Ensures better support in the event of legal case

International Acceptance through NABL Accreditation

NABL maintains linkages with the international bodies like International Laboratory Accreditation Co-operation (ILAC) and Asia Pacific Laboratory Accreditation Cooperation (APLAC). NABL Is signatory to ILAC as well as APLAC Mutual Recognition Arrangements (MRA), which is based on mutual evaluation and acceptance of other MRA Partner laboratory accreditation systems. Such international arrangements make foundations for acceptance of test/ calibration results between countries which MRA partners represent.

Contact:

NABL Secretariat

National Accreditation Board for Testing & Calibration Laboratories3rd Floor, NISCAIR Building, 14, Satsang Vihar Marg, New Mehrauli Road, New Delhi – 110067 (India)Tel.: 91–11–46499999, Fax: 91–11–26529716, E-mail: Info@nabl-India.org

Jawaharlal Nehru Centre for Advanced Scientific Research

Jakkur, Bangalore-560 064,

Jawaharlal Nehru Centre for Advanced Scientific Research (JNCASR) is a multidisciplinary research institution with a **mandate to pursue and promote research and training** at the frontiers of science and engineering. Established in 1989 to commemorate the birth centennary of Pandit Jawaharlal Nehru, it has come to be associated with high quality research and innovative science outreach activities.

Research at the Centre is focused on three key branches: **materials science, fluid mechanics and biology.** The pursuit of such diverse topics in a relatively small institution lead naturally to cross-disciplinary collaborations.

JNCASR is one of the world's leading centres of research on nanoscopic forms of matter. Several new forms of carbon and other inorganic compounds have been synthesized and their novel electrical, thermal, magnetic and optical properties, arising out of their nanoscale, studied. Experimental research in the center, on novel materials, is carried out in close collaboration with both theoretical and computational efforts. Transport processes, occurring at scales larger than atomic, in a whole spectrum of complex fluids and flows is another **important research discipline at Centre.** We have also examined fundamental questions posed in the context of an organism embedded in its ecology and shaped by evolution. Using tools, techniques, and information from a variety of disciplines, we carry out primarily empirical research to address questions in the areas of adaptive evolution, developmental evolutionary biology, chronobiology, animal behaviour, neurogenetics, and phylogeography. One of the major thrust areas of research in this centre is biomedical science to improve human health. We focus on basic problems that deal with a range of diseases including genetic, infectious and non-infectious diseases.

As a relatively young member of the scientific research fraternity, JNCASR has made its presence felt in the scientific world through high quality research publications, patents, and in the society at large, through its many **outreach programmes,** including the summer research programmes for under- and postgraduate students, the innovative project based chemical and biological education programmes, respectively, for undergraduate students, and many activities designed to share the excitement of science with schoolchildren.

Research facilities at the Centre are at par with any in the world in terms of technology as well as in the ambience. The Centre, is, in addition, recognized as a Deemed University. **The faculty-to-student ratio is 1:4,** making it an ideal place for a budding researcher to receive the finest guidance and exposure available.

JNCASR actively promotes networking among researchers and collaborations. The International Centre for Materials Science is the first body of its kind in India. Set up to facilitate the exchange of ideas as well as human resources, it attracts some of the finest international talent. The Nehru Centre has **active collaborative programmes** with institutions such as NIMS, Japan, Purdue and Northwestern Universities, US.

As a forum for the exchange of scientific thought, and a research facility that seeks to inspire and encourage scientists, JNCASR has a reputation that far outweighs its years of existence. The Centre's focus on selected advanced areas of research, underlines its contemporaneity.

INSTITUTE OF HIMALAYAN BIORESOURCE TECHNOLOGY

ISO 9001: 2000 certified lab by DNV (RvA)
a constituent lab of Council of Scientific & Industrial Research
Post Box No.6, Palampur (H.P.) – 176061, India

Providing R&D services on economic bioresources in western Himalayan region leading to value added plants, products and processes for industrial, societal, and environmental benefits

Thrust Areas : Biodiversity mapping & conservation; Plant genomics & metabolomics; Tea sciences; Floriculture; Plant health management; Chemical characterization; Value addition and product development.

National Recognition : Bioresource Development Unit (NBDB, DBT, GOI)

Recognised as a National facility for virus indexing of ornamental plants.

Recognised as a National Centre for Pesticide residue analysis of tea

Technologies Developed

- Varieties Damask Rose (Himroz and Jwala); Gladiolus; Tagetes (Himgold); *Valeriana jatamansi;* (Himbala); *Hedychium spicatum* (Himkachri),' *Curcuma aromatica* (Himhaldi).
- Recombinant enzymes Superoxide dismutase, Polyphenol oxidase, Catalase, Ascorbate peroxidase
- Processes Stevioside, Ascein, Vanillin, 4-Vinyl guaiacol, Analogue of natural whisky lactone, Tea wine, Ready to drink tea, Theaflavin, Natural yellow & red dye
- Cosmetics & health care products UV protection cream, Moisturizing lotion, Rose talc, Body lotion, Tooth picks, Pain balm
- Equipments / machines Mini-Distillation Unit, Tea Leaf Plucking Machine, Tea Withering Machine, Steriflow (Mini Laminar Flow Unit), Gel Transfer Device, Rooting Vessel.
- Protocols Micropropagated Bamboos, Tea, Rose, Lilies, Orchids etc.
- Agrotechnologies Tea, scented rose, geranium, lavender, *Tagetes minuta,* lilies, Alstroemeria, Bird of Paradise, Chrysanthemum etc.

Services : Project Formulation and Evaluation, Consultancy Services, Collaborative Research, Turnkey Ventures, Plant Virus Testing, Chemical Analysis of Aromatics and Herbals, Training and HRD.

Contact :
Dr. P.S. Ahuja, Director
Phone: (91-01894)230411, Fax: (91-01894) 230433
E-mail: director@ihbt.res.in; Website http://www.ihbt.res.in

ADVANCED MATERIALS AND PROCESSES RESEARCH INSTITUTE (AMPRI)

Council of Scientific and Industrial Research
BHOPAL

Major R&D Areas

Light Weight Materials
Natural Fibers and Composites
Industrial Waste Utilization

FRP Gear Case

MATERIALS CHARACTERIZATION & DEVELOPMENT

Instant House

Al MMC Brake Drum

- Metal Matrix Composites
- Natural Fiber Composites
- Industrial Wastes Utilization
- Building Materials
- Nano Materials

Redmud Furniture

Blast Resistant Panel

Radiation Shielding Material

Zn-Al Bush

FEM of Piston Block

COMPUTER SIMULATION & PROCESS MODELING

Extruded Tubes

- Process Modeling
- Electro Magnetic Forming
- Computer Simulation & Design
- Natural Resources
- Environment & Disaster Modeling

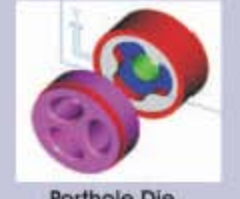

Porthole Die

Process Modeling Map

www.ampri.res.in

Contact :
Director
Advanced Materials and Processes
Research Institute (AMPRI)
Bhopal 462 064, M.P., India
Tel : +91-755-2457105 Fax: +91-755-2457042
Email: director@ampri.res.in

THERMAL CONSTANTS ANALYSER

Hot Disk®

The Hot Disk® Thermal Constants Analyser for quick and accurate measurement of Thermal Conductivity, Thermal Diffusivity and Heat Capacity in a wide variety of materials.

MODEL TPS 2500 S

- Model TPS 2500 S is a new improved R&D instrument designed for analyzing thermal transport properties.
- The TPS 2500 S meets ISO Standard.
- The patented TPS technique is used to simultaneously determine thermal conductivity, thermal diffusivity and specific heat capacity.
- The operative simplicity of the TPS2500 S with optimally designed Hot Disk sensors, makes this system a robust and ideal tool for tests of Solids, Liquids, Powders, Pastes, Fibres, Biomaterials etc.
- Optional software modules allows the instrument to be used in special applications, such as measurements of thin films, coatings or adhesive layers (Thin Films module), high-conducting sheets or slabs (Slabs module) and anisotropic samples or layered structures (Anisotropic module).
- Applications in the Electronics, Automotive, Aerospace, Nuclear, Biomedicines and Chemical Industries.
- The Test & Analysis software for automated measurements & temperature control of external devices.
- The software incorporates tools for exporting results to MS Excel for additional statistical analysis.
- Installed at NPL-UK, Bayer AG-Germany, Hitachi R&D- Japan, Mitsui Chemicals- Japan, IGCAR, Uni. Of Jaipur, Allahabad University, Laird Technology, BARC – Mumbai, Banaras Hindu Uni. Etc.

KEY FEATURES

- Sensors. Wide variety of TPS sensors suitable for different materials and applications.
- Temperature Control. Using either an optional external Furnace or Liquid-Temperature Bath.
- Everything to Get Started. With Std. Software, One Sensor, SS Ref. for data verification & RT Sample Holder.
- Optional: PC with Windows XP, MS Office 2007SBE, Monitor, Keyboard and Mouse.
- Optional Software. For Slab, Thin Film, Anisotropic and Specific Heat Capacity modules are available.

Transforming the complex into the simple

We also deal with HPTLC, GPC, HT GPC, OPLC, Hydrogen/Nitrogen/ Zero Air Generators, Refractometer, Polarimeter, Density Meter, GC, CE, Flash Chromatography and Ion Chromatography.

Chromline

CHROMLINE EQUIPMENT (I) PVT. LTD.
152-D, Udyog Bhavan, Sonawala Road, Goregaon (E) Mumbai 400 063. India
• Tel: 26860816 / 26860767 / 3263 [illegible] Fax: +91-22-26860306
• E-mail: mail@chromlineindia.com • Website: www.chromlineindia.com
Branches: New Delhi, Kolkatta, Lucknow, Bangalore, Hyderabad & Baroda

A Wide Range of Nano Technology Solutions

EVO®
Future assured
SEM platform

ULTRA
FESEM for
structural analysis

SUPRA™
Ultra high resolution
analytical FESEM

CrossBeam®
The ultimate
3D analysis tool

ORION™
He-Ion
microscope

LIBRA®
EFTEM with In-column
OMEGA filter

Visualization and Inspection

Making structures with nanoscopic dimensions far below the wavelength of light visible is the domain of imaging using electrons or ions. Intelligent detector technologies enable this technology to also display the structural and physical composition of material and analyse their chemical make up.

Si Solarcell
(using ZEISS ULTRA).

Nano-Structuring and Nano-Machining

By combining our outstanding core competencies in electron beam, focused ion beam technology (FIB) and gas injection system (GIS) into one system, unprecedented capabilities for cutting-edge nanoscopic imaging, structuring and analysis are the result.

In-situ Lift-out of semiconductor sample. The lamella is cut out and picked up with a micro-manipulator tip
(using ZEISS CrossBeam®).

Quantification and Analysis

Particle beam systems are irreplaceable tools for global basic research, the development of innovative products, and the production or quality-relevant process control. The latter is especially supported by a wide range of methods for detection, analysis and quantification of ultra-fine particles.

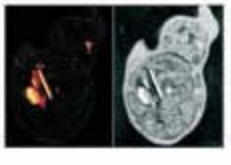

Malaria germ in a red blood cell.
Specimen by courtesy of B. T. Sewell, University of Cape Town
(using ZEISS LIBRA®120).

The Nano Technology Systems Division of Carl Zeiss SMT provides its customers with the latest leading-edge E-beam technology. Within this division you will find over four decades of accumulated experience in the field of scanning electron microscopy and six decades of experience in the field of transmission electron microscopy. Development and production facilities are based in Oberkochen (Germany), Cambridge (UK), and Peabody (USA).

The company's extensive know-how, which nowadays also comprises ion-beam technology and E-beam based analysis technology enable us to deliver innovative solutions for your business.

As a reliable, professional, worldwide provider of cutting-edge nanotechnology solutions your investment is in professional hands. Carl Zeiss heritage in quality optics generates a positive contribution to the performance of your enterprise and science institute. Carl Zeiss SMT strives for business excellence by developing processes for turning customer ideas into reality. The quality, precision and power of the Nano Technology Systems Division's instruments satisfy our customers with a foundation of operational excellence and a culture of continuous improvement.

As a learning organisation, market trends and first hand customer feedback worldwide are pro-actively incorporated into our processes and roadmaps.

The Division's business services also include outstanding support from sales consultancy to technical service options.

Carl Zeiss SMT
Nano Technology Systems Division
Carl-Zeiss-Str. 56
73447 Oberkochen
Germany

Tel. +49 7364 / 20 44 88
Fax +49 7364 / 20 43 43
info-nts@smt.zeiss.com
www.smt.zeiss.com/nts

Carl Zeiss India
Level 4, NDM II Building,Block 'D'
Netaji Subhash Place,Pitam Pura
New Delhi -110034
Ph: +91 11 45156000
Fax: +91 11 45156010/11
Email: nts.india@zeiss.co.in

ZEISS

LASER SCIENCE
SERVICES (I) PVT LTD

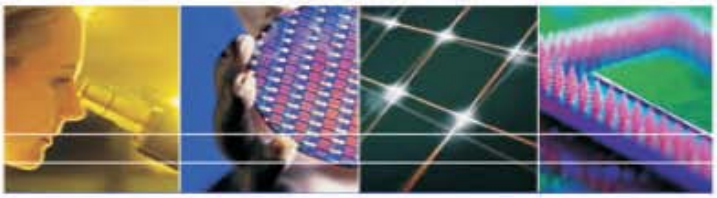

Bringing Tomorrows Technology Today!!

Ultrafast Laser:

COHERENT.

- **Micra** : One-box Ti:Sa Oscillator with adjustable Bandwidth & Repetition Rate

- **Chameleon Ultra-II** – Single Box Hands-free Oscillator with widest Tunability (400nm) from 680nm – 1080nm and fastest scanning speed (40nm/sec).

- **MiraHP :** Ultrafast Oscillator with Highest average power of > 3.3W @ 800nm

Excimer Laser

- **CompexPro** series excimer laser with max pulsed energy of 700mJ at 248nm

- **LpxPro** series Heavy duty excimer laser with max pulsed energy of 1.2J at 248nm

CCD & ICCD Cameras:

pco.
imaging

- **Pixelfly qe** :1K x 1K resolution 12 bit ccd camera with 62% QE.
- **Dimax** : 2K x 2K resolution 12 bit fast frame camera with 1000fps
- **DicamPro:** 1K x 1K resolution Iccd camera with interframing time of 75ns and exposure time down upto 3ns (1.5ns optional).

Atomic Layer Deposition

beneq

Features:

- Surface conformality
- Pinhole free Film & Repeatability
- Very thin films

- **TFS200:** ALD reactor for R&D application
- **TFS500:** ALD reactor for R&D and small scale Production

Materials: Oxides, Nitrides, Fluorides, Metals, Carbides, Sulfides Mixed Structures, Nanolaminates etc

Nanoparticle Synthesizer

Particles of: Metals (eg. Ag, Au, Ag-Pd etc), Metal oxides (eg. Fe, Co, Cu, TiO2-Ag etc)

For more details please write to us on sales@laserscience.in or call +91-22-41553232
Add: A-454, TTC Industrial Area, MIDC, Mahape, Navi Mumbai – 400701
www.laserscience.in

Nanotechnology is our Profession

High-Performance Routine Analysis

Imaging ESCA with < 200 nm Resolution

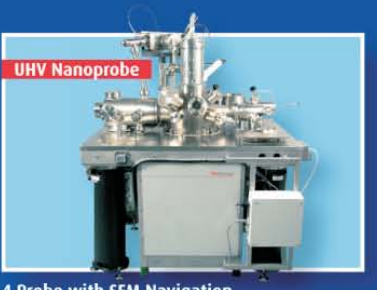

4 Probe with SEM Navigation

The Leading UHV STM and AFM Technology

20 nm Lateral Resolution

MBE & Deposition

Customised MBE, Thin Film
and Surface Analysis Solution

3nm SEM / 5nm SAM, SPM & FIB

AD More than UHV SPM / 05-11

World's Leading Technology for Nanotechnology Research and Analysis

MACK INTERNATIONAL
5/IA, Grants Building, Arthur Bunder Road,
Colaba, Mumbai 400 005, INDIA
Tel.: +91 (0) 22 22855261 / 22834962
Fax: +91 (0) 22 22852326
Email: sales@mack.in

Omicron NanoTechnology GmbH
Limburger Str. 75
D-65232 Taunusstein, Germany
Tel: +49(0) 6128 / 987 - 0
e-mail: info@omicron.de
Web: www.omicron.de

Building Modern Temples : Pandit Jawaharlal Nehru, Vice President of the Interim National Government of India laying the foundation stone of the National Physical Laboratory on January 4, 1947

SCIENTIFIC ADVISORY COMMITTEE

Designed and Printed at Deep Printers, 70A, Rama Road, Ind. Area, Kirti Ngaar, New Delhi-110015. Ph. : 9871196002